INVESTIGATIONS INTO THE THERMAL COMFORT AND INDOOR AIR QUALITY OF ROOMS IN LOW ENERGY HOMES USING A COMBINED HEATING AND VENTILATION SYSTEM

A thesis submitted for the degree

of

DOCTOR OF PHILOSOPHY

in the

Faculty of Engineering

UNIVERSITY OF LONDON

by

Patrick Kwaku Ata

ProQuest Number: 10055419

ProQuest 10055419

Dedicated to my Parents

ABSTRACT

The objective of the research was to identify a suitable heating and ventilation system for the provision and control of thermal comfort in rooms of future low energy homes. This was to be achieved whilst allowing for the provision of good indoor air quality (IAQ) and minimisation of energy consumption.

The thesis describes the investigations of individual room airflow and the implications on thermal comfort, indoor air quality and energy consumption. Using a commercial computational fluid dynamics package, numerical simulations were performed to produce airflow patterns and distributions of temperature and pollutants within a room. A numerical model was validated for use in indoor airflow. The model was used, first of all, in the identification of a suitable configuration of supply and extract air terminal devices, over the expected range of boundary conditions. Further to this, parametric and sensitivity studies were performed on the proposed system to establish the influence of the airflow rate, supply air temperature and room specific parameters such as internal heat sources, furniture etc. on the indoor environment. Time dependent variations were considered in order to provide a better understanding of the transient nature of the system. The research also included determination of necessary locations of sensor/measurement points which provide representative conditions of the thermal environment in the room.

The investigation found a high level supply combined with a low level extract configuration to be most appropriate over the range of operation expected of the heating and ventilation system. Limits of operation of the system were identified to prevent local thermal discomforts due to excessive vertical air temperature gradients and draught. As a result of the investigations, a simple control strategy was proposed to achieve thermal comfort control, while providing good IAQ and energy efficiency.

ACKNOWLEDGEMENTS

TABLE OF CONTENTS

LIST OF FIGURES

Chapter 4

Chapter 5

LIST OF TABLES

NOMENCLATURE

A	body/wall surface area
$A_{\mu,b,CI}$	constants in LB turbulence model
A_{on}	supply area of air terminal device
Ar	Archimedes number
A_s	individual wall surface areas
$b_n,\ c_n,\ d_n$	conduction transfer function coefficients
c,C	pollutant concentration
$C_{1,2,3,D,\mu}$	constants used in the turbulence models
C_p	specific heat capacity at constant pressure
E	formaldehyde emission rate
f_{cl}	clothing area factor
$f_{1,2,\mu}$	constants used in the LB turbulence model
g	acceleration due to gravity
$g_n,\ p_n$	space air transfer function coefficients
$g_n{}^*$	normalised space air transfer function coefficients
h_c	convective heat transfer coefficient
H	enthalpy
I_{cl}	thermal resistance of clothing
k	thermal conductivity, turbulent kinetic energy
K_{tot}	total conductance of the room envelope
L_m	constant used in the 2L turbulence model
$\dot{m}$	mass flow rate
m_f	rate of moisture generation within the building
m_g	rate of moisture diffusion through the building fabric
M	metabolic activity rate
n	summation index, constants
N	room air changes per hour
p_a	partial water vapour pressure of the room air
P	static pressure
PD_{iaq}	percentage dissatisfaction with the indoor air quality
PD_v	percentage dissatisfied due to draught
$PD_{\delta T}$	percentage dissatisfied due to vertical air temperature differences
PMV	predicted mean vote
q	heat load
q_e	heat gain through a square meter wall section
$Q_{C,E,K,RES,S,W,M}$	heat exchange/loss by convection, evaporation, conduction, radiation, respiration, body, mechanical work, metabolic activity.
$R_{N,K}$	turbulence Reynolds numbers
s	individual wall surfaces
S_ϕ	source terms in the transport equations
t,T	air temperature, air temperature in the room centre
t_a	air temperature, air temperature in the occupied zone
t_{cl}	surface temperature of clothing
t_e	sol-air temperature
t_{off}	extract-air temperature
t_{on}	supply-air temperature

t_{rc}	constant indoor room air temperature
$\bar{t}_r$	mean radiant temperature
t_s	wall surface temperatures
$T_{loc1, loc2}$	air temperature measurements at sensor locations
TI	turbulence intensity
u'	random fluctuating velocity
$\bar{u}$	mean velocity
U	conductance
$\dot{v}$	local air velocity
$\dot{v}_g$	CO_2 production rate
$\dot{v}_{olf}$	outdoor air flow rate per olf
$\dot{v}_{wwal}$	air velocity measurement at a sensor location on the west wall
V	air volume of room
$\dot{V}_o$	volume flow rate of outdoor air
W	work rate
x, y, z	directions on a cartesian coordinate
y_l	local distance to a wall
$y+$	Reynolds number in terms of a non dimensional transverse coordinate

Greek symbols

δ	time interval
δT	temperature difference between fixed heights
Δ	offset
ε	dissipation rate of turbulent kinetic energy
Γ	diffusion coefficient
μ	laminar viscosity
μ_t	turbulent viscosity
ϕ	dependent variable
ρ	density
σ	Prandtl number, Schmidt number
$\sigma_\varepsilon, \sigma_k$	constants in turbulence models
Σ	summation
τ	shear stress
θ	time
ω_i	specific humidity of indoor air
ω_o	specific humidity of outdoor air

Subscripts

ave	average
e, E	east
i	inside
o	outside
ref	reference value

sd   standard deviation
w, W   west

Abbreviations

ACH	air changes per hour
AIC	acceptable indoor concentration
ASHRAE	American society of heating refrigeration and air-conditioning engineers
ATD	air terminal device
BRE	building research establishment
BS	British standards
CEN	comite european de normalisation
CFD	computational fluid dynamics
CHAM	concentration heat and momentum
CI	comfort index
CIBSE	chartered institute of building services engineers
CO	carbon monoxide
CO_2	carbon dioxide
CTF	conduction transfer functions
DCV	demand controlled ventilation
ECA	European collaborative action
FVM	finite volume method
H & V	heating and ventilation
IAQ	indoor air quality
IEA	international energy agency
ISO	international standards organisation
LB	lam bremhorst
LHS	left hand side
LW	light weight
MAC	maximum allowable concentration
PDE	partial differential equation
PMV	predicted mean vote
pp	per person
ppm	parts per million
RHS	right hand side
RSP	room specific parameters
SATF	space air transfer functions
SBS	sick building syndrome
SCC	simple comfort control
S.S.	steady state
TDMA	tri-diagonal matrix algorithm
TFM	transfer function method
TLV	threshold limit values
vtg	vertical temperature gradient
WO	with obstacle
2L	two layer

1. INTRODUCTION

In cold climates, the energy consumption of the built environment's domestic sector constitutes a substantial proportion of national energy production. Within this, winter space-heating accounts for a significant percentage of the total energy consumed. Initiated by the energy crisis of the 70's and followed by recognition of the need to conserve fossil fuel reserves and more recently, the ecological implications of energy production by fossil fuels - CO_2 emissions, there has been a concerted effort to reduce energy consumption in all sectors. In the building sector, this has led to steadily improving levels of insulation and air tightness of the building envelope. Greater air tightness, whilst resulting in reductions in fortuitous air infiltration, and therefore heat losses, also resulted in high concentrations of indoor air pollutants. This brought about the need for some form of ventilation system to provide outside/fresh air to attain or maintain satisfactory indoor air pollutant concentrations. These ventilation systems resulted in additional and inevitable heat losses (known as the ventilation losses) in the provision of cold outside air (during winter) and extraction of warm room air. As building insulation levels were further improved, the ventilation losses constituted more significant proportions of the total heat loss. In recent years, attempts to minimise these losses have seen reductions in outside air supply rates. This era, not coincidentally, has been synonymous with the onset of the term 'sick building syndrome' (SBS). SBS refers to a host of indoor air quality related complaints which include the sensation of stuffy and stale air, irritation of mucous membranes and eyes, headaches, lethargy and so forth. Consequently, the impact of the indoor air quality (IAQ) on the health and productivity of the occupants has taken on greater importance, prompting extensive research activities into the causes and implications of poor IAQ. These studies have primarily addressed the following areas: the identification of the sources of indoor air pollution, ventilation rates required to achieve comfortable and healthy indoor environments for extended occupancy and the influence of the air distribution systems.

The thermal environment is influenced by air movement and as a consequence by the ventilation system, irrespective of whether air is used as the transport medium for space heating. Achieving satisfactory thermal comfort conditions is therefore

dependent on both the heating *and* ventilation systems. The provision of adequate levels of IAQ and thermal comfort in a room is thus an interdependent process, with a common variable: the air movement. This triangulation of *air movement, IAQ* and *thermal comfort*, together with the implicit *energy* implications, is the subject of this research, in the application domain defined below.

1.1 Application domain

The application domain of this research is in the heating and ventilation of low energy homes, located in the temperate climate of mid European countries. These will be air tight buildings with high standards of thermal insulation. The study will focus on a combined heating and ventilation system with individual room conditioning and control. The system is to operate intermittently, providing ventilation (outside air) along demand controlled principles, (i.e. the supply of outside air should satisfy requirements at any given moment). The concept of comfort control of the thermal environment as opposed to temperature control is to be assessed.

Reasons for the *choice* of ventilation and heating system and mode of operation will be highlighted in the following sections. These sections include a brief outline of the current status in the three broad fields which affect this investigation, namely the indoor air quality (IAQ), thermal comfort and air distribution systems. Within these sections, relevant data and mathematical expressions will be identified which were used in the course of the study. All mathematical expressions listed in this chapter will be used in subsequent chapters. Following the outline of the three fields, the chapter proceeds to review a number of recent studies which had a bearing on this research. This is followed by the definition of the objectives and methodology of this research.

1.1.1 Low energy homes

Low energy homes, refers to buildings with high levels of thermal insulation and air tightness, essentially surpassing most national standards. Several terms in use today include: *low energy* homes, *super insulated* homes and *passive* homes, representing increasing levels of thermal insulation and air tightness of the building envelope. The thermal insulation and air tightness standards currently associated with these

expressions may be approximately represented by the values shown in Table 1.1. The transition from *low energy* to *passive* homes is often accompanied by the introduction of heat recovery devices (e.g. air-to-air heat exchangers and exhaust-air heat pumps) and the use of alternative energy (or heat) sources, such as solar and geothermal energy sources. The use of the term *low energy home,* within this study, refers to buildings with insulation standards of 0.4 W/m²K or lower, i.e. all three levels in Table 1.1. The implications of the building insulation and air tightness level on the selection of heating and ventilation systems is discussed below.

	U value of the building envelope U (W/m^2K)	Air infiltration across the room envelope ACH (/h)
low energy homes	0.4	0.5
super insulated homes	0.2	0.35
passive homes	0.1	0.25

Table 1.1 Typical thermal conductivity and air infiltration rates of today's low energy homes (Infiltration rate is usually of the order of $1/20^{th}$ of the measured air change rate at 50 Pa. *Liddament,* 1986)

1.1.2 Natural vs. mechanical ventilation

Natural ventilation is the provision of outdoor air into a space via openings within the building fabric as a result of pressure differences which are caused by wind and stack effects. The stack effect arises from the differences in air temperature and therefore density causing pressure gradients both inside and outside the building. When the inside air temperature is greater than the outside air temperature, colder outside air enters the building through low level openings and warm air escapes at high levels. Natural ventilation may be provided by various strategies:

- ventilation through windows
- ventilation through purpose-provided openings (vents)
- passive stack ventilation - via purpose-provided openings and vertical stacks
- controllable air inlets

Although the provision of natural ventilation systems tends to be cheaper and simpler than mechanical systems, these are subject to a major drawback: the inherent uncontrollability due to the unpredictable nature of wind pressures and temperature differences. The need to conserve energy and avoid indoor air quality problems has seen natural ventilation evolve from arguably its most basic form: infiltration through cracks and gaps in the building envelope. Greater control has been achieved by the reduction of adventitious infiltration and the provision of windows and vents which are controlled by the occupants. In addition, the stack effect has been used in buoyancy driven exhaust systems, with outside air provided through purpose built openings. Further improvements (*Knoll*, 1992) have seen the development of controllable air inlets such as *trickle vents*; *self regulating inlets* (by temperature or pressure) and *humidity controlled inlets* which are combined with a buoyancy driven exhaust system. The latter have found applications in colder climates, but still encounter practical difficulties in the modulation of flow rates, due to their dependence on the climatic conditions. Where good control is required, the tendency is to employ mechanical ventilation systems.

Mechanical ventilation implies the use of one or more fans to achieve one of the following:

- mechanical supply of outside air
- mechanical extraction of room air
- a combination of the above (balanced system)

Supply-only or extract-only mechanical ventilation essentially operate on the principle of over and under pressurisation of the room, with the resulting exfiltration/infiltration of air by natural means. These exfiltration/infiltration air routes may be through cracks or gaps in the building fabric or through purpose built openings. Both of these systems, however, suffer from a number of drawbacks:

a) difficulties in precise control

b) difficulties in controlling the flow distribution in the room, and

c) they do not allow for the application of heat recovery devices between the supply and extract air.

In buildings with air tight envelopes, balanced mechanical ventilation systems (supply & extract) should be used for close control of IAQ by good distribution and mixing of the supply air and of the flow rates. These systems allow recirculation of room air and the incorporation of filters and heat recovery devices.

1.1.3   Demand controlled ventilation

Demand controlled ventilation (DCV) refers to the provision of appropriate quantities of outdoor air according to the needs and demands at the time. This concept was introduced to reduce energy consumption while maintaining good IAQ. This is achieved by avoiding unnecessary continuously high outdoor air supply rates. These systems vary in complexity from the application of simple devices such as timers, to the use of sensors for the evaluation of the IAQ, occupancy detection etc.

The concept of DCV is in itself nothing new e.g. providing ventilation during occupancy by the use of timers or manual activation of the system. Advances in technology however, both in communication (e.g. network/bus systems) and instrumentation (e.g. measuring instruments/sensors) give a new meaning to the concept of DCV today. In today's use, DCV refers to the provision of sufficient rates of outdoor air during occupancy, to meet the fluctuating requirements for satisfactory IAQ. This is to provide optimisation between the demands for good IAQ and the energy of the ventilation system.

The application of DCV systems is currently under assessment in several studies (*Liddament*, 1994). These studies address the necessary measurements to evaluate the IAQ, the identification of threshold limit values (TLVs) of individual pollutants for acceptable IAQ and the development of sensors to measure pollutant concentrations. DCV systems currently being evaluated include the use of CO_2, relative humidity and mixed gas sensors. Performance evaluation of these DCV systems is beyond the scope of investigation of this work. Further information on practical results with DCVs and the developments of components such as sensors can be found in various publications of International Energy Agency (IEA) Annex 18 "Demand Controlled Ventilation Systems". Within this study, a heating and ventilation system is to be investigated over

a range of flow rates which may be required of DCV systems. To determine the possible range of flow rates for DCV operation, the major pollutants will be identified together with the necessary ventilation rates to achieve satisfactory concentrations of these.

1.1.4 Space heating

In most of the Scandinavian countries, new housing is equipped with balanced mechanical ventilation systems with heat recovery devices (air-to-air heat exchangers or air-to-air/water heat pumps) which also provide space heating using air as the heat transport medium. In more moderate climates (mid-Europe) there is a similar trend with increasing thermal insulation and tightness of the building envelope.

The presence of a balanced ventilation system (with its associated components e.g. fans, ducts, dampers etc.) makes the use of an air heating system an attractive and economically viable option, in particular in terms of initial cost. The increasing supply rates of outside air with building tightness, have resulted in greater volumes of air movement and had implications on fan sizing, duct sizing and the energy consumed in the distribution process. Simultaneous improvements in thermal insulation and space heat requirement have meant reductions in air quantities required in the provision of the space heat requirement. The greater the reduction in space heat requirement, the closer these two flow rates converge. It has thus become economical both from the perspective of initial cost and operating cost to integrate the heating and ventilation into the same distribution system.

The configuration of the heating and ventilation systems and choice of primary heat source could have implications on the most efficient mode of operation of the systems i.e. optimisation in flow rates and supply air temperature. For example with the availability of low grade heat sources, operation at increased flow rates could be more economical despite the higher fan costs. Evaluation of the relative economies of operation, in a similar manner to the use of DCVs is beyond the scope of this investigation. Some consideration though will be given to this in the recommendation of a control strategy for the energy efficient provision of thermal comfort and IAQ in a room.

1.2   Indoor air quality

A person's perception of indoor air quality is subjective, mainly on the basis of an individual's sensation to various odours. This is acceptable for most organic substances, which are olfactory stimuli. In these cases, the human olfactory system is superior to most measuring instruments. Inorganic substances however, including harmful pollutants such as carbon monoxide, cannot be perceived even at high concentrations. Good indoor air quality thus requires fresh air supply rates to dilute odours and maintain harmful pollutants within healthy levels. Outdoor air flow rates for human respiration are between 0.1-0.9 l/s, depending on metabolic activity rate. These requirements fall well within the demands for pollutant dilution from for example human bioeffluents and need not be taken into consideration.

Two approaches will be identified to determine a possible range of flow rates required for ventilation purposes:

a) identification of the major indoor air pollutants and the minimum outdoor airflow rates required in order not to exceed threshold limit values (TLVs) for acceptable indoor concentrations, and

b) the use of two new units developed by *Fanger* (1988), the olf and the decipol.

1.2.1   Indoor air pollutants

Comprehensive reviews of research into common indoor pollutants and the ventilation rates required to control pollutant levels within acceptable limits are given in various annexes of the IEAs energy conservation in buildings and community systems programme, *Haberda & Trepte* (1989), *Raatschen* (1989), and *Limb* (1994) and also by *Awbi* (1991). These publications are the main data sources in the following sections on individual pollutants and corresponding minimum ventilation rates required. Where specific references are quoted from these, they are accompanied by superscripts [1], [2], [3] and [4], representing the order of appearance above.

Odours

The main sources of odours in habitable rooms have, until recently, been assumed to be due mainly to the occupants. Recent studies contradict this assumption. These studies have identified sources such as building materials, furnishings and the ventilation system to produce greater concentrations of odorous pollutants, when combined, than human bioeffuents. It is now widely accepted that other odour sources are at least as significant as those from human bioeffluents. This position is reflected in the revisions of the proposed new standards in the US in *ASHRAE standard 62* (1996) and in Europe in Comite Europeen de Normalisation (CEN) pre-standard *prENV 1752* (*Fanger*, 1996). These new standards specify minimum flow rates to cater for odour dilution from persons as well as from materials. The proposed *ASHRAE* standard is currently restricted to commercial buildings and does not apply to dwellings.

Laboratory and field study results have correlated a persons degree of dissatisfaction (based on a large sample of persons) with body odour from a sedentary person against outdoor air supply rate. For unadapted persons, freshly entering the space, the degree of dissatisfaction with outdoor airflow rate may be estimated from Figure 1.1[2]. *ASHRAE standard 62* (1989) recommends the use of similar limits of acceptable dissatisfaction level (20%) due to indoor air pollution as those used in the *ISO standard 7730* (1993) for thermal comfort. This results in the recommendation of outdoor air flow rates of 8 l/s per person (from Figure 1.1).
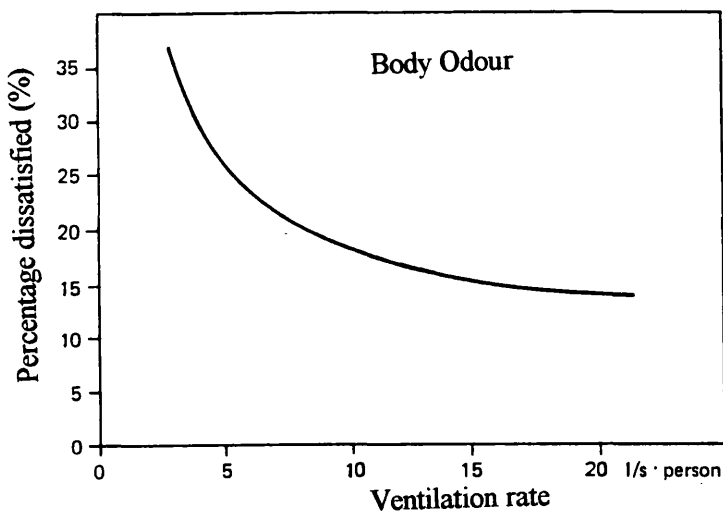
Figure 1.1 Degree of dissatisfaction of odour level with outdoor airflow rate [2]

Odours due to building materials and/or ventilation systems are difficult to quantify, partially due to the large variations found in materials, furnishings, and systems between buildings. Average building stock has been estimated (*ECA*, 1994) to require approximately 0.75 l/s per square metre of floor area for living rooms and bedrooms to achieve acceptable odour levels.

Carbon dioxide (CO_2)

The rate of production of CO_2 ($\dot{v}_g$, l/s) by human respiration is related to metabolic rate by the following expression:

$$\dot{v}_g = 4 \times 10^{-5} M \cdot A \qquad\qquad 1.1$$

where

M = metabolic rate (W/m^2)
A = body surface area (m^2)

The maximum allowable concentrations (MAC) for 8 hour occupation recommended in various standards is 5000 ppm. For acceptable indoor concentrations (AIC), the recommendation[2] in various countries is to keep the concentrations to minimum levels of between 800 and 1500 ppm. *Jannsen* (1994) and his associates studied the response of school children to CO_2 controlled ventilation. They found an acceptance of the environment at CO_2 levels of 1000 ppm with a rise in discomfort at 1600 ppm with complaints of stuffy, more stagnant and warmer air and the sensation of warmer hands and feet with respect to the rest of the body. Although CO_2 is not poisonous to humans below a concentration of 50000 ppm, physiological effects have been observed at concentrations above 10000 ppm. It is not known whether these are harmful in the long term.

The CO_2 concentration in outside air is approximately 350 ppm, with minor increases year on year. The variation of the environmental concentration of CO_2 rarely exceeds 150 ppm. This relatively minor variation in CO_2 concentration combined with the large percentage of CO_2 in expired air (4.4 % by volume) and the fact CO_2 cannot be filtered or absorbed, has led to the use of CO_2 as an index for occupant related pollution (i.e. odours).

Assuming perfect mixing, outdoor air flow rates ($\dot{V}$, l/s) can be estimated from a steady state mass balance:

$$\dot{V} = \dot{v}_g \left(\frac{1 - C_i}{C_i - C_o} \right)$$

1.2

where

$\dot{v}_g$ = internal generation rate of CO_2 (l/s)

C_o = outdoor concentration of CO_2 (ppm)

C_i = indoor concentration of CO_2 (ppm)

This expression will be used in the estimation of required air flow rates to prevent indoor CO_2 concentrations from exceeding the recommended limit (1000 ppm) for acceptable indoor concentration.

Formaldehyde

Formaldehyde exists extensively in today's environments. It is present in building materials such as compressed wood boards, plastic foam insulation, bonding and laminating agents, adhesives, as well as in packaging products, toiletries and cosmetics. Combustion appliances and tobacco smoke also generate appreciable amounts. At low concentrations, formaldehyde may cause discomfort due to odours or irritations to the eyes, nose, throat and related symptoms such as headaches. In higher concentrations, tests on animals suggest this may pose carcinogenic risks to humans. Most current ventilation standards allow MAC of formaldehyde of 1 ppm and recommend AICs of 0.1 ppm. It is however, not currently proven that health risks do not exist at the AIC level, particularly over long term exposures. Currently, the health implications at 0.1 ppm are suspected to be minimal or at least tolerable. Various studies (*Cain et al*, 1986) have found differing human sensitivity levels to the detection of formaldehyde, ranging from 0.03 ppm to 1.00 ppm. Tests have also shown decreasing irritation levels to formaldehyde with the introduction of other odorous sources. Numerous questions about the true impact of formaldehyde still exist and are being addressed in ongoing research[4].

Studies in the UK and Germany have recommended minimum air changes per hour (ACH) of between 0.5 and 0.8, thus maintaining concentrations within AIC levels. However, results (*Walsh et al*, 1984[4]) from an energy efficient house in the USA obtained formaldehyde concentrations well in excess of the 0.1 ppm threshold. Concentrations of up to 0.35 ppm were obtained at ACH of 0.83. These high formaldehyde concentrations were attributed to the insulation materials.

Typical formaldehyde emission rates of today's materials are given in Table 1.2. Its concentration in room air is dependent on various factors: the area of the emitting surface, total air volume, air change rate, and other parameters such as temperature, humidity and age of the formaldehyde source. Where no formaldehyde sinks are present within a room (i.e. assuming unsupressed emission), the room concentration (C, ppm) may be estimated by the expression[4]:

$$C = \frac{A \cdot E}{\rho \cdot N \cdot V}$$

1.3

where

A	= area of emitting surface, (m^2)
E	= net emission rate, (mg/hm^2)
ρ	= density, (kg/m^3)
N	= air change rate, (/h)
V	= air volume of room (m^3)

Equation 1.3 may be used together with the data in Table 1.2 in the estimation of necessary outdoor air flow rates to maintain formaldehyde concentrations within AIC levels (0.1 ppm).

Material	Emission Rate, E (mg/hm^2)
woodchip boards	0.46 - 1.69
compressed cellulose boards (hardboards)	0.17 - 0.51
plasterboards	0 - 0.13
wallpapers	0 - 0.28
carpets	0
curtains	0

Table 1.2 Typical formaldehyde emission rates (*Walsh et al*[4])

Water vapour

High moisture levels may have an impact on the occupants comfort and health. Low humidity levels are believed to contribute to increased risks of infection, whereas high humidity levels may result in condensation within the room. Condensation, when combined with inadequate ventilation, may cause musty smells as a result of mould and fungal growth. As well as having an adverse effect on the occupants health, long term condensation often leads to structural damage to walls and materials within the room.

Relative humidities of between 30-70 % are recommended in habitable rooms. High moisture levels can be restricted by adequate ventilation rates, due to relatively dry outdoor air, particularly during cold seasons. Moisture production within a dwelling is mainly from occupants and their activities. Assuming well zoned buildings, moisture production in habitable rooms would be due mainly to the emission from the occupants of approximately 2-3 1 per 24 hours for active occupants (Building Research Establishment [4]). Allowances may be made for activities such as meals and some spill-over from other higher production zones. Assuming perfect mixing of the indoor air, the outdoor airflow rate ($\dot{V}_o$, m^3/s) required to attain specified indoor air moisture levels (or relative humidity) can be estimated from a moisture balance for the zone:

$$\dot{V}_o = \frac{m_g - m_f}{\rho_o (\omega_i - \omega_o)}$$

1.4

where

m_g = rate of moisture generation within the building (kg/s)
m_f = rate of moisture diffusion through the building fabric (kg/s)
ρ_o = density of outdoor air (kg/m^3)
ω_i = specific humidity of indoor air (kg/kg)
ω_o = specific humidity of outdoor air (kg/kg)

Tobacco and Carbon monoxide (CO)

Tobacco smoke consists of approximately 90 % gaseous contaminants and 10 % particulates. Contaminants include amongst others acrolein, nicotine, tar, carbon monoxide and formaldehyde's which may have serious health effects on the occupants in poorly ventilated environments. The particulates lead to irritation of the eyes and nasal passage. Odours emanate mainly from the gaseous products.

Carbon monoxide levels have been found to give a good indication of levels of tobacco smoke that cause irritation and dissatisfaction due to odour intensity. Field studies suggest the restriction to a 1 ppm increase in indoor CO levels in comparison to the outdoor levels to be desirable to non smokers. MACs of CO in IEA member countries varies between 25-50 ppm and AICs between 9-18 ppm.

Various recommendations exist for required ventilation rates. *Haberda & Trepte* (1989) list a requirement of a 3 to 4 fold increase in outdoor airflow rate to prevent discomfort and irritations to non smokers. For an average smoker consuming 1.3 cigarettes per hour, *BS 5925* (1981) recommends an additional 7 l/s in addition to the airflow rates required for other pollutants. *CIBSE guide* (1986) recommends the values in Table 1.3. Assessment of the level of smoking is subjective and indicates some of the problems in evaluation of acceptable ventilation rates.

Condition	recommended outdoor air supply rate (l/s pp)
No smoking	8
Some smoking	16
Heavy smoking	24
Very heavy smoking	32

Table 1.3 Recommended outdoor supply rates (*CIBSE*, 1986)

A summary of recommendations obtained within the previous sections, for minimum outdoor airflow rates (or ventilation rates) required for individual pollutant dilution and/or the TLV concentrations is compiled in Table 1.4. The recommendations will be used in the Chapter 3 in estimating airflow rates required in the heating and ventilation system.

It was obvious in the review of the indoor pollutants that there are considerable differences in the standards of different countries. These differences are similarly observed in the minimum flow rates specified in the various ventilation standards listed in Appendix A.1 (ventilation standards, as at 1994, *Limb* (1994)). The current standards are widely acknowledged to be inadequate, and cannot be used as proficient guidelines. Most of these are currently under review and will no doubt be modified in the years to come.

Pollutant	MAC (ppm)	AIC (ppm)	Recommended minimum airflow rates
Human bioeffluents	-	-	8 l/s pp
Odours, materials & ventilation system	-	-	0.75 l/s m^2 floor area
Carbon dioxide	5000	1000	-
Formaldehyde	1	0.1	-
Water vapour		30-70% RH	-
Tobacco			15 -32 l/s per smoker

Table 1.4 Summary of TLV concentrations of the major pollutants or minimum flow rates recommended for acceptable indoor concentration.

1.2.2 The olf and decipol

Two units have been introduced by *Fanger* (1988), the olf, to quantify air pollution sources and the decipol, to quantify air pollution perceived by a person. These units are only applicable to odorous pollutants.

- 1 **olf** is defined as the emission rate of air pollutants from a standard person (bioeffluents). This is used to quantify air pollution sources.

- 1 **decipol** is defined as the pollution caused by one standard person (1olf) ventilated by 10 l/s of unpolluted air. This is used as a measure to quantify the air pollution perceived by a person.

The olf is a unit based on the perception of odours by the human olfactory system using a large sample of judges. Other pollution sources are quantified relative to the pollution source from a standard person. *Fanger* correlated the dissatisfaction of a large number of people to various rates of outdoor air when subjected to 1 olf of pollution. The response to the environment was taken immediately after entering the space. He obtained the following correlation:

$$PD_{iaq} = 395e^{(-1.83\dot{v}_{olf}^{0.25})}$$

1.5

where

PD_{iaq} = percentage dissatisfaction with the IAQ (%)
$\dot{v}_{olf}$ = outdoor airflow rate per olf (l/s)

From field measurements in numerous buildings, *Fanger* produced average/typical pollution loads from materials (olf/m² of floor area) and persons (olf/person) as shown in Table 1.5. This quantification process is being extended for individual building materials, which should aid the designers in the selection of low olf materials. By compiling the olf loads of a building or zone under investigated, Equation 1.5 can be used to determine the necessary flow rates to achieve a satisfactory indoor odour level (ASHRAE recommendation, 20% dissatisfaction).

Pollution source		Load (olf)
Occupants	sedentary activity (1 Met)	1
(per person)	active (4 met)	5
	very active person (6 Met)	11
	smoker (during smoking)	25
	smoker (average)	6
Materials and ventilation systems		
(per m² floor area)	average existing building stock	0.4
	low pollution building	0.1
Total load (occupants & materials)		
(per m² floor area)	average in existing building with 40% smokers	0.7
	low pollution building without smoking	0.2

Table 1.5 Pollution sources for various activities and within buildings[4] (1 Met = 70 W / m² of body surface area)

1.3 Thermal comfort

Thermal comfort   This is defined as that condition of mind which expresses satisfaction with the thermal environment

Thermal neutrality   This is defined as that condition in which the subject would prefer neither warmer nor cooler surroundings.

Thermal comfort and thermal neutrality may initially appear to have identical meaning. However, a person can be in thermal neutrality and at the same time experience discomfort for a number of reasons. This may be from local heating or cooling due to non-uniformities in the thermal environment or unacceptably high air movement, i.e. draught. These are known as the *local thermal discomforts*.

It has long been established that a person's perception of warmth or coolness is not solely dependent on temperature but on a combination of six variables: air temperature, mean radiant temperature[1], air velocity, water vapour pressure in the air, relative humidity, the persons activity and the persons clothing. Substantial research has been carried out on the relationship between thermal perception and one or more of these *environmental* (air temperature, mean radiant temperature, air velocity and water vapour pressure) and *personal* parameters (metabolic activity rate, clothing insulation level). These may be broadly categorised into:

1. Comfort chamber studies
2. Field studies

Comfort chamber studies have been the main contributor to the development of heat exchange models to predict a person's or group of persons response to a thermal environment. The most comprehensive and currently accepted of these studies is by *Fanger* at the Technical University of Denmark, and resulted in a thermal comfort index called the predicted mean vote (*PMV*). This is the recommended index in *ISO standard 7730* (1993) for measuring and evaluating thermal environments. It is also the measure by which guidelines are specified, in the standard, for acceptable conditions of thermal comfort. There is, however, an ongoing debate relating to the discrepancy between the *preferred* thermal comfort level predicted with comfort models (including the *PMV*) and results of field studies. The *PMV* is nevertheless considered to be appropriate for this study and will be used in the assessment of thermal comfort. The reasons for this choice and a partial discussion of the above-mentioned debate will be given below. Prior to this, however, the *PMV* model and the relations for evaluation and restrictions of local thermal discomforts will be described.

1.3.1 Thermal sensation measured by the *PMV*

The *PMV* is a so-called empirical comfort index. These indexes are developed on the basis of fundamental heat transfer theory, modelling the heat transfer between the body

---

[1] The *mean radiant temperature* of the environment is defined as the temperature of an imaginary isothermal enclosure with which the human body would exchange the same radiation as with the actual environment.

and its environment. These models include physiological variables to take into account the thermo-regulatory mechanisms of the body such as skin temperature and sweating. The physiological variables are determined from empirically derived relations. Details on the construction of heat transfer models and the physiological relations for the human body may be found in various texts, including *Fanger* (1970), *ASHRAE handbook* (1993) and *Awbi* (1991). Heat transfer from a body to its environment can be represented by a general expression such as:

$$Q_S = Q_M + Q_W + Q_R + Q_C + Q_K - Q_E - Q_{RES} \qquad 1.6$$

where

Q_S	= heat load of the body (W) *
Q_M	= mechanical work (W)
Q_W	= metabolic rate (W)
Q_R	= heat exchange by radiation (W)
Q_C	= heat exchange by convection (W)
Q_K	= heat exchange by conduction (W)
Q_E	= evaporative heat loss (W)
Q_{RES}	= heat loss by respiration (W)

*Q_S = 0 represents thermal equilibrium, positive values represent body temperature rises and negative values falling body temperature.

Fanger (1970) assumed a number of requirements for thermal comfort under steady state conditions. Firstly, the body needs to be in thermal equilibrium i.e. its rate of heat loss is equal to its rate of heat gain (i.e. Q_S = 0). Secondly, he assumed a person's mean skin temperature and sweat secretion rate must fall within narrow limits which change with activity rate. Studies have shown that a person's thermal sensation is influenced by mean skin temperature and some internal body temperature, possibly the hypothalamic temperature. The internal body temperature is taken into consideration by using the sweat secretion rate, which is a function of both the internal body and the mean skin temperature. Therefore, although a wide range of environmental variables may achieve a heat balance of the body, thermal comfort is restricted to a narrow range, which satisfies the criteria for both skin temperature and sweat secretion rate.

In establishing his thermal comfort equation, *Fanger*, in the absence of data on the acceptable range of skin temperatures and sweat secretion rates, made a further assumption. He assumed that the *mean* values of persons preferred skin temperature

and sweat secretion rates (from experiments on a large sample of persons at various activity rates), would approximately correspond to the mid range of the acceptable limits. Assuming a normal distribution about this mid-range, these mean values should lie within the comfort range. Integrating expressions for the variation of skin temperature and sweat secretion rate for persons in thermal comfort, *Fanger* arrived at his *thermal comfort equation* . This can be used to investigate any combination of variables to achieve thermal neutrality. However, it gives no indication of the thermal sensation if thermal neutrality is not achieved. To address this last issue and also to allow for variations between persons, he extended the algorithm to include a prediction of a person's rating on the ASHRAE thermal sensation index (*ASHRAE handbook*, 1993) as shown in Table 1.6. In doing this, *Fanger* assumed a person senses his or her *own* temperature and not the temperature of his or her surroundings. Therefore, by relating the heat imbalance (heat storage, Q_S in Equation 1.5) to experimental data on recorded thermal sensation at similar combinations of personal and environmental parameters, he obtained the relation for *PMV*. This is expressed in terms of the air temperature, mean radiant temperature, air velocity, vapour pressure and the persons activity and clothing insulation as:

$$PMV = \left(0.303e^{-0.036M} + 0.028\right)\left\{\begin{array}{l} (M-W) - 3.05\times10^{-3}\left[5733 - 6.99(M-W) - p_a\right] \\ -0.42\times\left[(M-W) - 58.15\right] - 1.7\times10^{-5} - 0.0014M\left(34 - t_a\right) \\ -3.96\times10^{-8}f_{cl}\times\left[\left(t_{cl} + 273\right)^4 - \left(\overline{t_r} + 273\right)^4\right] - f_{cl}h_c\left(t_{cl} - t_a\right) \end{array}\right\}$$

1.7

M = metabolic activity rate per m^2 of body surface area (W)
W = work rate (W)
I_{cl} = thermal resistance of clothing (m^2 °C/W)
f_{cl} = factor of clothing area i.e. ratio of clothed to exposed surface
t_a = air temperature (°C)
$\overline{t_r}$ = mean radiant temperature (°C)
$\dot{v}$ = relative air velocity (m/s)
p_a = partial water vapour pressure (Pa)
h_c = convective heat transfer coefficient (W/ m^2 °C)
t_{cl} = surface temperature of the clothing (°C)

The surface temperature of the clothing (t_{cl}) is represented by Equation 1.8. The clothing area factor (f_{cl}) is related to the thermal resistance of the clothing by the

expression in Equation 1.9 and the convective heat transfer coefficient (h_c) is the higher value obtained from the two expressions in Equation 1.10 which represent free and forced convection respectively.

$$t_{cl} = 35.7 - 0.028(M - W) - I_{cl}\left\{3.96 \times 10^{-8} f_{cl} \times \left[(t_{cl} + 273)^4 - (\overline{t_r} + 273)^4 + f_{cl} h_c (t_{cl} - t_a)\right]\right\}$$

1.8

$$f_{cl} = \begin{cases} 1.00 + 1.290 I_{cl} & \text{for } I_{cl} \leq 0.078 \text{ m}^2 \ ^\circ C / W \\ 1.05 + 0.645 I_{cl} & \text{for } I_{cl} > 0.078 \text{ m}^2 \ ^\circ C / W \end{cases}$$

1.9

$$h_c = \begin{cases} 2.38(t_{cl} - t_a)^{0.25} & \text{(represents free convection)} \\ 12.1\sqrt{v} & \text{(represents forced convection)} \end{cases}$$

1.10

cold	-3
cool	-2
slightly cool	-1
neutral	0
slightly warm	+1
warm	+2
hot	+3

Table 1.6 *ASHRAE* (1993) seven point thermal sensation scale

International standard *ISO standard 7730* (1993) recommends that *PMV* in spaces for human occupancy should be within the following limits:

$$-0.5 < PMV < 0.5$$

For reliable prediction, the standard also recommends the application of the index to be restricted to *PMV*s between -2 and +2, over the following ranges of the variables:

M $= 46$ to 232 W/m^2

I_{cl} $= 0$ to 0.31m^2 °C/W

t_a $= 10$ to 30 °C

$\overline{t_r}$ $= 10$ to 40 °C

v $= 0$ to 1 m/s

The metabolic rates corresponding to various activities are shown in Appendix A.2 together with estimates of the thermal resistance of various clothing ensembles (*ISO standard 7730*, 1984).

For a combination of personal and environmental parameters, the thermal sensation of persons under steady conditions may be predicted, with the neutral *PMV* corresponding to the optimum level of thermal comfort. *Fanger* found no consistent or significant bias due to factors such as sex, age, build, racial origin, geographic location (i.e. acclimatisation). The *PMV* was thus proposed to be universally applicable. It is both this universal applicability and the prediction of the level of thermal sensation that is the current subject of debate. The validity of the *PMV* i.e. its mathematical basis, with regard to the relative influences of individual parameters is not questioned. This mathematical validity, as well as the prediction of the *PMV*, has been confirmed by various climate chamber studies (*Fanger* 1970, *Awbi* 1991, *Oseland & Humphreys* 1994). As previously mentioned, the discrepancy exists between the prediction of the *PMV* (and other models derived from comfort chambers studies) and the results of field studies. The discrepancies indicated by earlier field studies were often attributed to poor estimates of the personal parameters or poor measurements of the environmental parameters, particularly the mean radiant temperature and air velocity. More recently, the application of more detailed data on the insulation values of various clothing ensembles and improved instrumentation in the measurement of environmental parameters, has confirmed that discrepancies do exist. The following are some of the main criticisms (*Humphreys* 1992, *Olesen* 1993, *Gan & Croome* 1994 and *Oseland & Humphreys* 1994) levelled at the *PMV* on the basis of field study results:

- underestimation of the 'feeling of warmth' (and therefore overestimation of the prediction of air temperatures required).
- poor performance for non sedentary activity.
- acclimatisation: various studies in hot climates obtained preferences for warmer environments.
- steady state assumptions (used in the heat exchange model) are said to be applicable only where the changes in the thermal environment are slow and steady.

- psychological variables, such as misinformation of temperature, knowledge of energy consumption, and even colour of decor have been found to influence the preferred comfort level.

These criticisms do not have any impact on the choice of the *PMV* for the purposes required in this research. The reasons for this are outlined below.

1. The mathematical basis of the *PMV*, with respect to the influence of the individual parameters, appears to be sound. Therefore, the comparison of different systems at similar levels of thermal sensation will be consistent.

2. Comfort levels are to be controlled according to individual requirements. Over or under estimation of the thermal sensation measured by the *PMV* for a given thermal environment is thus not significant. Once a person has determined their preferred comfort level, the environment can be controlled by maintaining this *preferred* comfort level according to the *PMV*. This will be explained in more detail in the recommendation of the control strategy in Chapter 5.

3. A comfort index, which takes different parameters into consideration, is required. The *PMV* caters for this as well as any other comfort index.

The *PMV* will be used in Chapters 4 & 5 in the evaluation of the thermal environment provided by the heating and ventilation systems. In addition, the local thermal discomforts due to draught and vertical air temperature differences will be taken into consideration. These are discussed below.

1.3.2 Local thermal discomforts

As stated earlier, thermal neutrality is a prerequisite for thermal comfort but it is not the *sole* requirement. Although a person may be thermally neutral in an environment, one part of the body may be too warm and another too cool, causing discomfort. These discomforts may be caused by a number of conditions: asymmetric radiant fields, local convective cooling or draught, vertical air temperature differences or contact with a warm or cool floor. The influences of asymmetric radiant fields and warm or cold floors are not addressed here. These are unlikely to have any influence in the current application. Asymmetric temperature differences are expected to fall well

within *ISO standard 7730* (1993) limits (5 °C in the vertical direction and 10 °C in the horizontal) using an air heating system. Floor temperatures have no influence on the thermal comfort when feet are clothed, which would be expected during cold periods. The following sections will provide information for the assessment of discomforts due to the remaining two factors: draught and vertical air temperature gradient, and the recommended limits of these. Greater detail on all of the local thermal discomforts can be obtained in *Awbi* (1991) and *ASHRAE Handbook* (1993).

Percentage dissatisfied due to draught

Draught is defined as the undesired local cooling of the body, caused by air movement. This is one of the most common complaints in heated or cooled buildings. Draught produces a cooling effect on the skin, caused by temperature differences between the air and the skin, air velocity and velocity fluctuations (turbulence level). The perception of draught may cause occupants to raise the room temperature to counteract this cooling effect (thereby resulting in increased energy consumption) or to turn off the ventilation system, with adverse effects on air quality. The parts of the body most sensitive to draught are the neck and ankles, of which the neck is particularly sensitive. Recognition of the influence of the air velocity fluctuation (measured by the turbulence intensity) is fairly recent and has been taken into account in a model developed by *Fanger et al* (1988, as quoted by *Awbi*, 1991). This model predicts the percentage dissatisfaction due to draught (PD_v, %) in the head region in terms of the air temperature, velocity and turbulence intensity. This is expressed as:

$$PD_v = (34 - t_a)(\dot{v} - 0.05)^{0.6233}(3.143 + 0.3696\dot{v}TI) \qquad 1.12$$

where

t_a = local air temperature (°C)
$\dot{v}$ = relative velocity (m/s)
TI = turbulence intensity (%)

valid for: 20° C < t_a < 26° C, 0.05 m/s < $\dot{v}$ < 0.4 m/s and 0 < TI < 70 %.

For velocities of less than 0.05 m/s no discomfort is predicted irrespective of temperature or turbulence level. *ISO standard 7730* (1993) and *ASHRAE Standard 55* (1992) specify maximum dissatisfaction levels of 15 % due to draught. These were

both revised from the previous standards which specified maximum velocities in winter of 0.15 m/s.

Percentage dissatisfied due to vertical air temperature difference

In heated enclosures in particular, air temperature gradients exist between the ceiling and the floor. If this gradient is sufficiently large, local discomfort (warm) may occur at the head or discomfort (cold) at the feet. Few studies have been performed on the effect of vertical air temperature differences. The most comprehensive data available is from studies by *Olesen et al* (1975, 1979 as quoted by *ASHRAE handbook*, 1993). By exposing subjects in thermal neutrality to various temperature differences between the ankle and neck (0.1 - 1.1 m, for a seated person), they obtained a relationship between the percentage dissatisfied and vertical temperature difference, as shown in Figure 1.2.
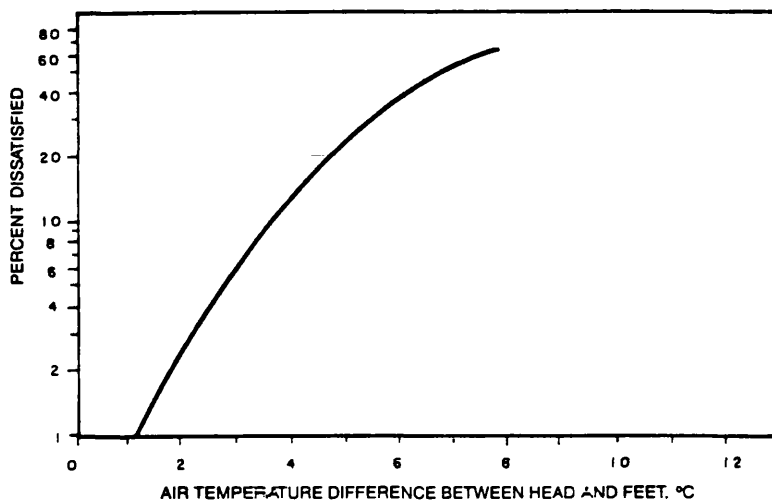
Figure 1.2 Percentage dissatisfied with vertical air temperature difference between heights of 0.1 m and 1.1m

ISO standard 7730 (1993) recommends a maximum vertical air temperature difference of 3 °C between the head and ankle. For a seated person (ankle 0.1 m, head 1.1 m) this corresponds to a percentage dissatisfaction of 6.5 %. *ASHRAE Standard 55* (1992) recommends the same temperature differences between heights of 0.1 m and 1.7 m.

1.4   Indoor airflow

Indoor airflow patterns and temperature distributions influence the IAQ and thermal comfort within a room and may also have an impact on the energy requirements of the combined heating and ventilation system.

Air movement as a result of the supply air is not caused by virtue of the *movement* of the supply air volume alone, but is also due to the entrainment of the room air by the supply air jet. The momentum and direction of the supply air volume have considerable influence on air motion within a room. Return airflow approaches the extract device(s) from various directions, resulting in considerably lower velocities in its vicinity than for the supply device. In addition, this extract air volume is only a fraction of the total volume of air movement within the room (supply and entrained air) and therefore has relatively little impact on the airflow in the room. The type and location of the extract device is not of great significance as long as the supply air is not short circuited. Where possible, the extract should be located in stagnant zones or regions of high contaminant sources.

ASHRAE handbook (1993) and *CIBSE guide* (1986) provide guidelines for the selection and application of air terminal device (ATD) types and locations. These suggest the suitability of both high level and low level supply grills and diffusers in air heating systems. ASHRAE, on the basis of work by *Straub et al* (1956, 1957, as quoted by ASHRAE), caution of the risk of air temperature stratification with high level supplies. Supply temperature differentials are recommended not to exceed 15 °C. Low level supplies are said to result in smaller stagnant regions and therefore less thermal stratification. Both vertical and horizontal discharge of the supply air is said to be possible, with horizontal discharge recommended not to exceed supply velocities of 1.5 m/s for diffusion directly into the occupied zone (to avoid excessive air velocities in the occupied zone).

Investigations or predictions into the airflow and temperature distribution in a room are performed by two methods: experimental investigations and numerical modelling.

Experimental investigations

Experimental investigations involve either full scale tests or reduced scale models. Full scale tests, in principle, provide the most realistic information from direct measurements of the conditions within the room. These are usually performed in climate chambers with instrumentation to obtain the distribution within the room of air velocities, temperatures, velocity fluctuations and pollutants concentrations. Difficulties (*Chen et al*, 1992) are encountered in accurate measurement of the flow direction at low velocities and of the velocity fluctuations. Full scale studies are expensive and, in some cases, impractical. For specific design tasks, these are mostly uneconomical, if at all possible. The alternative to these is reduced scale models. The results gained from these, however, need to be extrapolated to full scale values. This is a complex process which is reported (*Zhang et al*, 1990) to produce distortions where internal heat production is present, due to contradictory scaling factors of the Reynolds (ratio of inertial to viscous force) and the Archimedes number (ratio of thermal buoyancy to inertial force), both important non-dimensional terms in determining room air distribution. A review of the non-dimensional terms relevant to room airflow is provided in *Moser*, 1988.

Numerical flow modelling

Numerical modelling of indoor airflow is performed by solving the equations that govern fluid flow. This is based on a number of fundamental principles: the conservation of mass, conservation of momentum and the conservation of energy and concentration. These fundamental physical principles can be expressed in terms of mathematical equations which in their most general form, are either integral equations or partial differential equations. In computational fluid dynamics (CFD) these integrals and partial derivatives are replaced by algebraic equations, which are solved to obtain numerical values of the flow variables at discrete points in time and space. The larger the number of grid points within the space, the greater the accuracy of the solution. Solution of these equations requires the specification of initial and boundary conditions of the flow variables.

CFD has the following advantages and disadvantages in comparison to experimental techniques:

Advantages:

- results are produced quicker and cheaper than predictions for specially conducted experimental studies.

- do not suffer from scaling difficulties experienced with reduced scale models. Results are obtained for full scale predictions.

- detailed information is available over the entire domain (information is available at all points of the computational grid in the flow field). It is also possible to obtain data in locations which would not be easily accessible.

- simple to investigate the effect of a wide range of conditions which may influence the flow. Therefore, parametric and sensitivity studies are relatively straightforward and trends are more easily established than by experiment.

Disadvantages:

- the accuracy of the solution depends on the grid resolution and the quality of information specified for the boundary conditions and fluid properties.
- false solutions or unconverged solutions may be obtained.
- difficulties in modelling of flow phenomena such turbulence.
- requires experienced users to obtain reliable predictions.

Recent years have seen increasing application of computational fluid dynamics as a tool for the prediction of airflow in buildings. This increase has come about through a number of developments:

a) The rapid development and cost reduction in powerful computer systems.

b) The development and validation of improved flow models for indoor airflow.

c) The availability of commercial CFD programs within which specific flow models may be selected.

With these developments, CFD can offer substantial benefits in the design and evaluation of the IAQ and thermal comfort provided by air distribution systems and their energy consumption.

1.5   Review of findings of previous work

This is divided into two sections: *air distributions systems*, followed by *thermal comfort control*.

1.5.1   Air distribution systems

Relatively little detailed information appears to be available on the effect of supply and extract ATD configuration (location and type) in air heating systems, on the thermal comfort and IAQ within a room and their energy implications. Despite the wealth of data available for cooling and ventilation, information concerning air heating is still relatively scarce. The influence of buoyancy on airflow patterns, restricts the use of cooling and ventilation data in a heating application.

From the available studies, a few of these which contributed to the direction and procedures of this investigation are outlined and commented on below. These consist of results from field studies, full scale experimental studies in comfort chambers and from numerical models.

Werner (1990) measured air velocities and temperatures in rooms of well insulated and airtight houses in Stockholm using an integrated heating and ventilation system. Outdoor air temperatures were in the range of -10 to -20 ° C. Two methods of air distribution were tested; a) exterior wall supply beneath a window via a vertically discharging floor supply, and b) high level supply on the internal wall. At flow rates corresponding to normal ventilation rates of approximately 0.8 ACH, it was possible to meet the heating requirements of the room without exceeding supply temperatures of 30 °C. Vertical temperature gradients between the floor and ceiling did not exceed 3 °C. The high level system did not cause large down draughts at the cold window surface. This was found to provide better comfort requirements than the low level supply, due to lower air velocities in the occupied zone.

Carlson (1991) investigated the performance of an air heating system utilising 100 % outside air (i.e. no recirculation) with 70 % heat recovery from the exhaust air. In a house of thermal insulation value of 0.3 W/m^{2}K, it was possible to provide the heating requirements at the outdoor design condition of -16 °C, at a maximum supply temperature of 50 °C and at 1 ACH. The temperature in each apartment was maintained at 22 °C. A poll of voter satisfaction found 95 % satisfaction with the environment i.e. of both the IAQ and the thermal environment.

Awbi (1991) studied the effect of the position and type of supply device on the comfort level of a heated room, using a warm air heating system. Using grills and diffusers, investigations were performed in an experimental chamber of dimensions 5.5 x 3.5 x 2.5 m^3. Both low and high level supplies were investigated, with measurements of the air velocity and air temperature taken at 385 points in the room, between the heights of 0.15 m and 1.8 m. High level supplies obtained considerably higher vertical air temperature gradients than for low level supplies. Low level supplies produced higher velocities at the same ACH. In both of these cases, the results were found to be almost independent of the supply device used. To provide acceptable indoor conditions over a range of 4 - 23 ACH, *Awbi* found it necessary to use a low level supply for ACH below 10 (to prevent high vertical air temperature differences), and a high level supply for ACH above 10 (to prevent draught). The low level supply was found to provide a comfortable environment up to 14 ACH. This appears to be based on the mean room air velocity not exceeding 0.15 m/s. To meet the space heat requirements at a design ambient of -1 °C, high level supplies exceeded vertical temperature differences of 3 °C (between the height of 0.1 m and 1.8 m) at supply temperature exceeding 28 °C. It is not clear what the thermal insulation level of the chamber was. It is assumed from the date of the investigation, 1983, that these would not have been below a U value of 0.6 W/m^{2}K.

Gan (1995) investigated the influence of the positioning of supply and extract ATD devices in a warm air heating system by CFD modelling. The investigation was performed on a room of dimension 4.9 x 3.7 x 2.75 m^3 with an internal heat and pollution source. At 4 ACH and a supply temperature of 25 °C, a number of different

supply and extract locations were investigated as shown in Table 1.7. Comfort was assessed using *Fanger's PMV*. Similar temperature and comfort levels were obtained for both high level supply locations (systems 1 & 3). However, system 1 (with the supply device on the side wall and extract at low level on the opposite wall) achieved better IAQ and energy utilisation. At low level supply, the best IAQ was obtained for the vertical discharge, with a low level extract on the opposite wall (system 2). The supply along the floor length (system 4) achieved similar temperature distribution and comfort level in the occupied zone, however poorer IAQ. The low level side wall supply, with a high level extract on the opposite wall (system 5), obtained the lowest temperature and comfort level as well as the poorest IAQ. Comparison of the two optimum cases of the high level and low level supplies (systems 1 & 2) showed similar temperatures and IAQ with better energy utilisation for the low level supply (approximately 10 %). The vertical temperature gradient did not exceed 3 °C between the heights of 0.1 m and 1.1m for any of the systems.

System	No of supply devices	Supply area (m^2)	Supply location	Extract location all North wall
1	1	0.05	South wall - high level	Low level
2	1	0.05	Floor - near south wall	Low level
3	1	0.05	Ceiling - centre	Low level
4	2	0.25 (total)	Floor - along room length	High level
5	1	0.1	South wall - low level	High level

Table 1.7 ATD configurations used by *Gan* (1995)

Chen et al (1992) used CFD predictions in the comparison of three heating systems: an air heating system; a radiant panel and a radiator. Discomfort due to draught was assessed using *Fanger's* draught risk model. The air heating system used a low level supply with high level extract on the same wall. The results obtained for the air heating system at 5 ACH and a room temperature of 21 °C produced high levels of draught in some locations. In the floor region, discomfort due to draught approached 20 % dissatisfaction levels. High levels of draught were also obtained in those parts of the room surrounding the buoyant plume of supply air, thereby affecting a considerable portion of the occupied zone.

Comments

The results by *Werner* show that in well insulated homes, the space heating requirement may be satisfied at relatively low airflow rates (below 1 ACH) and supply air temperatures (below 30 °C). The flow rates were of similar magnitudes as those required for ventilation purposes. These results would be applicable to continuous systems, however do not provide any information for requirement of an intermittently operating system.

The work by *Awbi* suggests the *location* of the supply ATD device is not of prime importance in air heating applications, and the *type* of ATD has similarly little impact. The implication of this is that a simple (and low cost) supply slot device may be used for the heating and ventilation system.

The ASHRAE guidelines which restrict excessive supply temperature differentials of 15 °C do not, however, provide any detail on the flow rate or the design condition for which this is applicable. It is assumed that the ASHRAE limit is based on commonly used unit type heating systems which are usually able to circulate a relatively fixed quantity. The air quantity is therefore fixed within a narrow range, with control of the supply temperature used for modulating heat requirements. The flow rate is assumed to be of similar magnitude as that commonly used for air conditioning purposes: approximately 4 ACH. This is normally the higher of the requisite flow rates for a system which is to provide both heating and cooling i.e. for a constant air volume system. The maximum supply temperature of 28 °C at 4 ACH which was determined by *Awbi* to prevent discomfort due to excessive vertical air temperature differences (using the ASHRAE limit of 3 °C between the heights of 0.1 m and 1.8 m) would appear to confirm the assumption of the flow rate of 4 ACH for which the ASHRAE limit is applicable. This provides some guidance in estimation of operation limits of the heating and ventilation equipment (also assuming the limits are applicable for a room of insulation value of approximately 0.6 W/m^{2}K at ambient temperatures of -1 °C). It would also appear that the ASHRAE guideline is based on measurements/estimates of temperature difference between the specified heights, as opposed to occupant responses.

In dwellings, it would be reasonable to assume that the occupants would mostly be seated, therefore the vertical temperature difference between the ankle and head is better represented by the ISO limit of 3 °C, between the heights of 0.1 m and 1.1 m than between 0.1 m and 1.8 m as specified by ASHRAE. This would allow for the use of greater supply air temperatures and would also increase the range of ACH (to lower values than those determined by *Awbi*) of the high level supply system which would achieve comfortable indoor environments. The acceptability of higher supply temperatures is also supported by the study by *Carlson* which shows a high degree of user acceptability with systems operating at supply temperatures of up to 50 °C. Supply air temperature differentials of 16 - 27 °C are commonly used (*McQuiston* and *Spitler*, 1992) in air heating equipment in the USA. Assuming a room temperature of about 22 °C, this corresponds to supply temperatures of between 38 and 50 °C.

The results of the experiments by *Chen et al* with regard to the acceptability of the environment with respect to draught, provide a stark contrast to the observations by *Awbi* and *Gan*. At similar ACH, the results by *Chen*, using a draught model, indicate high levels of draught in large parts of the occupied zone. The results by *Awbi* and *Gan*, however, would suggest the acceptability of much greater ACH. These limits of flow rate to prevent discomfort due to draught appear to be based on the previous *ASHRAE standard 55* (1981) and *ISO Standard 7730* (1984) guideline of restricting maximum velocities in the occupied zone to below 1.5 m/s. This is clearly inappropriate and the range of acceptable ACH, stated by *Awbi*, for a low level supply is therefore questionable. *Chen's* results, with respect to draught, would also question the similarity in comfort of both the high and low level supply systems in *Gan's* investigation.

1.5.2 Thermal comfort control

The purpose of comfort control systems is to create and maintain thermal conditions within a zone which will provide comfort to the occupants. Conventional control systems measure only air temperature and ignore the remaining environmental parameters (air velocity, mean radiant temperature and water vapour pressure), which also have an influence on thermal comfort. In conventional systems, the air

temperature is controlled with the remaining variables finding their own level, corresponding to the given conditions and ambient air temperature. Conventional systems also do not consider changes in the personal parameters (clothing insulation level and activity rate). Variations in any of these personal parameters and the three remaining environmental parameters (air velocity, mean radiant temperature and water vapour pressure) may cause fluctuations in comfort sensation.

The comfort level in a room may be measured using a comfort index such as the *PMV*. Measurement of the *PMV* may be accomplished by individual measurement of the environmental parameters, from which (with knowledge of the personal parameters) the *PMV* is evaluated. Alternatively, this may be measured directly with the use of so-called *thermal comfort meters* which combine the effect of the environmental parameters and allow input of the personal parameters. These thermal comfort meters are commercially available and are used in the assessment of thermal environments. The comfort meters do not isolate the effect of individual parameters and have found limited application in thermal comfort research, where the effect of the individual environmental parameters is of interest. Similarly, for control purposes, it would be beneficial to determine the changes to the comfort level which may be brought about by variation of any one parameter. Thermal comfort may therefore be attained/restored through the most energy efficient control action. Recently, *climate analysers* have become commercially available, which consist of four sensors for measuring the four environmental parameters. Although these have found application in the assessment of thermal environments, very little application of this, or similar *PMV* based control (i.e. with sensors in different locations), has been reported in the *control* of the thermal environment.

A review is provided below of two significant exercises, on the assessment and benefits of comfort control. The first of these reviewed, is a theoretical study and the second by experiment/measurements in a demonstration house.

MacArthur (1986) assessed the use of two comfort control strategies in terms of the comfort level and energy consumption and compared these with a conventional air temperature control system. The purpose of the comfort control strategies were to maintain uniform comfort levels during plant operation throughout the cooling season.

Investigations were performed using a computational model with the simulation consisting of four components, the cooling plant, the house, the controller and external and internal disturbances (weather and internal load). The two comfort control strategies used were: 1) based on the *PMV* index and 2) using a temperature reset algorithm based on the internal humidity level. The latter may be seen as emulating a *PMV* controller with two indices being taken into consideration and all the others assumed constant. The algorithm is based on the fact that the *PMV* decreases with decreasing relative humidity and vice versa. Relative air velocity in the room was assumed in evaluation of the *PMV* to be 0.1 m/s. The conventional system was specified to operate at a fixed air temperature setpoint of 25.5 °C. It was assumed in the evaluation of the control strategies that an acceptable comfort profile was obtained for the conventional system when operating at design conditions. This comfort profile was used as the basis for comparison of the control strategies and the corresponding energy requirements. The results of the comparison suggested substantial seasonal energy savings may be possible with the application of comfort control strategies in comparison to the conventional system. This was mainly due to variations in mean radiant temperature and relative humidity during the cooling season with the variations in mean radiant temperature being the dominant factor. At design capacities, the estimated annual saving in energy consumption, in comparison to the conventional system, was 7 % with humidity/temperature reset control and 10 % with *PMV* control.

Scheatzle (1991) applied what appears to be the first application of a *PMV* controller, in the control of the thermal environment of a residence. He demonstrated a year round comfort control in one (occupied) room of the residence during heating, cooling and intermediate seasons. The performance of a *PMV* based system, using *expert system*[2] control methods (to optimise equipment operation), was compared with conventional air temperature control using fixed air temperature setpoints. The evaluation of the comfort control, relative to the conventional control was based on the following criteria: 1) capability to achieve year round control 2) ability to maintain conditions within the established comfort range and 3) energy consumed to achieve comfort conditions. The room was equipped with sensors to measure the four environmental

---

[2] An *expert System* is a computer application program that makes decisions or solves problems in a particular field using knowledge and analytical rules defined by experts in the field.

parameters. Space conditions were provided and controlled using the following equipment: an air conditioner (cooler), a furnace, evaporative cooler, ventilation fan and a ceiling fan. Velocities in the room were pre-recorded/measured at the centre of the room for various fan (ventilation and ceiling) settings. The *PMV* based control algorithm was developed using expert system techniques to select and control the equipment in order to provide the required comfort level in the most economical manner. The control logic was based on two components: 1) the *PMV* model and 2) knowledge of occupancy scheduling, equipment capabilities and operation and weather predictions. The second component allowed energy saving actions to be taken in addition to the requirements for comfort. The combination of the *PMV* and expert system control logic was referred to as comfort index control (CI control). The system incorporated seasonal and night time activity and clothing specifications. On the basis of user responses, upper and lower *PMV* limits of a comfort envelope was identified. These were found to be (for the specific group of occupants) -1 < *PMV* < 0.5. The system modulated, with a throttling range of 0.15 (*PMV*) to maintain conditions within this envelope in the most energy efficient manner. For instance, in an air conditioning only scenario, as the *PMV* rose above 0.5, the air conditioner was turned on. As a result of its operation and after some time lag the *PMV* begun to drop. When the *PMV* dropped to a value of 0.35, the air conditioner was switched off. Sensor readings were made every 3 seconds, and preventative action was taken before discomfort levels were reached. Energy comparisons were obtained for typical seasonal days. The study listed the following advantages of CI control over conventional control:

- Provides year round control with a single controller. Conventional control would require multiple thermostats whose operation would not be automatically coordinated.

- Provides a greater percentage of time that conditions are within the comfort range (also according to the occupant response) and at a lower operating cost.

The main disadvantage *Scheatzle* identifies of CI control is the high initial cost in comparison to conventional systems.

Comments

With relevance to the current research, the most important results obtained from the reviewed studies were:

1. The feasibility and user acceptance of a *PMV* based comfort control system.
2. The apparent potential for energy saving using a comfort control system/strategy.

The first point, as a result of *Scheatzles* work, suggested user acceptance and indeed preference of the comfort controlled system. This result provides a mandate for further development and application of such comfort controlled systems. Scheatzles work also provides a throttling range in the control of the *PMV* of 0.15 (*PMV*). Assuming modulation of the *PMV* by air temperature alone, this *PMV* range of 0.15 corresponds to an air temperature range of 1.5 °C (using Equations 1.7 - 1.10 and assuming sedentary activity, typical winter indoor clothing, mean radiant temperature of approximately 20 °C and a partial water vapour pressure of 1400 Pa). This agrees with typical control ranges of air temperature thermostats of between 1 and 2 °C.

The comfort envelope obtained in *Scheatzles* study, of -1 < *PMV* < 0.5 may be somewhat misleading. From the control strategy used, it can be seen that the high and low end of the comfort envelope values correspond to summer and winter conditions respectively. In theory, this *PMV* should be the same in both seasons. This deviation could be due to incorrect estimation of the clothing insulation values during the different seasons. This could also be due to the pre recorded velocity measurements. It is not known whether these were recorded during the summer or winter season, nor what the difference between these would be.

On the second point, with regard to the energy consumption, *Scheatzles* study is subject to a major restriction, which explains why more detail on the estimated energy saving were not provided in the review above. In the investigation, the conventional system was assumed to operate at a fixed air temperature setpoint through the 24 hour period, without night time air temperature setback. In the *PMV* based system, night time setback was taken into consideration. In addition the *PMV* based system (CI index) did not isolate the effect of *PMV* as the control variable, but integrated this with

the use of more sophisticated control decisions which were not applied to the conventional system.

The study by *MacArthur* however, provided encouraging results for the application of comfort controlled systems with respect to the energy consumption. Despite the fact that the assessment was performed for cooling season, the results, in particular with respect to the effect of the mean radiant temperature, indicate the potential for energy saving in a heating season with the use of comfort control. This would have particular relevance with the use of intermittent heating systems, where variations in mean radiant temperature will occur due to changes in the wall surface temperatures.

1.6   Objectives of the present research

The main objective of the research described in this thesis was the identification of a suitable combined air heating and ventilation system for the provision and control of thermal comfort in rooms of low energy homes. This heating and ventilation system was assumed to work on demand controlled principles and operate intermittently. This system will subsequently be referred to as *the* H & V system.

The review in the early sections of this Chapter, projected the trend of an increasing use of combined air heating and ventilation systems with the increasing air tightness and thermal insulation of homes. These systems need to provide healthy and comfortable indoor environments, while minimising energy consumption. Rising living standards and expectations of the indoor environment, both in terms of the air quality and thermal comfort provided, impose even greater demands on such systems. Although this has, in part, resulted in new and additional energy requirements to meet these expectations, this is seen as an inevitable and unavoidable element of human evolution. The challenge facing today's technological society is to utilise this technology to minimise the energy required to meet the users expectations and requirements of the indoor environment.

The preceding sections highlighted a lack of existing data for the design and operation of air heating systems. Relatively little information is available on the relative merits of different air distribution systems with respect to thermal comfort, IAQ and energy

requirements. Although some data has been produced on the influences of the air distribution systems on thermal comfort, IAQ and energy consumption, this is restricted to a limited range of steady state conditions, with no detailed parametric or time dependent (for intermittent systems) observations. This existing data is unsatisfactory for the design of heating and ventilation systems, which in order to provide good thermal comfort and IAQ in an energy efficient manner, may operate over a wide range of flow rates and supply air temperatures. This clearly highlights the need for further research into the flow behaviour of forced air heating systems. The research in this thesis contributes to the knowledge in this field, in the process of determining a suitable combined heating and ventilation system for the rooms in low energy homes.

The literature review also indicated the potential for application of thermal comfort control systems, in particular for use with intermittently operating systems. Future low energy homes are expected to experience increasing use of innovative technology, leading to home automation and intelligent systems (*Seyer* and *Trepte*, 1990). The infrastructure of these systems, with the presence of a network or bus system and the developments in sensors and microcomputers, improve the economic feasibility of more sophisticated control, such as thermal comfort control. Several research projects are currently targeted to the development of the hardware for the implementation of thermal comfort control, such as the sensors (*Kon*, 1994) and controllers (*Federspiel* and *Asada*, 1994). Very little work appears to have been done on the required number and locations of these sensors, required to effectively control an environment for thermal comfort. The necessary sensor/measurement locations are addressed as a part of this research.

The investigation was approached in two phases:

1. The identification of a suitable room air distribution system for the H & V system. The evaluation criteria were the thermal comfort measured by the *PMV*, IAQ and energy consumption of the systems over the range of operation expected.

2. For the *proposed* configuration, detailed studies were performed to determine the behaviour of this system at various supply conditions (airflow rate and temperature) with respect to thermal comfort and IAQ. The effect of various

parameters, such as obstacles within the room, heat sources etc. and time dependent variations on the thermal comfort within the room was investigated.

The information gained from this investigation was then used in the recommendation of a control strategy to achieve thermal comfort control, while providing good IAQ in an energy efficient manner.

1.7   Research methodology and outline of the thesis

Comparisons of heating and ventilation systems, or more precisely air distribution systems was performed with the aid of theoretical predictions, using CFD, of indoor airflow patterns, temperature and pollutant distributions. The task in hand, with numerous parametric studies to be performed was perfectly suited to a CFD investigation. Experimental investigations were anyhow eliminated due to economic considerations.

An introduction to CFD modelling is provided in **Chapter 2**. This Chapter also identifies a number of suitable indoor airflow models and validates one of these for use in these investigations. A description of the flow model/configuration used to define or represent the room and air distribution system is provided.

The range of operation of the H & V system, which refers to both flow rate and supply air temperature, is dependent on both the thermal and IAQ requirements. Thermal or space heat requirements were determined by transient heat analysis of the heat transmission through the enclosure surfaces. Flow rates for acceptable IAQ were determined using the criteria identified in Section 1.2. The supply parameters determined provided the boundary conditions for the CFD simulations. Determination of the boundary conditions for the simulations is described in **Chapter 3**.

In **Chapter 4**, various air distribution systems are investigated with the aid of the predictions from the CFD model. A suitable system is proposed for the H & V system.

Chapter 5 provides a description of detailed investigations into the behaviour of the proposed H & V system and assesses the feasibility of thermal comfort control. This concludes in the recommendation of a control strategy.

The final Chapter, **Chapter 6**, gives a brief summary of the findings of this investigation.

2. INDOOR AIRFLOW MODELLING USING COMPUTATIONAL FLUID DYNAMICS (CFD)

A commercial CFD program was used in this study to predict the airflow patterns, air temperature and pollutant distributions in a heated and ventilated room. Commercial CFD packages are general purpose codes which provide facilities for the definition of a flow problem, specification of mathematical airflow models and solution techniques of the fluid flow equations. In other words they eliminate the time-consuming computer programming aspect, by providing well developed tools to speed up these processes. The use of a commercial CFD code, by no means implies accurate or reliable prediction of the flow problem under investigation. The accuracy of the prediction is dependent on the validity of the mathematical models used to simulate the occurring flow phenomena, the accuracy of the flow definition, satisfactory grid representation and the ability to obtain a converged[1] solution.

This Chapter is divided into two main sections, the first (Section 2.1) of which provides the background to common CFD modelling techniques. This section presents standard forms of the governing equations of fluid flow, heat and pollutant transfer. Common procedures applied to obtain numerical solutions of these equations are outlined as well as numerical considerations required to achieve convergence of the solution.

The second section (Section 2.2) provides detail of the CFD program used and the mathematical models applied in this research. This begins with a brief description of the format of the commercial CFD code used for the simulation task, followed by the identification of a suitable indoor airflow model. The application of CFD to indoor airflow is still relatively new, with extensive research still taking place into the development and validation of suitable airflow models. A number of these models are identified and the procedure described which was used in the validation and choice of one of these for use in this study. The flow configuration used to model the heated and ventilated room is then specified. The section is completed with a listing of some of the problems encountered in obtaining the CFD solutions.

2.1 Fundamentals of CFD

2.1.1 Governing equations of fluid flow

The *transport* equations that describe the flow of a fluid, heat and concentration within an enclosure are based on the conservation of mass, momentum, thermal energy and the concentrations within an enclosure. The flow equations are presented for an incompressible fluid flowing through an infinitesimal control volume ($dx \cdot dy \cdot dz$). These equations are in the form of partial differential equations (PDEs), with each PDE describing the conservation of one dependent variable within the flow field. The equations are stated in cartesian form (x, y, z) assuming a unit control volume and instantaneous velocities of u, v and w in the x, y, and z directions respectively. The fluid density is represented by ρ. The governing equations are not derived within this text. Details of the derivation procedure can be found in various texts (*Anderson* 1995, *Versteeg & Malalasekera* 1995).

Conservation of mass

A mass balance over the control volume produces the continuity equation, which is expressed as:

$$\frac{\partial \rho}{\partial t} + \frac{\partial}{\partial x}(\rho u) + \frac{\partial}{\partial y}(\rho v) + \frac{\partial}{\partial z}(\rho w) = 0 \qquad \qquad 2.1$$

Where turbulent flow is considered, which is the case in indoor airflow, the velocities may be expressed as the sum of a time mean component and a fluctuating component:

$$u = \bar{u} + u', \quad v = \bar{v} + v', \quad w = \bar{w} + w'$$

where, for instance $\bar{u}$ is the mean velocity and u' the random fluctuating component over the mean value. The integrals of the fluctuating components over time are equal

---

[1] A CFD solution is said to converge if the values of the variables at the points in the domain tend to move towards some fixed value as the solution progresses.

to zero. The conservation of mass equation can therefore be represented as in Equation 2.1 with the instantaneous velocities replaced by the mean velocities:

$$\frac{\partial \rho}{\partial t} + \frac{\partial}{\partial x}(\rho \overline{u}) + \frac{\partial}{\partial y}(\rho \overline{v}) + \frac{\partial}{\partial z}(\rho \overline{w}) = 0 \qquad\qquad 2.2$$

Conservation of momentum

Application of the laws of conservation of momentum (or Newton's second law) over the control volume, produces the momentum or Navier-Stokes equations. These take into consideration the normal and shear stresses on the fluid patch and can be expressed in the x, y and z components:

x-direction:

$$\rho \frac{\partial u}{\partial t} + \rho u \frac{\partial u}{\partial x} + \rho v \frac{\partial u}{\partial y} + \rho w \frac{\partial u}{\partial z} = -\frac{\partial P}{\partial x} + \frac{\partial}{\partial x}\left(\mu \frac{\partial u}{\partial x}\right) + \frac{\partial}{\partial y}\left(\mu \frac{\partial u}{\partial y}\right) + \frac{\partial}{\partial z}\left(\mu \frac{\partial u}{\partial z}\right)$$

$$2.3$$

y-direction:

$$\rho \frac{\partial v}{\partial t} + \rho u \frac{\partial v}{\partial x} + \rho v \frac{\partial v}{\partial y} + \rho w \frac{\partial v}{\partial z} = -\frac{\partial P}{\partial y} + \frac{\partial}{\partial x}\left(\mu \frac{\partial v}{\partial x}\right) + \frac{\partial}{\partial y}\left(\mu \frac{\partial v}{\partial y}\right) + \frac{\partial}{\partial z}\left(\mu \frac{\partial v}{\partial z}\right)$$

$$2.4$$

z-direction:

$$\rho \frac{\partial w}{\partial t} + \rho u \frac{\partial w}{\partial x} + \rho v \frac{\partial w}{\partial y} + \rho w \frac{\partial w}{\partial z} = -\frac{\partial P}{\partial w} + \frac{\partial}{\partial x}\left(\mu \frac{\partial w}{\partial x}\right) + \frac{\partial}{\partial y}\left(\mu \frac{\partial w}{\partial y}\right) + \frac{\partial}{\partial z}\left(\mu \frac{\partial w}{\partial z}\right)$$

$$2.5$$

where P is the static pressure and μ the laminar viscosity of the fluid. To include the influence of gravity in the momentum equation, an additional term (ρg) can be added to the right hand side of the momentum equation, in the relevant component. For turbulent flow, substitution of the velocity terms does not, however, eliminate the fluctuating terms as for the continuity equation. This is because the products of the fluctuating terms do not produce zero integrals over time. Replacing the instantaneous velocities with the time-mean and fluctuating components produces the following

additional terms on the right hand sides of Equations 2.3 - 2.5 in the x, y and z directions respectively:

x-direction:

$$+\frac{\partial}{\partial x}\left(-\rho\overline{u'u'}\right)+\frac{\partial}{\partial y}\left(-\rho\overline{u'v'}\right)+\frac{\partial}{\partial z}\left(-\rho\overline{u'w'}\right)$$

y-direction:

$$+\frac{\partial}{\partial x}\left(-\rho\overline{u'v'}\right)+\frac{\partial}{\partial y}\left(-\rho\overline{v'v'}\right)+\frac{\partial}{\partial z}\left(-\rho\overline{v'w'}\right)$$

z-direction:

$$+\frac{\partial}{\partial x}\left(-\rho\overline{u'w'}\right)+\frac{\partial}{\partial y}\left(-\rho\overline{v'w'}\right)+\frac{\partial}{\partial z}\left(-\rho\overline{w'w'}\right)$$

These additional terms are known as the *Reynolds* (or turbulent) *stresses* and are taken into account by so-called turbulence models. Turbulence models vary in complexity and in accuracy. Most of these though, for convenience of numerical modelling, treat the additional terms in the momentum equations as additional viscous stresses produced by the turbulent flow, hence the term Reynolds stresses. These Reynolds stresses may thus be expressed in the x-direction as:

$$\frac{\partial}{\partial x}\left(\mu_t\frac{\partial u}{\partial x}\right)+\frac{\partial}{\partial y}\left(\mu_t\frac{\partial u}{\partial y}\right)+\frac{\partial}{\partial z}\left(\mu_t\frac{\partial u}{\partial z}\right)$$

where μ_t is the additional viscosity due to turbulence. This is referred to as the turbulent (or eddy) viscosity. This turbulent viscosity can be combined with the dynamic viscosity in Equations 2.3 - 2.5 by substitution of $\mu+\mu_t$ for μ, thereby retaining the same equation format. The turbulence models applicable to indoor airflow will be outlined in Section 2.2.2.

Conservation of energy

For low velocity flow with negligible viscous dissipation, the energy equations can be written as:

$$\rho\frac{\partial H}{\partial t} + \rho u\frac{\partial H}{\partial x} + \rho v\frac{\partial H}{\partial y} + \rho w\frac{\partial H}{\partial z} = \frac{\partial}{\partial x}\left(\frac{k}{C_p}\frac{\partial H}{\partial x}\right) + \frac{\partial}{\partial y}\left(\frac{k}{C_p}\frac{\partial H}{\partial y}\right) + \frac{\partial}{\partial z}\left(\frac{k}{C_p}\frac{\partial H}{\partial z}\right)$$

2.6

where k is the thermal conductivity of the fluid and C_p the specific heat capacity at constant pressure and H the instantaneous enthalpy of the air. A source term may be added to the right hand side of the energy equation to allow for internal heat sources or sinks. The energy equation can similarly be expressed in terms of temperature.

Conservation of chemical species (pollutant concentration)

The pollutant concentration equation is expressed as:

$$\rho\frac{\partial C}{\partial t} + \rho u\frac{\partial C}{\partial x} + \rho v\frac{\partial C}{\partial y} + \rho Cw\frac{\partial C}{\partial z} = \frac{\partial}{\partial x}\left(\frac{\mu}{\sigma}\frac{\partial C}{\partial x}\right) + \frac{\partial}{\partial y}\left(\frac{\mu}{\sigma}\frac{\partial C}{\partial y}\right) + \frac{\partial}{\partial z}\left(\frac{\mu}{\sigma}\frac{\partial C}{\partial z}\right)$$

2.7

where μ is the dynamic viscosity and σ the Schmidt number of the fluid, which is obtained in agreement with Fick's law of diffusion (Patankar, 1980). In a similar manner as in the enthalpy equation, a source term can be included in Equation 2.7 to account for internal pollutant sources.

The general transport equation

The transport equations of momentum (Equations 2.3 - 2.5), energy (Equation 2.6) and concentration (Equation 2.7) can all be seen to have the general form:

$$\frac{\partial}{\partial t}(\rho\phi) + \frac{\partial}{\partial x}(\rho u\phi) + \frac{\partial}{\partial y}(\rho v\phi) + \frac{\partial}{\partial z}(\rho w\phi) = \frac{\partial}{\partial x}\left(\Gamma_\phi\frac{\partial\phi}{\partial x}\right) + \frac{\partial}{\partial y}\left(\Gamma_\phi\frac{\partial\phi}{\partial y}\right) + \frac{\partial}{\partial z}\left(\Gamma_\phi\frac{\partial\phi}{\partial z}\right) + S_\phi$$

2.8

where ϕ is the dependent variable (which may stand for a velocity component, enthalpy, pollutant concentration etc.) and S_ϕ is the source term which may have different expressions for the different transport equations. The transport equation can be described as consisting of four terms, a transient term (the 1st term on the left hand

side of Equation 2.8), convection terms (the 2nd, 3rd and 4th term on the LHS), diffusion terms (the 1st, 2nd, and 3rd term on the RHS) and a source term (4th term on the RHS).

Identical convection and diffusion terms occur for all the transport equations with Γ_ϕ representing the diffusion coefficient of the scalar variables (e.g. enthalpy). The characteristic equation is also seen to represent the continuity equation with $\phi = 1$ and $S_\phi = 0$. Representation of all the transport equations in this characteristic format provides numerical advantages, since the numerical solution can be formed on the basis of the solution of one equation only - Equation 2.8. This may then be used repeatedly with different representations of the dependent variable (ϕ), the diffusion coefficients (Γ_ϕ) and the source terms (S_ϕ). A numerical solution procedure is outlined below.

2.1.2 Numerical solution procedures of the transport equations

Analytical solutions of the PDEs that represent the transport equations cannot always be obtained. This is either because a solution does not exist for the integration of the differential equations or that the solution can only be achieved by invoking numerous simplifications and assumptions which impair the accuracy of the solution. Numerical methods provide a simplification on the solution *procedure* without simplifying the differential equations themselves. For numerical solution, the partial differential equations are transformed into algebraic equations by numerical *discretisation* techniques. In this discretisation process each term in the PDEs is translated into an algebraic expression which can be solved directly using computers. The discretised forms of the PDEs are produced by a variety of numerical procedures. The most common technique in current use is the finite volume method, which evolved as a special formulation of the finite difference method. This is said to provide advantages in computational economy (*Patankar*, 1980) and is used in most of the major commercial CFD codes available, such as, PHOENICS, FLUENT, FLOW3D and STAR-CD.

Discretisation using the Finite Volume Method (FVM)

Numerical solutions imply that time and space dimensions of the flow domain are broken into finite intervals. The dependent variables (ϕ) are therefore evaluated at a

finite number of locations in a four dimensional coordinate system (t, x, y and z). This means that the continuous solution of the differential equation is replaced by a number of discrete values. Discretisation requires the use of a computational grid with the dependent variables computed at the grid or node points (intersection of the computational grid lines). The numerical method treats the values of the dependent variables at the grid points as its basic unknowns. A set of algebraic equations are used to describe the variation of ϕ in the flow domain and therefore produce distributions of the unknown ϕs at the grid points. These algebraic equations are known as the discretisation equations. As the number of grid points in the flow domain are increased the solution of the discretisation method gets closer and closer to the exact solution of the PDEs. Increasing the number of grid points however also increases the computational task and a compromise is required between the accuracy of the solution obtained and computational demands/costs.

The concept of the finite volume method is to divide the flow domain into a number of non-overlapping control volumes such that there is one control volume enclosing each grid point. The discretisation method is demonstrated below using a one-dimensional transport equation containing a convection and a diffusion term as shown in Equation 2.9.

$$\frac{\partial}{\partial x}(\rho u \phi) = \frac{\partial}{\partial x}\left(\Gamma \frac{\partial \phi}{\partial x}\right) \qquad\qquad 2.9$$

A control volume and grid convention may be defined as shown in Figure 2.1, where the shaded region represents the control volume. The notations W and E represent the neighbouring West and East volumes (in the x- direction). The faces of the control volume are represented by the subscripts w and e.
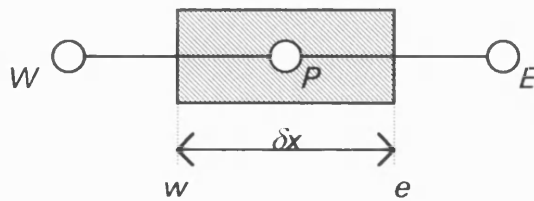
Figure 2.1 Grid points and control volume for a one-dimensional field.

Volume integration of Equation 2.9 over the control volume P (assuming a scalar dependent variable (ϕ)), obtains the following expression:

$$\left(\rho u \phi\right)_e - \left(\rho u \phi\right)_w = \left(\Gamma \partial \phi / \partial x\right)_e - \left(\Gamma \partial \phi / \partial x\right)_w \qquad 2.10$$

Equation 2.10 can be solved, provided that the unknowns (u, ϕ) are interpolated in a manner that relates their values at the control volume faces to the stored values at the control volume centres. The relation is made by assuming a profile for the variation of the variable ϕ from one grid point to another. Assuming the most obvious and simple profile between the grid points - a linear profile, and uniform grid spacing, the variable ϕ at the control surfaces can be expressed as:

$$\phi_e = 0.5\left(\phi_E + \phi_P\right) \text{ and } \phi_w = 0.5\left(\phi_P + \phi_W\right)$$

substituting these in Equation 2.10 obtains:

$$\frac{1}{2}\left(\rho u\right)_e\left(\phi_E + \phi_P\right) - \frac{1}{2}\left(\rho u\right)_w\left(\phi_P + \phi_W\right) = \frac{\Gamma_e}{\delta x_e}\left(\phi_E - \phi_P\right) - \frac{\Gamma_w}{\delta x_w}\left(\phi_P - \phi_W\right)$$

where the diffusion coefficient at the control surfaces Γ_w and Γ_e are similarly expressed by:

$$\Gamma_e = 0.5\left(\Gamma_E + \Gamma_P\right) \text{ and } \Gamma_w = 0.5\left(\Gamma_P + \Gamma_W\right)$$

The discretised equation (Equation 2.10) can conveniently be expressed as:

$$a_P\phi_P = a_E\phi_E + a_W\phi_W \qquad 2.11$$

where

$$a_E = \frac{\Gamma_e}{\delta x_e} - 0.5\left(\rho u\right)_e$$

$$a_W = \frac{\Gamma_w}{\delta x_w} + 0.5\left(\rho u\right)_w$$

$$a_P = \frac{\Gamma_e}{\delta x_e} + 0.5\left(\rho u\right)_e + \frac{\Gamma_w}{\delta x_w} - 0.5\left(\rho u\right)_w, \text{which by continuity gives } a_P = a_E + a_W$$

Therefore using Equation 2.11, it is possible to determine the value of a variable at the node point ϕ_P, from its values at the neighbouring points. Sets of discretised equations are set up at each grid point and the resulting system of linear algebraic equations are then solved to obtain the distribution of the property ϕ at the grid points.

The profile assumed in the interpolation of the values of ϕ at the grid points is known as the central difference scheme. Several other interpolation schemes are commonly used in CFD, such as the Upwind, Hybrid, Power law and QUICK schemes, which make different profile assumptions for the variation of ϕ between grid points. Details of these schemes may be found in *Vertseeg* and *Malalasekera* (1995). These however all produce a general discretisation equation of the format expressed in Equation 2.11, the solution of which is discussed in the following section.

Solution procedures

The discretised form of the differential equations that govern fluid flow, temperature and pollutant transport were expressed as the algebraic equation of the general form as shown in Equation 2.11. This resulted in sets of linear algebraic equations for each dependent variable, which need to be solved. The complexity and size of the set of equations depends on the dimensionality of the problem, the number of grid nodes and the number of variables being solved for. Solution of the algebraic equations can be obtained by various solution techniques for linear algebraic equations. The solution techniques generally fall into two categories: *direct methods* and indirect *iterative methods*. *Direct methods* may apply matrix procedures such as Cramer's rule or Gaussian elimination (*Versteeg* and *Malalasekera*, 1995). Where a large number of equations need to be solved, therefore resulting in large matrixes, direct methods require large amounts of computational effort to produce a solution. This computational effort is reduced by using iterative methods, which is the procedure used in CFD. An *iterative solution* starts from guessed values of the dependent variables (ϕ) for the whole field. These values are then improved by solving the equations line-by-line until the whole field is swept. This process is repeated until eventually convergence of the solution is achieved. The main advantage of the iterative

method over the direct methods is that only non-zero coefficients of the equations need to be stored in the core memory.

The most popular and computationally economical iterative solution technique is the well known tri-diagonal matrix algorithm (TDMA). The TDMA is essentially the result of a Gaussian elimination applied to a tri-diagonal system of equations i.e. a matrix representation with all its non zero elements on the main diagonal and in the positions immediately adjacent to the main diagonal. The solution procedure is not described within this text. Detail of the application of this to the solution of the discretised transport equations are given in *Anderson* (1995), *Vertseeg & Malalasekera* (1995). Let it suffice to say, that the TDMA is applied iteratively to a succession of grid lines from top to bottom of each grid line until the whole field is swept from east to west.

Boundary conditions

The procedure for numerical solution of the flow field has been described above. To apply these techniques to real flow problems requires the definition of the flow geometry and the specification of the conditions of the flow variables at the boundaries of the geometry i.e. where the control volumes border for example a wall, an object or supply device. These boundary conditions are represented as linearised sources for cells adjacent to the boundaries. In general these conditions can be constant values or constant fluxes at the flow boundaries for any vector or scalar quantity. For instance the thermal boundary conditions could be specified as a constant value of temperature on the wall or as a constant heat flux through the wall.

Numerical considerations

CFD programs normally provide a number of devices for the user to monitor the convergence and stability[2] of the numerical solution as it continuously improves/updates the values of the variables from one sweep of the flow field to the next. These devices allow monitoring of the *residuals* (or *residual errors*) in the numerical solution and the observation of the variation in the values of a variable at a particular point in the flow field. The residual errors are the imbalances or errors in the

---

[2] A numerical process is said to be stable if the intermediate results of the process are reasonable

finite volume equation (Equation 2.8) during the solution procedure. When the numerically correct solution is approached these inbalances in the equations will approach zero i.e. the right hand side of the equation will be equal to the left hand side. The aim of the iteration process is to diminish these errors. When these residuals reduce the solution is converging. A converged solution is normally characterised by residuals of several orders of magnitude below those obtained at the start of the solution.

There are several guidelines (CHAM, 1993) to follow and observe when trying to assess whether a run has converged or not:

- have the values at a monitoring point in the flow field stopped changing ?
- have the residuals reached the cut-off point, or reduced by several orders of magnitude ?
- do the sums of the source terms balance ? e.g. enthalpy balance, mass balance etc.

Due to the inherent non-linearities in the flow phenomena, difficulties are frequently experienced in obtaining converged solutions. A commonly used device to promote convergence is the use of *relaxation* to slow down the changes made to the values of the variables during the solution procedure. This can be expressed as:

$$\phi_{new} = \omega\phi_{calc} + (1 - \omega)\phi_{old}$$

where ϕ_{old} is the value of the variable at the start of the iteration, ϕ_{calc} is the value of the variable at the end of the iteration. With the application of the scaling factor ω the new value of the variable is set ϕ_{new}, which is in between the values of ϕ_{old} and ϕ_{calc}. Relaxation therefore involves changing the values obtained from the solution algorithm, so that they are closer to the pre-existing ones. Excessive relaxation will slow down the rate of convergence unnecessarily and too little relaxation may not avoid divergence. The choice of relaxation values is mostly a matter of experience or trial and error. As a starting point, the general rule is to set the relaxation to be proportional to a characteristic time scale of the problem e.g. the ratio of the characteristic length to the characteristic velocity, or the turbulent kinetic energy to its

dissipation rate. Relaxation does not change the converged solution, but aids the achievement of convergence and the rate at which this is obtained.

Although a numerically accurate solution may be obtained, this is not necessarily an accurate solution of the flow conditions. Good predictions of the flow conditions is also dependent on correct specification of the boundary conditions, sufficient grid representation of the flow phenomena and the validity of the mathematical models to the application field.

2.2 CFD program and models applied in this research work

2.2.1 CFD program used: PHOENICS

PHOENICS is an acronym for Parabolic, Hyperbolic or Elliptic Numerical Integration Code Series and is a general purpose CFD code for simulating single and multi phase flow, heat and mass transfer and chemical reaction phenomena. It employs finite volume techniques to solve the transport equations for both steady and unsteady/transient flow in one, two and three-dimensional geometries. In a similar format to most commercial codes it consists of three main elements: a pre-processor, a solver and a post processor.

The pre-processor

The pre-processor allows the input of the flow problem through a user friendly interface. The pre-processor facilitates the set-up of the flow problem by specification of :

- *geometry* of the flow (or computational) domain
- *grid* or mesh
- *dependent variables* to be solved (e.g. velocity components, enthalpy/temperature, concentration, variables required in the turbulence models if turbulent flow is being modelled)
- *airflow models* e.g. laminar or turbulent flow and specification of turbulent model and specification of the turbulent model

- *steady or unsteady flow*

- *fluid and material properties*

- *boundary conditions* e.g. wall temperatures or heat fluxes, conditions at the supply and extract faces, heat or concentrations sources or sinks within the geometry

- *initial conditions* of the dependent variables within the flow field

- *solution controls* e.g. choice of solvers to aid the convergence of the numerical solution and relaxation.

- *output format* of the results

The solver

The solver is the part of the program that solves the numerical equations for the problem under consideration. The solver is provided with all the relevant data defined in the pre-processor. The solver contains sequences for:

- storage allocation

- formulation of the finite volume equations

- iterative solution of the finite volume equations

- termination of iterations

- outputs of the results

PHOENICS offers a choice of the upwind and hybrid interpolation schemes. Built in features such as the turbulence models, the solvers and other coding sequences may be inspected and modified or replaced by the user.

The post-processor

The post-processor facilitates graphical viewing of the results. As a large number of points have been created within the flow domain and several variables are stored at these points, computer graphics are often the most useful means of displaying these results e.g. vector or contour plots, lines, iso-lines, stream lines etc.

2.2.2 Identification of a suitable airflow model for Indoor airflow

Room airflow is dominated by turbulence which is generated by relatively high supply velocities, the flow through the supply devices, and air temperature differences within the room. As yet, no complete theory on turbulence exists because its full nature is not well understood. Turbulence is characterised in terms of its irregularity, diffusivity, large Reynolds Numbers, three dimensional vorticity fluctuations, dissipation, and continuum (*Chen* and *Jiang*, 1992). Due to these features, it is difficult to identify whether a room airflow is laminar unsteady, locally artificially induced turbulent flow, transitional airflow or fully developed turbulent airflow. Very few room airflows are however laminar.

The representation of turbulence relies substantially on empirically derived parameters. A review of some of the turbulence models applied to indoor airflow is given in *Whittle* (1986) and *Liddament* (1991). Common turbulence models include what are described as zero, one and two equation turbulence models. The prefixes refer to the number of additional transport equations which need to be solved to account for turbulence. The two equation eddy viscosity k-ε model, or variants of this, has for some time been considered (and still is) to be the most appropriate for turbulent flow in most practical airflow applications and is the most validated of turbulence models. In this k-ε model the turbulent diffusivity is expressed in terms of the kinetic energy of turbulence k, and the dissipation rate of the kinetic energy of turbulence ε. This results in two further transport equations which express the spatial distribution of k and ε. These are solved simultaneously with the transport equations previously defined.

The standard k-ε model by *Harlow* and *Nakayama* (*CHAM*, 1993), is by far the most widely used two-equation eddy viscosity turbulence model. This model is suitable for flow at high Reynolds Number or high turbulence flow. In indoor airflow, especially in the regions close to the walls, low turbulence regions occur (*Moser*, 1988). These need to be accounted for when modelling turbulence. Two approaches are commonly used to deal with low turbulence conditions: wall functions and low Reynolds number extensions of the turbulence model.

Wall functions use empirically derived expressions to represent the variation of the dependent variables between the wall boundaries and the fully turbulent region. This approach however is dependent on the universality of the turbulent structure near the wall. In the vicinity of hot or cold walls, airflow may be strongly affected by buoyancy, with large viscous effects. In these conditions, conventional wall functions which are based on local equilibrium velocity and temperature assumptions, have been found to provide poor predictions. *Chen* (1988) reports that using the high Reynolds Number model with wall functions, placement of the first grid point outside the viscous sub-layer resulted in underestimation of the convective heat transfer coefficients. On the other hand, when the grid point was within the viscous sub-layer, the heat exchange coefficients were overestimated.

The second approach is a modification/extension of the k-ε model to incorporate viscous effects, or low Reynolds number effects. Low Reynolds number extensions incorporate additional terms in the transport equations of turbulence kinetic energy and its dissipation rate. These additional terms provide damping of the viscous stresses at low Reynolds numbers and in the viscous sub-layer adjacent to the solid walls. A comprehensive review of various low Reynolds number extensions has been given by *Patel et al* (1984) in which it was concluded that the models by *Launder* and *Sharma* (1974), *Chien* (1982), and *Lam* and *Bremhorst* (1981) performed considerably better than the other models for various flat-plate boundary flows. *Chen et al* (1990) recommend the use of the *Lam* and *Bremhorst* extension of the k-ε turbulence to predict airflow in rooms. They obtained good agreement between predictions and measurements using the *Lam* and *Bremhorst* low Reynolds number k-ε model for buoyant airflows with mixed regime of natural and forced convection. Few validations of other low Reynolds number models have been performed at these conditions which are typical of ventilated and heated rooms. However, *CHAM* (1993) suggested the use of a two-layer k-ε model as an economical (due to a reduced grid requirement) and often more accurate alternative to the low Reynolds number k-ε models. The two layer k-ε model uses the high Reynolds number k-ε away from the wall regions in the fully turbulent region. The near wall viscosity affected layer is resolved using a one equation model.

The *Lam* and *Bremhosrt* k-ε turbulence model and the two-layer k-ε model were chosen for investigation and validation of an airflow model to be used in the investigations in this study. The validation hereby referred to is on the basis of agreement of the predictions with existing experimental measurement data. The formulations of the turbulence models used are listed below. The standard high Reynolds number k-ε model, which forms a part of the two layer (2L) model is presented first. The additional features of the 2L model are then listed followed by the formulation and constants of the Lam-Bremhorst (LB) model. These model formulations and flow constants were obtained from *CHAM* (1993).

Standard k-ε turbulence model

The transport equation for turbulent kinetic energy (k) can be represented by the general transport equation in Equation 2.8 with the dependent variable as k, a turbulent diffusion coefficient of kinetic energy (Γ_k) and a source term S_k as expressed below:

$$S_k = \mu_t \left\{ 2\left[\left(\frac{\partial u}{\partial x}\right)^2 + \left(\frac{\partial v}{\partial y}\right)^2 + \left(\frac{\partial w}{\partial z}\right)^2 \right] + \left(\frac{\partial u}{\partial y} + \frac{\partial v}{\partial x}\right)^2 + \left(\frac{\partial u}{\partial z} + \frac{\partial w}{\partial x}\right)^2 + \left(\frac{\partial w}{\partial y} + \frac{\partial v}{\partial z}\right)^2 \right\}$$

$$- C_\mu \rho \varepsilon + \beta g \frac{\mu_t}{\sigma_t} \frac{\partial T}{\partial y} \qquad\qquad 2.12$$

where σ_t is the turbulent Prandtl number and C_μ is a constant as shown in Table 2.8. The turbulent viscosity (μ_t) is represented by:

$$\mu_t = \frac{C_\mu \rho k^2}{\varepsilon}$$

Similarly in the transport equation of the dissipation rate of turbulent kinetic energy (ε), the source term (S_ε) in the general transport equation is expressed as:

$$S_\varepsilon = C_1 \frac{\varepsilon}{k} \mu_T \left\{ 2\left[\left(\frac{\partial u}{\partial x}\right)^2 + \left(\frac{\partial v}{\partial y}\right)^2 + \left(\frac{\partial w}{\partial z}\right)^2 \right] + \left(\frac{\partial u}{\partial y} + \frac{\partial v}{\partial x}\right)^2 + \left(\frac{\partial u}{\partial z} + \frac{\partial w}{\partial x}\right)^2 + \left(\frac{\partial w}{\partial y} + \frac{\partial v}{\partial z}\right)^2 \right\}$$

$$- C_2 \rho \frac{\varepsilon^2}{k} + C_3 \beta g \frac{\varepsilon}{k} \frac{\mu_t}{\sigma_t} \frac{\partial T}{\partial y} \qquad\qquad 2.13$$

C_1, C_2 and C_3 are constants shown in Table 2.1. The diffusion coefficients of k (Γ_k) and ε (Γ_ε) in the transport equations are expressed as:

$$\Gamma_k = \frac{\mu + \mu_t}{\sigma_k} \text{ and } \Gamma_k = \frac{\mu + \mu_t}{\sigma_\varepsilon} \text{ where } \sigma_k \text{ and } \sigma_\varepsilon \text{ are constants shown in Table 2.1}.$$

Constant	σ_k	σ_ε	C_μ	C_1	C_2	C_3
Value in standard k-e model	1.0	1.31	0.09	1.44	1.92	0.2

Table 2.1 Constants used in the Standard high Reynolds number k-ε model

The two layer k-ε model (2L)

The two-layer k-ε model uses the standard high Reynolds number k-ε model in the turbulent regions away from the wall, and a one-equation model in the near-wall viscosity affected layer. In the near wall layer, the two layer k-ε model fixes the dissipation rate ε as:

$$\varepsilon = C_D f_2 k^{1.5}$$

where

$$f_2 = 1 + \frac{5.3}{R_N} \text{ and } C_D = 0.1643, \text{ with } R_N \text{ defined as:}$$

$$R_N = \sqrt{k}\,\frac{y_l}{\mu}$$

and y_l is the minimum distance to the nearest wall and μ is the laminar viscosity. The turbulent viscosity (μ_t) in the near wall layer is defined as:

$$\mu_t = C_\mu f_\mu L_m \sqrt{k}$$

where

$$f_\mu = 1 - e^{(-0.0198 R_N)}$$

$$L_m = A_k y_l$$

and $C_\mu = 0.5478$ and $A_k = 0.41$ (the von Karman's constant).

Lam-Bremhorst k-ε turbulence model (LB)

The Lam-Bremhorst k-ε turbulence model is an extension of the standard high Reynolds number k-ε model. No additional source terms are required. In the Lam-Bremhorst model the transport equations of the kinetic energy (k) and the dissipation rate of the turbulence energy (ε) are the same as for the standard k-ε model (Equations 2.12 and 2.13) with C_μ, C_1 and C_2 multiplied respectively by f_μ, f_1 and f_2 where,

$$f_\mu = \left(1 - e^{-A_\mu R_k}\right)^2 \left(1 + \frac{A_t}{R_t}\right)$$

$$f_1 = 1 + \left(\frac{A_{C1}}{f_\mu}\right)^3$$

$$f_2 = 1 - e^{-R_t^2}$$

where R_N and R_K are the local turbulence Reynolds numbers defined as:

$$R_N = \sqrt{k}\frac{y_l}{\mu} \quad \text{and} \quad R_K = \frac{k^2}{\varepsilon\mu}$$

The model specifies setting of a value of zero for k and a zero gradient condition for ε at the wall boundaries.

Constant	C_1	C_2	C_μ	A_μ	A_t	A_{C1}
LB value	1.44	1.92	0.09	0.0165	20.5	0.05

Table 2.2 Constants used in the *Lam-Bremhorst* low Reynolds number k-ε model

Since the low Reynolds number extension does not employ wall functions, the flow field needs to be meshed into the laminar sub-layer and down to the wall. In general the grid normal to the main flow direction needs to be distributed so as to give a high concentration of grid cells near the wall, with the wall adjacent node located at a y+ value of not exceeding 11.6 (edge of the laminar sub-layer). y+ is the Reynolds number in terms of the distance from the wall (y_l), the friction velocity ($\sqrt{\tau/\rho}$) at the wall and the laminar viscosity (μ). It is defined as:

$$y+ = \sqrt{\frac{\tau}{\rho} \frac{y_i}{\mu}}$$

In all of the above cases buoyancy production terms were included in the prediction terms of k and ε. This was found by *Chen et al.*(1990) to improve the predictions of the low Reynolds number models. The 2L and LB model were investigated in the validation task described below.

2.2.3 Validation of a turbulence model

A comparison was performed between the predictions of the turbulence models and experimental data for airflow in a full scale cavity, under conditions similar to those in heated and ventilated rooms. The validation of a model for further use in this study was on the basis of obtaining good agreement between the predicted and experimental data.

Experimental data

The experimental results of *Cheesewright et al* (1986) were employed for the validation procedure. In a series of experiments in a full scale air filled cavity *Cheesewright et al* produced velocity profile data for a cavity at a Rayleigh number of 5×10^{10} (based on the cavity height). This magnitude of Rayleigh number is typical of room airflow with buoyancy influences (*Chen et al*, 1992). The Rayleigh number is a non dimensional parameter which characterises the relative buoyant to viscous forces in a flow.

The experiment was performed in an air-filled cavity designed to a height of 2.5 m and a width of 0.5 m as shown in Figure 2.2. The temperature difference between the side walls was 45.8 °C and the top and bottom walls were well insulated. Air velocities and velocity fluctuations were measured by a laser-Doppler anemometer system. *Cheesewright's* experiments experienced considerable heat losses through the side walls and also through the top (insulated) wall. This produced asymmetric effects in the flow. Comparisons of the experimental and predicted data of the velocity and turbulence intensity was restricted to the mid-height of the cavity where asymmetric effects are expected to be smallest.

Adiabatic wall (0.5 m)

Hot wall   Cold wall (2.5 m)

z

x

Adiabatic wall
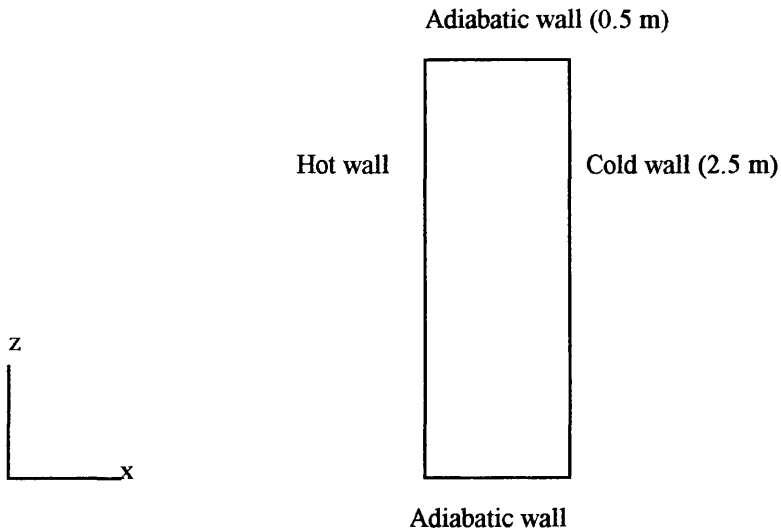
Figure 2.2 Sketch of the air-filled cavity used in *Cheesewright's* (1986) experiment

Prediction of cavity airflow using the 2L and LB model

Predictions of the air flow in the cavity were performed for a two dimensional cavity of dimensions as shown in Figure 2.2. Side wall temperatures were specified as shown in the diagram with the top and bottom walls assumed to be adiabatic.

Four grid distributions were investigated, as shown in Table 2.3. Initial simulations were performed using grid type 1 with progressive grid refinements through grid types 2, 3 and 4. Grid refinements were performed to obtain both greater grid density in the wall regions (where greater variations in flow direction and magnitude occur) and also throughout the flow domain. The grid power in Table 2.3 refers to the exponential in grid spacing from the wall to the symmetry plane, therefore an index of one obtains uniform spacing and an increase in the index obtains greater grid density in the wall regions. The table also includes the range of y+ values obtained at the grids adjacent to the wall.

Grid type	Grid (x, z)	Power (grid spacing)	y+ (2L model)	y+ (LB model)
1	31	1 (uniform)	8-12	5-15
2	31	1.3	4-8	2-8
3	51	1 (uniform)	5-10	3-10
4	51	1.3	1-4	-

Table 2.3 Grid distributions used in simulation of the buoyant cavity airflow.

Simulations were performed using a hybrid interpolation scheme for both the 2L and LB model. In simulations with the 2L model, convergence of the solution was obtained after 2000 sweeps. This utilised under-relaxation of the variables of the order of 10^{-1} for the enthalpy solution and of the order of 10^{-2} for the remaining scalar and vector quantities. On a DEC Alpha 3000 these runtimes took approximately 900 seconds for the smaller number of grid points (31 x 31) and 3000 seconds for the larger (51 x 51).

The LB model required stronger relaxation of k and ε, than for the 2L model equations to achieve convergence of the solution. The relaxation applied to these was of the order of 10^{-3}. Convergence of the solution of the LB model with grid type 4 could not be achieved, despite the use of alternative solvers. This is discussed in Section 2.2.5. Comparison of the simulation results with the experimental values was thus restricted to grid types 1-3 for the LB model. For these grid types convergence was achieved with similar number of sweeps and run-times as for the 2L model.

Results

Results of the velocity field (vectors) are shown in Figure 2.A1 for the 2L model (grid type 4) and in Figure 2.A2 for the LB models (grid type 3). In both of these, the flow is dominated by two anti-clockwise vortices, one in the upper right quadrant of the cavity and the other in the lower left quadrant. Differences in magnitudes of velocity in these vortices can be seen between the predictions of the two model, with higher velocities occurring in the LB model.

The comparison of the predicted and experimental data of the velocity and velocity fluctuation in mid-height of the cavity are shown in Figures 2.A3 and 2.A4 for the 2L model and in Figures 2.A5 and 2.A6 for the LB model.

No large difference is observed between the velocity predictions (Figure 2.A3) of the 2L model for the different grid distributions. All four grid types produced good agreement with the experimental data in the mid-width of the cavity. Towards the sides however, there is a greater deviation from the experimental data, with an underestimation of the predicted velocities in the approach to the walls. The difference

between the predicted and experimental data was however not large with reasonably good overall agreement with the experimental data.

Distributions of velocity fluctuations obtained from the experiment versus predictions of the 2L model are shown in Figure 2.A4. All the grid types predicted similar velocity fluctuations at the cavity centre, with differences towards the cavity sides, in particular between grid type 1 and the other types. Grid types 2,3 and 4 obtained similar predictions of the velocity fluctuations, which are in reasonably good agreement with the experimental data. The predictions of grid type 1 underestimate the velocity fluctuations at the sides of the cavity.

The LB model obtained good agreement between the predicted and experimental velocities (Figure 2.A5) for grid type 3. Grid types 1 and 2 predicted similar velocity distributions. However both underestimated the velocities at the sides of the cavity, and were also not in close agreement in the mid-section.

Greater similarities were obtained between grid types 1 and 2 than grid type 3 in the predictions of the velocity fluctuations using the LB model (Figure 2.A6). Grid types 1 and 2 obtained similar velocity fluctuations in the mid-section of the cavity, with grid type 2 overestimating the values in the wall regions. Grid type 3 achieved reasonable agreement with the experimental values both in the mid-point of the cavity and also in the side regions. This is also in closer agreement with the distribution of velocity fluctuations obtained for the 2L model. It would therefore appear that the LB model requires both a closely meshed grid in the wall region and also a greater grid density in the flow domain away from the wall in comparison to the 2L model.

Both the LB model (grid type 3) and the 2L model (grid type 2,3,4) produced satisfactory predictions of the turbulent airflow in the cavity, with the LB model obtaining better agreement with the experimental velocity distribution in the cavity mid-height. The results obtained, confirm the results of Chen et al (1990) on the suitability of the LB model for the modelling of indoor airflow. Similarly the 2L model would appear to be a good alternative which is less demanding in grid requirements and therefore of greater computational economy. The LB model was at this stage chosen as the preferred model for indoor airflow simulations. This was for two

reasons. Firstly, this produced somewhat improved prediction of the velocity distributions than the 2L model in the validation exercise. Secondly, this model has been applied successfully to room airflow by researchers such as *Chen et al.*

2.2.4 Room and H & V system setup/specification

Two room geometries were used in the investigation of the H & V system in Chapter 5. Preliminary investigations on the performance of the airflow model and generation of a suitable grid were performed using a room geometry of 6 x 6 x 2.5 m^3. The second geometry used in the ensuing investigations was of dimensions 4 x 4 x 2.5 m^3 and employed the same near wall grid distribution (i.e. distances to the wall). Various locations of air terminal devices (ATDs) were used as will be described in Chapter 4. A number of methods were considered for modelling of airflow from the supply devices and are discussed below.

Air supply device

The momentum of the supply air jet has been found to be the most significant parameter of the supply airflow to influence room air movement (*Nielsen*, 1989). The maximum velocity in the occupied zone has for example been found to be proportional to the inlet velocity times the square root of the supply area, which expresses the square root of the supply momentum. It is therefore very important that the inlet conditions used in the numerical method can adequately represent the momentum flow. *Heikkinen* (1991) provides a review of several methods which have been used for simulating complex inlet ATDs, namely the:

- *basic model*, where the ATD is replaced with a simple opening which has the same effective area as the free area of the ATD.

- *wide slot model*, in which a much larger aspect ratio is used in the model than that of the ATD whilst retaining the same effective area.

- *momentum model*, in which the area of the supply device is set as equivalent to the gross area (total free and blocked area) of the ATD. The supply momentum may then be set by the specification of separate boundary conditions for the continuity and momentum equations.

- *box model*, in which the boundary conditions are given at the surface of an imaginary box around the ATD. This is usually obtained by prior measurements.

- *prescribed velocity model*, where the boundary conditions are given both at a simple opening and also in the flow field as in the box model. The idea is to minimise the necessary measurements required.

The preferred model for use in the current work was the momentum model. This has been found by several researchers (*Heikkinen* 1991, *Chen* and *Moser* 1991) to perform well in the prediction of airflow through complex inlet devices. However due to inconsistencies obtained in preliminary tests using the model (which are mentioned in section 2.2.5) simulations of the cases investigated in Chapters 4 and 5 were performed using the basic inlet model. This model has been found (*Heikinnen*, 1991) to give fairly accurate predictions outside the initial stages of the supply jet. This was chosen in preference to the remaining supply models for the following reasons:

1. The box model and prescribed velocity model require existing experimental results. This data is not available.

2. The wide slot model has in tests been found to perform no better than the basic model (*Heikkinnen*, 1991).

Grid

Using the results of the validation section as guidelines for the grid requirement in the near wall region (y+ values), the grid distribution in the room was refined progressively until a satisfactory balance was obtained between the accuracy of the solution and the computational time required. At this point, further increases in grid number did not have a significant influence on the flow pattern obtained. Nor did increases in the grid proximity to the wall have any further impact on the heat transfer between the wall and the room air. The final grid selected consisted of 33 x 35 x 27 cells in the x, y and z directions respectively with a finer grid distribution in the near wall region. ATD supply areas were simulated by approximately 15 cells, with small variations in the cell number for different locations of the supply devices.

Simulations

Initial simulations were performed using the LB model. Difficulties were however experienced in obtaining stable and converged solutions of the room airflow simulation using this model and the 2L model was eventually used in preference to the LB model. The difficulties encountered and attempts at resolving these are mentioned in Section 2.2.5.

The simulations in this study were all performed using the 2L model with a basic supply model. The same relaxation parameters were used as in the validation exercise. The simulations required on average 2500 sweeps for convergence. On the DEC Alpha 3000 this resulted in a run-time of approximately 25000 s.

2.2.5 Problems encountered

A number of problems have been cited in the text in the use of particular flow models. These problems influenced the final choice of models and are briefly commented on below. Some of the difficulties encountered with the use of the selected model are also mentioned.

Momentum model for simulation of supply airflow: This model produced inconsistent predictions of the velocities at the supply outlet. The required or specified momentum of the supply airflow could only be achieved over small ranges of flow rate and supply area. For example, doubling of the airflow rates did not result in doubling of the supply velocity at the supply outlet. The use of the momentum model requires separate specification of the momentum and continuity boundary conditions. Some CFD codes utilise combined boundary conditions for both equations and do not allow for this. PHOENICS does however cater for this. The agreement obtained between the specification and outputs over small ranges and not over wider margins would suggest the error did not arise from incorrect specification but in the handling and solution of these conditions within the code. Correspondence with the code suppliers did not resolve the solution to this problem.

LB model: Two problems were cited with regard to the LB model. The first was in the validation exercise where convergence could not be achieved for a dense grid

distribution in the wall regions, with the first grid point in close proximity to the wall. The use of various alternative solvers (such as a conjugate gradient solver, recommended by *Ludwig*, 1993) failed to improve the convergence of the solution. The second was in the simulation of the room airflow, in which convergence could sometimes be achieved, but with great difficulty. At high airflow rates (in the range of 6-9 ACH) and low supply air temperatures using very strong relaxation of the iterative solution, convergence was obtained. This however required run-times of up to two or three days to obtain a converged solution. The run time required for each of these simulations made the use of this model impractical for the extensive simulations performed in this study. In addition convergence could not be achieved at low flow rates in particular with high supply air temperatures (e.g. 3 ACH, 45 °C), which would have eliminated a vital range of investigation of the study. The difficulty encountered at low flow rate and high supply air temperature may be a result of the buoyancy influence. Application of several recommended (*Madhav*, 1993) solution schemes to the energy flow and turbulent kinetic energy equation failed to improve the convergence.

A number of difficulties were encountered with the use of the 2L model in the course of the investigations. These were:

1. Greater difficulties in convergence when using a symmetry plane i.e. modelling the flow in a symmetrical half of the room. All simulations were therefore performed for the full 3D representation of the room.

2. Some difficulties were encountered in convergence of the energy equation at low flow rates and high supply air temperatures as commented on for the LB model above. This again appears to be due to the buoyancy effect. A solution could however mostly be achieved by increased numbers of iterations or by 'coaxing' the solution e.g. having obtained a solution at a lower supply air temperatures, the solved flow field serves as initial conditions at the higher supply air temperature. This was performed in various stages.

Figure.2.A1

Velocity vectors in the cavity using the 2L model, grid type 4.
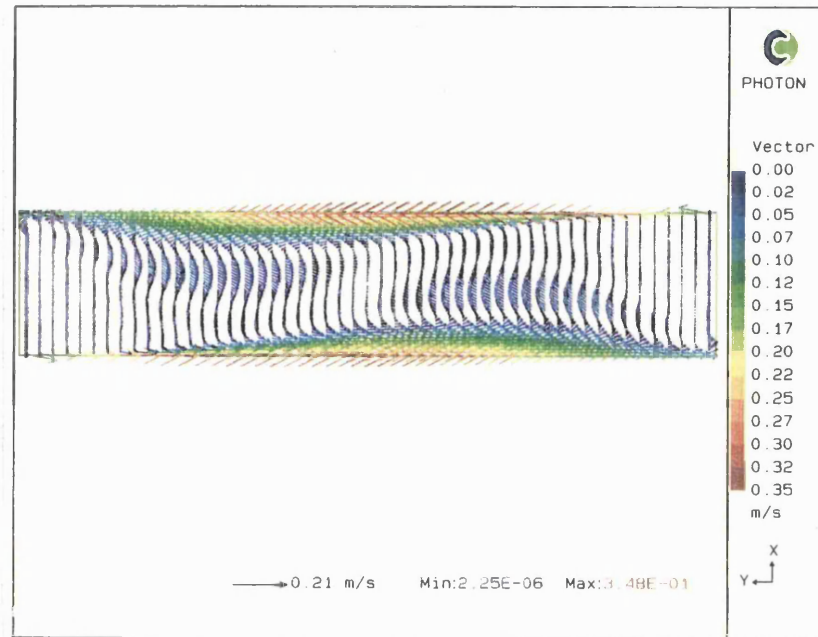
Figure.2.A2

Velocity vectors in the cavity using the LB model, grid type 3.
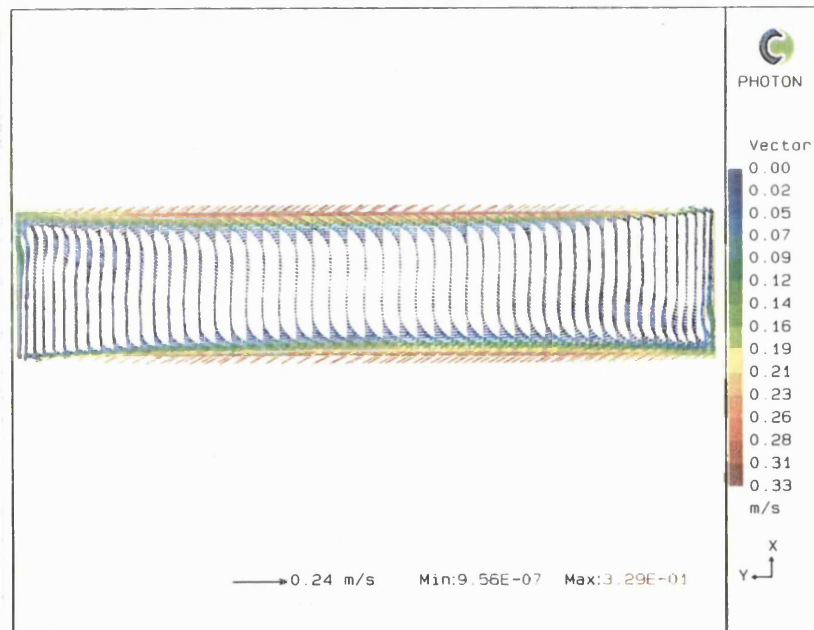
Figure.2.A3

Velocity distribution in the cavity mid-height using the 2L model, grid types 1 - 4.
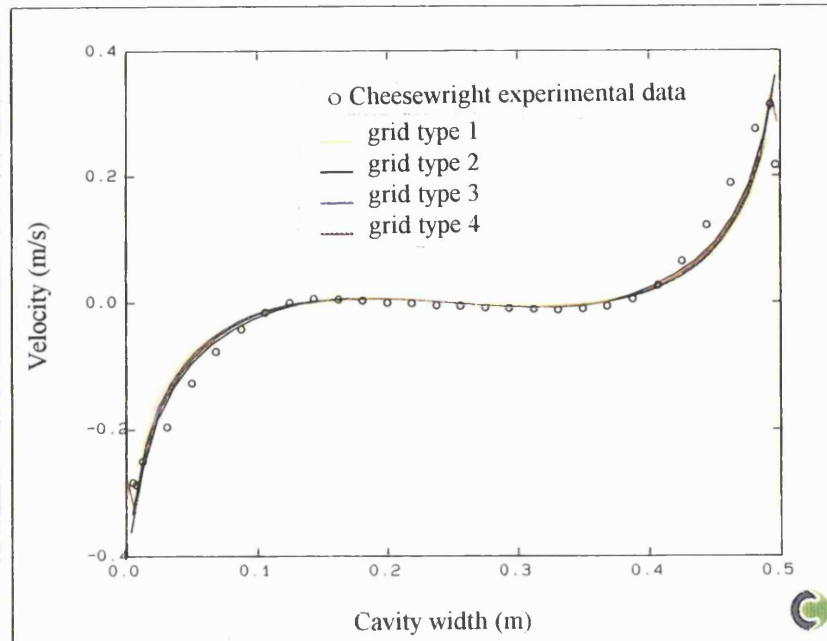
Figure.2.A4

Velocity fluctuations in the cavity mid-height using the 2L model, grid types 1 - 4.
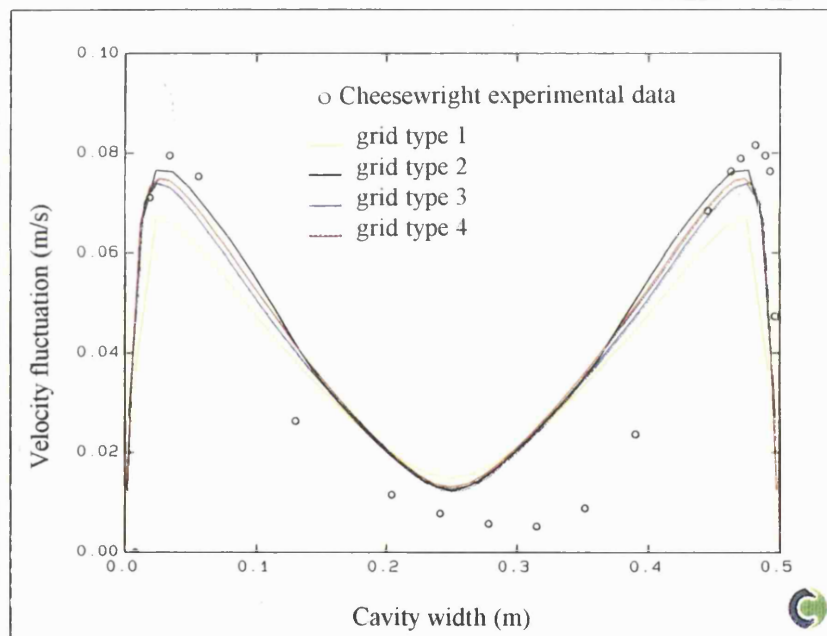
Figure.2.A5

Velocity distribution in the cavity mid-height using the LB model, grid types 1 - 3.
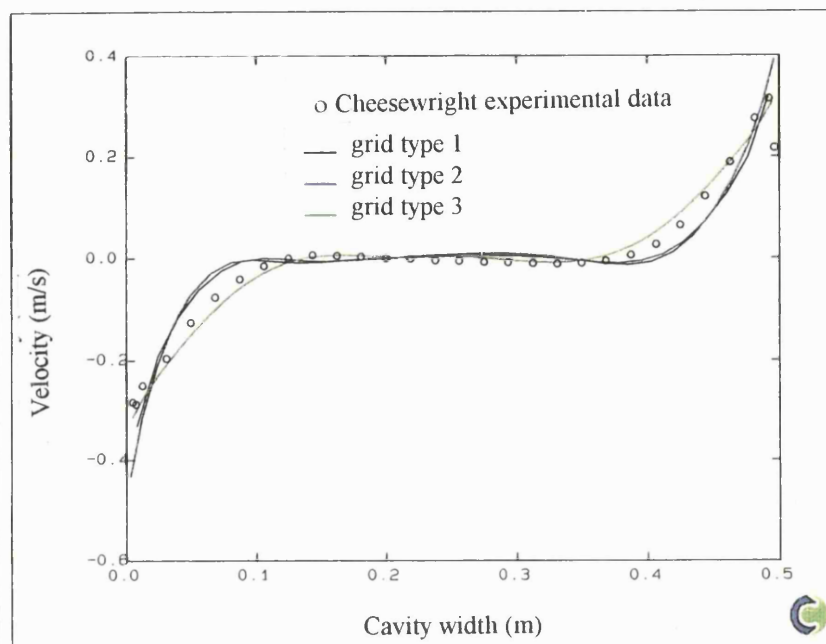
Figure.2.A6

Velocity fluctuations in the cavity mid-height using the LB model, grid types 1 - 3.
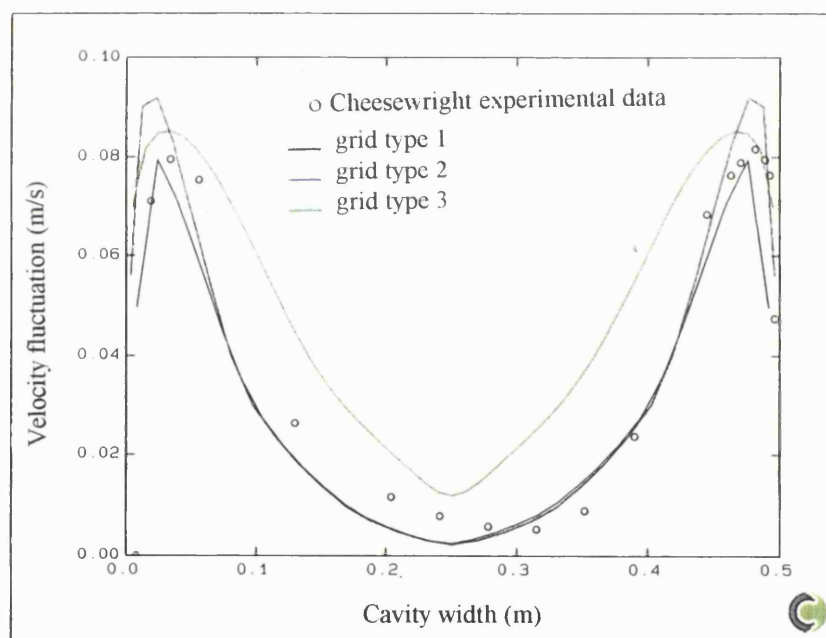
3.   BOUNDARY CONDITIONS

The objective of the work described in this chapter was to provide estimates of:

- the thermal boundary conditions which may occur in a room of a low energy home.

- the flow rates required of the H & V system for ventilation and space heating purposes.

Heat transmission through enclosure boundaries or walls, is dependent on the conductance of the wall and the convection and radiation heat transfer at the internal and external wall surfaces, and may be expressed in terms of a heat flux at the internal wall surface or by internal surface temperatures. These surface temperatures and heat fluxes are referred to as the thermal boundary conditions. The heat loss from the room influences the space heat requirements and consequently, the required flow rates and supply air temperatures. High supply air temperatures may cause excessive vertical air temperature differences, resulting in discomfort to the occupants. The space heat requirement therefore has an influence on the airflow rates required from the H & V system. Additional reasons for determination of the conditions at the individual enclosure surfaces are:

a) the influence of the radiant temperature and therefore wall surface temperatures on thermal comfort.

b) the individual surface temperatures (or heat losses) may have an impact on the airflow patterns and temperature distributions in the room.

Outside air needs to be supplied to the room in sufficient quantities to dilute indoor air pollutants to acceptable concentrations during occupancy regardless of the space heating requirement. Ventilation requirements are therefore assessed independently.

The analysis will be presented in two major sections, the first of which is concerned with the *thermal boundary conditions* and the latter with the *required flow rates*. These sections are each split into two further sections. A brief description of the objectives of each   section is given below.

Thermal boundary conditions:

Heat transmission through the room envelope. Analytical methods were used to determine the transient heat transmission through the enclosure envelope. This established variations in heat flux and surface temperature, both in time and within the space. (Sections 3.1-3.5)

Vertical temperature gradients in the side walls. A heated room will experience temperature gradients between the floor and ceiling. Using a conjugate heat transfer CFD model, the corresponding temperature gradients which might occur in the side walls were estimated. (Section 3.6)

Flow rates:

Flow rates required for space heating. Using the heat transmission data from the thermal boundary conditions together with guidelines from the literature review of maximum supply temperatures, approximate flow rates which may be required for space heating purposes were determined. (Section 3.7.1)

Flow rates required for ventilation purposes. Using the information identified in the literature review the possible flow rates required from the H & V system were determined. (Section 3.7.2)

The results of this analysis provided realistic boundary conditions for the CFD investigations in Chapters 4 & 5.

3.1 Heat transmission through the room envelope

The analysis proceeded with the identification of representative climatic data, building fabric and an operation/occupancy schedule. This information was required to perform a detailed analysis of heat transmission into the space. The procedures and results of this process will be laid out in the following sections.

An accurate prediction of individual wall surface temperatures in a room is an unrealistic prospect. The approach adopted was to determine the minimum and maximum values of individual surface temperatures which may occur simultaneously.

3.1.1 External climatic conditions

External climatic conditions refer to both the ambient temperatures and solar radiation. The effect of both on heat transmission through an opaque surface may be combined in the use of the sol-air temperature. The sol-air temperature represents an outside air temperature resulting in the same heat flow in the absence of sunlight and long wave radiation. Further information on sol-air temperature and solar irradiance can be found in standard texts, *Jones* (1994), and *ASHRAE handbook* (1993).

Using the concept of sol-air temperature, three climate 'scenarios' were considered using weather data (*CARRIER E20-ii*, 1994) for Munich (latitude 48° North, longitude 12° East) to be representative of a mid-European climate. These climate scenarios were:

a) a typical winter day without solar radiation

b) a typical winter day with solar radiation

c) a design day with no solar radiation. (winter/minimum design temperatures)

Typical winter day, without solar radiation

In the absence of solar radiation either due to overcast conditions or the wall surface orientation, the sol-air temperature is approximately equal to the ambient air temperature. External climatic conditions in this case were represented by the ambient air temperatures for a typical day in January. The hourly ambient temperatures are shown in Figure 3.1. These ambient temperatures were used in the determination of minimum internal surface temperatures.

Typical winter day, with solar radiation

The current research is targeted towards homes in mid-European climates. In such locations within the northern hemisphere, greatest exposure to solar radiation is on south facing building surfaces, with little or no direct radiation on north facing surfaces. A south facing wall would therefore experience the highest internal surface temperatures. This surface orientation was used in determining maximum internal

surface temperatures which may occur on a typical winter day. Sol-air temperatures for a south facing wall are shown in Figure 3.2. These were determined using solar flux data for the 21st of January assuming an external heat transfer coefficient of 22.7 W/m^{2}K, as recommended for winter conditions by *ASHRAE handbook* (1993).

Design day, without solar radiation

The coldest weather spells are often accompanied by sustained periods of overcast skies with very small variation in outdoor air temperature over the day. It is therefore satisfactory to use a fixed outside temperature for the analysis of the design conditions to meet peak heating requirements. A winter dry bulb temperature of -16 °C was used. This condition was used in determining 'lows' of possible internal surface temperatures.
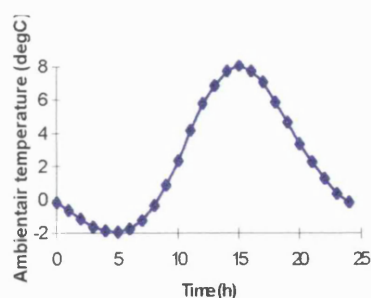
Figure 3.1 Ambient temperature, Jan., Munich
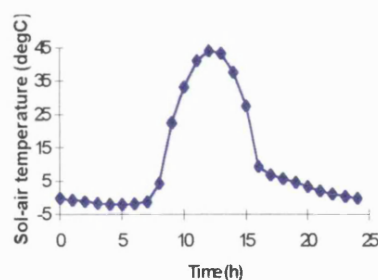
Figure 3.2 Sol-air temperature, 21st Jan Munich (South facing wall)

3.2 Building fabric

The focus of the application is towards a rapid-response, intermittent heating and ventilation system. The inclination in building fabric is therefore towards a lightweight low thermal capacity structure which warms up quickly, together with the room air, when the space is heated. In addition to the options in building *materials*, options in the distribution of thermal capacity within the wall configurations also exist. These need to be taken into consideration in the analysis of heat transmission into the space. Wall configurations which may be used in low energy construction are identified and commented on below.

Four wall configurations were found to be in common use in dwellings (*Foster* 1983, *Diamant* 1986, *Feist* 1990), as shown in Figure 3.3, namely:

a) walls with external placement of insulation

b) wall with internal placement of insulation

c) insulation in cavity walls

d) insulated wood-frame walls

Insulation external   *Insulation internal*   *Insulation sandwiched*   *Insulated frame wall*
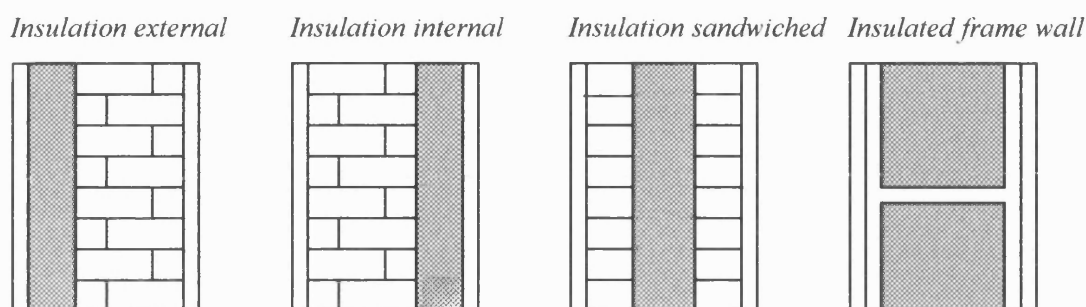
Figure 3.3 Wall configurations in common use.

When thermal mass is positioned internally it takes considerably longer to warm up the room air and the internal surfaces, than with a low thermal capacity layer (insulation) on the inside. The placement of insulation therefore effectively changes the thermal capacity of the room as opposed to the wall structure as a whole, with internal placement of insulation corresponding to a lower *room* thermal capacity. Internal placement of insulation would thus be preferential for an intermittently operated system, both from a comfort and energy perspective. Rapid warming up of the room surfaces has an additional benefit in that it reduces heat loss from the room air with a corresponding rate of increase in the mean radiant temperature. This allows for a reduction in the required supply air temperatures for equivalent comfort conditions and would result in further energy savings.

Having stated the configuration which in theory would be suitable for a rapid-response intermittent heating system, limitations exist when considered in a wider context. From a practical perspective, the wall configuration may result from criteria such as suitability of external insulation for retrofit purposes or central type insulation for use with insulation material of low compressive strength and stability. From a thermal

perspective, the considerations are normally (*Burberry*, 1983) based on the influence of the following on the thermal behaviour of a room:

a) *Winter vs. summer optimisations*: a balance is needed to achieve a combination of winter economy and avoidance of summer overheating. The qualities which lead to rapid warming up of the room in winter, similarly lead to rapid over heating of the room in summer due to solar heat gains through the fenestration and from internal heat sources.

b) *The system response times*: rapid variations in indoor air temperature in low thermal capacity rooms may pose difficulties in controlling heating systems with large 'time' constants. Slow response times of the heating system result in indoor air temperature swings.

The latter point is not expected to pose problems with a variable capacity air heating system. These would be expected to have considerably lower time constants than the thermal response of the surfaces. The first point is more complicated. If intermittent summer cooling were to be provided, similar thermal properties would be appropriate as those for intermittent heating. Summer cooling is however, unlikely to be widely implemented in the foreseeable future. No formalised optimisation process for the selection or use of thermal mass currently exists. The approach adopted in this study was to identify representative thermal boundary conditions irrespective of the possible configuration, by determining conditions for *all* the configurations.

3.3   Scope of the investigation

Low energy buildings commonly use similar insulation values for exterior walls and floors and somewhat higher insulation values for roofs. In a typical room, the exterior walls are the most likely to experience the highest heat losses and gains and therefore the highest and lowest surface temperatures. The consideration was therefore restricted to the exterior walls.
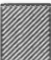
The four wall configurations identified and shown in Figure 3.3 were investigated. Using current UK building regulations [Section 1/C (*Stephenson*, 1995)] as guidelines, external walls were blockwork of minimum dimension 190 mm for solid walls and 90

mm for cavity walls. Lightweight material was used at two insulation levels, U values of 0.4 and 0.2 W/m^2K, the former being consistent with UK standards and the latter approaching that of 'super insulated homes'. The precise components and dimensions of these walls will be identified in greater detail in the following sections.

An occupancy schedule for the room was assumed, as shown in Table 3.1. This assumes an occupied period thermostat setpoint of 23 °C, with the temperature allowed to float during other times. This occupancy schedule (and therefore mode of operation of the heating system) does not follow an intermittent pattern. The main feature in the selection of this occupancy schedule was to create a short and long heating period, with a large time gap between these to allow the walls to lose heat. The short heating period is of particular interest for the identification of conditions which may occur during intermittent heating.

h	1	2	3	4	5	6	7	8	9	10	11	12	13	14	15	16	17	18	19	20	21	22	23	24
							▨	▨									▨	▨	▨	▨	▨	▨		

Table 3.1 Occupancy schedule assumed in the heat transmission analysis

▨ Occupied period,   Set point: 23 °C

☐ Unoccupied period, Set point: -

3.4   Transient heat transmission using the Transfer Function Method (TFM)

The design of heating systems is based mostly on steady state calculations, using winter design temperatures for determination of peak heating capacity. For continuous heating systems, these calculations provide reasonable accuracy due to relatively constant outdoor air temperatures. When using temperature setback or intermittent heating, large indoor air temperature variations occur and transient variations need to be considered. The transient heat transmission through the wall was analysed using the transfer function method (*ASHRAE handbook*, 1993). This analysis process utilises the previously defined conditions (climate conditions, building fabric and heating schedule) in determination of instantaneous heat fluxes at the internal wall surfaces and therefore internal surface temperatures. An outline of the information flow in the heat transmission analysis is shown in Figure 3.4.
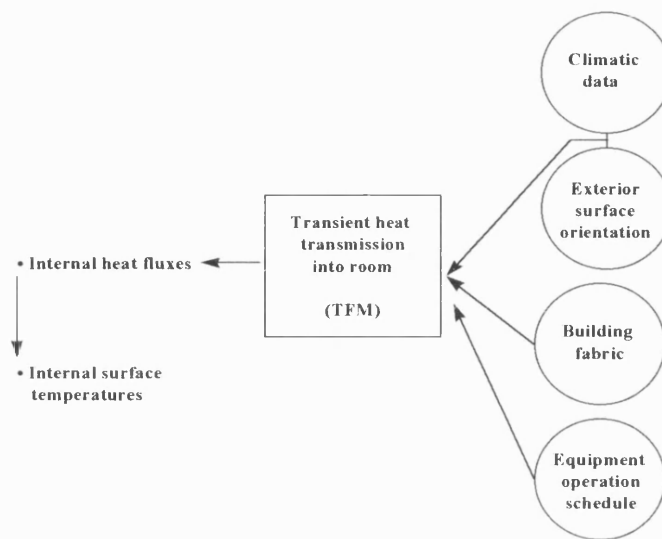
Figure 3.4 Overview of information inputs and outputs of transient heat transmission analysis.

The transfer function concept involves the conversion of a theoretically infinite set of response factors into a time series i.e. relating a current variable to past values of itself and other variables, at discrete time intervals. In building analysis these time intervals are one hour periods. The following sections present the key principles involved in the calculation of heat transmission into a space, using the TFM and the application of these in the current analysis.

Space heating/cooling load calculation is a complex process involving determination of different types of heat gains into a space and the interaction between the heat gains with the storage and release of energy in the thermal mass. The TFM breaks down the calculation into three sets of transfer functions which apply to the following three stages:

a) instantaneous heat loss[1]

b) time lag in conversion to space heating load[2]

c) influence of plant and control on the heat supply[3]

---

[1] *Heat loss*: Rate of convective and radiative heat loss from the space at a given time.
[2] *Heating load*: Instantaneous rate of heat convected from the space or rate at which heat must be supplied to maintain a constant indoor air-temperature.
[3] *Heat supply*: Rate at which heat is supplied to the conditioned space.

The sequential solution of these transfer functions allows predictions of conditions within a space on an hourly basis for a variety of systems, control strategies and operating schedules. The transfer function applicable to the above mentioned stages are the *conduction transfer functions*, *weighting factors* and *space air transfer functions* respectively.

3.4.1 Conduction Transfer Functions (CTF)

The CTFs describe the heat fluxes on the internal surfaces of walls as a function of previous values of: heat fluxes, room air temperatures, and the outside air temperatures. The room air temperature is assumed to be constant and uniform within the space. Combined heat transfer coefficients for radiation and convection are assumed to be constant on the internal and external wall surfaces and the transfer function is driven by the sol-air temperature on the outside and room air temperature on the inside. The CTF is calculated by:

$$q_{e,\theta} = A\left[\sum_{n=0} b_n(t_{e,\theta-n\delta}) - \sum_{n=1} d_n\{(q_{e,\theta-n\delta})/A\} - t_{rc}\sum_{n=0} c_n\right]$$

3.1

where

$q_{e,\theta}$ = heat gain through wall at time θ (W)
A = indoor surface area of wall (m^2)
θ = time (h)
δ = time interval (h)
n = summation index (as many terms as non negligible coefficients)
$t_{e,\theta-n\delta}$ = sol air temperature at time ,$\theta-n\delta$ (° C)
t_{rc} = constant indoor room temperature (°C)
b_n, c_n, d_n = conduction transfer function coefficients

The first stage of the calculation procedure involved the identification of the CTF coefficients, b_n, c_n, d_n , for the wall configurations in consideration. This was done using the CTF routines (*Mcquiston* and *Spitler*, 1992) developed as part of ASHRAE TC 4.1, Load Calculations. The CTF routines facilitate automated procedures for accessing a database of conduction transfer function coefficients for representative wall types and matching the wall configuration under consideration to a corresponding wall type. The matching process was developed as a result of investigations by *Harris* and *Mcquiston* (1988) into characterisation of walls, based on their transient heat transfer

characteristics. By classifying walls and roofs on the basis of their thermal lag and amplitude they found that all common wall configurations could be represented by 41 distinct wall groups and 42 distinct roof groups. These are categorised as wall types 1 - 41, which represent increasing thermal lags (time) and amplitudes. The matching process between a wall/roof configuration and a wall/roof group allows selection from a wide range of building materials, insulation values and thermal mass, as well as the location of the thermal mass relative to the insulation (in, out or integral).

The wall configurations outlined in Section 3.2 were matched with their corresponding wall types on the basis of the building materials, thermal mass location and U value of the wall configuration. This resulted in the categorisations as specified in Table 3.2 and the corresponding CTF coefficients in Table 3.3 (The c coefficients are not required for reasons explained shortly). The CTF coefficients had to be unnormalised for the specific U value of the wall configuration under investigation. The d coefficients are non dimensional and therefore remained the same. The b coefficients were unnormalised by multiplication with the ratio of the U value of the wall being investigated to the U value of the equivalent wall type obtained from the matching process. This can be explained by consideration of the steady state conditions:

At steady state conditions, where $d_0 = 1$ and q_e, t_e and t_{rc} are constant, Equation 3.1 becomes:

$$q_e \sum_{n=0} d_n = A\left(t_e \sum_{n=0} b_n - t_{rc} \sum_{n=0} c_n \right)$$

Description	U=0.4 W/m^{2}K wall type	U=0.2 W/m^{2}K wall type
LW block, external insulation	10	16
LW block, internal insulation	10	15
cavity wall, LW block, face brick	10	15
frame wall	2	2

Table 3.2 Categorisation of wall type.

LW: Light weight wall with internal or external insulation: 200 mm LW concrete block, 20 mm internal plaster/gypsum board.
Cavity wall: 100 mm LW concrete block, insulation,100 mm face brick.
Frame wall: 20 mm internal plaster/gypsum board, external stucco.

Wall Group	coefficient	n=0	n=1	n=2	n=3	n=4	n=5
2	b_n	0.00089	0.03097	0.05456	0.01224	0.00029	0.00000
	d_n	1.00000	-0.93389	0.27396	-0.02561	0.00014	0.00000
10	b_n	0.00004	0.00578	0.02505	0.01476	0.00136	0.00001
	d_n	1.00000	-1.66360	0.82440	-0.11098	0.00351	0.00000
15	b_n	0.00000	0.00018	0.00342	0.00824	0.00418	0.00050
	d_n	1.00000	-2.00000	1.36800	-0.37388	0.03885	-0.00140
16	b_n	0.00000	0.00080	0.00959	0.01534	0.00491	0.00032
	d_n	1.00000	-2.00260	1.32890	-0.32486	0.02361	-0.00052

Table 3.3 CTF coefficients for wall types (*ASHRAE handbook*, 1993), b_n (W/m^{2}k), d_n - non-dimensional.

This may be compared with the common steady state conduction equation:

$$q_e = U \cdot A\left(t_e - t_{rc}\right)$$

and implies that the sum of the coefficients of t_e and t_{rc} must be equal:

$$\sum_{n=0} b_n = \sum_{n=0} c_n \qquad\qquad 3.2$$

and also

$$U = \frac{\sum_{n=0} b_n}{\sum_{n=0} d_n} \qquad\qquad 3.3$$

The relation in Equation 3.2 explains why the c coefficients need not be determined at constant indoor air temperatures (t_{rc}). The sum of the b coefficients, being equal to the sum of the c coefficients, these may be used in Equation 3.1. The relation between the U values and the b and d coefficients is shown in Equation 3.3. Since the d coefficients are non-dimensional, the U value of the wall configuration must be consistent with the magnitudes of the b coefficients. This relation allows the unnormalisation of the b coefficients to the required U value.

Having identified the CTF coefficients, the calculation was performed in a spreadsheet with Equation 3.1 expressed as a simple algebraic equation as shown in Equation 3.4

The heat fluxes at the internal wall surfaces were evaluated per unit wall area at a fixed indoor air temperature of 23 °C.

$$\frac{q_{e,\theta}}{A} = \frac{d_1 q_{e,\theta-1}}{A} \cdots\cdots - \frac{d_5 q_{e,\theta-5}}{A} + b_0 t_{e,\theta} + b_1 t_{e,\theta-1} \cdots\cdots + b_5 t_{e,\theta-5} - t_{rc} \sum_{n=0} c_n \qquad 3.4$$

CTF Outputs

At constant indoor air temperatures the wall types obtained in Table 3.2 for the various wall configurations investigated fell into two wall categories (types) for walls of U value of 0.4 W/m²K and three categories (types) for walls of U value of 0.2 W/m²K. At the U value of 0.4, the same wall type was obtained for the block walls irrespective of the placement of insulation relative to the thermal mass (blockwork). At the U value of 0.2, the same wall types were obtained for wall configurations with internal and integral insulation. External placement of insulation obtained a wall type with only minor differences in thermal properties (thermal lag and amplitude). This was indicated by the single increment in wall type (i.e. wall type 15 to 16). The frame wall was of the same type (but obviously with different CTF coefficients) for both insulation values. Further analysis was therefore restricted to the CTF outputs obtained from wall type 2, representing the frame wall, and wall types 10 and 15 representing the block walls at U values of 0.4 and 0.2 W/m²K respectively.

The heat fluxes obtained (per square metre of exterior wall area) for the three climatic data sets and for wall configurations identified above are shown in Figures 3.5 and 3.6 for the walls of U value 0.4 and 0.2 W/m²K respectively. Negative heat fluxes represent heat losses from the room and positive values heat gains to the room. These heat fluxes were used in the next stage of the analysis.
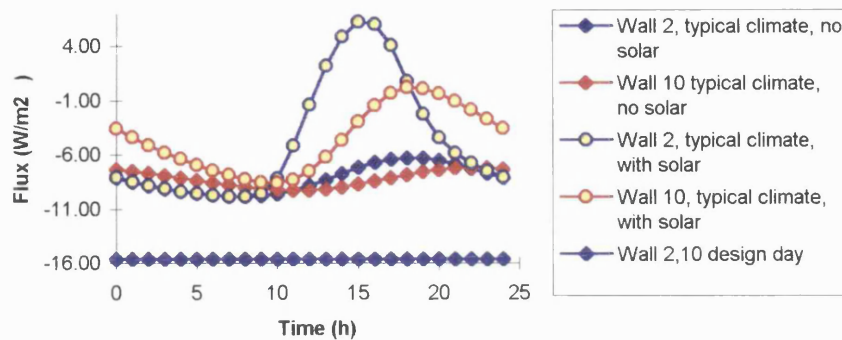
Figure 3.5 Heat fluxes for walls of U values of 0.4
Wall type 2   frame wall
Wall type 10   walls with internal, external and integral insulation i.e. cavity wall
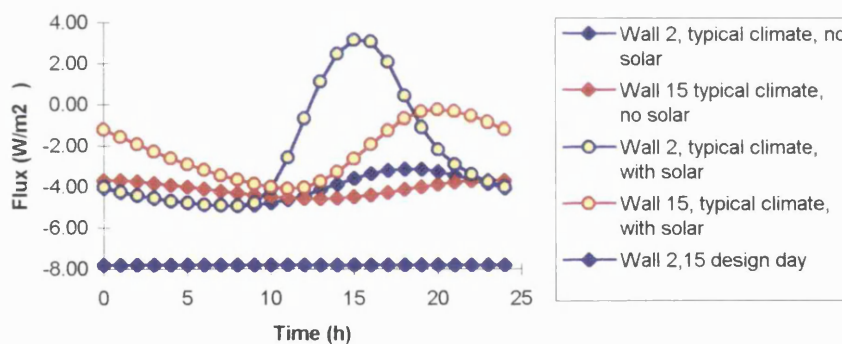
Figure 3.6 Heat fluxes for walls of U values of 0.2
Wall type 2   frame wall
Wall type 15   wall with internal and integral insulation

3.4.2   Weighting factors

This transfer function relates hourly space loads due to instantaneous heat loss/gain to previous values of space load due to the heat loss. As mentioned earlier, this effectively represents the time lag in conversion of a heat loss/gain to a space load. This delay is due to the radiative and convective interactions within the space, with convective heat loss/gain immediately transmitted to the space load but the radiant absorbed by the thermal mass and later converted to the space load.

In the current analysis, the heat loss was considered to be equivalent to the space load. This was for the following reasons:

- Use of a lightweight building structure would imply that radiant heat gains would fairly rapidly be convected into the space. This includes heat gains due to lighting, solar heat gains etc.

- In an intermittent heating system there would be wall temperature equalisation during the off-periods. Therefore at start-up, using an air heating system, the mode of heat transfer in the space would be predominantly convective. It is these early periods of operation that are of primary importance.

For a particular wall surface, the instantaneous heat loss/gain was therefore assumed to be equal to the heating load with no time lag.

3.4.3 Space air transfer functions (SATF)

The space heat loads calculated as a result of the CTFs and consequent weighting factors (if applied) are imposed to a major restriction: that of a fixed indoor air temperature. The indoor air temperature will depend on: thermostat setpoints, operating schedules and the capacity of the heating equipment. The indoor air temperature varies as a consequence of the heat supply rate and vice versa. The SATF accounts for this by relating a deviation in temperature from the constant values assumed in the CTF to a deviation in heat supply to the space. If the capacity of the heating system, control permitting, can match the space heat load, the heat supply rate will be equal to the space heat load. This equality of space load and heat supply rate was assumed. In this analysis, for reasons stated in the previous section on weighting factors, this was also assumed to be equivalent to the instantaneous heat gain. The space air transfer function is calculated by:

$$\sum_{n=0} p_n \Delta q_{\theta-n\delta} = \sum_{n=0} g_{n,t} \Delta t_{rc,\theta-n\delta} \qquad\qquad 3.5$$

where

Δq = variation of heat load from that at constant t_{rc} (W)
Δt_{rc} = temperature offset from constant t_{rc} (°C)
p_n, g_n = coefficients of space air transfer function

and

$$g_{0i,\theta} = g_0{}^*A + p_0K_{tot}$$ 3.6

$$g_{1,\theta} = g_1{}^*A + p_1K_{tot}$$ 3.7

$$g_{2,\theta} = g_2{}^*A + p_2K_{tot}$$ 3.8

where

K_{tot} = total conductance of the room envelope. (W/K)

A = floor area (m^2)

g_n *   = normalised coefficients of g_n (W/m^{2}K)

The SATF coefficients (p_n, g_n) were determined using the data listed in Table 3.4 as per *ASHRAE handbook* (1993) for light, medium and heavyweight construction. The p coefficients are non dimensional. The g^* coefficients are normalised values for a room with zero heat conductance and unit floor area. These had to be unnormalised to obtain values of g_n using Equations 3.6, 3.7 and 3.8. With the use generally lightweight construction, rooms with external frame walls and LW concrete walls with internal insulation were classified in the lightweight category. The LW concrete wall with exterior insulation, and the cavity wall were classified as medium construction.

Room envelope construction	p_0	p_1	p_2	$g_0{}^*$	$g_1{}^*$	$g_2{}^*$
Light	1.0	-0.82	0	9.54	-9.82	0.28
Medium	1.0	-0.87	0	10.28	-10.73	0.45
Heavy	1.0	-0.93	0	10.50	-11.07	0.57

Table 3.4 Space air transfer function coefficients, ASHRAE (1993) p- non-dimensional, g- W/m^{2}K.

Light construction: such as frame exterior wall, 50 mm concrete floor slab, approximately 150 kg of material per square metre of floor area.

Medium construction: such as 100 mm concrete exterior wall, 100 mm concrete floor slab, approximately 340 kg of material per square metre of floor area.

Heavy construction: such as 150 mm concrete exterior wall, 150 mm concrete floor slab, approximately 630 kg of material per square metre of floor area.

The SATF in Equation 3.5 is valid for either of the variables (air temperature or heat supply rate) as the driving term. In other words, the evaluation may be based on either the deviation in heat flux (Δq) in terms of specified offsets in air temperature (Δt_{rc}) or the evaluation of offsets in temperature in terms of specified deviations in heat flux. The validity also holds for mixtures of the two regimes, i.e. setting Δq for certain hours and Δt_{rc} for others.

The calculation was again performed in a spreadsheet. Using the occupancy schedule in Table 3.1 and the heat fluxes obtained from the CTFs, the occupied periods were specified with values of Δt_{rc} (offset from temperature used in the CTF) and the corresponding Δq expressed as in Equation 3.9. For unoccupied periods, the Δq was set to correspond to a zero heat supply rate with the corresponding Δt_{rc} expressed in a rearrangement of Equation 3.9. The SATF was calculated using an envelope to floor area ratio of 3.6 (assuming a room of dimension 6 x 6 x 2.5 m^3). From the solutions to the Δt_{rc} and Δq the corresponding air temperatures and heat supply rates were determined.

$$\Delta q_\theta = (-p_1 \Delta q_{\theta-1} + g_0 \Delta t_{rc,\theta} + g_1 \Delta t_{rc,\theta-1} + g_2 \Delta t_{rc,\theta-2}) / p_0 \qquad 3.9$$

where

$$\Delta t_{rc} = t_{rc,ref} - t_{rc}$$
$$\Delta q = q_{ref} - q$$

$t_{rc,ref}$ is the room air temperature used in the CTF, and the q_{ref} is the heating load (in this case equal to the instantaneous heat loss) previously established.

SATF Outputs

The resultant heat supply rates are shown in Figures 3.7, 3.8 and 3.9. These were used in the determination of the wall surface temperatures, which is described below and also in determination air flow rates required for space heating purposes in Section 3.6.1.

Estimated wall surface temperatures

Wall surface temperatures were determined on the basis of the assumption made during the course of the analysis (i.e. instantaneous heat loss being equal to the space heat load, which in turn is equal to the heat supply rate during equipment operation). The transient heat supply rates determined for the occupancy/operation schedule, using the SATF, were therefore assumed to be equivalent to the instantaneous heat loss. The wall surface temperatures were determined using this supply rate and assuming an internal heat transfer coefficient of 5.0 W/m^2K for a mixed convection regime (*Chen et*

al., 1989). It was also assumed that the room air temperature would rapidly approach the surface temperatures when the system was not in operation. The air temperature and wall surface temperature were therefore taken to be equal during floating periods. The estimated wall surface temperatures and corresponding air temperatures are shown in Figures 3.10, 3.11 and 3.12.

3.5   Wall surface temperature variations

Estimates of the surface temperatures in a room which might occur during the heating system operation were determined. This included the lowest temperatures expected after short periods of operation of the H & V system (these are referred to as the minimum surface temperatures) and the maximum temperature differences between the room surfaces. These results provided guidelines for the range of investigation of the H & V system in Chapters 4 & 5.

3.5.1   Minimum surface temperatures

If the neighbouring zones of a heated space are unconditioned, the wall temperatures within a room during unheated periods will approach the temperature of the exterior wall surfaces. Thus, the surface temperature of the exterior wall may be assumed to be the same as that of the remaining wall surfaces in the room enclosure at the start-up of the intermittent heating system. 'Minimum' surface temperatures were to be determined which would be experienced for a given insulation standard after short periods of operation of the system. These were determined for two climatic scenarios: the typical winter day; and the design day. Both of these ignore solar radiation.

The results of the surface temperature variation for the typical winter day without solar radiation and for the design day (Figures 3.10 -3.12) indicate a large increase in the surface temperature during the first hour of heating, followed by smaller and reducing increases in the subsequent hours. As expected, the configurations resulting in lower room thermal capacities, the frame wall (2) and wall with internal insulation (10a), exhibit more rapid increases and decreases of surface temperature at start-up and shut-down of heating, respectively. The lower thermal capacity rooms experience both the lowest and highest surface temperatures. These were however of similar magnitude to

those obtained in the rooms of greater thermal capacity during the first few hours after start-up. The surface temperatures achieved in the first hour after start-up were estimated from the Figures 3.10 - 3.12 and are shown in Table 3.5. The average ambient temperatures temperature of 2.4 °C is for the typical winter day and -16 °C to the design day.

U Value of wall (W/m^{2}K)	Ambient temperature (°C)	Surface temperatures within first hour (°C)
0.4	2.4 (average)	18
	-16	15
0.2	2.4 (average)	20
	-16	18

Table 3.5 Estimated minimum wall temperatures within an hour of start-up (from Figures 3.10 - 3.12).

3.5.2 Maximum variations in surface temperature

The maximum surface temperature variations were determined on the basis of the maximum and minimum coincident surface temperatures (i.e. in effect, presuming two exterior wall surfaces in the room: one exposed to solar radiation and the other not). Surface temperatures of walls with solar radiation were obtained for a south facing wall facade. These surface temperatures would in actual fact be overestimates, since similar conditions were assumed on the other wall surfaces within the room and therefore ignore radiant heat transfer to what, in practice, would be colder wall surfaces. The floating air temperature of the room is therefore also an overestimation. This was taken into consideration in the determination of the maximum surface temperatures likely to occur.
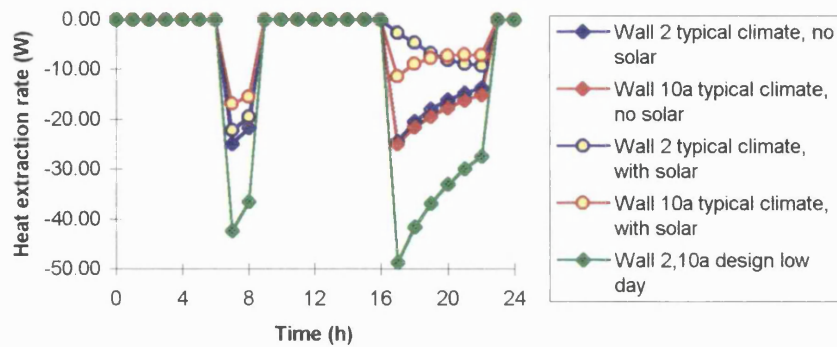
Figure 3.7 Heat supply rate for walls of U value 0.4. (per m^2 of wall area).
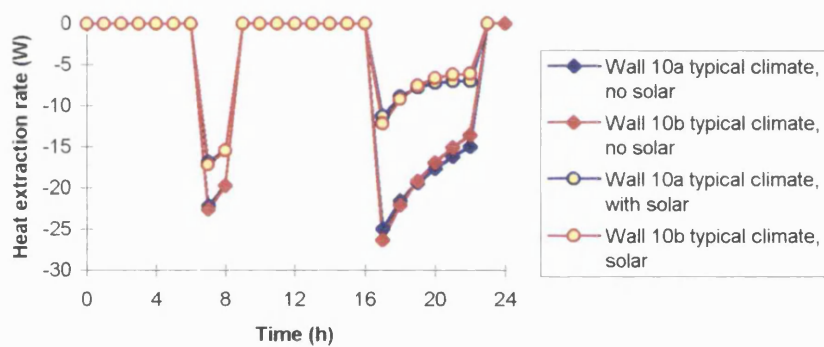
Figure 3.8 Heat supply rate for walls with internal and external insulation, U values 0.4.
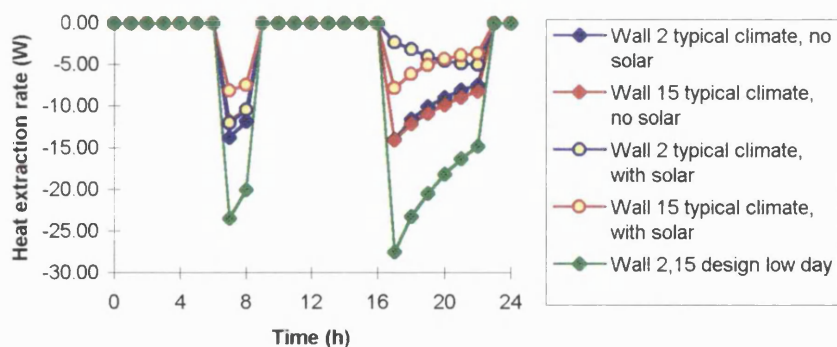
Figure 3.9 Heat supply rate for walls of U value 0.2.

Wall type 2   frame wall

Wall type 10a   wall with external insulation and integral insulation

Wall type 10b   wall with internal insulation

Wall type 15   wall with internal and integral insulation
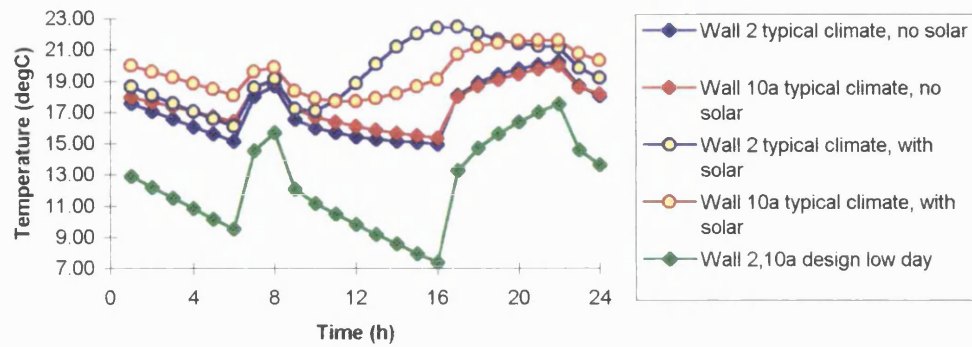
Figure 3.10 Wall temperature variations for wall with U value 0.4.
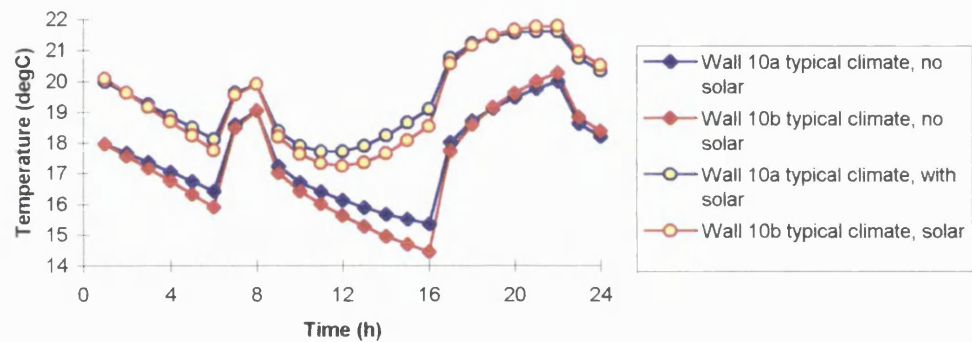
Figure 3.11 Temperature variation for wall type 10, with internal (10a) and external insulation (10b), U value 0.4.
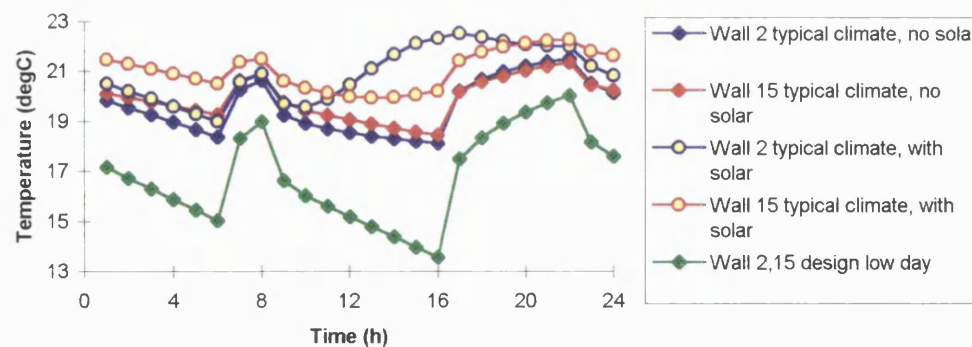
Figure 3.12 Wall temperature variations for wall with U value 0.2.

Wall type 2   frame wall
Wall type 10a   wall with external insulation and integral insulation
Wall type 10b   wall with internal insulation
Wall type 15   wall with internal and integral insulation

The surface temperatures obtained for the walls on a typical winter day with solar radiation (Figures 3.10 - 3.12) show large differences between the frame wall and the solid walls with greater swings in temperature of the frame wall. The solid walls, with greater thermal mass, retain higher and more moderate surface temperatures over longer periods into potentially more useful application times (assuming evening occupancy). This was expected and highlights the benefits of the use of thermal mass in south facing facades of 'passive' design. The positioning of the thermal mass within a solid wall appeared to have little influence on the internal surface temperatures (Figure 3.11). The maximum differences in surface temperatures during operation of the heating system were extracted from Figure 3.10, for the frame wall (2) and block wall (10a/b) for U values of both 0.4 and 0.2. (i.e. between each wall type with and without solar radiation). These are shown in Table 3.6. It was assumed that the surface temperatures of the frame wall in 'real' situations would not greatly exceed the 'overestimates' obtained for the block wall. It is these surface temperature differences, obtained from the block walls, that were used as guidelines in the investigation range in Chapter 5.

| Wall type	U Value of wall (W/m^2K)	Maximum difference in surface temperatures during heating (°C)
Frame wall	0.4	4.3
(2)	0.2	2.3
Block wall	0.4	2.7
(10a/b)	0.2	1.2

Table 3.6 Estimated maximum differences in surface temperatures on a typical winter day (from Figures 3.10-12).

3.6 Vertical temperature gradient in the side walls

In the provision of space heating, vertical air temperature gradients occur in the space/room. These air temperature gradients in turn, cause vertical temperature gradients in the side walls. The effect of these on the airflow pattern and air temperature distributions in a room were to be assessed (Chapter 5). To facilitate this investigation, a simple model was set up to estimate the magnitudes of vertical temperature gradients which may occur in the side walls.

A two dimensional, steady state, conjugate heat transfer model was set up in PHOENICS, using the two layer k-ε turbulence airflow model which was validated for indoor airflow in Section 2.2.3. This essentially consisted of two air streams flowing on either side of the conjugate wall structure of height 2.5m as shown in Figure 3.13. Supply air temperatures of 26 °C and 0 °C were used to represent the interior (warm side) and exterior zones (cold side) respectively. For both of these, the airflow rates were adjusted to obtain air temperature differences of the air bordering the wall surfaces of approximately 4 °C on the warm side and 1 °C on the cold side. This corresponded to bulk velocities of 0.03 and 0.3 m/s on the warm and cold sides respectively.
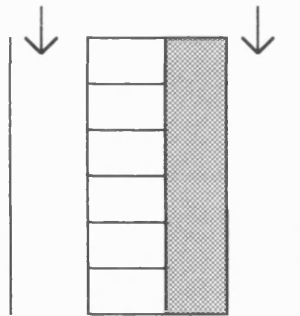
Figure 3.13 Sketch of flow setup used in the CFD investigation in Chapter 2.

Two wall configurations were assessed. One with internal placement of the insulation and the other with the insulation placed externally. Both of these walls were of U value of 0.4 W/m^{2}K and consisted of the same wall components: 80 mm of polystyrene (ρ = 25 kg/m^3, k = 0.035 W/m°C) and 100 mm of concrete block (ρ = 1400 kg/m^3, k = 0.51 W/m°C).

The internal surface temperatures obtained from the simulations are shown in Figure 3.14. These indicate a somewhat larger vertical temperature gradient for the wall with internal insulation. This result was to be expected, due to the lower thermal conductivity of the insulation. The estimated surface temperature differences between the top and bottom of the wall (for a 4 °C air temperature difference) are approximately 2.4 °C for external insulation and 3.1 °C for internally placed insulation.
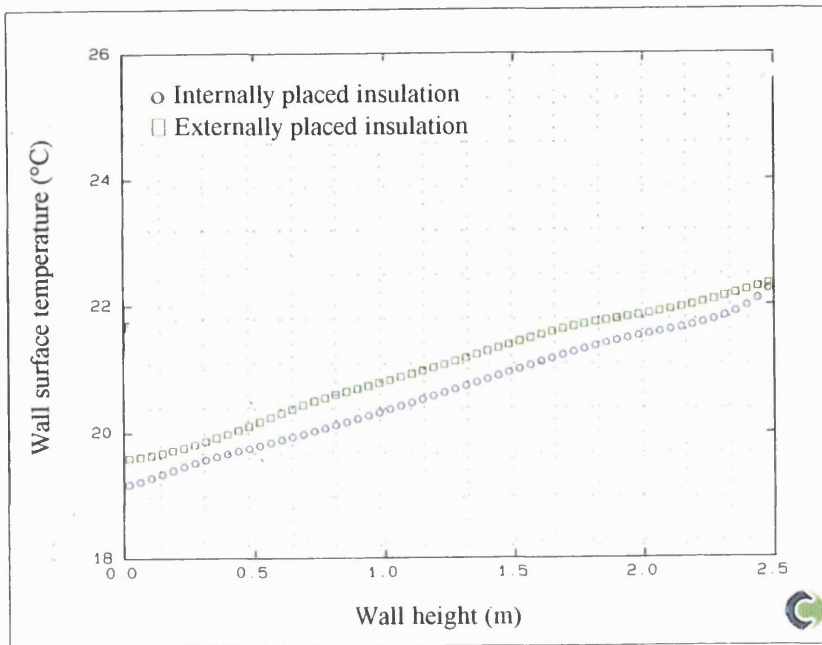
Figure 3.14 Vertical wall temperature variations obtained from CFD simulation.

3.7 Airflow rates

3.7.1 Space heating

Airflow rate requirements for space heating were determined for two climatic scenarios: the typical winter day and the design day within the first hour of operation of the heating system. The heat supply rates were extracted from Figures 3.7 - 3.9 using average values of the two construction types (solid and frame walls). In determination of the flow rates for space heat requirements internal heat gains were ignored for simplicity.

From Figure 3.7 heat supply rates at start-up were estimated to be 25 W/m^2 of wall area for the typical winter day and 40 W/m^2 for the design day. This resulted in peak heat supply rates for the room of approximately 3.3 and 5.3 kW for the two climatic scenarios (total wall surface area of 132 m^2). Assuming an extract air temperature equal to the occupied zone temperature, the flow rates and supply temperatures estimated to attain an occupied zone air temperature of approximately 22.5 °C are shown in Table 3.7.

ACH (/h)	Mass flow rate (kg/s)	Typical winter day Supply air temperature (° C)	Design day Supply air temperature (° C)
1	0.03	131	198
3	0.09	59	81
6	0.18	41	52
9	0.27	35	42

Table 3.7 Estimated supply air temperatures required to provide space heat demands at various flow rates.

For maximum supply temperature differentials of 15 °C (*ASHRAE handbook*, 1993), at a room temperature of 22.5 °C, supply air temperatures would be limited to magnitudes below 37.5 °C. This would require flow rates of up to 9 ACH for intermittent operation of the heating system on a typical winter day and somewhat beyond this for a design day. However as discussed in Section 1.4.1 supply air temperatures of up to 50 °C are frequently encountered in existing systems. This would correspond to airflow rate requirements of up to approximately 4.5 ACH for a typical winter day and 6 ACH for the design day.

3.7.2 Ventilation rates

Outdoor airflow rates were to be provided to satisfy the IAQ requirements, assuming a room of dimensions 6 x 6 x 2.5 m^3 and four persons in the room. One of these persons was assumed to be a smoker.

Two approaches were adopted in the determination of the required flow rates to meet the IAQ requirements (as mentioned in Section 1.2):

1. On the basis of the fresh air required in order to meet the recommended minimum ventilation rates i.e. not exceeding AIC levels for individual pollutants.

2. Using the olf/decipol criteria for perceived discomforts due to odours.

The ventilation rates required to maintain AIC values of the individual pollutants were evaluated on the basis of the data summarised in Table 1.4. The estimated ventilation rates (in ACH) evaluated are shown in Table 3.8. The table includes a listing of assumptions made in establishing the required flow rates. The ventilation rates required to meet the AIC values of CO_2, formaldehyde and water vapour were determined using Equations 1.1 - 1.4 listed in Section 1.2.1 with the assumptions listed in Table 3.8.

Pollutant	Assumptions	Recommendation of flow rate (l/s)	ACH (/h)
Human bioeffluents	sedentary activity, 4 persons (8 l/s pp)	32 l/s	1.2
Odours, materials & ventilation system	0.75 l/s per m^2 floor area	27 l/s	1.0
Carbon dioxide	sedentary activity, body surface area 1.8 m^2, CO_2 concentration inside 1000 ppm, outside 350 ppm, assuming 4 persons.	32 l/s	1.2
Formaldehyde	emission levels of 0.2 mg/h/m^2 from room surfaces excluding the floor.	45 l/s	1.8
Water vapour	3 l/24 h pp, outside air 0.004 kg/kg, 4 persons	7 l/s pp	1.1
Tobacco	additional 7 l/s pp .	15 l/s pp	0.6

Table 3.8 Minimum flow rates (in ACH) required for acceptable IAQ due to individual pollutants.

Similarly using the data listed in Table 1.5 on the olf loads due to materials, equipment and persons, the ventilation requirements (in ACH) were determined as listed in Table 3.9. The required flow rate of outside air was based on the perceived outdoor air pollution being negligible in comparison to the indoor air pollution. The required flow rates were evaluated using Equation 1.5 and using the *ASHRAE standard 62* (1989) recommendation of a maximum dissatisfaction level of 20% due to indoor air pollution.

Assumptions	Olf load (olf)	ACH to meet 20 % PD level (/h)
Average existing building stock + 4 sedentary persons	18.4	5.2
Average existing building stock + 4 sedentary persons, one smoker (average)	23.4	6.6
Low pollution building + 4 sedentary persons	7.6	2.2
Low pollution building + 4 sedentary persons, one smoker (average)	12.6	3.6

Table 3.9 Minimum flow rates (in ACH) obtained using the olf.

The range of ventilation rates obtained by the consideration of individual pollutants is therefore between 1.0 and 2.2 ACH (sum of odorous pollutants, persons + materials) assuming four non smokers in the room and extending to approximately 2.5 ACH with the presence of one smoker. The olf/decipol criteria in contrast obtained greater ventilation rate requirements in the range of 2.2 to 5.2 ACH for non smokers and 3.6 to 6.6 ACH with the presence of one smoker.

The ventilation rates obtained gave an indication of the minimum ACH required of the system if a 100% fresh air system was used. Using recirculating air systems, higher ACH would occur in the room.

The flow rates obtained for ventilation requirements were based on the continuous operation of the systems. Ventilation rates required for intermittent operation of the system were investigated in the CFD analysis described in Chapter 5.

3.8 Overview

The work described in this chapter was performed to identify the possible range of operation of the H & V system and the conditions within the room at start-up and during operation of the system. Using a combination of thermal and IAQ analysis. estimates of the following were obtained:

- Minimum wall surface temperatures in the room. These were determined for two climatic scenarios, a typical winter day and a winter design day. Climatic data for Munich was used as representative of a mid-European climate.

- Maximum differences in wall surface temperatures in a room. These were again determined for the typical winter day and winter design day with incident solar radiation on the external surface of one of the walls in the room. This wall was assumed to be south facing.

- Vertical surface temperature differences in heated rooms between the top and bottom of side walls.

- A range of flow rates and supply air temperatures required for space heating purposes.

- A range of outside airflow rates required for ventilation purposes.

4. CHOICE OF SUPPLY AND EXTRACT AIR TERMINAL DEVICE (ATD) CONFIGURATION

The position, type and size of air terminal devices (ATDs) influence air distribution within a room. Good air distribution should achieve effective air movement and distribution within the room to attain satisfactory levels of thermal comfort and indoor air quality throughout the occupied zone, whilst minimising the non-uniformity of these. This includes the elimination of excessive temperature variations and air movement (draught) within the room. This Chapter presents the investigation of the influence of ATD configuration on the indoor environment, and concludes with the identification of a suitable configuration for the required H & V system. The H & V system needs to provide optimum levels of thermal comfort and indoor air quality over the possible range of flow conditions. Energy considerations will be a part of the assessment criteria. The investigation was conducted by CFD modelling of the indoor airflow, heat and pollutant transfer.

The procedure/sequence of the investigation is presented in the order shown below:

1. Identification of ATD configurations for investigation (Section 4.1)
2. Definition of the room configuration used in the CFD simulations (Section 4.2)
3. Evaluation criteria and procedures (Section 4.3)
4. Specification of the investigative range (Section 4.4)
5. Simulations (Section 4.5)
6. Analysis of the results and proposal of a suitable configuration of the H & V system (Section 4.8)
7. Discussion of the results (Section 4.9)

4.1 ATD Configurations

The ATD configurations investigated are listed below and shown in Figures 4.1a-f. These evolved as a consequence of the review in Chapter 1 and also as a result of feedback from initial investigations which were performed on the following two ATD configurations:-

Configuration A   High level supply, low level extract; on the same wall surface. (Figure 4.1a)

Configuration B   Low level supply, high level extract; on the same wall surface. (Figure 4.1b)

As a consequence of observations made from the initial investigations, three other configurations were evaluated:-

Configuration C   High level supply, high level extract, on the same wall surface. (Figure 4.1c)

Configuration D   Low level supply, low level extract, on the same wall surface. (Figure 4.1d)

Configuration E   Low level inlet, low level outlet, on opposite wall surfaces. (Figure 4.1e)

All configurations used slot type openings located on the side walls. The effect of using two supply/extract ATDs located on the sides to replace the single central device was also investigated. This configuration is shown for configuration A in Figure 4.1f and is applicable to all of the above configurations. These will be denoted as 'configuration A-2', for example.

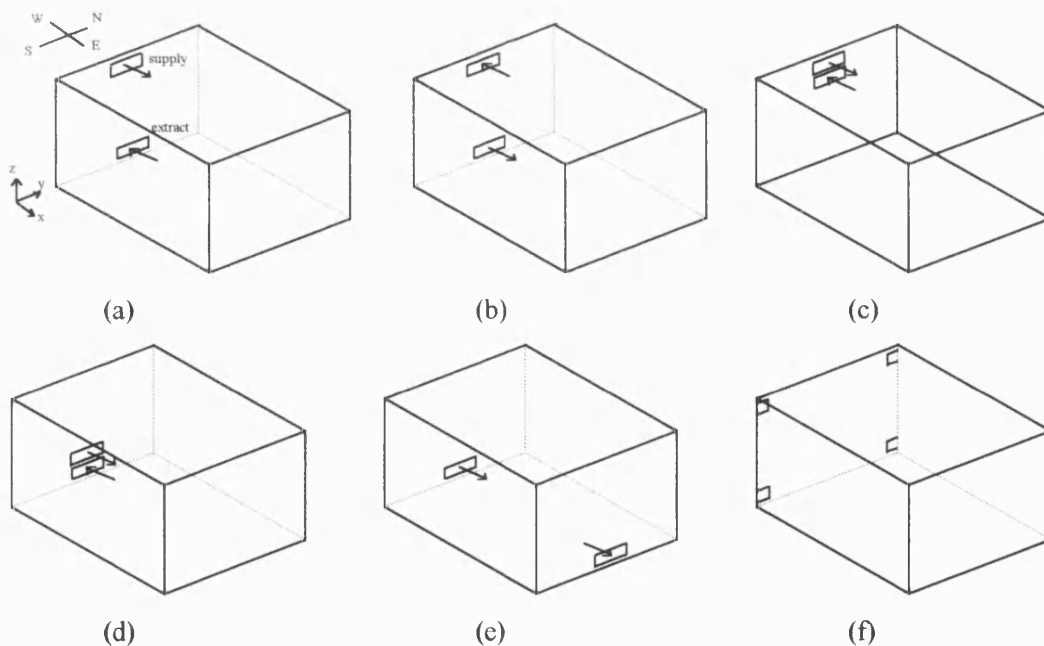

Figure 4. 1a-f Supply and extract ATD configurations investigated. (a) Configuration A, (b) Configuration B, (c) Configuration C, (d) Configuration D, (e) Configuration E, (f) Configuration A-2.

4.2 Room Configuration

A bare enclosure of dimension 6 x 6 x 2.5 m^3 was used in the comparison of the ATD configurations. This enclosure was represented by a Cartesian grid of 33 x 35 x 27

cells in the x, y and z directions respectively, corresponding to the grid orientation shown in Figure 4.1a. This grid distribution was determined in Section 2.2.4, using criteria outlined therein. An occupied zone was designated (with boundaries to match the grid used) as the space within the room, up to approximately 10 cm from the side walls and between the heights of 0.07 m to 1.43 m above the floor. The following convention is adopted throughout: low x: WEST, high x: EAST, low y: SOUTH, high y: NORTH, low z: FLOOR, high z: CEILING (x, y, z orientation in the room is as shown in Figure 4.1a).

Supply and extract ATDs were all of height 0.17 m. Variations in ATD area were accounted for by increases or decreases in the width of the devices. The centre heights of the ATD were located at the heights shown in Table 4.1.

Configuration	Supply ATD height (m)	Extract ATD height (m)
A	2.3	0.2
B	0.2	2.3
C	2.3	2.0
D	0.3	0.1
E	0.3	0.3

Table 4.1 Supply and extract ATD centre heights.

Enclosure surface temperatures were specified as fixed and uniform temperatures, the magnitude of which is given in Section 4.4. Pollution sources were specified as being at the enclosure surfaces. Pollutant source fluxes were prescribed as fixed fluxes per unit surface area on all enclosure surfaces.

4.3 Evaluation criteria and procedures

The CFD outputs consist of distributions of air temperature, air velocity, turbulent kinetic energy and pollutant concentrations within the room. These were used in the evaluation of the thermal environment, IAQ and energy consumption. The analysis of IAQ and energy consumption is relatively straightforward. IAQ was assessed in terms of the magnitude and distributions of the pollutant concentration within the space. Energy requirements was assessed on the basis of the enthalpy difference between the supply and extract air stream. The assessment of thermal comfort was performed on

the basis of the thermal sensation (measured by the *PMV*) and local thermal discomforts due to draught and vertical air temperature difference. In the following sections, the numerical criteria used in the assessment of thermal comfort will, first of all, be specified. This includes the specification of limiting values (i.e. acceptable limits) of the local thermal discomforts which were applied in the evaluation. These will be referred to as the acceptable limits to distinguish between the limits herein specified and the recommendation of the International Standards. Following the specification of the numerical evaluation criteria, and therefore identification of the necessary variables in the calculation of these, the procedure used to obtain the relevant variables (for the assessment of the comfort criteria) from the CFD outputs files is outlined. This is however preceded by a description of the format of the CFD output files.

Thermal sensation

Thermal sensation was measured using *Fanger's* predicted mean vote (*PMV*). This was calculated using Equations 1.7 - 1.10. The mean radiant temperature (t_r) was determined using the area-weighted average of the room surface temperatures. This disregards a person's location or orientation within the room.

$$t_r = \sum_s \left(t_s A_s \right) / \sum_s A_s \qquad\qquad 4.1$$

where

A_s = individual wall surface areas (m^2)
t_s = surface temperature (°C)
s = individual surfaces

ISO standard 7730 (1993) recommends *PMV* in habitable rooms be maintained between the range of $-0.5 < PMV < 0.5$. The investigation performed comparisons at average *PMV*s in the occupied zone of close to neutral values (i.e. zero). Initial comparisons were based on the magnitudes and uniformity of *PMV*s in the occupied zone for the various configurations, at similar supply air conditions (temperature and flow rate). In addition, some comparisons were made at similar *PMV*s in the occupied zone. The latter enabled direct comparison of the comfort conditions and energy requirements of the configurations at similar comfort levels.

Vertical air temperature difference

Using a polynomial fit to the data derived by *Olesen et al* (1979) and shown in Figure 1.2, the percentage dissatisfied ($PD_{\delta T}$) due to vertical air temperature difference between a height of 0.1 and 1.1m was calculated by:-

$$PD_{\delta T} = 0.0004 + 0.3276\delta T + 0.2580\delta T^2 + 0.1177\delta T^3 \qquad 4.2$$

where

$PD_{\delta T}$ = percentage dissatisfied due to vertical air temperature difference (%)
δT = vertical air temperature difference between 0.1 m and 1.1 m (°C)

Vertical air temperature differences were evaluated between the heights of 0.07 m and 1.0 m (matching the grid used). This was assumed to produce similar temperature differentials as those that would be obtained between the heights of 0.1 m and 1.1 m, as specifed in the standard. The *ISO standard 7730* recommendation of a maximum temperature difference of 3 °C was to be applied. This corresponds to a percentage dissatisfied of 6.5%.

Draught

Draught was measured using *Fanger's* model of draught risk, which includes the influence of velocity fluctuations. This was calculated using Equation 1.12. The limit for acceptable levels of draught was specified as 6.5% dissatisfaction level, to correspond with the dissatisfaction limit due to vertical air temperature differences. This dissatisfaction limit surpasses the requirements of the current international standards (as listed in Section 1.3.2). The turbulence intensity in Equation 1.12 was determined using the relation between the turbulence intensity (TI) and turbulent kinetic energy (k) as defined by Equation 4.3 where $\dot{v}$ is the relative air velocity.

$$TI = 100(2k)^{0.5} / \dot{v} \qquad 4.3$$

4.3.2 CFD outputs

CFD distribution outputs may be obtained in graphical or numerical format, the latter being required for application in numerical processes. The numerical outputs were written into a 'result' file which also included a combination of the input conditions (initial and boundary conditions) and values of variables or constants used in the

solution of the flow equations/variables. The solutions include the distributions of air temperature, velocity, turbulent kinetic energy and pollutant concentration. For economy of computer storage, this result file typically contains the distributions of the output variables at a reduced number of nodes. For the application in room airflow, a reduced number of nodes provides satisfactory representation due to the gradual nature of the change in conditions within the room.

The CFD results were output in a standard format to allow the use of the same numerical evaluation scheme (program) for all cases. Distributions of variables at 270 nodes were written into the result file, with the largest distances between the nodes being 0.25 m. (nodes: $x = 5,8,11,14,17,20,23,26,29$, $y = 3,6,9,12,15,18$ (symmetrical half) and $z = 3,6,9,12,15$). These node points covered the occupied zone and extended into regions beyond, in the vicinity of the side walls. The region in the wall vicinity is not of immediate interest in this section, however it will be used in Chapter 5 in the assessment of sensor locations. Within the occupied zone, the distribution of selected nodes is relatively even with inter-node distances of approximately 0.25 m. Smaller distances are chosen in the near-wall region.

The variables of interest in the evaluation of thermal comfort, IAQ and energy consumption are the:

> air temperatures in the occupied zone, t_a (°C)
>
> surface temperatures of the enclosure, t_s (°C)
>
> supply air temperature, t_{on} (°C)
>
> extract air temperature, t_{off} (°C)
>
> air velocities in the occupied zone, v (m/s)
>
> turbulent kinetic energies in the occupied zone, k (kg m^2/s^3)
>
> pollutant concentrations in the occupied zone, c (ppm)
>
> mass flow rate, $\dot{m}$ (kg/s)

Solutions to the energy equation were obtained in terms of enthalpy with the specific heat capacity of air at a constant value of 1005 J/kgK. The air temperatures were determined from these.

4.3.3 Evaluation scheme

A numerical evaluation scheme was constructed to calculate the *PMV* and local thermal discomforts at designated points (from the CFD result file) in the occupied zone. The *PMV* was evaluated for pre-defined values of personal activity rate and clothing insulation and water vapour pressure in the zone. The values of the *PMV* and local thermal discomforts due to draught and vertical air temperature difference were stored for graphical assessment and also summarised in statistical format (average, minimum, maximum and standard deviations within the occupied zone) in an output file.

4.4 Range of investigation (flow rates, supply air temperatures and wall surface temperatures)

Flow rates

An estimate of the possible range of flow rates was determined in Chapter 3. This estimated airflow rates of up to 6 ACH for space heating requirements and flow rates of between 1 and 6 ACH for ventilation purposes. On the basis of this, two flow rates were selected for comparison of the configurations. These were airflow rates of 3 and 6 ACH to represent a mid-range and possible high end value of the likely range.

Supply air temperatures

Fixed supply air temperatures were used at each of the flow rates. These were determined by trial runs on configuration A. At each of the flow rates, the supply air temperature was varied to achieve average *PMV*s in the occupied zone of close to zero (i.e. neutral *PMV*).

Wall surface temperatures

Design wall surface temperatures were determined as explained in Section 3.5.1. This produced estimates of internal wall surface temperatures for a building of U value of 0.4 W/m²K of approximately 18 °C within an hour of commencement of space heating, at outside ambient temperatures of approximately 0 °C. Similarly, at U values of 0.2 W/m²K the surface temperatures approached 20 °C within the first hour. An average

of these values was used in this assessment (i.e. wall surface temperatures of 19°C). All surfaces within the room were assumed to be at this temperature.

4.5   Simulations

CFD simulations were performed using the two layer k-ε turbulence model, validated for indoor airflow as discussed in Chapter 2. Supply outlets were modelled using the basic inlet model (i.e. the ATD geometry equivalent to the effective area[1]).

The simulations and subsequent analysis were performed in three stages:-

1. Determination of suitable ATD areas and therefore supply momentum.
2. Investigation of the influence of the location of the ATD devices.
3. Comparison of ATD configurations, for the optimum size/location of each of these.

In *Stage 1* the influence of the supply momentum on the IAQ and thermal comfort in the room was assessed. On the basis of this, optimum ATD sizes for each of the configurations were identified. Due to the reduced influence of the extract device, the investigation was restricted to just some of the configuration types which have the same supply location. The evaluations were performed on configuration A for the high level supply and configurations B and D for the low level supply. These were also used in the investigation of the locations in *Stage 2*, which used the alternative configuration of supply devices shown in Figure 4.1f. In *Stage 3*, on the basis of the results from *Stages 1 & 2*, simulations were performed for the remaining configurations, C and D, at the optimum sizes and locations identified.

The simulations performed are shown in Table 4.1. The table groups the simulations according to ATD configuration type. Within each group (ATD type), the simulations performed are listed in rows, in order of increasing supply area. At each supply area, the supply parameters used are listed in the corresponding columns. The extract ATDs are of approximately equal area to the supply and are not listed.

---

[1] *Effective area:* Sum of free areas of ATD device

4.6 Results

A summary of numerical results obtained for the various configurations is shown in Table 4.3, which uses the same order of presentation as for the simulations performed in Table 4.2. For ease of reference in the ensuing discussions, the Table includes an allocation of a Run Number for each case. This Run Number does not represent the sequence of the investigation. The table lists the values of interest in the evaluation of the thermal comfort, IAQ and energy consumption. This includes the extract air temperature (t_{off}) and the average and standard deviation within the occupied zone of the following:-

- air temperature (t_{ave}, t_{sd})
- air velocity (v_{ave}, v_{sd})
- PMV (PMV_{ave}, PMV_{sd})
- percentage dissatisfied due to draught $(PD_{v\,ave}, PD_{v\,sd})$
- percentage dissatisfied due to vertical air temperature difference $(PD_{\delta T\,ave}, PD_{\delta T\,sd})$
- pollutant concentration within the occupied zone (c_{ave}, c_{sd})

In the evaluation of the PMVs, typical winter indoor clothing values were assumed with the occupants at sedentary activity rate. A water vapour pressure in the air (P_a) was specified to correspond with a relative humidity of 50 % at 22 °C. The values of these used in the analysis were:-

$M = 70$ W/m^{2}K   (sedentary activity)

$W = 0$ W/ m^{2}K   (no external work)

$I_{cl} = 0.16$ m^2°C/W   (typical winter indoor clothing ensemble)

$P_a = 1400$ pa   (corresponding to approximately 50% RH at 22 °C)

For economy of presentation, graphical illustrations of the flow variables will be restricted to a number of locations which were found to be representative of the conditions in the room. Graphical results were grouped for each configuration type and within these by flow rate. These illustrations are added as an appendage at the end of this chapter, and will be denoted in the following format: Figure 4.Axx.

ATD Configuration (as listed in section 4.1)	Supply Area (m2)	ACH (/h)	Supply velocity (m/s)	Supply air temperature °C
A	0.07	3	1.1	42
	0.12		0.62	
	0.17		0.44	
	0.25		0.3	
	0.07	6	2.2	30
	0.12		1.24	
	0.17		0.88	
	0.25		0.6	
B	0.17	3	0.44	42
	0.25		0.3	
	0.17	6	0.88	30
	0.25		0.6	
C	0.25	3	0.3	42
	0.25	6	0.6	30
D	0.25	3	0.3	42
	0.44		0.17	
	0.25	6	0.6	30
	0.44		0.34	
E	0.25	3	0.3	42
		6	0.6	30
A-2	0.23	3	0.33	42
		6	0.66	30
B-2	0.23	3	0.33	42
		6	0.66	30
D-2	0.24	3	0.31	42
		6	0.62	30

Table 4.2 Simulations performed to investigate appropriate ATD configuration(s).

Config uration	A_{on}	t_{on}	t_{ave}	t_{sd}	t_{off}	v_{on}	v ave	v sd	PMV ave	PMV sd	PD_v ave	PD_v sd	$PD_{\delta T}$ ave	$PD_{\delta T}$ sd	c_{ave}	c_{sd}	Run No.
	(m²)	(°C)	(°C)	(°C)	(°C)	(m/s)	(m/s)	(m/s)			(%)	(%)	(%)	(%)	(ppm)	ppm)	
A	0.07	42	22.0	1.5	20.9	1.10	0.021	0.033	-0.10	0.16	0.9	3.9	7.6	2.8	13.5	7.0	1
	0.12	42	21.8	1.4	20.8	0.62	0.018	0.026	-0.11	0.15	0.6	2.5	6.6	2.6	13.4	6.9	2
	0.17	42	21.8	1.4	20.7	0.44	0.017	0.023	-0.11	0.15	0.5	2.0	6.3	2.6	13.3	6.6	3
	0.25	42	21.8	1.4	20.7	0.30	0.017	0.022	-0.11	0.15	0.5	1.7	6.1	2.6	13.3	6.4	4
	0.07	30	22.5	1.0	22.0	2.20	0.107	0.073	-0.09	0.11	9.5	10.8	3.4	2.9	9.2	4.5	5
	0.12	30	22.4	1.2	21.9	1.24	0.054	0.057	-0.06	0.12	3.3	6.8	5.1	2.8	7.6	4.8	6
	0.17	30	22.4	1.2	21.8	0.88	0.039	0.048	-0.06	0.13	2.1	5.2	5.2	2.6	7.0	4.0	7
	0.25	30	22.4	1.2	21.7	0.60	0.033	0.041	-0.06	0.12	1.8	4.3	5.1	2.6	6.8	3.7	8
B	0.17	42	22.0	1.9	27.3	0.44	0.052	0.090	-0.09	0.25	1.9	4.3	5.3	13.2	25.1	4.5	9
	0.25	42	21.7	1.6	27.8	0.30	0.045	0.075	-0.13	0.17	2.3	6.3	4.5	8.7	27.6	4.8	10
	0.17	30	22.5	1.1	23.2	0.88	0.094	0.098	-0.07	0.12	8.4	13.3	2.4	5.6	10.2	2.1	11
	0.25	30	22.2	1.1	23.7	0.60	0.083	0.072	-0.10	0.12	6.5	9.3	2.7	4.3	11.4	2.5	12
C	0.25	42	19.3	0.5	24.6	0.30	0.002	0.003	-0.37	0.06	0.0	0.0	0.1	0.3	115	84	13
	0.25	30	19.5	0.8	24.3	0.60	0.004	0.009	-0.35	0.09	0.0	0.6	0.2	0.5	100	89	14
D	0.25	42	22.9	1.6	21.9	0.30	0.057	0.072	0.00	0.17	2.7	5.7	7.1	12.0	13.1	3.0	15
	0.44	42	22.8	1.5	21.8	0.17	0.050	0.067	-0.02	0.16	2.5	5.5	7.4	10.9	12.8	3.4	16
	0.25	30	21.8	1.0	24.7	0.60	0.078	0.060	-0.13	0.10	6.1	9.3	1.8	2.9	11.5	2.3	17
	0.44	30	22.3	1.1	23.4	0.34	0.075	0.058	-0.09	0.11	5.0	7.1	2.9	4.4	8.2	2.4	18
E	0.25	42	22.8	1.3	22.2	0.30	0.055	0.069	-0.02	0.13	3.1	6.5	6.2	9.3	16.5	4.2	19
	0.25	30	22.8	1.0	22.5	0.60	0.090	0.058	-0.04	0.11	6.6	6.9	2.9	3.3	8.5	2.1	20
A-2	0.23	42	21.8	1.4	20.7	0.33	0.016	0.022	-0.11	0.15	0.5	1.8	6.0	2.6	13.6	7.5	21
	0.23	30	22.3	1.2	21.7	0.66	0.034	0.038	-0.06	0.12	1.7	4.3	5.1	2.5	7.1	4.2	22
B-2	0.23	42	21.6	1.8	27.7	0.33	0.044	0.092	-0.13	0.20	1.8	5.2	5.6	15.4	28.7	6.3	23
	0.23	30	22.4	1.2	23.1	0.66	0.087	0.084	-0.08	0.12	7.2	10.1	2.6	5.3	10.5	2.5	24
D-2	0.24	42	22.9	1.9	21.9	0.31	0.056	0.087	0.00	0.22	2.5	5.1	8.3	18.2	14.0	4.3	25
	0.24	30	21.1	1.0	25.4	0.62	0.070	0.063	-0.16	0.10	5.5	9.7	1.5	2.4	14.4	2.9	26

Table 4.3 Summary of numerical evaluation data obtained from the simulations listed in Table 4.2

4.8 Analysis of the results

As stated earlier, analysis of the configurations will be performed using graphical representations of the distributions of variables within the room and the numerical results listed in Table 4.3.

In the evaluation of thermal comfort, the distribution of the *PMV* and the local discomforts are of particular importance. These are however dependent on the flow parameters, in particular the air temperature and velocity. Therefore, air temperature (enthalpy) and velocity distributions will be shown to provide a better insight into the flow, and the resultant effects on thermal comfort. These distributions will not be described in any detail, but will be referred to mainly for the purposes of clarification. 'Average values' refer solely to the occupied zone.

Distributions of *PMV* and the percentage dissatisfied due to draught (PD_v) will be presented in two planes. These are both in the East-West plane: the *symmetry* plane (grid $y = 18$) and an *outer* plane at distance of approximately 10 cm from the side wall (grid $y = 3$). Velocity and temperature distributions unless otherwise stated are in the symmetry plane of the room (grid $y = 18$).

4.8.1 Influence of ATD-area / supply-momentum on thermal comfort and IAQ

The results obtained on the influence of the supply area/momentum in the high level supply configurations are discussed first, followed by those on the low level supply configurations.

High level supply (Configuration A)

Four supply ATD areas and supply velocities were investigated. These were not pre-selected before the investigation began, but evolved from observations of the initial case and the effect of the ensuing increments in ATD area. Initial simulations were performed at 3 and 6 ACH, for an ATD supply area of 0.07 m^2. The resulting supply velocities of 1.1 and 2.2 m/s are fairly standard magnitudes in air conditioning (cooling/ventilation) applications. The early analysis was performed on numerical results (as in Table 4.2), indicating unacceptably high discomfort levels due to draught

(PD_v) in the occupied zone at 6 ACH. The attempt to reduce high velocities in the room and subsequent discomfort due to draught led to an increase in the supply ATD area from 0.07 m^2 to 0.12 m^2. This was seen to achieve considerably lower level velocities and draught. The supply area was further incremented until this had negligible effect on the thermal environment in the occupied zone.

For economy of presentation, the effect of the supply velocity/momentum will be shown in comparisons of the distributions of *PMV* and *PD$_v$* for the two extreme cases (minimum and maximum supply velocity) at ATD areas of 0.07 m^2 and 0.25 m^2. These will be referred to as the high and low supply velocity cases, respectively.

At 3 ACH, the high supply velocity resulted in marginally higher *PMV*s in the occupied zone than at the low supply velocity. This is seen in comparison of the iso-lines of constant *PMV* (contours) in Figures 4.A1a-b at the high supply velocity and in Figures 4.A5a-b at the low supply velocity, in the symmetry plane (*a*) and outer plane respectively (*b*). The contours show a *PMV* range of -0.4 to +0.1 between the floor and ceiling of the room at the high supply velocity, with a *PMV* at the centre of the room of approximately -0.05. In comparison, at the low supply velocity, a range of - 0.3 to -0.1 was obtained with the *PMV* in the room centre of approximately -0.1. This increase in *PMV*s may also be seen in the values in Table 4.3 (Run Nos. 1 & 4). The increase in *PMV* is seen to correspond with somewhat higher air velocities (Figure 4.A2) and air temperatures (Figure 4.A3) in the occupied zone at the high supply velocity in comparison to the low supply velocity (Figure 4.A6 - velocity and Figure 4.A7 - temperature). The high supply velocity therefore attained higher *PMV*s, despite the increased velocities. This may be explained by the mode of heat transfer, which at the pertaining velocities for both cases, is by free convection; the air velocity therefore had little or no influence on heat loss from the body or the *PMV* (transition from free to forced convection between 1-2 m/s (*Fanger*, 1970)). Distribution of *PMV*s in both cases were fairly uniform across the room.

At both supply velocities at 3 ACH, satisfactory comfort conditions were achieved with respect to draught i.e. draught levels below 6.5% dissatisfaction. This is seen in the contours of discomfort due to draught (*PD$_v$*) in the symmetry and outer planes respectively in Figures 4.A1c-d at the high supply velocity and 4.A5c-d at the low

supply velocity. These contours show discomfort levels due to draught in excess of 6.5% only in the immediate vicinity of the extract devices (Figures 4.A1c and 4.A5c), with higher magnitudes at the higher supply velocity. In the symmetry planes, the blank chart with no contours displayed was because draught dissatisfaction levels did not exceed 2% (which were not displayed in the contours). The low magnitudes of discomfort due to draught are also shown by the figures in Table 4.3 (Run. Nos. 1 & 4).

At both supply velocities (at 3 ACH) the vertical air temperature differences caused dissatisfaction levels ($PD_{\delta T}$) in excess of the 6.5% acceptable limit, as shown in Table 4.3 (Run Nos. 1 & 4). A lower dissatisfaction level due to vertical air temperature differences was obtained at the higher supply velocity, the difference was however minimal.

At 6 ACH, the effect of higher supply velocity on the *PMV*s was the reverse of that at 3 ACH. The high supply velocity (Figures 4.A9a-b) resulted in lower *PMV*s in the occupied zone than at the low supply velocity (4.A13a-b). These lower *PMV*s were however accompanied by both higher velocities *and* temperatures than for the low supply velocity case as seen in distribution of velocities in Figures 4.A10 and 4.A14 at the high and low supply velocities respectively, and similarly in the distribution of temperatures in Figures 4.A11 and 4.A15. At the high supply velocity, the resulting room air velocities therefore had an influence on the *PMV*, with the reduction in *PMV*s due to the increase in air velocities. The influence of the velocities on the *PMV* (and heat transfer from the body) is also observed in the dissimilar distribution between the *PMV* (Figure 4.A9a) and temperature (Figure 4.A11). Air velocities in the occupied zone at the low supply velocity, appear to have little influence on the *PMV*, with the distribution of *PMV* (Figure 4.A13a) across the room seen to be uniform and similar to that of the air temperature (Figure 4.A15).

In addition to the greater cooling effect, the high supply velocity (at 6 ACH) resulted in unacceptably high discomfort due to draught of between 5-10% dissatisfaction for most of the occupied zone (Figures 4.A9c-d). At the lower supply velocity, the discomfort level was within the acceptable limits (Figures 4.A13c-d).

Satisfactory vertical air temperature differences were obtained at both supply velocities (at 6 ACH), as seen in the dissatisfaction levels $(PD_{\delta T})$ in Table 4.3 (Run Nos. 5 & 8). Reduced vertical air temperature differences were obtained in the central region of the room at the higher supply velocity. This however was also accompanied by greater temperature non-uniformities across the room, as was seen in the distribution of temperatures in the symmetry plane (Figure 4.A11).

At both flow rates, the higher temperatures and velocities obtained in the occupied zone at the higher supply velocities appear to be as a direct consequence of these increased supply velocities. The increase in velocities would appear to be due to greater entrainment (of the air surrounding the supply air stream) and therefore air movement. The greater momentum of this induced air-stream achieves greater penetration into the eastern region of the occupied zone. This results in a larger proportion of the warm supply air being carried directly into the occupied zone with less dispersion of heat in regions above this. The penetration and spread of the incoming air-stream is shown in Figures 4.A4 and 4.A8 at 3 ACH and Figures 4.A12 and 4.A16 at 6 ACH, at the high and low supply velocities respectively.

To summarise, at the low flow rate of 3 ACH the supply velocity had little influence on thermal comfort within the room. Vertical air temperature differences exceeded the acceptable dissatisfaction limits. Therefore, at the specified thermal boundary conditions, higher flow rates would be required to avoid discomfort due to vertical air temperature differences. At the high flow rate of 6 ACH, the supply velocity was found to have a greater influence, with the possibility of unacceptably high air-movement in the occupied zone as well as thermal non-uniformities. The high air-movement may result not only in high levels of discomfort due to draught, but also contribute to additional cooling of the body.

The results indicate that a fixed geometry ATD device may be used for application over the range of flow rates required of the H & V system. For prevention of draught, this should be sized on the basis of the maximum flow rate. Over the investigated flow range, no significant advantage would be expected to be gained by the use of a variable

geometry device. For the current application, where flow rates are not expected to greatly exceed 6 ACH, a supply device of core area 0.25 m^2 would appear to be suitable for the room of dimension 6 x 6 x 2.5 m^3.

Low level Supply (Configurations B and D)

Following the observations made for the high level supply, initial investigations for a low level supply were performed using configuration B. These were at 3 and 6 ACH with supply ATD areas of 0.17 m^2 and 0.25 m^2. Configuration D evolved as a consequence of the observations made on configuration B. This used supply ATD areas of 0.25 m^2, and a further increase to 0.44 m^2. The observations made on each of these configurations are outlined below. As in the previous Section, the cases will be referred by the relative magnitudes of supply velocity for each case, i.e. low/high supply velocity.

Configuration B

Distributions of *PMV*, *PD$_v$* , air velocity and air temperature obtained at both 3 and 6 ACH and the two supply ATD areas are shown respectively in the figures indicated below:-

3 ACH:	high supply velocity	Figures 4.A17a-b, 4.A17c-d, 4.A18 & 4.A19
	low supply velocity	Figures 4.A20a-b,4.A20c-d, 4.A21 & 4.A22

6 ACH:	high supply velocity	Figures 4.A23a-b, 4.A23c-d, 4.A24 & 4.A25
	low supply velocity	Figures 4.A27a-b, 4.A27c-d, 4.A28 & 4.A29

At both 3 and 6 ACH, higher *PMV*s were attained for the high supply velocities in comparison to those at the low supply velocities, with associated increases in both velocity and temperature. These increases in *PMV* were therefore clearly, due to the increase in temperature in the occupied zone. The significant temperature increases were due to increased penetration of the warm air-stream directly into the occupied zone. This had a two-fold effect: a) greater enthalpy transport of the supply air directly into the occupied zone and b) reduction of the short-circuiting of the supply- air, particularly at the low flow rate. It can be seen that at 3 ACH, and low supply velocity, the buoyant plume rises directly towards the extract as illustrated in the sketch in

Figure 4.2. This assumption of short-circuiting of the (unpolluted) supply air is supported by the high values of pollutant concentration (c_{ave}) in the occupied zone at low supply velocity (Table 4.3, Run No. 10) in comparison to the case with high level supply (Table 4.3, Run No.4).
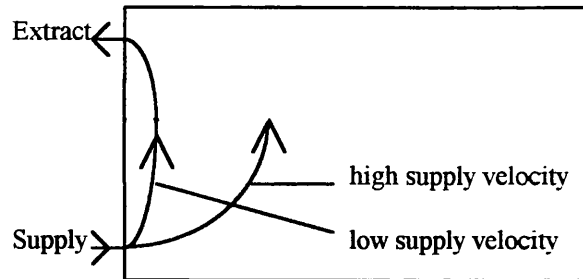
Figure 4.2 Illustration of short-circuiting of the supply air for low ACH of configuration B.

At 3 ACH, discomforts due to draught were within the acceptable limits for most of the occupied zone at both the high (Figures 4.A17c-d) and low supply velocities (Figures 4.A20c-d). Higher discomfort due to draught occurred in the region approaching the west-wall at the low supply velocity. This would be attributed to the lower air temperatures in the region, presumably as a consequence of the greater amount of short-circuiting of the warm supply air. At 6 ACH, unsatisfactory levels of draught were experienced in large parts of the occupied zone at both the high (Figure 4.A23c) and low supply velocity (Figure 4.A27c). (These contours in the symmetry plane were found to representative for most of the occupied zone). High air velocities are observed, not just in the warm supply air stream, but also in the regions surrounding this warm air plume. The low supply velocity resulted in less penetration of this warm supply air into the occupied zone and also in somewhat lower air velocities in the warm supply air plume itself. The surrounding regions, however, are at similar velocities as those obtained for the high supply velocity, with a similar proportion of the room exceeding the acceptable draught limits. This indicates the occurrence of high velocities in the occupied zone, being not in the path of the incoming warm air stream alone. High velocities also occur in the rest of the room presumably due to the air movement caused by the induction of the air surrounding the buoyant plume. This is seen in the velocities in the symmetry plane (Figures 4.A24, 4.A28) and across the mid-height of the room (Figures 4.A26, 4.A30) at the high and low supply velocities respectively. A further reduction in supply velocity is therefore

unlikely to result in significant improvements in draught in large parts of the occupied zone. The vertical air temperature differences were within acceptable discomfort limits for all the cases (Table 4.3, Run Nos. 9-12).

Configuration D

Configuration D evolved mainly as an attempt to eliminate the short-circuiting of the supply air experienced at low ACH of configuration B.

At 3 ACH, and at a supply velocity equal to the high supply velocity in configuration B (supply area 0.25 m^2), the velocity distributions obtained (Figures 4.A32) were very similar to those of configuration B (Figure 4.A21). The air temperatures (Figure 4.A33) in the room were considerably and uniformly higher than those obtained for configuration B (Figure 4.A22), confirming the high extent of short-circuiting of the warm supply air with the high level extract in configuration B. There is also seen to be a vast improvement in the average pollutant concentration (Table 4.2, Run Nos. 10 & 15). Increased *PMV*s accompanied the increases in air temperature of configuration D (Figure 4.A31a-b) in comparison to B (Figure 4.A20a-b).

At 3 ACH, a further reduction in supply velocity (supply area 0.44 m^2) in configuration D, was found to have little influence on thermal comfort. This is shown by the near identical distribution of *PMV*, *PD$_v$*, velocity and air temperature obtained at the low supply velocity (Figures 4.A37a-b, 4.A37c-d, 4.A38, 4.A39, supply area 0.44 m^2) in comparison to those obtained at the high supply velocity (Figures 4.A31a-b, 4.A31c-d, 4.A32, 4.A33, supply area 0.25 m^2). The vertical air temperature differences were within acceptable limits at both supply velocities, with a fractional reduction and therefore improvement in the discomfort level at the higher supply velocity (Table 4.2, Run Nos. 15 & 16).

At 6 ACH lower *PMV*s were obtained at the high supply velocity (Figure 4.A37a-b) than at the low supply velocity supply (Figure 4.A40a-b). Since both cases experience similar magnitudes of velocity distributions (Figures 4.A38, 4.A41), the reduction in *PMV* would be as a result of lower air temperatures at the high supply velocity. Lower air temperatures at the high supply velocity are confirmed in Table 4.3 (Run Nos. 17 & 18) and in the temperature distributions of the two cases (Figures 4.A39, 4.A42). This

is a somewhat surprising result in view of the previous observations on greater penetration and mixing of the supply air at high supply velocities. Examination of the vectors in the vicinity of the supply shows considerable interaction (or mixing) between the supply and extract air-streams at the high supply velocity (Figure 4.A38), effectively causing short-circuiting of the supply air with resulting loss of heat to the extract air-stream. This appears to be due to proximity of the supply outlet to the extract and may need to be considered in practice, when using simple supply ATDs at high flow rates. It may however, also have been caused by insufficient grid representation in the CFD. This mixing of the supply and extract air streams at the low supply velocity prevents the evaluation of the influence on thermal comfort of the reduction in supply velocity. However, the reduced penetration of high-velocity warm supply air stream at the low supply velocity (as was seen in Figure 4.A41, compared to the high supply velocity in Figure 4.A38) would make this the preferable option. The thermal plume at the low supply velocity is seen to be very close to the west-wall. This would suggest that a further reduction in supply velocity would have little impact on the distributions of velocity and temperature in the room.

Comparison of configurations B and D at 6 ACH, shows similar *PMV*s (Figures 4.A27a-b, 4.A40a-b) and air temperatures (Figures 4.A29, 4.A42) for both configurations with reduced levels of draught (Figures 4.A27c-d, 4.A40c-d), in the occupied zone for configuration D, mainly in the vicinity of the warm-air plume. These observations are also supported by the figures in Table 4.3 (Run Nos. 12 & 18).

To summarise, a low level air extract-device has been found to be preferable when combined with a low level air supply-device to avoid short-circuiting of the supply air at low flow rates. As with the high supply device, a fixed geometry ATD device has been found to be appropriate for use over a range of flow rates. This should be sized to prevent draught at the maximum required flow rate. Beyond a particular supply ATD area, further increases in supply area are not expected to bring about significant improvements in the comfort level, in particular with respect to draught. At flow rates of up to approximately 6 ACH, as anticipated of the H & V system, a supply device area of 0.44 m^2 would appear to be appropriate.

4.8.2 Influence of location of ATD device on thermal comfort

From a cost point of view, a single supply and extract device per room would be the preferable option. Due to the high velocities experienced for low level supplies, an alternative configuration was assessed with the single supply and extract ATD device replaced by two devices located adjacent to each of the side walls as described in Section 4.1. The reasoning was that, by supplying the air stream *adjacent* to the wall, it may be possible to achieve greater penetration and dispersion of the air-stream *along* the wall, resulting in improved distribution of the supply air and lower air velocities in the occupied zone. The alternative configuration was investigated for configurations A and B only, using the same total supply area as for single supply devices.

The average values of the flow variables obtained from the numerical analysis in Table 4.3 suggest little difference to the thermal environment of the occupied zone as a whole when using the alternative ATD configuration. Similar average and standard deviation values of PMV, PD_v, air velocity and air temperature were obtained for the single and double supply devices (Run Nos. compared: 4 & 20, 8 & 21, 10 & 23, 12 & 24, 15 & 25, 17 & 26). Graphical illustrations of the influence of the supply location are restricted to one of the low level-supply configurations at high ACH, at which draught has been observed to be a problem. These are shown for configuration B-2 at 6 ACH, and will be compared with the previous results obtained for configuration B. Distributions of PMV and PD_v are shown in Figures 4.A43a-d for configuration B-2. There is seen to be a re-distribution of the contours obtained for the single supply device (Figures 4.A27a-d), with the distributions of PMV and PD_v in the outer plane of the double-supply similar to those in the symmetry plane for the centrally-located supply and vice versa. Somewhat increased levels of draught are however obtained in the symmetry plane for the double inlet device than were obtained in the outer plane for the single supply device. This is due to high velocities occurring in the symmetry plane (Figure 4.A42) which appear to be due to the interaction of supply air from the two supply devices, causing a large down-flow of the returning air. Incidence of similar velocities in most of the occupied zone for both the single and double supply devices is

seen by the similar velocity magnitudes in the plane through the mid-height of the room as shown in Figures 4.A43 and 4.A30.

From the above observations, the double inlet device would appear to offer no significant advantage over the single, centrally located device.

4.8.3 Comparison of configurations, thermal comfort, IAQ and energy consumption

The previous section on identification of suitable ATD areas, effectively eliminated the use of configuration B in favour of configuration D. Therefore configuration B will not be considered any further. Similarly, the use of more than one supply device has not been found to provide any advantages. The following sections will therefore be restricted to comparisons between configurations A, C, D and E for single, centrally located supply and extract ATDs. These will be for ATD areas of 0.44 m^2 for configuration D and 0.25 m^2 for the rest.

The numerical data in Table 4.3, showed considerably higher average pollutant concentrations in the occupied zone for configuration C than for the other three configurations (Run No. 13 compared to 4, 16, 19 and Run No. 14 compared to 8, 18, 20). The PMVs are also seen to be significantly lower than those obtained for the other configurations. This is seen to be due to the supply air being drawn directly towards the extract (Figure 4.A44), which is in effect short-circuiting of the supply air. A large recirculating zone is seen in high end of the room between the supply and extract locations. No further consideration is given to this option.

Configurations D & E obtained very similar thermal and flow conditions within the occupied zone (Table 4.3). Configuration E experienced somewhat poorer mixing of the supply air in the occupied zone, due to the extract device being located in the path of the penetrating supply air stream at the bottom of the east-wall (Figure 4.A47). This results in fractionally higher pollutant concentration in the occupied zone than for configuration D. The location of the supply and extract device on opposite walls is likely to be less economical for installation purposes. Thus, for a low level supply system, Configuration D is considered more appropriate than configuration E.

Comparison and choice of a system, therefore, remains to be made between configuration A (high level supply and low level extract) and configuration D (low level supply and low level extract). To facilitate a more accurate comparison, the *PMV*s and temperatures at the centre of the occupied zone were used, as opposed to the average values in the occupied zone (in Table 4.2). This was to eliminate the bias of the warm supply air in the low level supply case on the average air temperatures of the occupied zone.

To allow comparison between the configurations at similar comfort levels (*PMV*s), a number of additional simulations were performed. These were for configuration A at 3 ACH and a supply air temperature of 46 °C and configuration D at 6 ACH and supply air temperature of 34 °C. Relevant data for the comparison of the cases is shown in Table 4.4. This is of a similar format to the previous tables, with the average and standard deviations of air temperature, *PMV* and *PD*$_{ST}$ replaced with their respective values at the centre of the occupied zone. The table also includes the enthalpy loss between the supply and return air-streams, ΔH.

Configuration	ACH	t_{on}	t_{off}	ΔH	t	PMV	PD_v	PD_{vsd}	PD_{ST}	c_{ave}	c_{sd}
	(/h)	(°C)	(°C)	(kJ)	(°C)		(%)	(%)	(%)	(ppm)	(ppm)
A	3	46	20.9	2.2	23.3	0.05	0.5	1.6	7.8	13.3	6.3
high level supply	6	30	21.7	1.5	23.2	0.04	1.8	4.3	5.8	6.8	3.7
D	3	42	21.8	1.8	23.5	0.07	2.5	5.5	6.2	12.8	3.4
low level supply	6	34	24.3	1.7	23.9	0.05	4.7	6.4	5.1	7.5	2.2

Table 4.4 Numerical evaluation data of additional cases to obtain similar *PMV*s

Vertical air temperature differences of the high level supply at 3 ACH exceeded the acceptable limits of 6.5 % at supply conditions to achieve neutral *PMV*s. In the absence of internal heat sources, this would require operation at higher flow rates to reduce the vertical air temperature difference to acceptable levels (i.e. at the pertaining wall temperatures and personal parameters). At low ACH, the low level supply system has distinct advantages: lower thermal stratification and better energy utilisation of the supply air. At similar *PMV*s, the low level supply requires between 15-20 % less heat input than the high level supply system. Similar pollutant concentrations occur in the occupied zone for the high (Figure 4.A48) and low level supply (Figure 4.A49) systems.

At higher flow rates (6 ACH) however, the high level supply system provides greater advantages. It experiences significantly lower levels of draught, while providing similar IAQ with greater energy efficiency. The high level supply configuration requires approximately 10% less heat input than the low level supply configuration to attain similar average *PMV*s. This is the case despite the higher air temperatures obtained for the low level supply configuration and is as a result of considerably higher air velocities in the occupied zone for the low level supply, which contribute to additional cooling of the body and thus reductions in the *PMV*s. The high levels of draught experienced with a low level supply have already been commented on in Section 4.8.1. Figure 4.A40c-d shows a relatively large proportion of the occupied zone experiencing draught dissatisfaction levels of between 5 - 10 %. These draught dissatisfaction levels would be further increased if the requirement of a high ventilation rate arose, together with a low space heat requirement. For instance, if a flow rate of 6 ACH were required for ventilation (DCV) purposes but the space heat demands require a supply air temperature considerably lower than the magnitudes currently investigated. This would lead to further increments in draught dissatisfaction level to those obtained between supply air temperatures of 34 °C (PD_v = 4.7 ± 6.4 %) and 30 °C (PD_v = 5.0 ± 7.1 %) as indicated by the average and standard deviations of these in the occupied zone. In addition, at low supply air temperatures, the reduction in buoyancy of the supply air stream would result in penetration of the high velocity supply into the occupied zone, thus affecting larger proportions of the room.

A high level supply with low level extract would thus appear to be most appropriate to satisfy the requirements of good thermal comfort and IAQ over the anticipated range of supply parameters (flow rates and supply air temperatures) and mode of operation of the H & V system. This is therefore the chosen system for the H & V system.

4.9   Discussion of the results

The results show the benefits of a low level supply system at low ACH. Even in severe climates, these low ACH may be capable of providing space heat requirements for continuously operating systems. At very high levels of insulation, it is likely that heat requirements may be provided for an intermittently operating system. These systems

may however require lead times in the operation of the ventilation system, to achieve satisfactory IAQ levels prior to occupancy. This to some extent defeats the purpose. However, reductions in the emissions of building materials and therefore ventilation requirement for satisfactory IAQ, may increase its applicability to the type of H & V system under investigation. In the long term therefore, there may be applications for low level supply systems in demand-controlled, intermittent H & V systems. However, at the current time, with lack of any clear position on acceptable IAQ and at intermediate insulation levels, the high level supply would appear to be more appropriate. This study will focus on the use of this system in the provision of heating and ventilation of individual rooms. This will be analysed in greater detail in Chapter 5, including the issue of control.

The investigation clearly raises doubts on the ASHRAE guideline (1993) of supply velocities for discharge into the occupied zone not exceeding 1.5m/s at the ATD face. Similarly, the range of flow rates (4 - 15 ACH) which *Awbi* (1991) found acceptable for low level supply device, are found to be inappropriate. This study however, set very high standards for acceptable draught levels of 6.5%. The draught levels observed for the low level supply device frequently occur in cooling applications (5-10%, from results of simulations by *Chen et al* (1992), using *Fanger's* draught risk model). Should higher draught levels be found to be acceptable, this may extend the application of low level devices. To allow the use of high ACH in ventilation mode these should however, be used with a vertical discharge of the supply air from the floor level. The extract device may be placed next to the supply device. This configuration was not used in this investigation for the following reasons:

1. At the design conditions (wall temperatures) investigated, this was not expected to be significantly different from the side wall supply. The reason for this being that, at the supply ATD areas used, (with low supply velocity/momentum), the buoyant air plume was seen to rise upwards, immediately after discharge. A vertical discharge would be expected to follow a similar flow-path, with the buoyant flow inducing similar air-movement in the occupied zone.

2. Although this would allow higher supply-rates than for the side wall supply, at low flow rates and supply temperature, the distribution and mixing of the supply air would be poorer than that provided by the high level supply.

The results obtained are in agreement with those of *Gan* (1995) on the improved energy utilisation of a low level air heating system at low ACH (*Gan's* observation were at 4 ACH). However, at flow rates beyond those investigated by *Gan*, this is no longer seen to be the case, due to the effect of the increased air-movement on heat loss from the body (and therefore the *PMV*). At these higher flow rates, the high level supply is found to obtain greater energy utilisation.

4.10 Conclusions

The aim of the work described in this Chapter was to identify a suitable ATD configuration to be used in the H & V system. The investigation compared several configurations and concluded in the choice of a high level supply and low level extract ATD configuration. This was found to be the most appropriate for the provision of good thermal comfort and IAQ over the range of operations anticipated of the H & V system. For application over the range of flow rates expected, an ATD supply area of 0.25 m^2 was identified as being suitable.

The following observations were also made in the course of the analysis:-

- Fixed ATD sizes were found to be suitable for variable flow air distributions systems for both low and high level supply locations. No appreciable benefit would appear to be gained from using a variable geometry device. These ATDs should be sized for prevention of draught at the maximum airflow rates.

- Low levels supply devices should be used together with low level extracts to eliminate short-circuiting of the warm and fresh supply air.

- The ASHRAE recommended limit of maximum supply velocities directly into the occupied zone of 1.5 m/s was found to be inappropriate.

- The upper limit of acceptable ACH for a low level supply device was between 3 and 6 ACH in order not to cause discomfort due to draught.

- Low level supply devices obtained greater energy efficiency than the high level supplies at low flow rates of 3 ACH. Application of these in an H & V system operating in DCV principles may however require vertical supply of the incoming air stream. These systems may find application with increasing insulation levels and reductions in internal pollutant emissions.

- Multiple supply devices offered no advantage over single supply devices for the airflow rates and room geometry investigated.
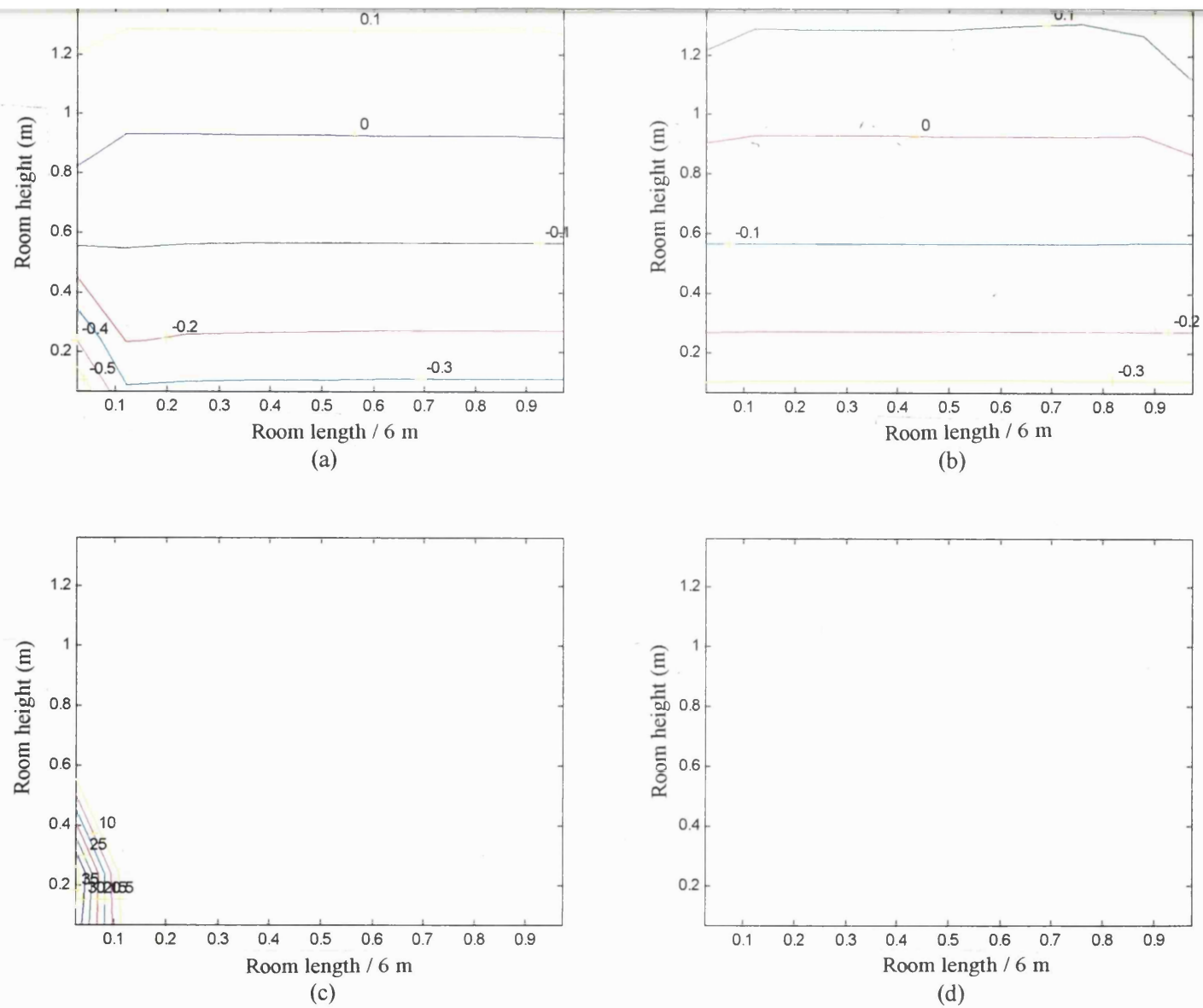
Figure 4.A1 *PMV* and *PD$_v$* contours of configuration A, 3 ACH, supply velocity 1.1 m/s, supply temperature 42 °C. (a) *PMV* contours in plane y = 3 m. (b) *PMV* contours in plane y = 5.7 m. (c) *PD$_v$* contours in plane y = 3 m (%). (d) *PD$_v$* contours in plane y = 5.7 m (%).

Figure.4.A2

Velocity vectors in plane
y = 3 m, configuration A at
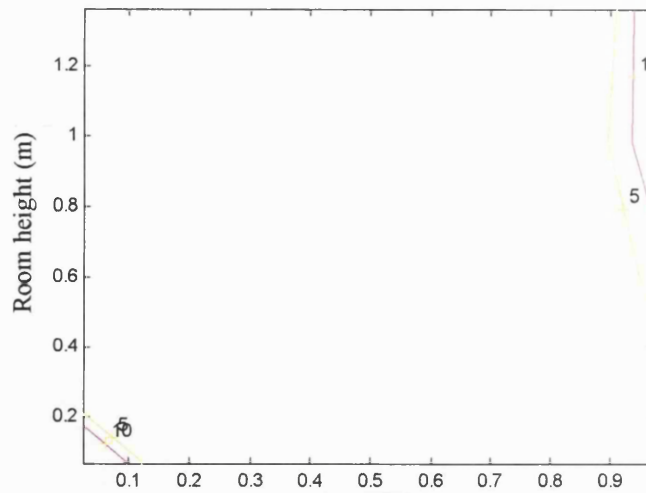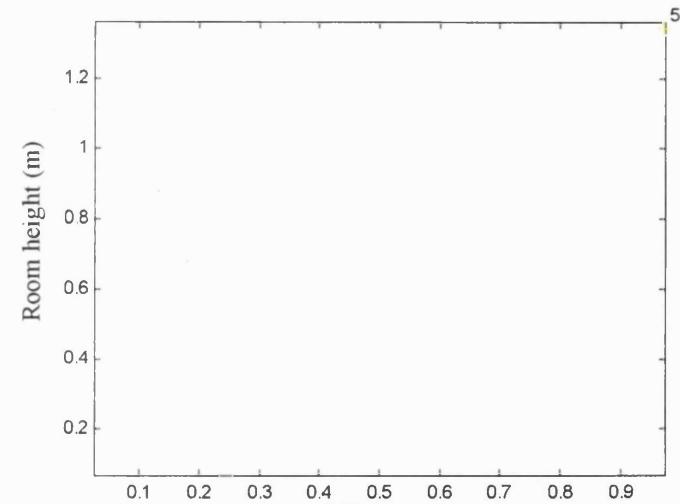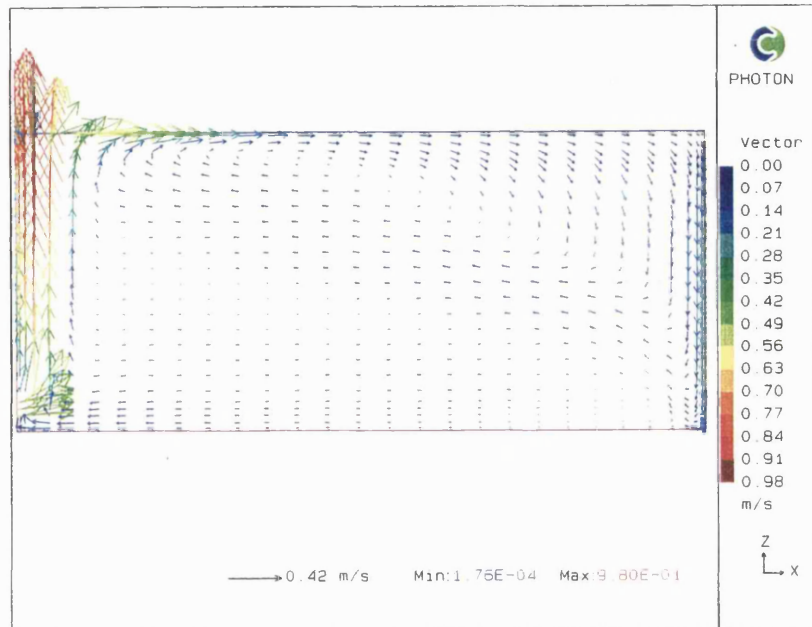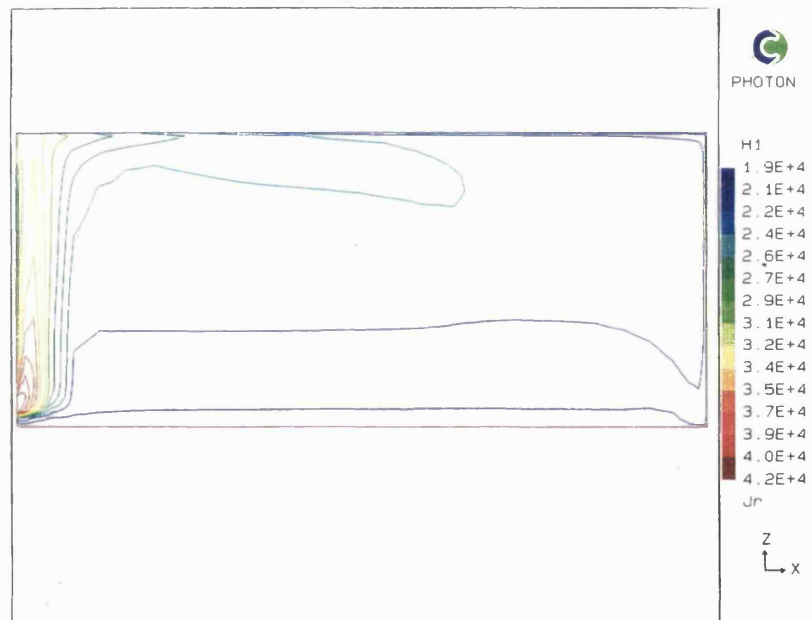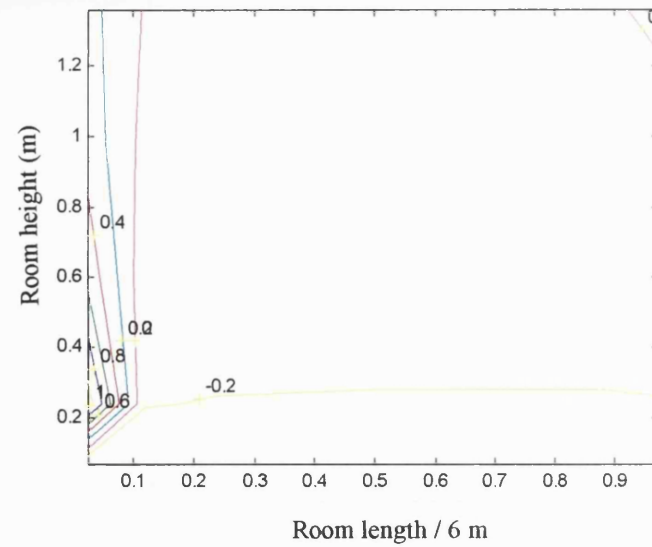3 ACH, supply velocity 1.1 m/s,
supply temperature 42 °C.
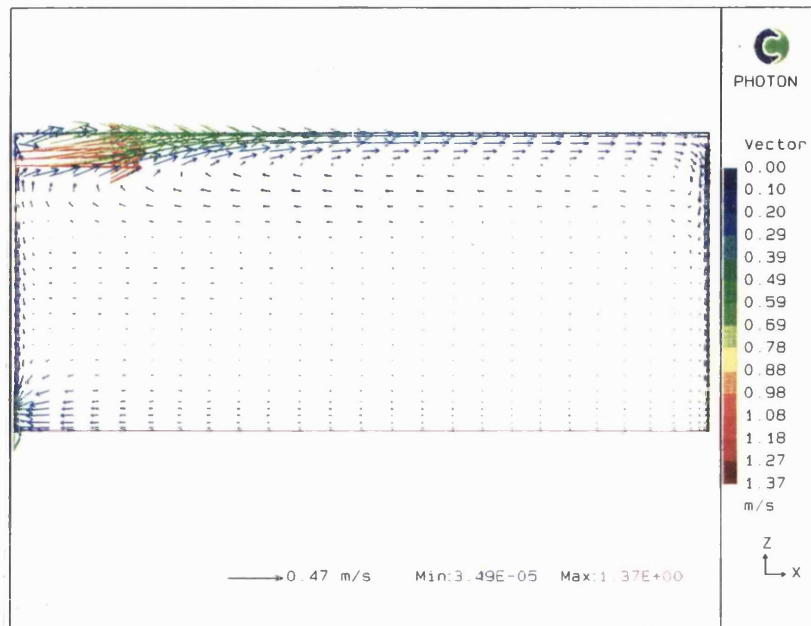
Figure.4.A3

Enthalpy contours in plane
y = 3 m, configuration A at
3 ACH, supply velocity 1.1 m/s,
supply temperature 42 °C.
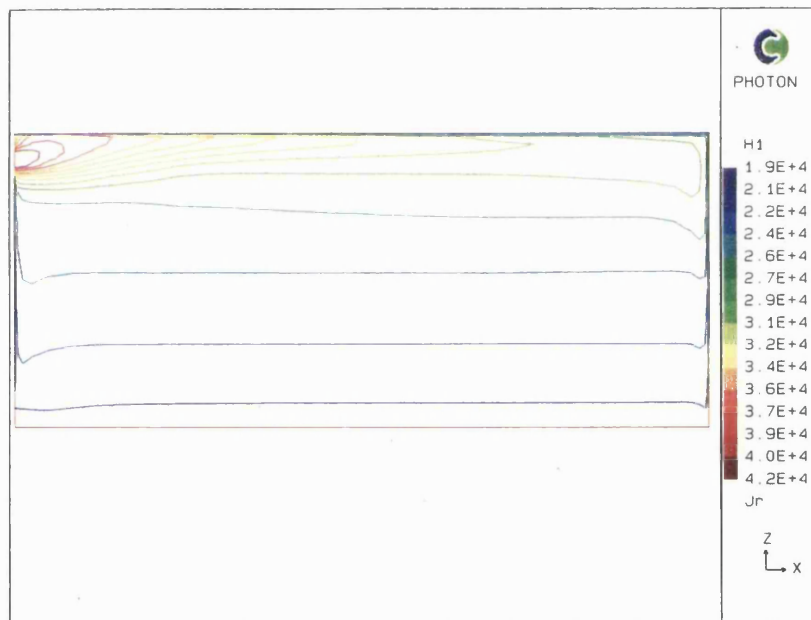
Figure.4.A4

Velocity vectors in plane
z = 2.3 m, configuration A at
3 ACH, supply velocity 1.1 m/s,
supply temperature 42 °C.
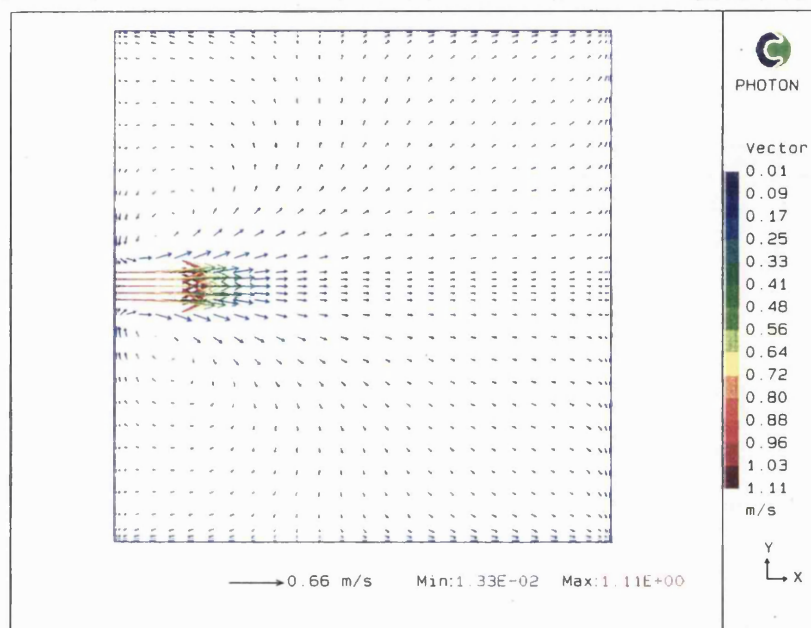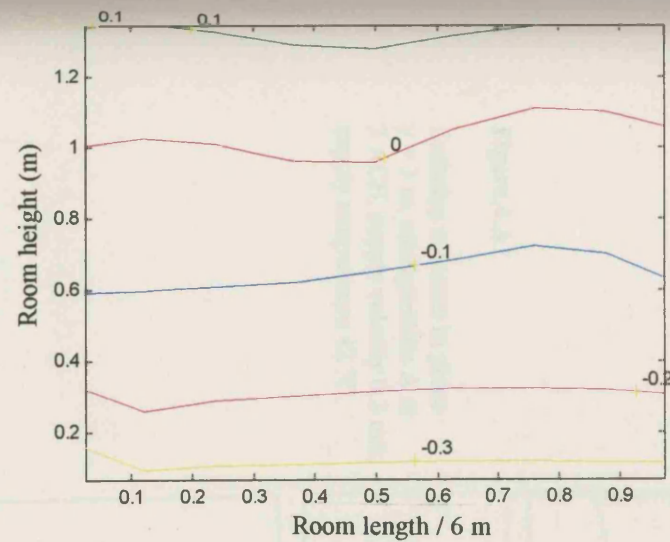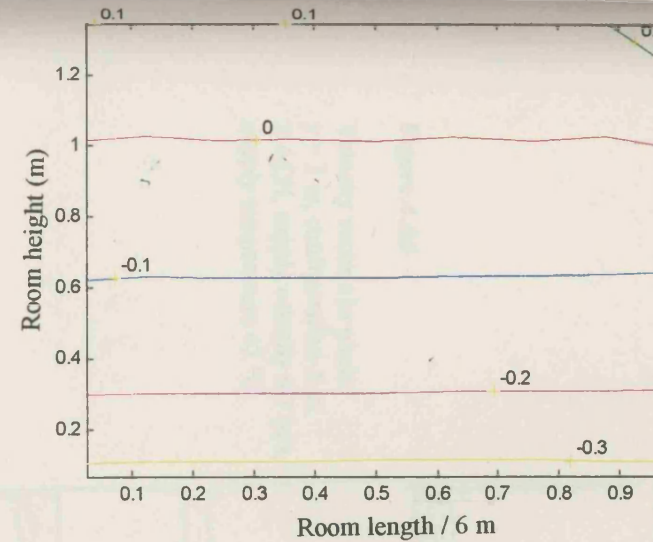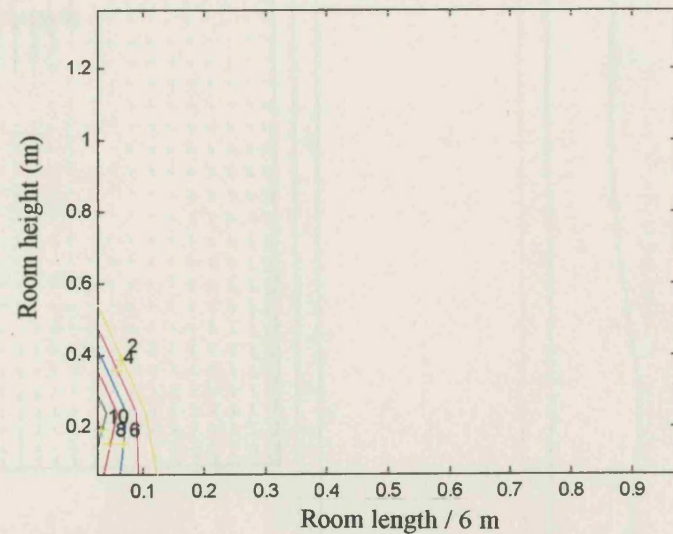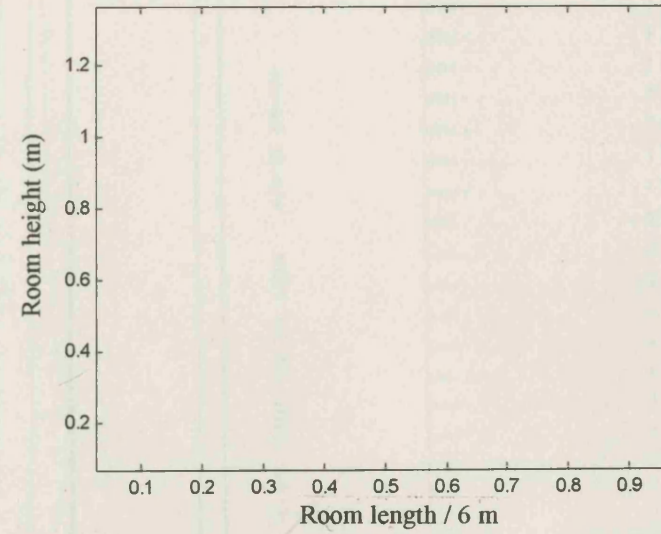
Figure 4.A5 *PMV* and *PD*$_v$ contours of configuration A, 3 ACH, supply velocity 0.3 m/s, supply temperature 42 °C. (a) *PMV* contours in plane y = 3 m. (b) *PMV* contours in plane y = 5.7 m. (c) *PD*$_v$ contours in plane y = 3 m (%). (d) *PD*$_v$ contours in plane y = 5.7 m (%).

Figure.4.A6

Velocity vectors in plane
y = 3 m, configuration A at
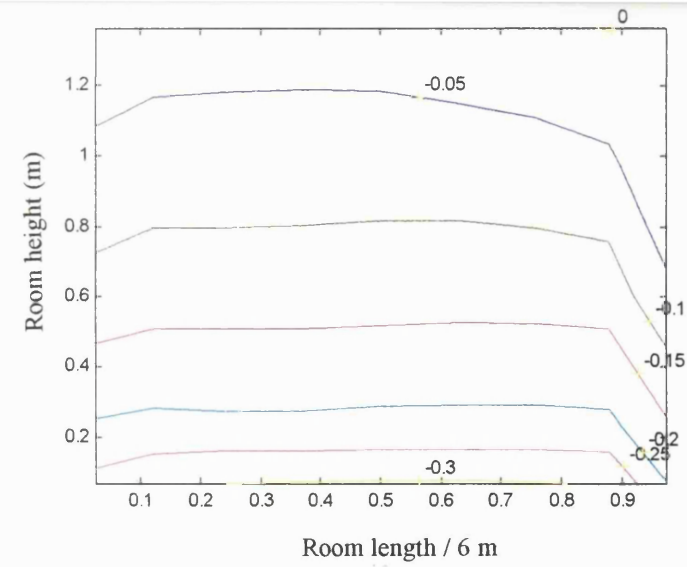3 ACH, supply velocity 0.3 m/s,
supply temperature 42 °C.
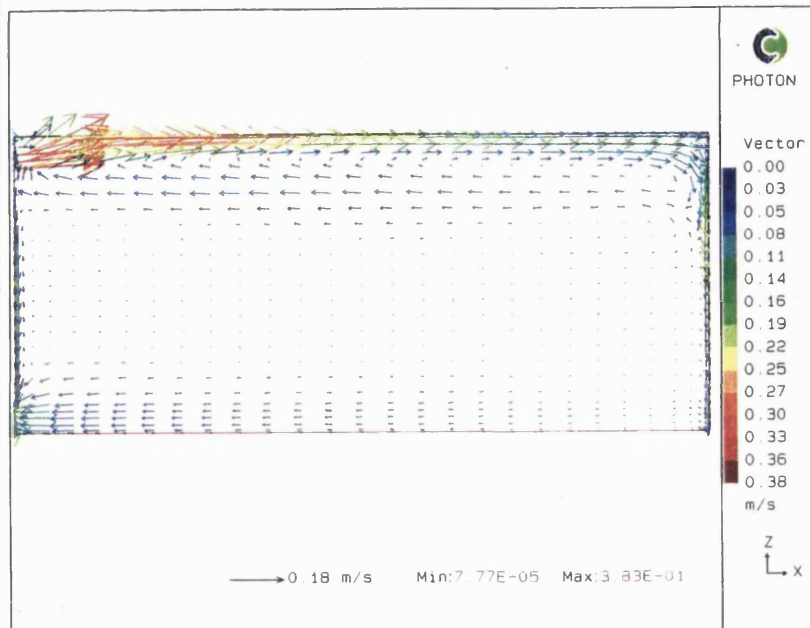
Figure.4.A7

Enthalpy contours in plane
y = 3 m, configuration A at
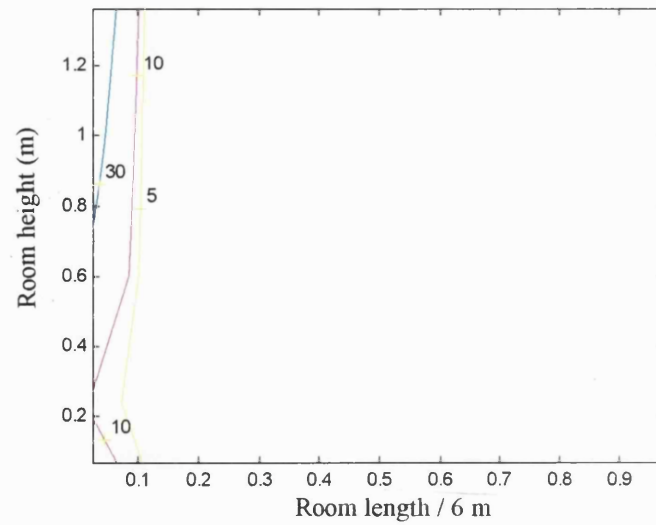3 ACH, supply velocity 0.3 m/s,
supply temperature 42 °C.
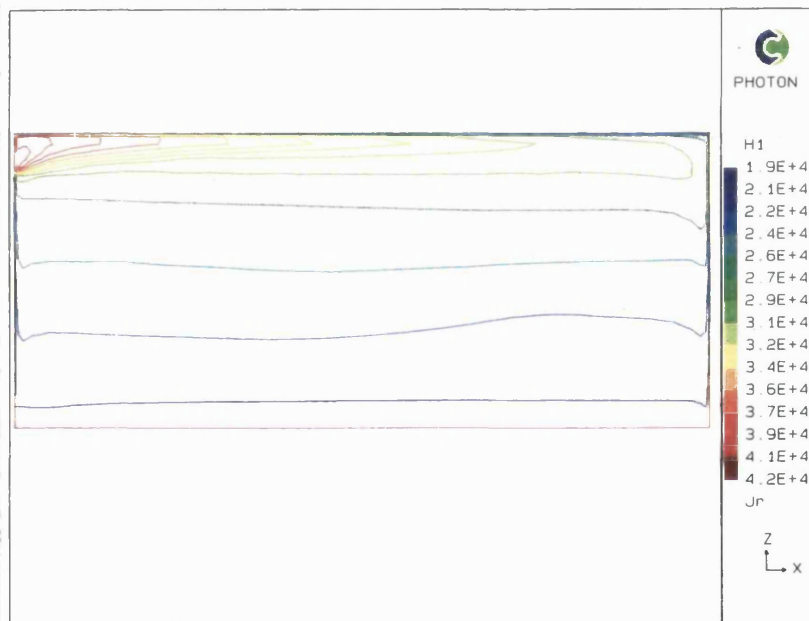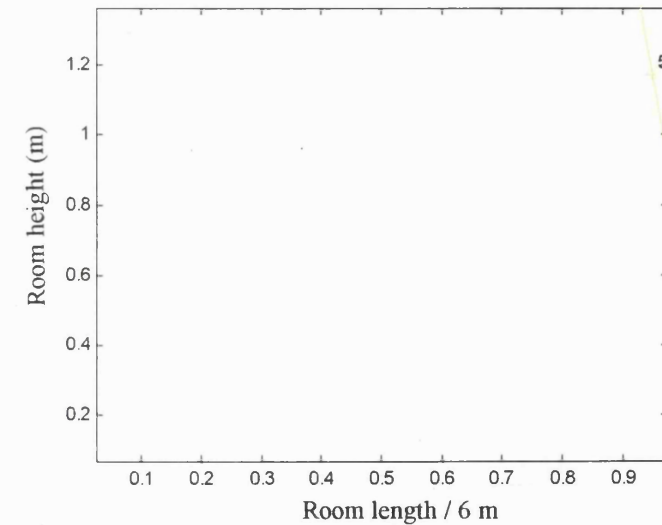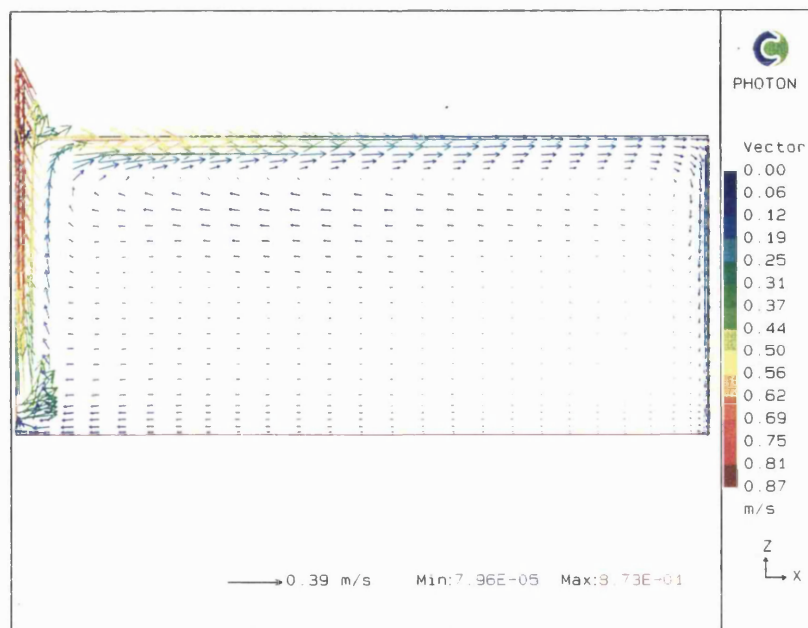

Figure.4.A8

Velocity vectors in plane
z = 2.3 m, configuration A at
3 ACH, supply velocity 0.3 m/s,
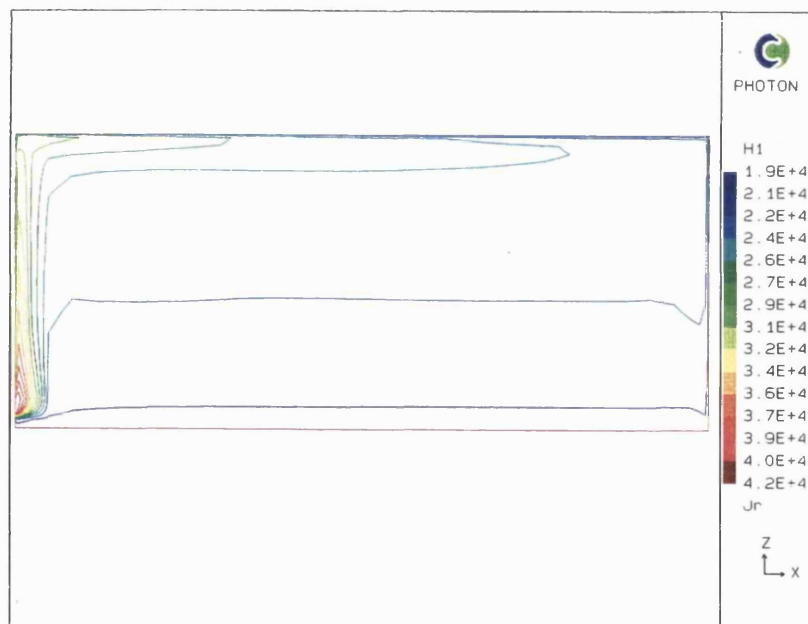supply temperature 42 °C.
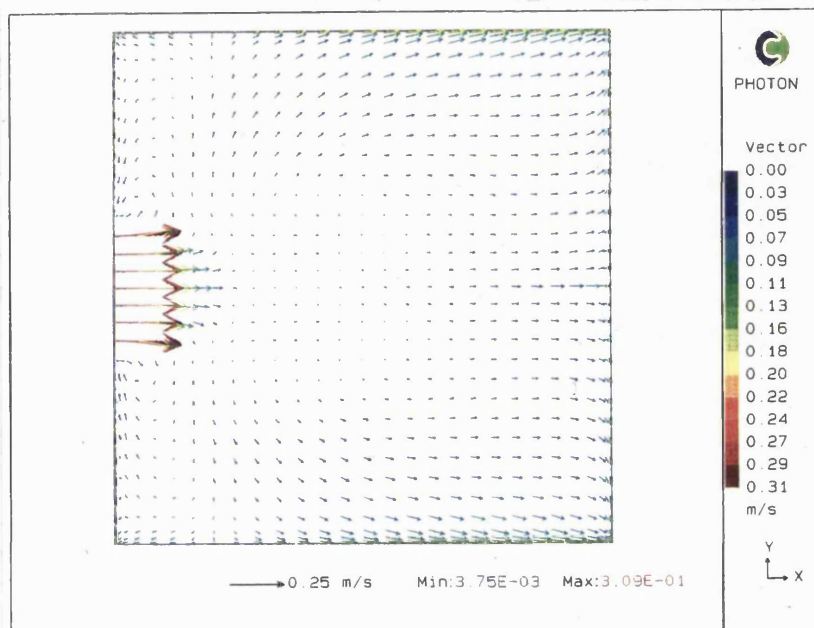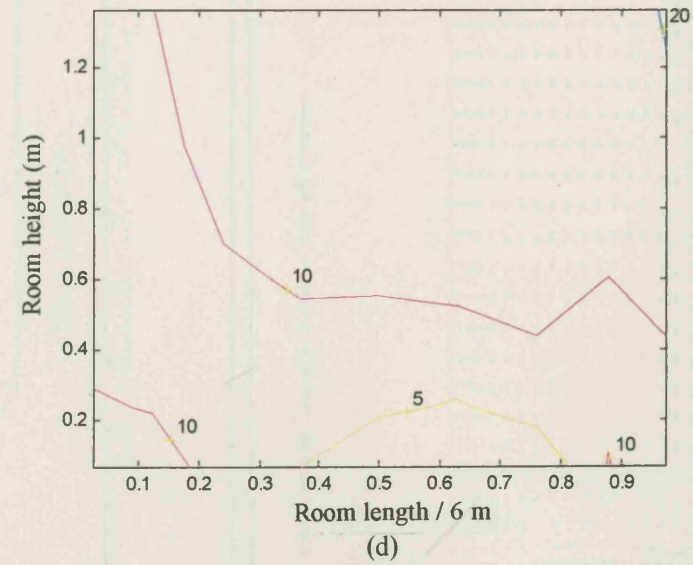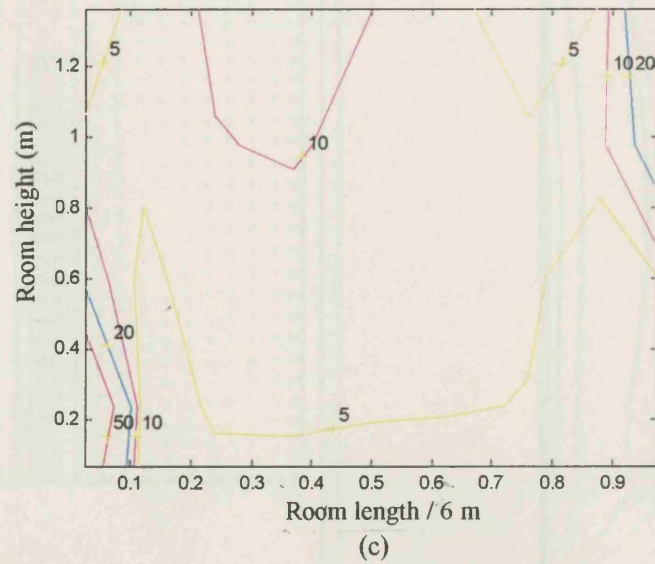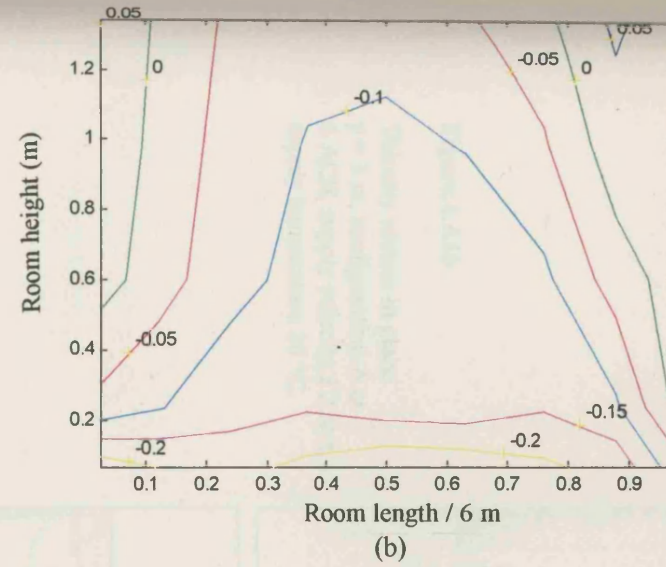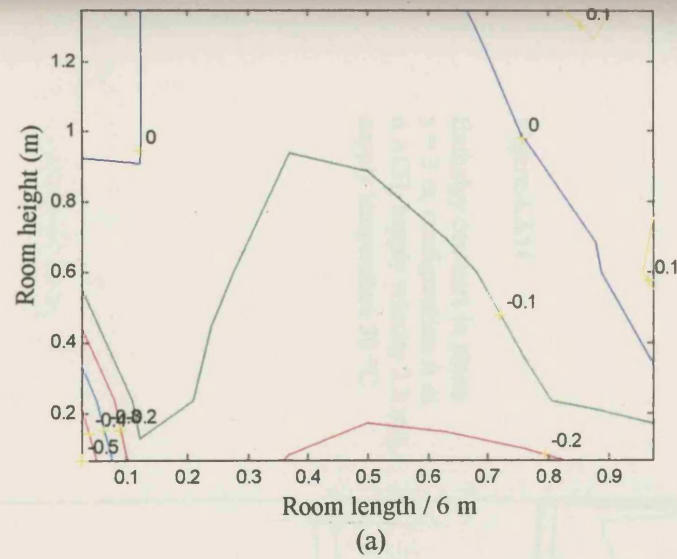
Figure 4.A9 *PMV* and *PD$_v$* contours of configuration A, 6 ACH, supply velocity 2.2 m/s, supply temperature 30 °C. (a) *PMV* contours in plane y = 3 m. (b) *PMV* contours in plane y = 5.7 m. (c) *PD$_v$* contours in plane y = 3 m (%). (d) *PD$_v$* contours in plane y = 5.7 m (%).
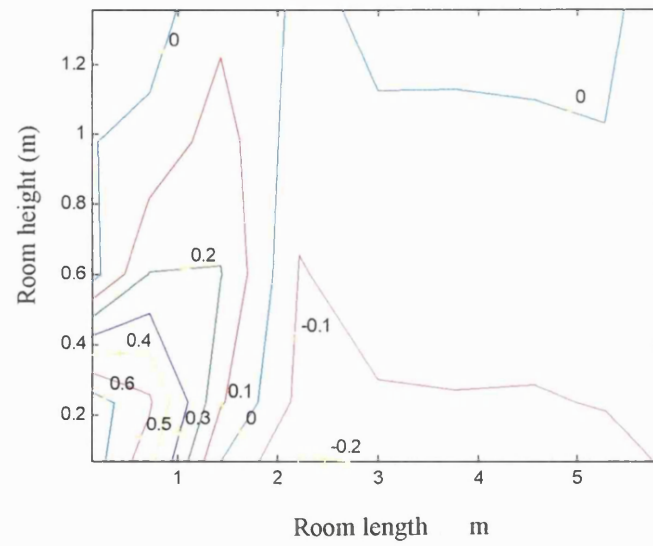
Figure.4.A10

Velocity vectors in plane
y = 3 m, configuration A at
6 ACH, supply velocity 2.2 m/s,
supply temperature 30 °C.
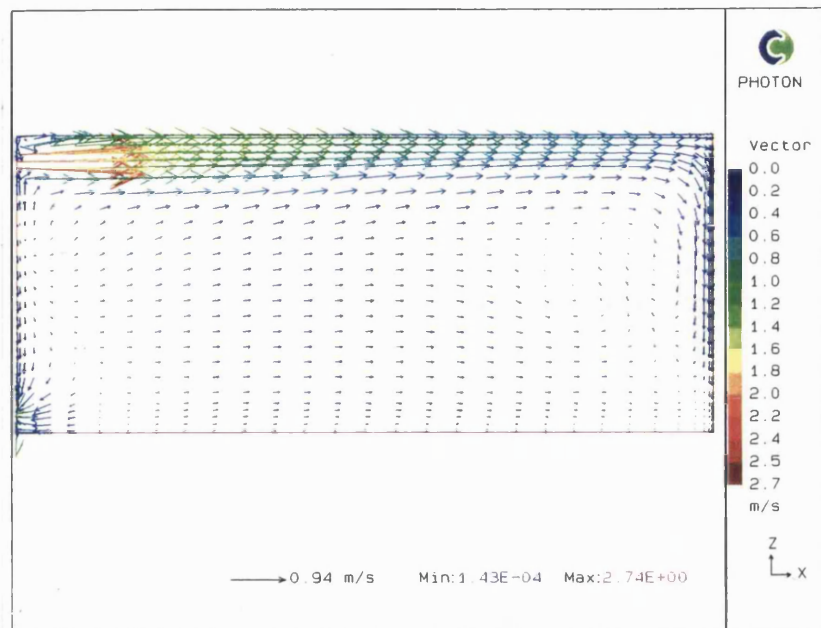
Figure.4.A11

Enthalpy contours in plane
y = 3 m, configuration A at
6 ACH, supply velocity 2.2 m/s,
supply temperature 30 °C.
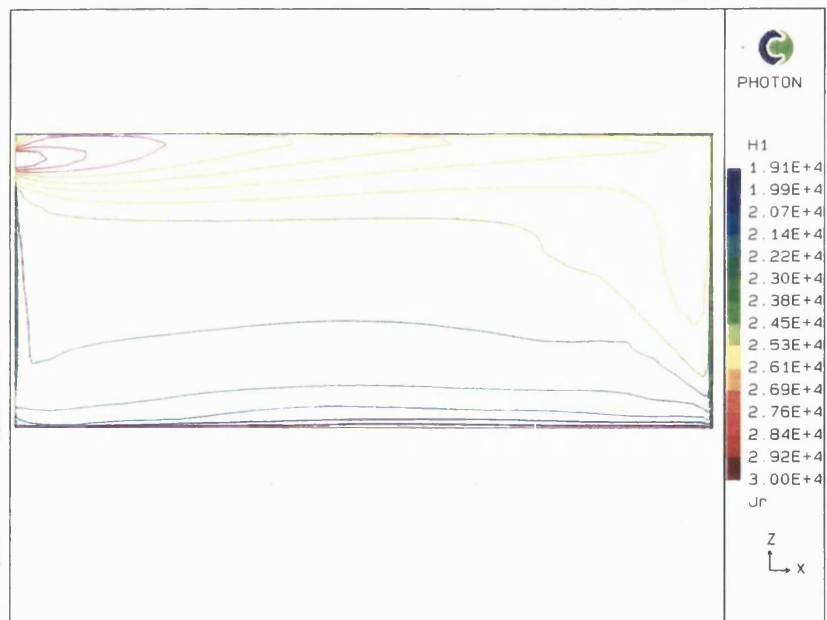
Figure.4.A12

Velocity vectors in plane
z = 2.3 m, configuration A at
6 ACH, supply velocity 2.2 m/s,
supply temperature 30 °C.
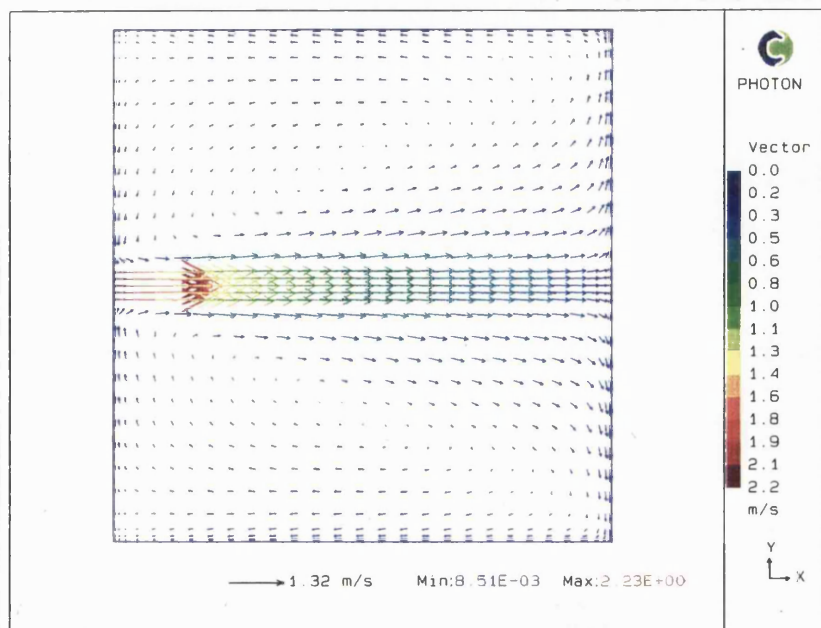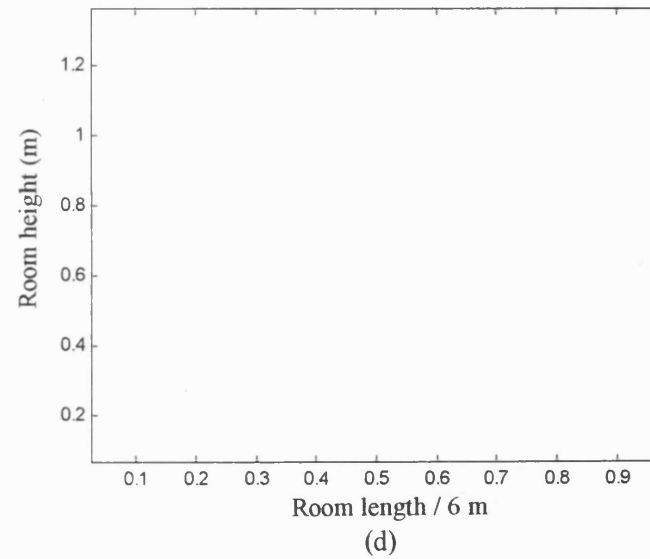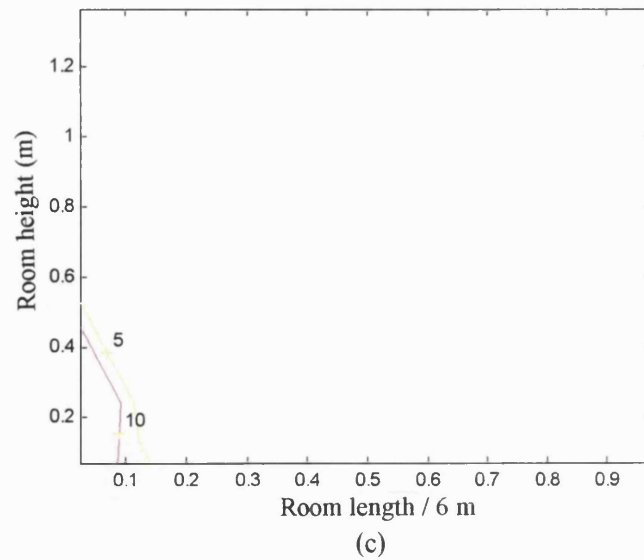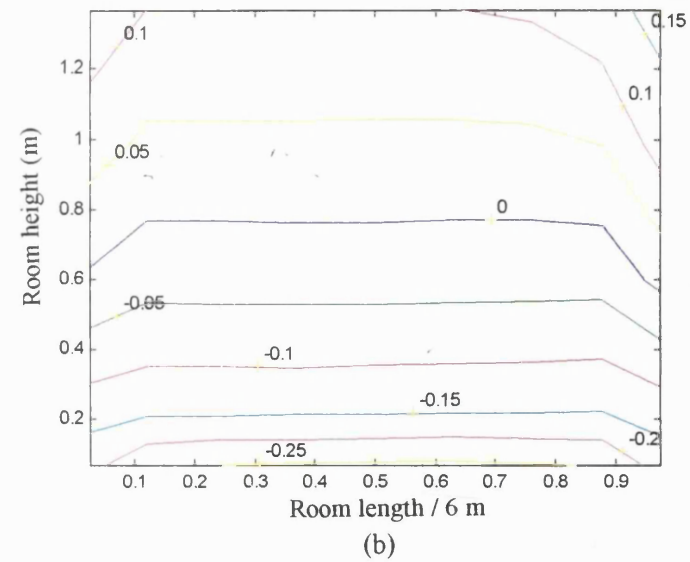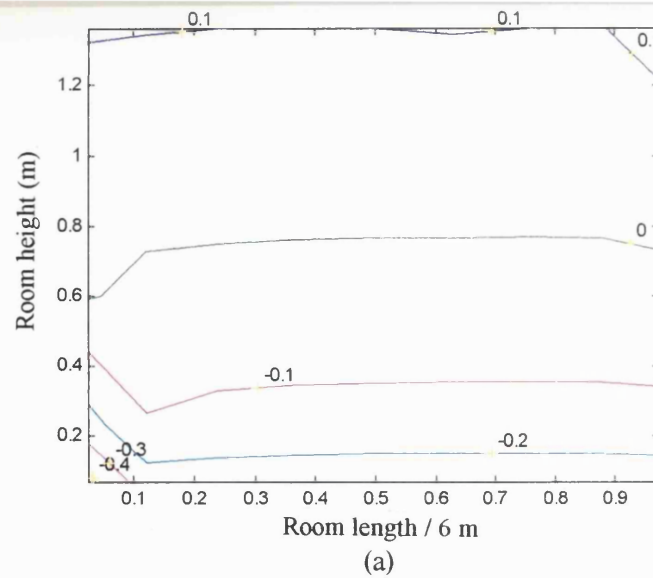
Figure 4.A13 *PMV* and *PD$_v$* contours of configuration A, 6 ACH, supply velocity 0.6 m/s, supply temperature 30 °C. (a) *PMV* contours in plane y = 3 m. (b) *PMV* contours in plane y = 5.7 m. (c) *PD$_v$* contours in plane y = 3 m (%). (d) *PD$_v$* contours in plane y = 5.7 m (%).

Figure.4.A14

Velocity vectors in plane
y = 3 m, configuration A at
6 ACH, supply velocity 0.6 m/s,
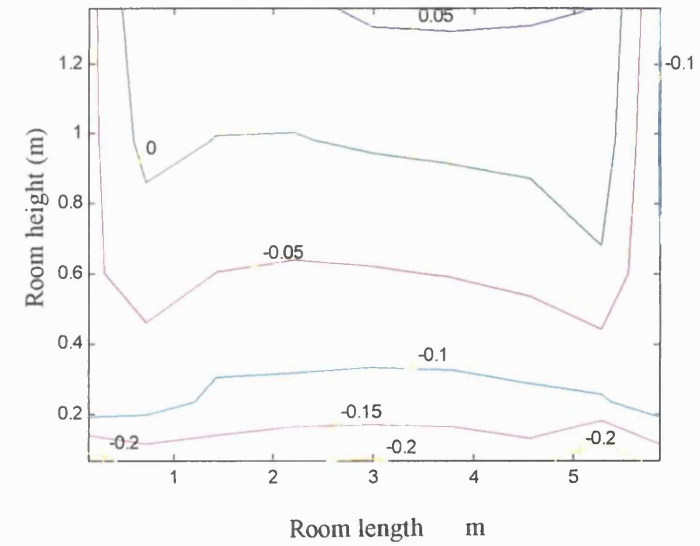supply temperature 30 °C.
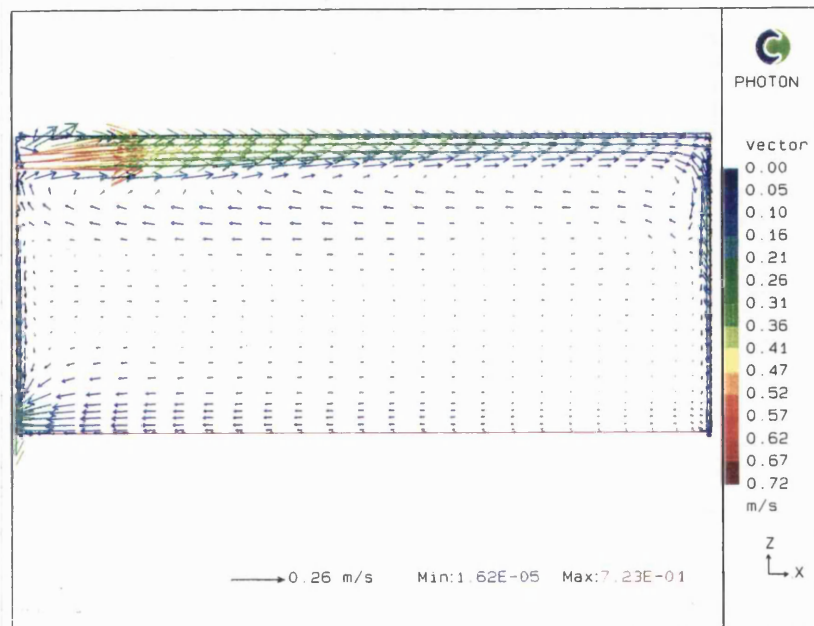
Figure.4.A15

Enthalpy contours in plane
y = 3 m, configuration A at
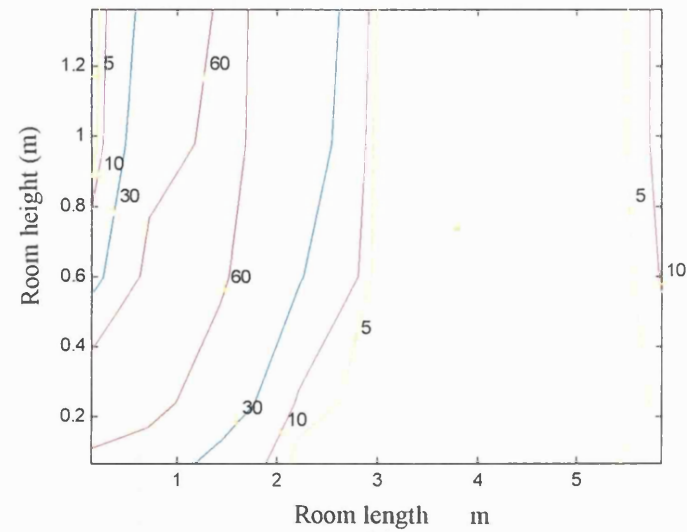6 ACH, supply velocity 0.6 m/s,
supply temperature 30 °C.
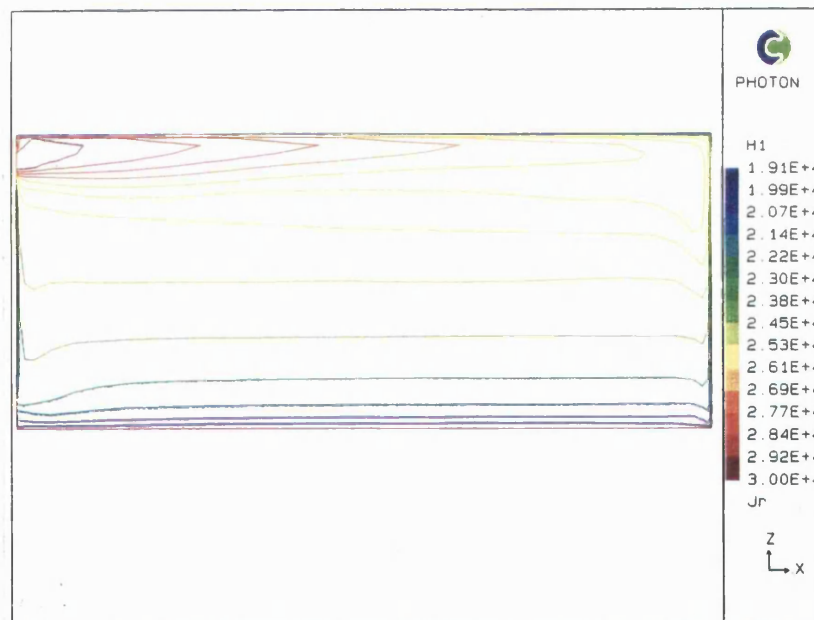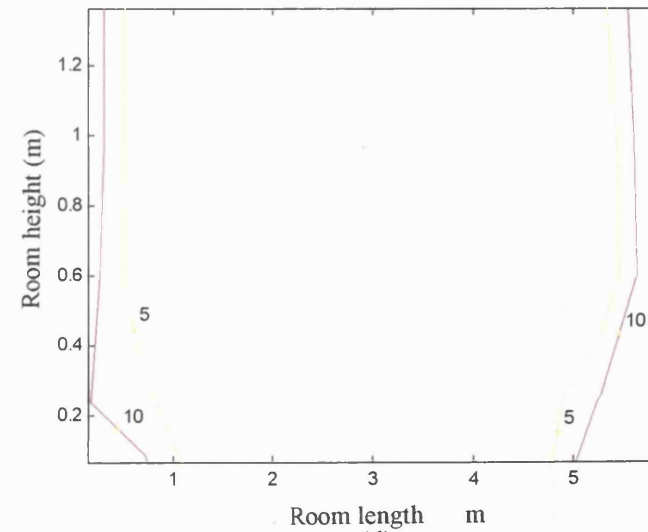

Figure.4.A16

Velocity vectors in plane
z = 2.3 m, configuration A at
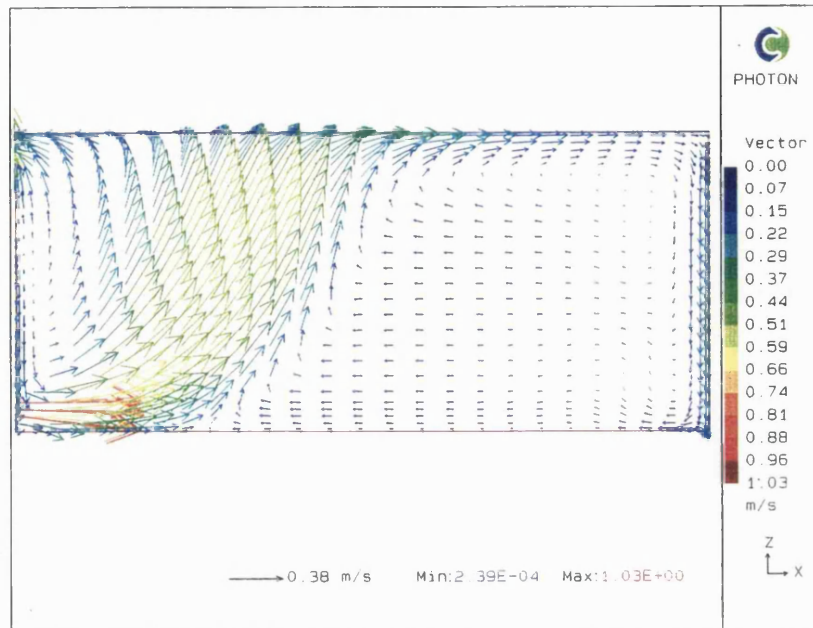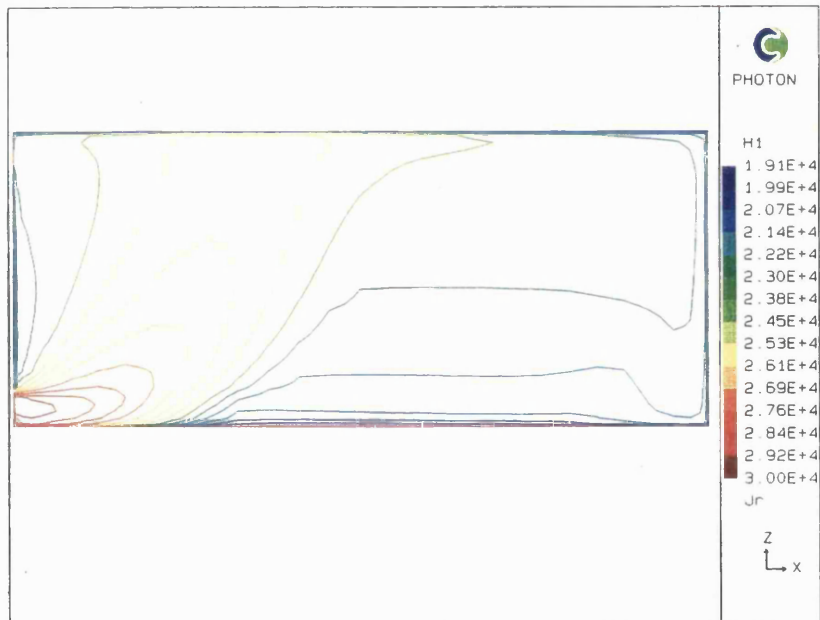6 ACH, supply velocity 0.6 m/s,
supply temperature 30 °C.
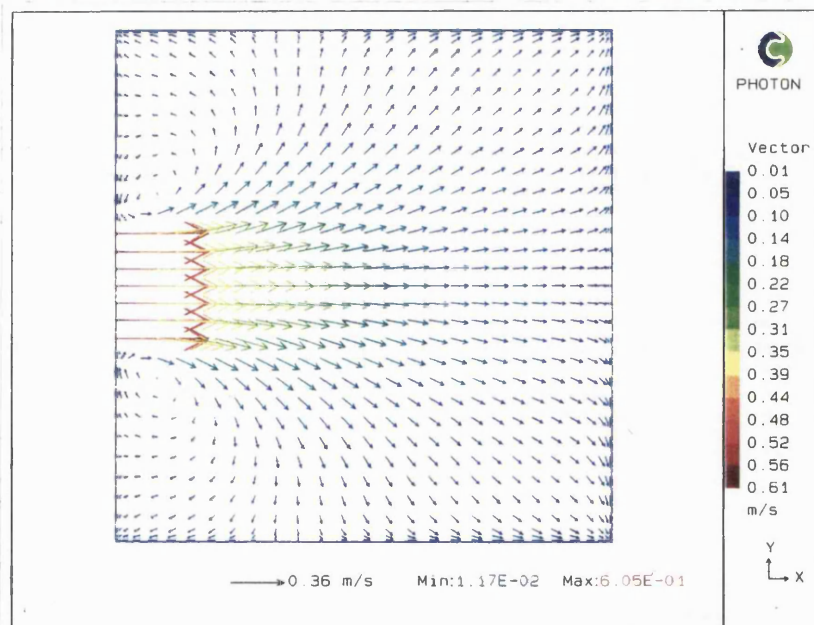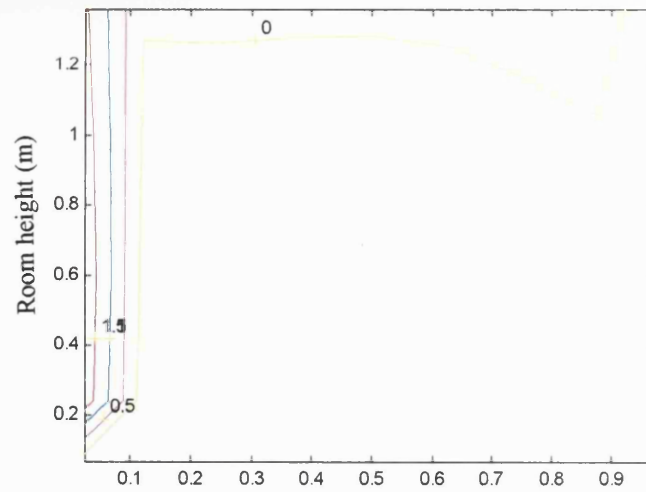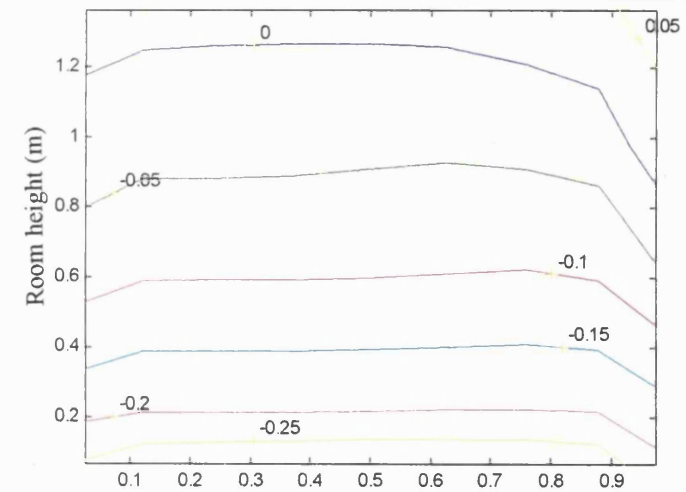
Figure 4.A17 *PMV* and *PD*$_v$ contours of configuration B, 3 ACH, supply velocity 0.44 m/s, supply temperature 42 °C. (a) *PMV* contours in plane y = 3 m. (b) *PMV* contours in plane y = 5.7 m. (c) *PD*$_v$ contours in plane y = 3 m (%). (d) *PD*$_v$ contours in plane y = 5.7 (%) m.
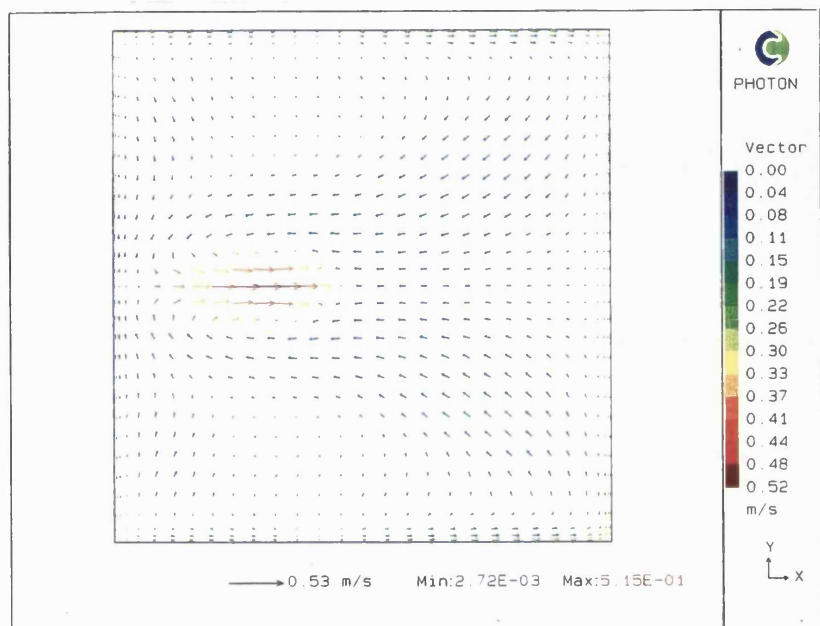
Figure.4.A18

Velocity vectors in plane
y = 3 m, configuration B at
3 ACH, supply velocity 0.44 m/s,
supply temperature 42 °C.

Figure.4.A19

Enthalpy contours in plane
y = 3 m, configuration B at
3 ACH, supply velocity 0.44 m/s,
supply temperature 42 °C.

Figure 4.A20 *PMV* and *PD$_v$* contours of configuration B, 3 ACH, supply velocity 0.3 m/s, supply temperature 42 °C. (a) *PMV* contours in plane y = 3 m. (b) *PMV* contours in plane y = 5.7 m. (c) *PD$_v$* contours in plane y = 3 m (%). (d) *PD$_v$* contours in plane y = 5.7 m (%).

Figure.4.A21

Velocity vectors in plane
y = 3 m, configuration B at
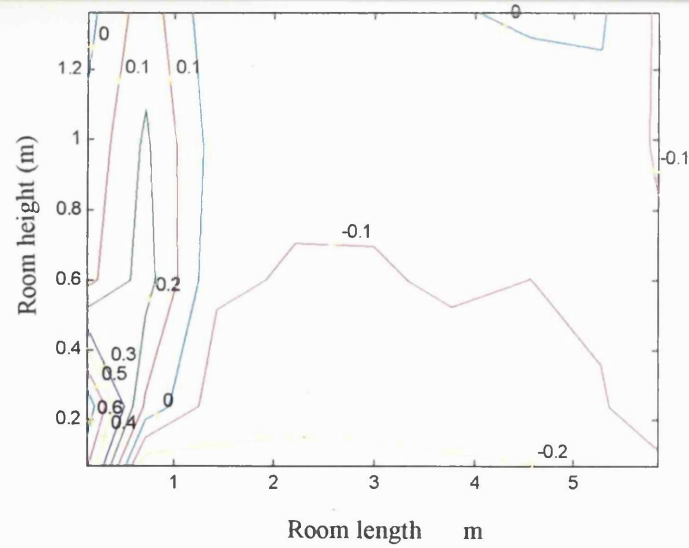3 ACH, supply velocity 0.3 m/s,
supply temperature 42 °C.

Figure.4.A22

Enthalpy contours in plane
y = 3 m, configuration B at
3 ACH, supply velocity 0.3 m/s,
supply temperature 42 °C.
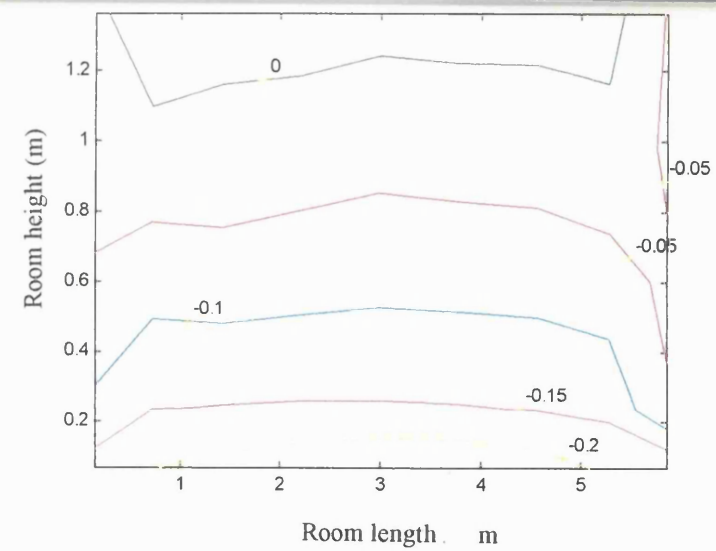
Figure 4.A23 *PMV* and *PD*$_v$ contours of configuration B, 6 ACH, supply velocity 0.88 m/s, supply temperature 30 °C. (a) *PMV* contours in plane y = 3 m. (b) *PMV* contours in plane y = 5.7 m. (c) *PD*$_v$ contours in plane y = 3 m (%). (d) *PD*$_v$ contours in plane y = 5.7 m (%).

Figure.4.A24

Velocity vectors in plane
y = 3 m, configuration B at
6 ACH, supply velocity 0.88 m/s,
supply temperature 30 °C.

Figure.4.A25

Enthalpy contours in plane
y = 3 m, configuration B at
6 ACH, supply velocity 0.88 m/s,
supply temperature 30 °C.

Figure.4.A26

Velocity vectors in plane
z = 1.2 m, configuration B at
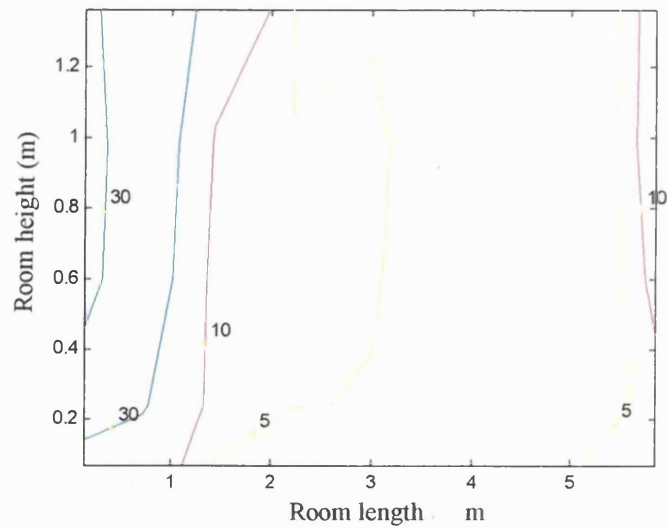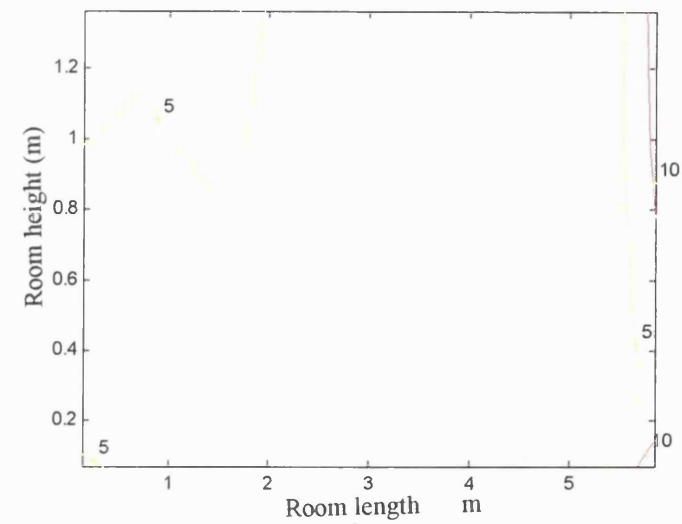6 ACH, supply velocity 0.88 m/s,
supply temperature 30 °C.

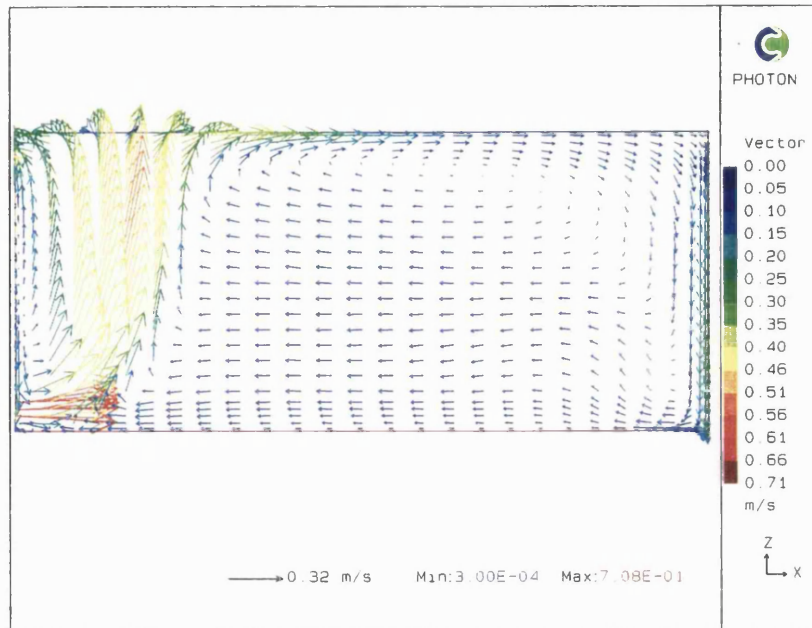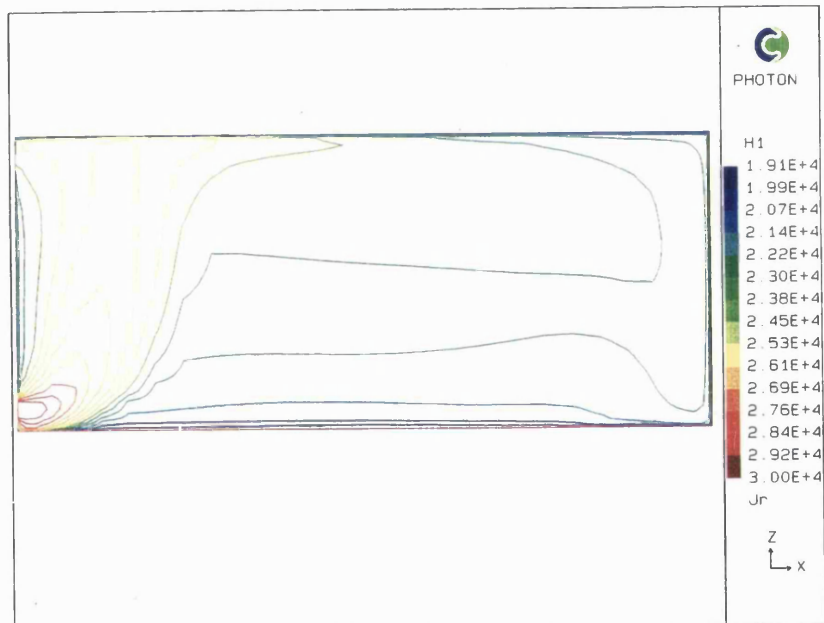**Figure 4.A27** *PMV* and *PD*$_v$ contours of configuration B, 6 ACH, supply velocity 0.6 m/s, supply temperature 30 °C. (a) *PMV* contours in plane y = 3 m. (b) *PMV* contours in plane y = 5.7 m. (c) *PD*$_v$ contours in plane y = 3 m (%). (d) *PD*$_v$ contours in plane y = 5.7 m (%).
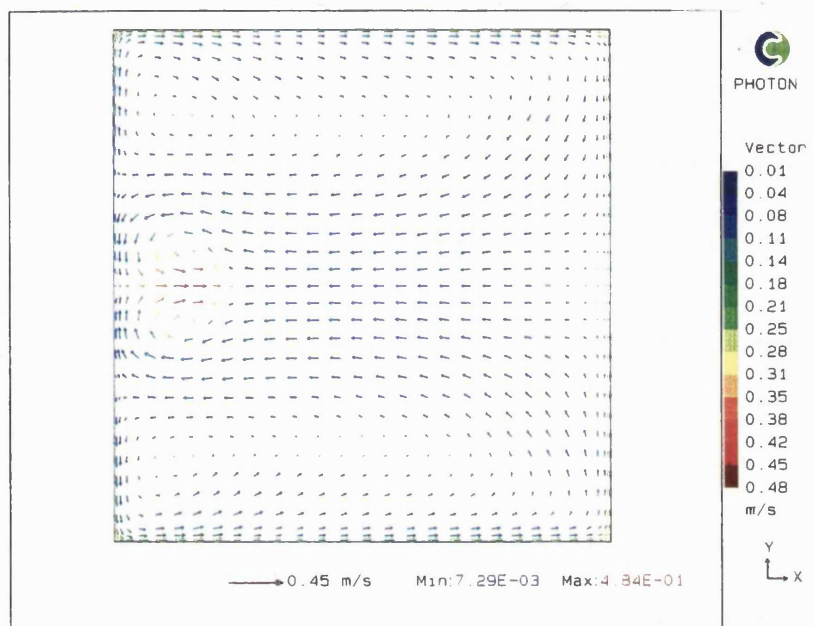
Figure.4.A28

Velocity vectors in plane
y = 3 m, configuration B at
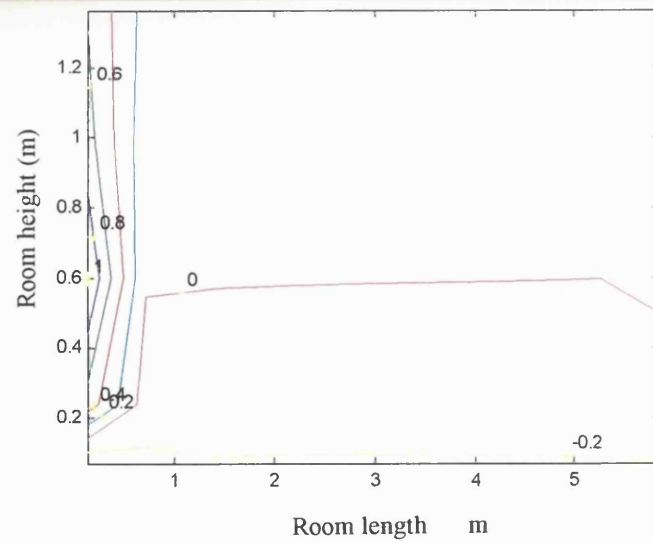6 ACH, supply velocity 0.6 m/s,
supply temperature 30 °C.

Figure.4.A29

Enthalpy contours in plane
y = 3 m, configuration B at
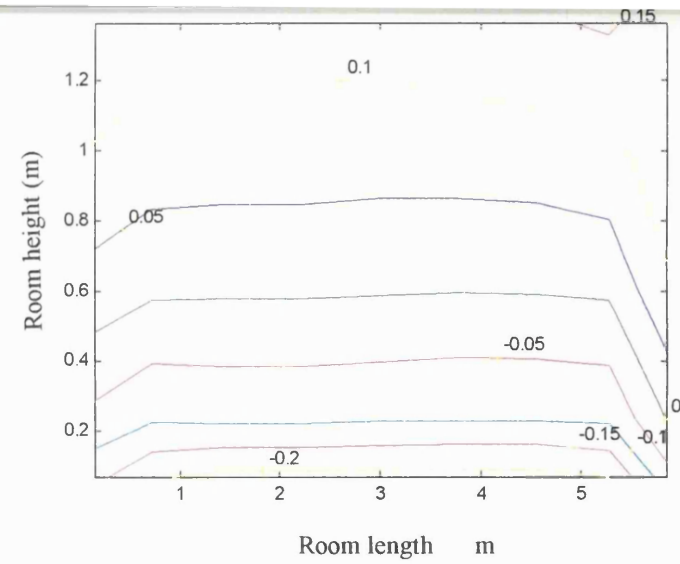6 ACH, supply velocity 0.6 m/s,
supply temperature 30 °C.

Figure.4.A30

Velocity vectors in plane
z = 1.2 m, configuration B at
6 ACH, supply velocity 0.6 m/s,
supply temperature 30 °C.

Figure 4.A31 *PMV* and *PD_v* contours of configuration D, 3 ACH, supply velocity 0.3 m/s, supply temperature 42 °C. (a) *PMV* contours in plane y = 3 m. (b) *PMV* contours in plane y = 5.7 m. (c) *PD_v* contours in plane y = 3 m (%). (d) *PD_v* contours in plane y = 5.7 m (%).

Figure.4.A32

Velocity vectors in plane
y = 3 m, configuration D at
3 ACH, supply velocity 0.3 m/s,
supply temperature 42 °C.

Figure.4.A33

Enthalpy contours in plane
y = 3 m, configuration D at
3 ACH, supply velocity 0.3 m/s,
supply temperature 42 °C.
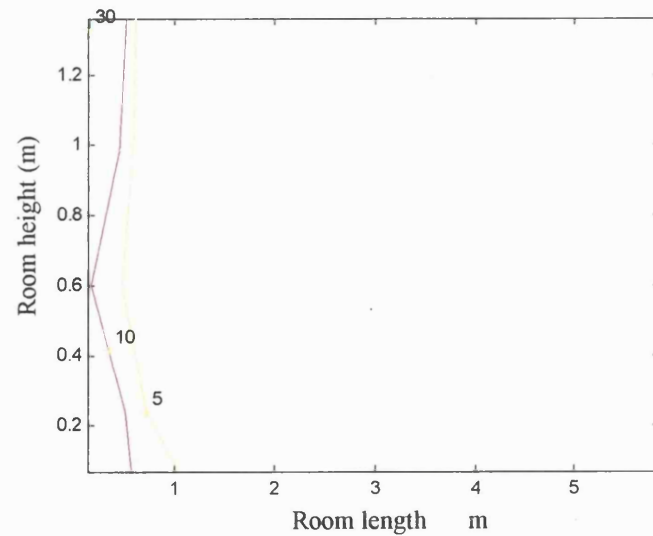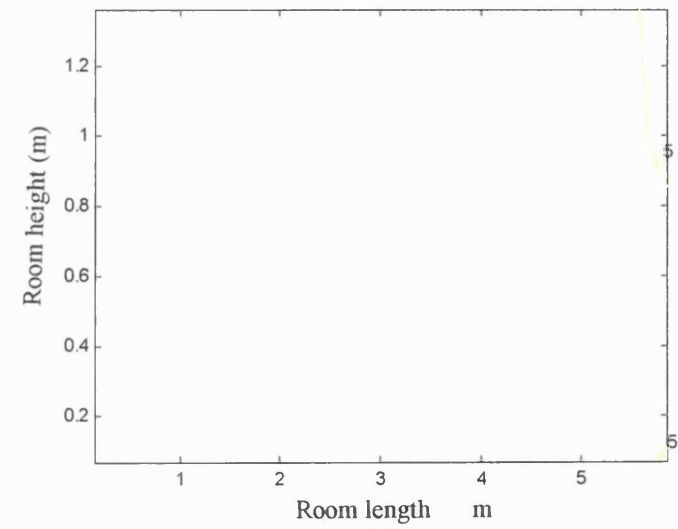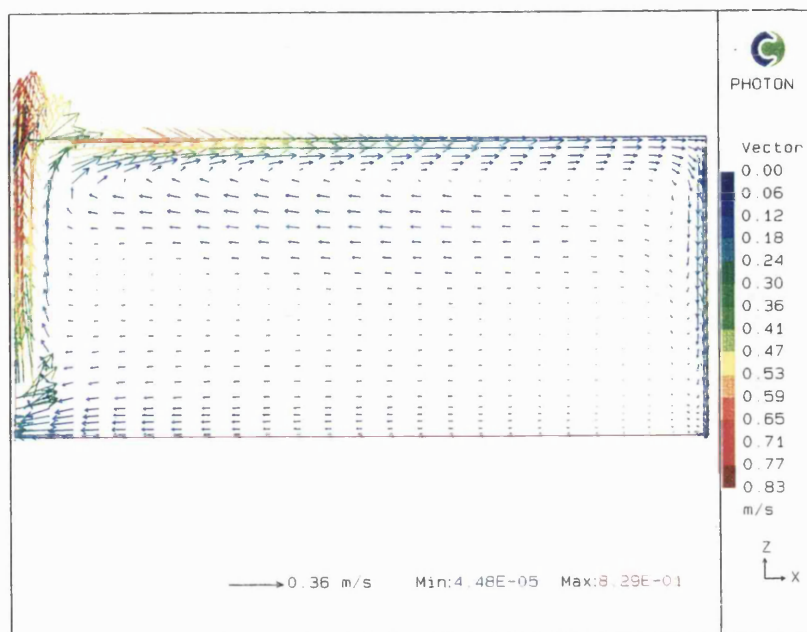
Figure 4.A34 *PMV* and *PD*$_v$ contours of configuration D, 3 ACH, supply velocity 0.17 m/s, supply temperature 42 °C. (a) *PMV* contours in plane y = 3 m. (b) *PMV* contours in plane y = 5.7 m. (c) *PD*$_v$ contours in plane y = 3 m (%). (d) *PD*$_v$ contours in plane y = 5.7 m (%).

Figure.4.A35

Velocity vectors in plane
y = 3 m, configuration D at
3 ACH, supply velocity 0.17 m/s,
supply temperature 42 °C.

Figure.4.A36

Enthalpy contours in plane
y = 3 m, configuration D at
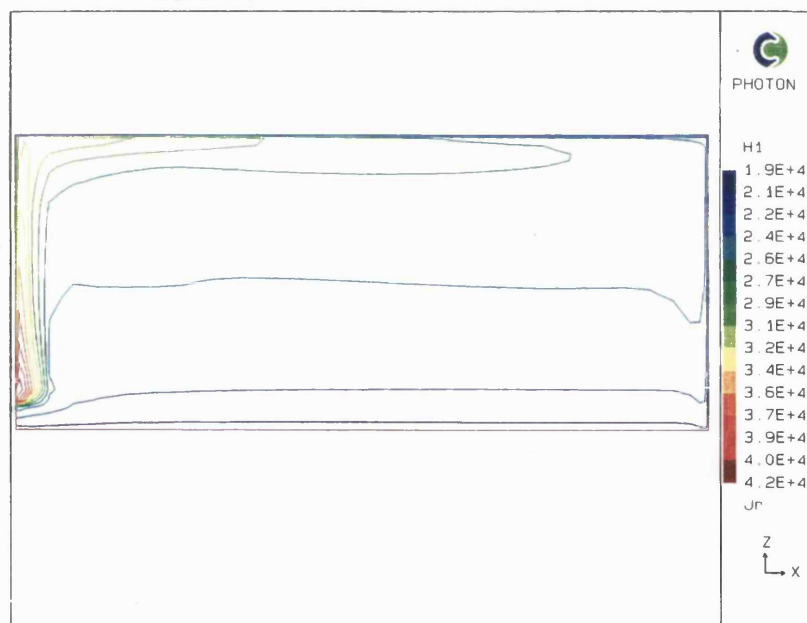3 ACH, supply velocity 0.17 m/s,
supply temperature 42 °C.

Figure 4.A37 *PMV* and *PD$_v$* contours of configuration D, 6 ACH, supply velocity 0.6 m/s, supply temperature 30 °C. (a) *PMV* contours in plane y = 3 m. (b) *PMV* contours in plane y = 5.7 m. (c) *PD$_v$* contours in plane y = 3 m (%). (d) *PD$_v$* contours in plane y = 5.7 m (%).
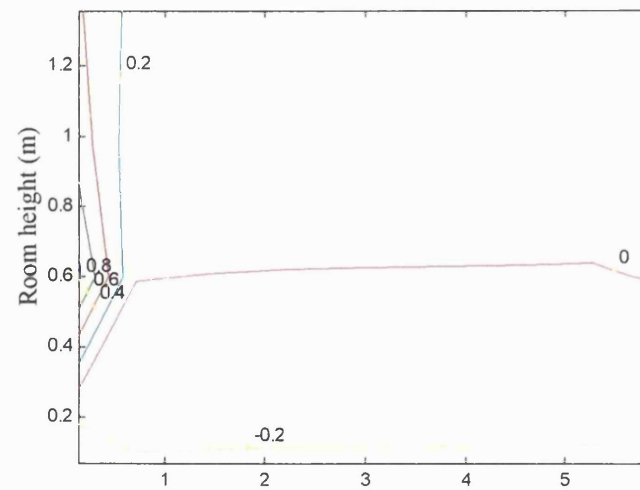
Figure.4.A38

Velocity vectors in plane
y = 3 m, configuration D at
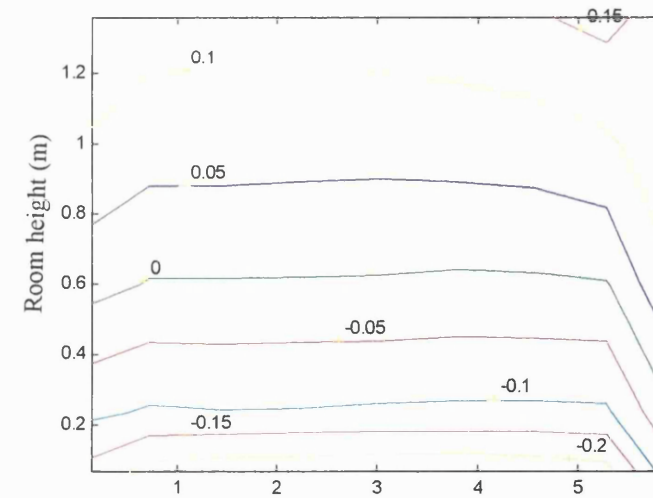6 ACH, supply velocity 0.6 m/s,
supply temperature 30 °C.

Figure.4.A39

Enthalpy contours in plane
y = 3 m, configuration D at
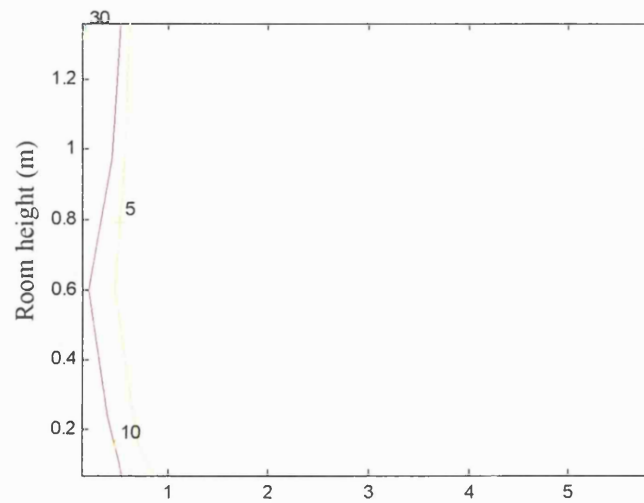6 ACH, supply velocity 0.6 m/s,
supply temperature 30 °C.
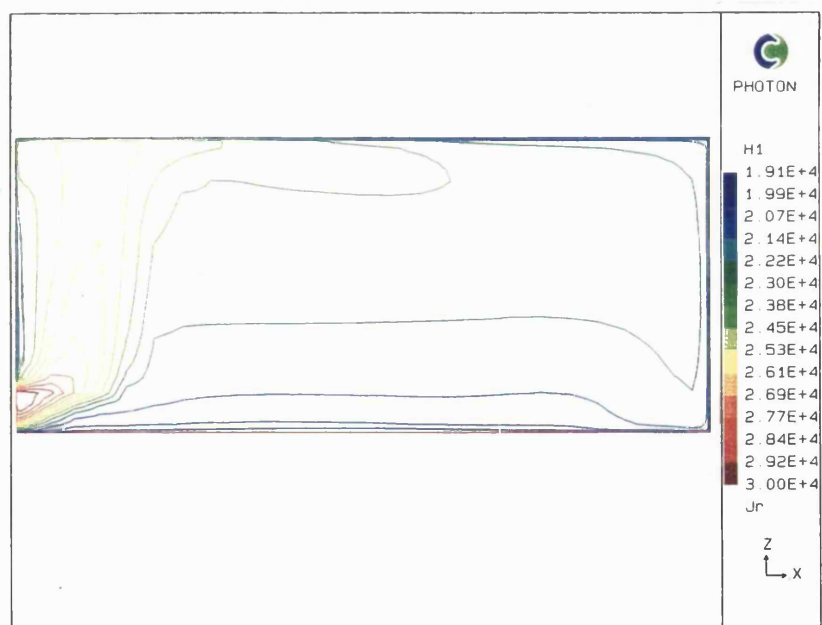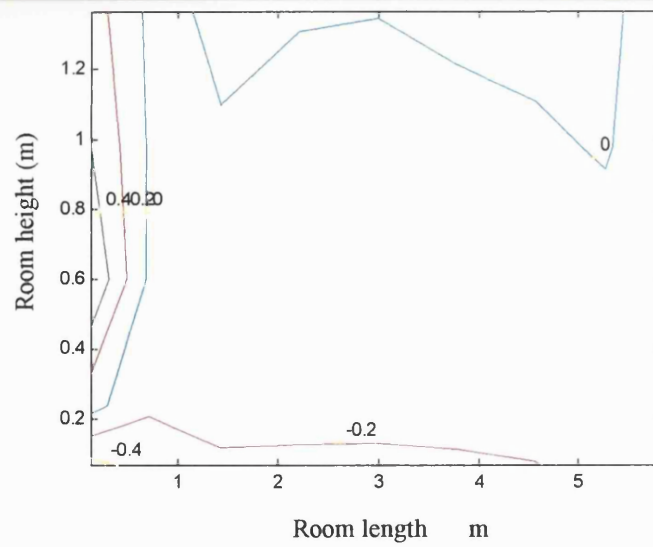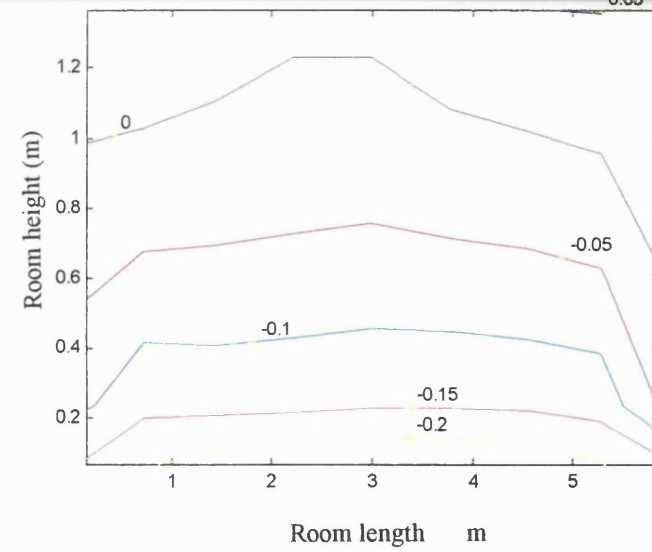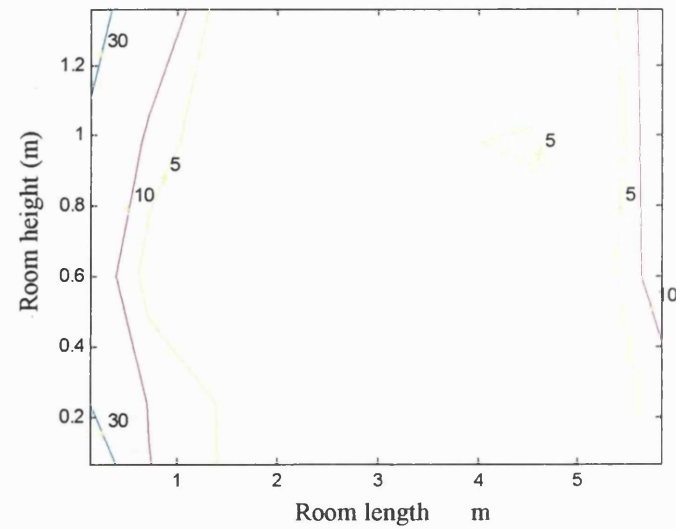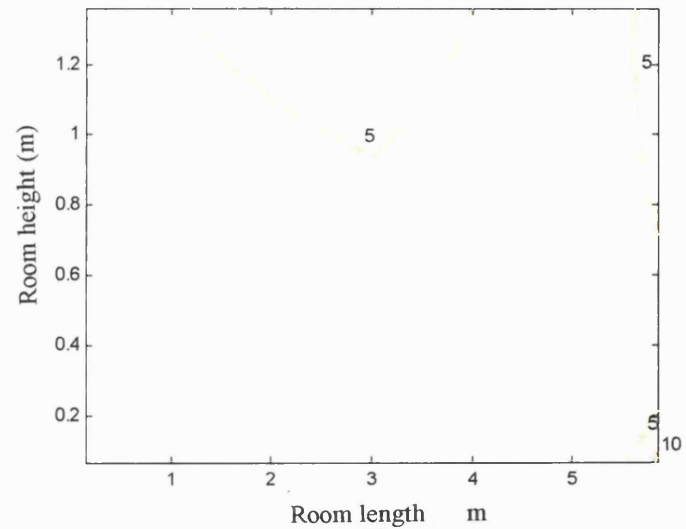
Figure 4.A40 *PMV* and *PD*$_v$ contours of configuration D, 6 ACH, supply velocity 0.34 m/s, supply temperature 30 °C. (a) *PMV* contours in plane y = 3 m. (b) *PMV* contours in plane y = 5.7 m. (c) *PD*$_v$ contours in plane y = 3 m (%). (d) *PD*$_v$ contours in plane y = 5.7 m (%).

Figure.4.A41

Velocity vectors in plane
y = 3 m, configuration D at
6 ACH, supply velocity 0.34 m/s,
supply temperature 30 °C.
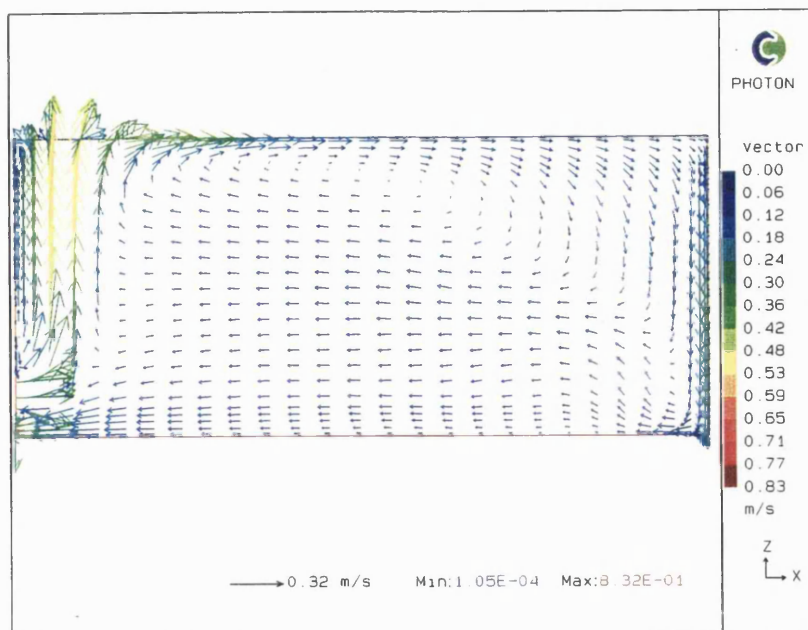
Figure.4.A42

Enthalpy contours in plane
y = 3 m, configuration D at
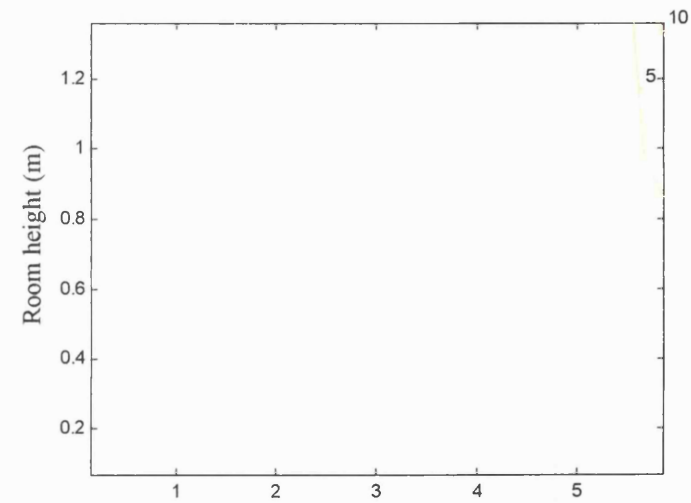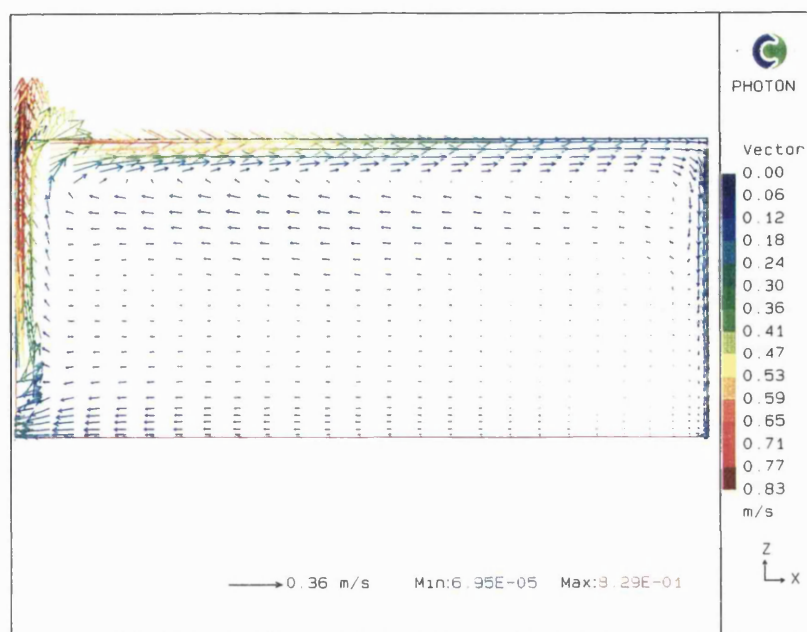6 ACH, supply velocity 0.34 m/s,
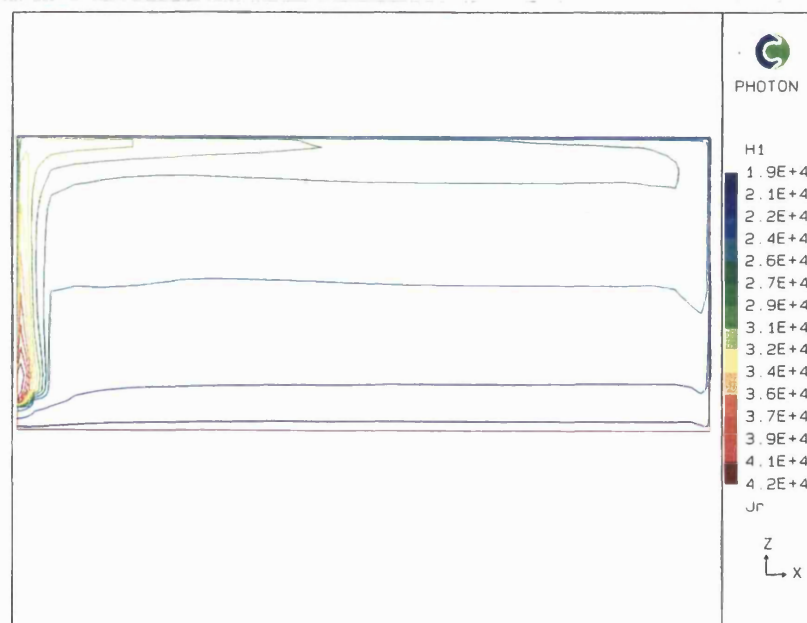supply temperature 30 °C.
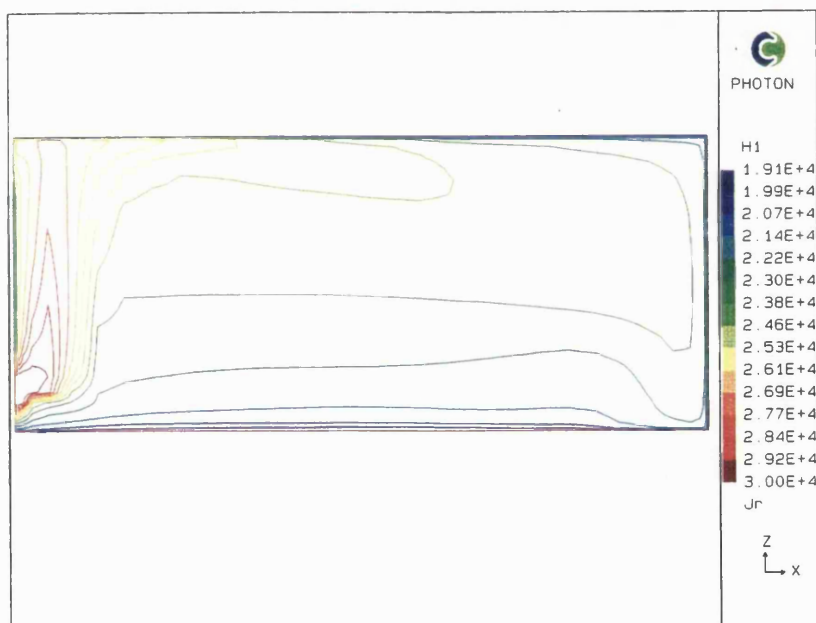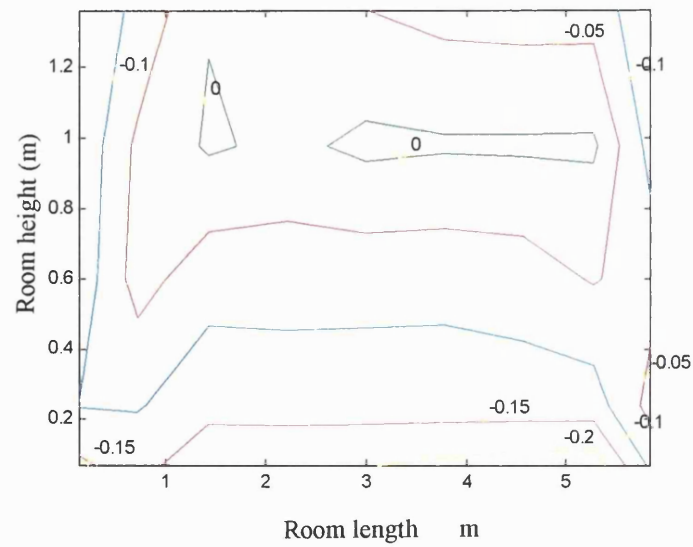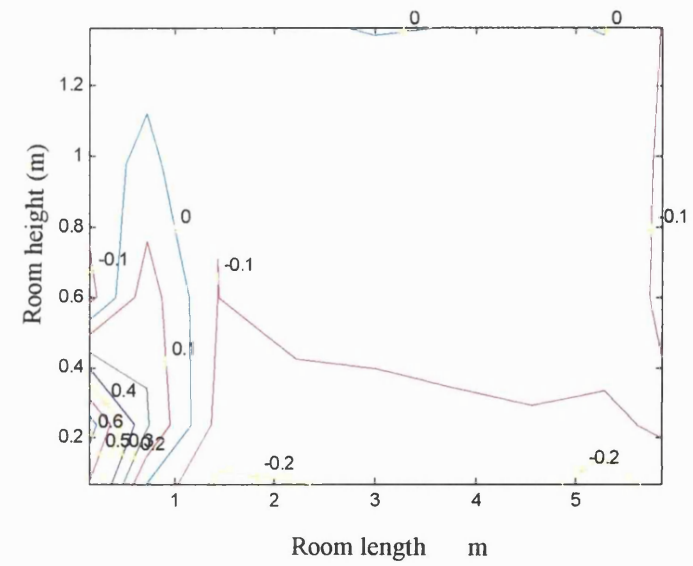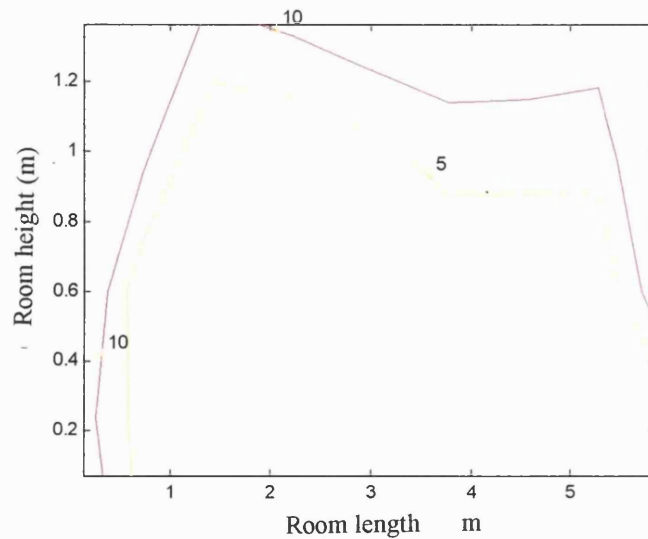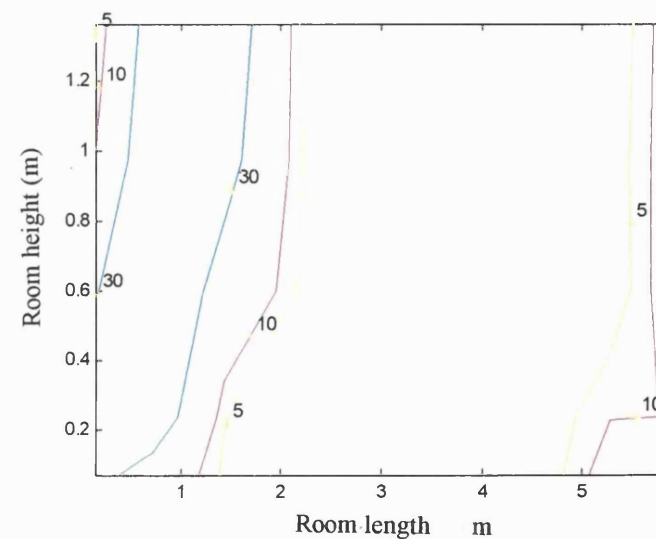
Figure 4.A43 *PMV* and *PD$_v$* contours of configuration B-2, 6 ACH, supply velocity 0.66 m/s, supply temperature 30 °C. (a) *PMV* contours in plane y = 3 m. (b) *PMV* contours in plane y = 5.7 m. (c) *PD$_v$* contours in plane y = 3 m (%). (d) *PD$_v$* contours in plane y = 5.7 m (%).
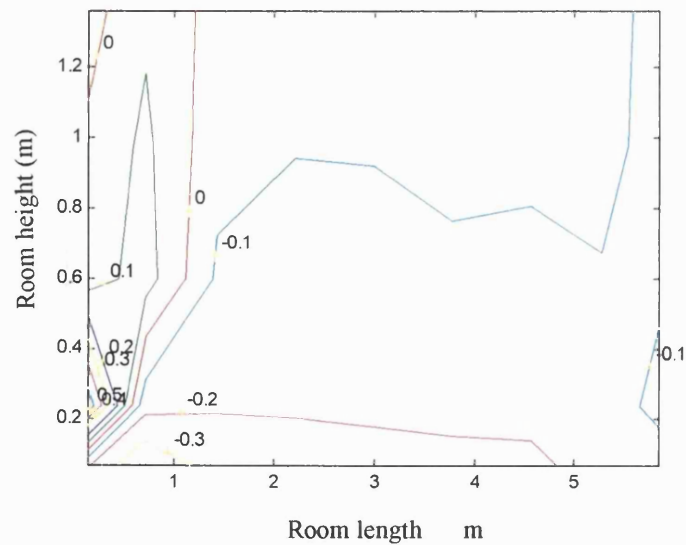
Figure.4.A44

Velocity vectors in plane
y = 3 m, configuration B-2 at
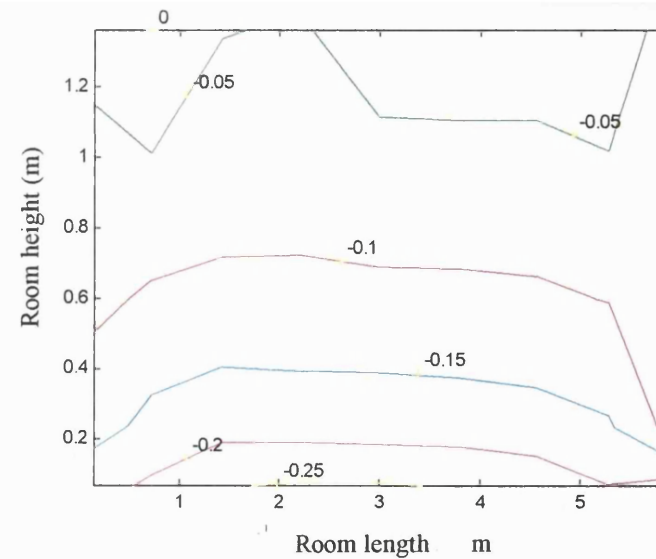6 ACH, supply velocity 0.66 m/s,
supply temperature 30 °C.
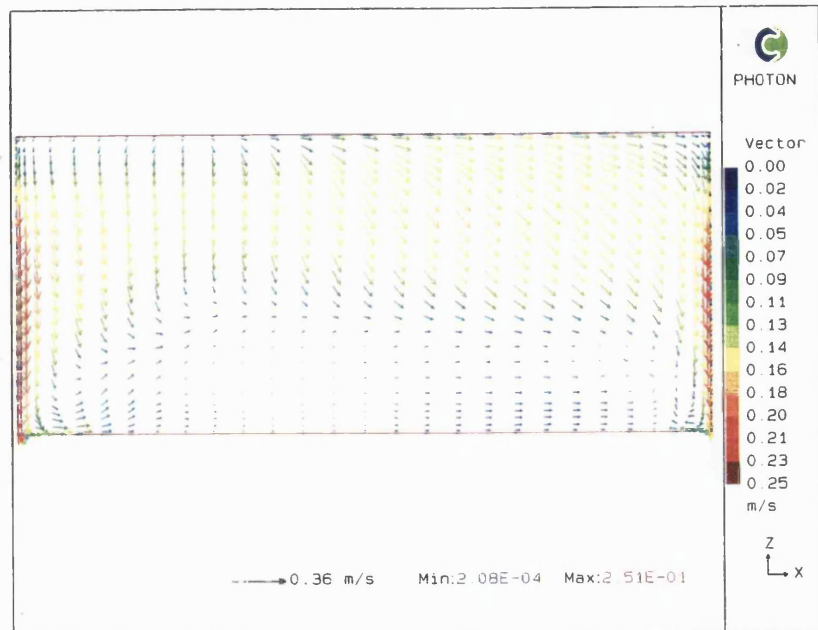
Figure.4.A45

Velocity vectors in plane
z = 1.2 m, configuration B-2 at
6 ACH, supply velocity 0.66 m/s,
supply temperature 30 °C.
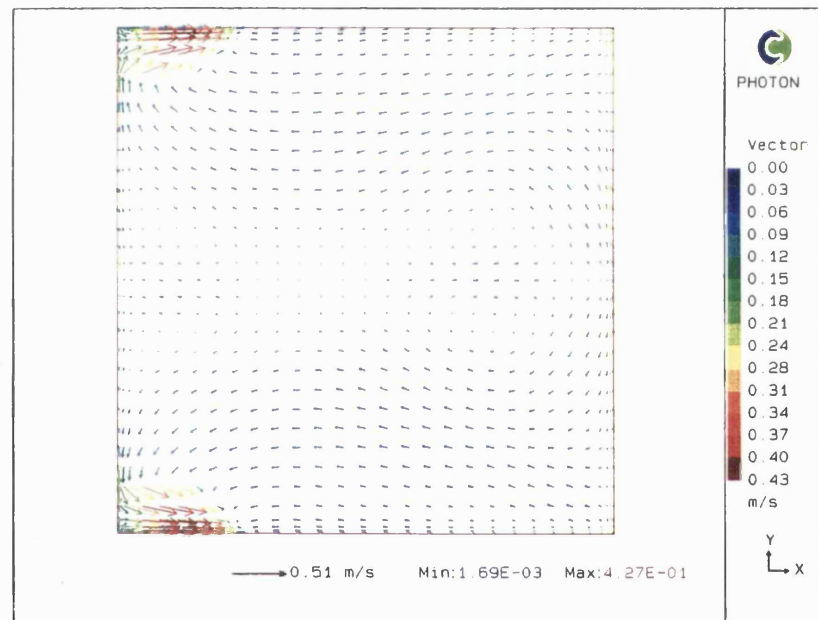
Figure.4.A46

Velocity vectors in plane
y = 3 m, configuration C at
6 ACH, supply velocity 0.6 m/s,
supply temperature 30 °C.
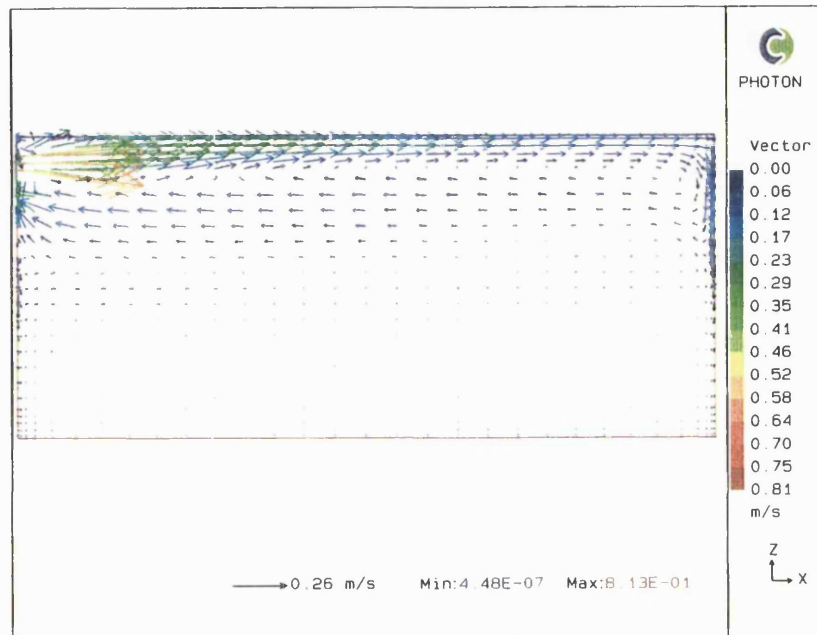
Figure.4.A47

Velocity vectors in plane
y = 3 m, configuration E at
6 ACH, supply velocity 0.6 m/s,
supply temperature 30 °C.
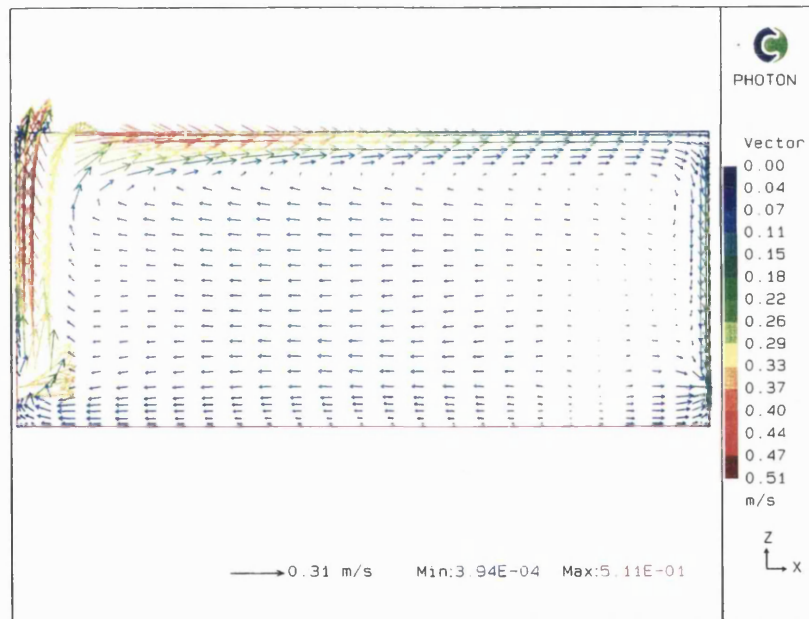
Figure.4.A48

Pollutant concentration contours
in plane y = 3 m, configuration A
at 3 ACH, supply velocity 0.3 m/s,
supply temperature 42 °C.
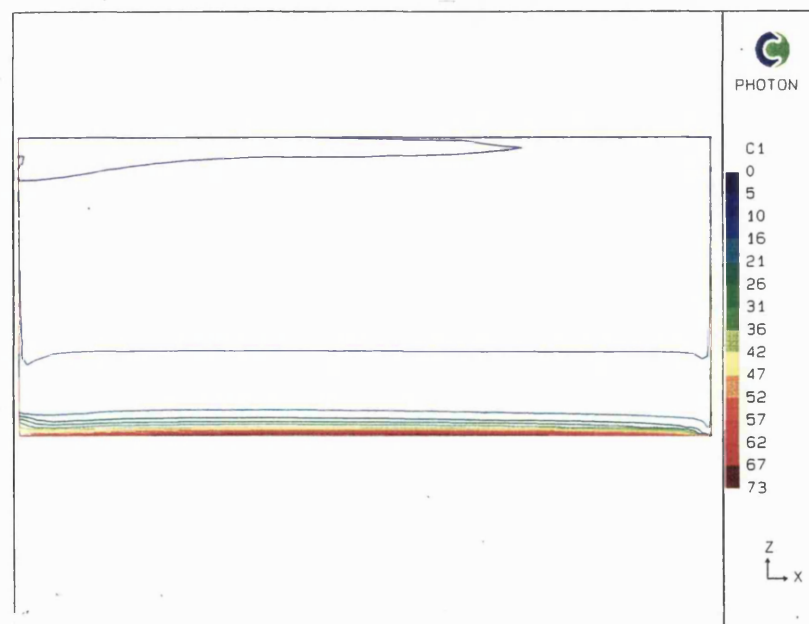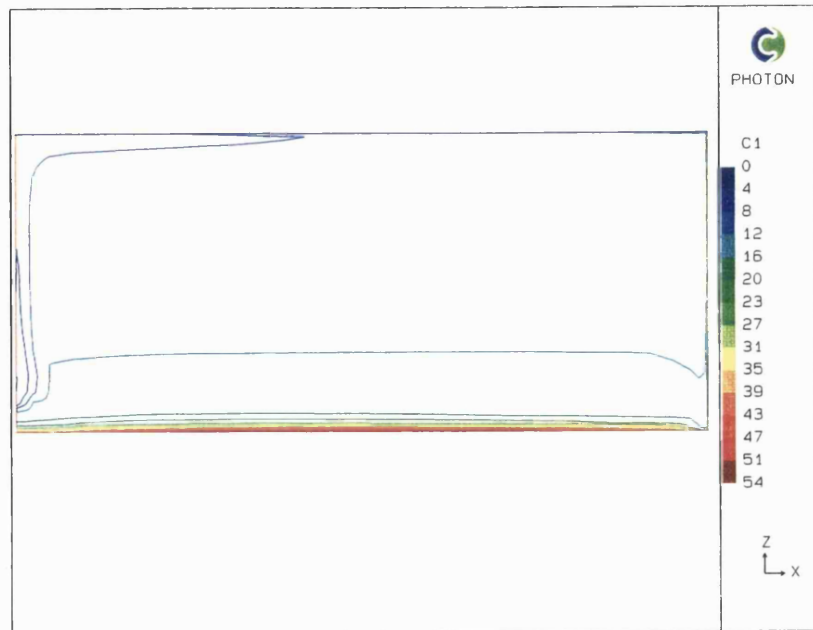
Figure.4.A49

Pollutant concentration contours
in plane y = 3 m, configuration D
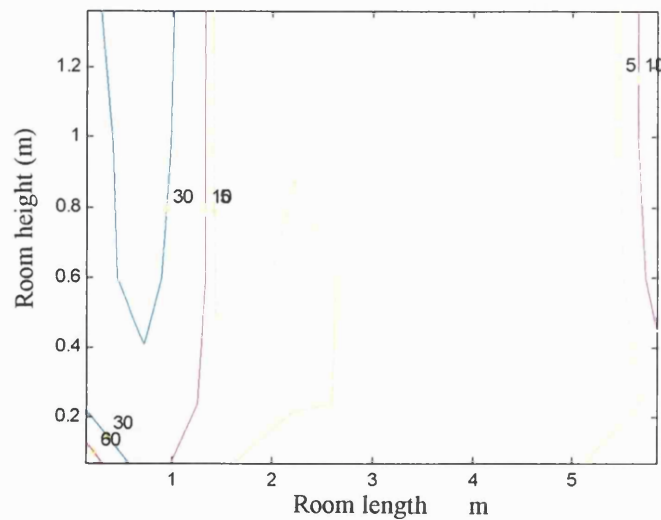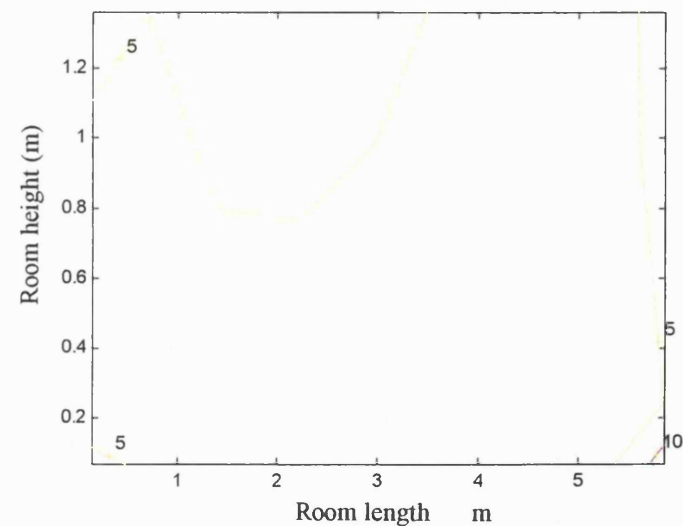at 3 ACH, supply velocity 0.17 m/s,
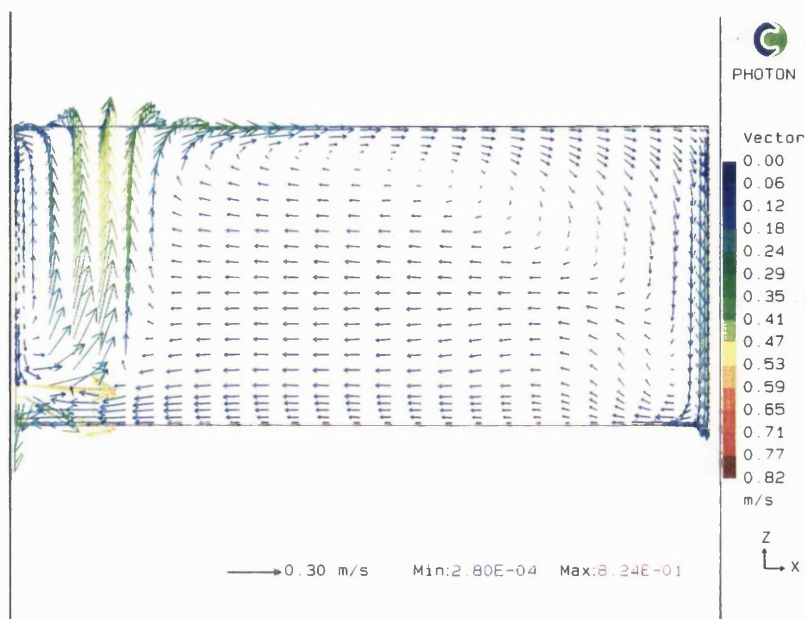supply temperature 42 °C.

# 5. ANALYSIS OF THE PROPOSED SYSTEM

In the following sections, the term *flow behaviour* is used in reference to the airflow patterns and distributions of air temperature, air velocity, turbulence and pollutant concentrations. The terms *personal parameters* and *environmental parameters* are as defined in Chapter 1. The H & V system unless otherwise stated, is assumed to be a demand controlled and rapid response heating and ventilating system.

5.1 Objectives

The previous chapter evaluated the influence of the *position* of the supply and extract air terminal devices (ATDs) on thermal comfort and indoor air quality (IAQ) within the occupied zone. The configuration of high level supply and low level extract, both mounted on the same wall surface, was selected as most appropriate in satisfying the requirements of the H & V system. These requirements were the provision of good thermal comfort and IAQ over the expected range of supply parameters (flow rates and supply air temperatures).

Having identified a suitable configuration of the H & V system, the work presented in this chapter investigates this configuration in a more thorough and detailed manner. This involves analysis of the flow behaviour over a wider range of flow rates and supply temperatures than in the previous section. Additionally the effects of further parameters, referred to as the *room specific parameters*, which may have an influence on the flow field are assessed. These include:

- wall surface temperatures
- internal heat sources and their locations
- obstacles (persons, furniture etc.) and their locations
- a cold window surface
- room geometry
- time dependent, or transient effects

The observations of the flow behaviour over the investigation range were used in addressing the following issues:

- *Limits of operation of the H and V equipment*

  For a system operating over a wide range of flow rates and inlet air temperatures, unacceptably high vertical air temperature differences may occur at low flow rates and high supply air temperatures. Similarly at high flow rates and particularly at low air temperatures, there is likely to be discomfort due to draught. It was to be investigated whether limits of operation could be identified for application in varied and changing environments (i.e. in rooms with different room specific effects or varying internal conditions).

- *Transient behaviour of the system*

  In continuous heating/ventilation systems, steady state solutions provide good representations of the room conditions. The rate at which steady state conditions are reached after start-up of the H & V system was to be investigated, together with the flow behaviour during this transition period. These observations were to provide an indication of the start-up times and conditions required to achieve satisfactory thermal comfort and IAQ *for* or *during* occupancy.

- *Thermal comfort control*

  The concept and feasibility of comfort control was addressed and the requirements for implementation of such comfort control identified. This included determination of the number and location of sensors that adequately provide representative values of the required conditions in the occupied zone.

The information gained from the above analyses contributed towards the recommendation of a control strategy with the aim of achieving good thermal comfort and IAQ in an energy efficient manner.

5.2   Approach

Room airflow modelling is commonly performed in simplified conditions, with a room represented as a bare enclosure at uniform surface temperatures. This case which will be referred to as the 'standard' configuration, is commonly used in providing an indication of the airflow patterns and air temperature distributions within a room. However in real environments, room specific parameters have an effect on the flow field, the magnitude of which depends on the type of ventilation system in use (e.g. mixing ventilation, displacement ventilation). These parameters are building and user specific and vary from one room to the next, with some variance over time (e.g. in the short term: heat sources and surface temperatures, and in the long term: room and furniture layout). In terms of time and cost efficiency, it would be unrealistic to perform simulations for every possible combination of room specific parameters. The approach adopted therefore was to perform extensive simulations using the standard case (parametric studies) and establish links to room specific cases and the time dependent variations (sensitivity studies).

5.3   Simulations

All simulations were performed using the two layer k-ε turbulence model. Two room dimensions were used: the room (6 x 6 x 2.5 m^3) used in the investigation of the ATD configuration in the previous chapter and a room of dimensions 4 x 4 x 2.5 m^3. These configurations used supply and extract ATD areas of 0.25 m^2 and 0.11 m^2 for the rooms of dimension 6 x 6 x 2.5 m^3 and 4 x 4 x 2.5 m^3 respectively. The ATD area used in the smaller room was sized to maintain the same supply velocity as that of the larger room at the same ACH.

The investigation and therefore simulation task was approached in simulation groups as listed below. A brief description of these groups and the investigations performed is given, although greater detail is provided within the 'analysis' section. Table 5.1 outlines the full range of simulations performed. Steady state solutions were obtained for the parametric and sensitivity studies. Time dependent simulations were performed on the standard configuration only. The default room dimension and wall surface temperatures are 6 x 6 x 2.5m^3 and 19 °C respectively.

Uniform wall temperatures

All surfaces are at the same temperature. No temperature variations occur over the surfaces. This is referred to as the 'standard' case.

Walls with vertical temperature gradients

During operation of the H & V system, vertical air temperature gradients in the room also impose temperature gradients in the side walls. These temperature gradients were approximated by temperature steps in vertical sections of side walls.

Obstacles

Solid objects of varying size were placed at different locations within the occupied zone. Two different obstacle sizes were used to represent a combination of persons and/or furniture.

Heat sources

The influence of heat sources both within and above the occupied zone was investigated. Heat fluxes within the occupied zone were used to represent heat losses from persons at two metabolic activity rates, 110 and 220 W. The heat source at the latter in particular could equally represent other heat sources within the room. The heat source above the occupied zone is located on the ceiling, representing heat gains from lighting appliances.

Unequal wall surface temperatures

Individual wall surfaces within a room will experience different temperatures. To investigate the effect of this, different surface temperatures were prescribed with each surface at a uniform temperature. Surface temperatures were specified, using the results obtained in Section 3.5.2.

Cold window surface

The influence of a cold window surface (dimension of 6 x 0.77 m^2) in the east-wall section was investigated. The temperature of the window was assumed to be 16 °C, with the wall surfaces at 20 °C.

Case	Wall surface temperature (°C)	ACH	Inlet temperature range (°C)	Heat source (W)
Steady-state				
Uniform wall	19	3	35-55	-
temperatures	19	4.5	25-45	-
	19	6	25-35	-
	19	9	25-35	-
	20	3	30-50	-
Walls with vertical	vtg 20,20,20	3	30	-
temperature gradients	vtg 19.5,20,20.5		30	-
	vtg 19,20,21		30-50	-
vtg: *temperatures in*				
three sections of vertical	vtg 19,20,21	9	25, 30	-
walls. From low to high.				
Obstacles	19	3	35	-
	19	9	25	-
Increased obstacle size	19*	9	25*	-
Heat sources	19	3	35, 40, 45	2 x 110W (2 persons)
	19	9	25, 30, 35	" "
	19*	3*	35*	" "
	19	4.5	30	2 x 220 W
Heat source moved	19	3	35	(2 x 110)+200W (light)
	19	3	35	200 W (light only)
Unequal wall surface	*19.55, 19, 20	4.5	30	-
temperatures	*19.39, 19, 20	4.5	30	-
	*19.27, 19, 20	3	42	-
Average, minimum and	*19.39, 19, 20	3	42	-
maximum wall surface	*19.55, 19, 20	3	42	-
temperatures	*19.27, 18, 20	3	42	-
Cold window surface	19.84*	3	30	-
Average surface				
temperature, window				
16°C, walls 20°C				
Varied geometry, 4 x 4 x	19	3	40	-
2.5 m³, uniform wall	19	6	30	-
temperatures				
Time dependent				
Transient, uniform wall	19	3	42	-
temperatures	19	6	30	-
	19	9	25	-
3 ACH: 3 x 15 min				
increments				
6,9 ACH: 2 x 15min				
increments				

Table 5.1 CFD simulations performed on the proposed system

5.4   Evaluation

As in the previous chapter the evaluation of the thermal and flow environment was performed through a combination of graphical and numerical analysis using the same numerical evaluation scheme. The evaluation will be presented in the following sections:-

i)   *Parametric studies* based on the standard case with variation of flow rate and supply air temperature. (Section 5.5)

ii)   *Sensitivity studies* taking into consideration the room specific parameters. (Section 5.6)

iii) *Limits of operation of the H and V system* will be established as a result of observations in parametric and sensitivity studies, to prevent local thermal discomforts. (Section 5.7)

iv)   *Thermal comfort control* will be assessed and the feasibility of this together with the measurements required to achieve this. (Section 5.8)

The parametric and sensitivity studies investigate the flow behaviour and its impact on the local thermal discomforts due to vertical temperature differences and draught. The influence of the flow behaviour on the thermal sensation is however assessed at a later stage (Section 5.8). To consider thermal comfort in two stages offers a number of advantages over the combined process. Firstly, the comfort criteria which are independent of personal parameters are valid at all times for the given flow and thermal environment, unlike the thermal sensation. These limits will be applicable independent of the activity or clothing insulation level of the person(s). Secondly, this allows for a more thorough evaluation of the thermal sensation (*PMV*) at varied activity rate and clothing insulation values. Although representative/typical values of activity rate and clothing insulation may be used in an evaluation of the *PMV* (as was done in Chapter 4), in practice, these will vary according to the individual. The use of representative values is acceptable for design purposes where the aim is usually to achieve satisfaction for the average user or majority of users. Independent evaluation allows for assessment of the thermal sensation over a wide range of personal parameters.

The result section for each simulation group includes a full table of the numerical results, as produced in Chapter 4. Although not all of these values were specifically referred to in the course of the analysis, these contributed in the development of the analysis and reaching the conclusions. These are also included for completeness and to allow the listing of all the results for a particular simulation group in one section. Where comparisons are made between groups, the comparison data is also included in the Table. The analysis in each section where possible, adheres to the following sequence:

Flow patterns and velocity distributions

Temperature distribution across the room

Vertical temperature distribution

Draught

Pollutant concentrations

Pollutant concentrations are discussed only in the parametric studies and in the time dependent cases. All reference to average values refer only to the occupied zone (as quoted by values in the result tables).

5.5 Parametric studies on the standard case

This section presents results for simulations using the standard case i.e. with all surfaces of the enclosure at the same temperature and no internal obstacles or heat sources. Simulations were performed at fixed flow rates, corresponding to 3, 4.5, 6 and 9 ACH, at a range of supply air temperatures shown in Table 5.2. The reducing trend in supply air temperature with increasing flow rate, seen in Table 5.2, was in order to attain similar ranges of room air temperatures. The Table includes the listing of the graphical illustrations of the airflow patterns (and distribution of velocities) in the symmetry plane and an outer plane of each of the cases. Wall surface temperatures were all at 19 °C. A summary of the numerical evaluation results is shown in Table 5.3. In addition to the variables previously defined (Chapter 4), this includes the Archimedes number and the air velocity at a point in the mid-height of the room and in the vicinity of the west-wall. The Archimedes number (Ar) is a non-dimensional

number that gives a measure of the ratio of the buoyant to inertia force of the supply air stream and is defined as:

$$Ar = \frac{\beta \cdot g\sqrt{A}\Delta T}{U^2}$$

where

β = Cubic expansion coefficient of air (/K)

g = acceleration due to gravity (m/s^2)

A = cross sectional area of the supply device (m^2)

ΔT = temperature difference between supply air and the bulk room air (°C)

U = velocity at supply outlet (m/s)

T_{on} (°C)	3 ACH (Figure No.)	4.5 ACH (Figure No.)	6 ACH (Figure No.)	9 ACH (Figure No.)
25		✓ (Figure 5.A6)	✓ (Figure 5.A11)	✓ (Figure 5.A16)
27.5			✓ (Figure 5.A12)	
30		✓ (Figure 5.A7)	✓ (Figure 5.A13)	✓ (Figure 5.A17)
32.5			✓ (Figure 5.A14)	
35	✓ (Figure 5.A1)	✓ (Figure 5.A8)	✓ (Figure 5.A15)	✓ (Figure 5.A18)
40	✓ (Figure 5.A2)	✓ (Figure 5.A9)		
45	✓ (Figure 5.A3)	✓ (Figure 5.A10)		
50	✓ (Figure 5.A4)			
55	✓ (Figure 5.A5)			

Table 5.2 Combination of ACH and supply air temperatures investigated for simulations of 'standard' configuration. Includes listing of figure numbers of graphical illustration of the airflow patterns.

Results

At flow rates of 3 (Figures5.A1-5) and 4.5 ACH (Figures 5.A6-10) no large variation in the magnitudes of velocity are observed with increases in supply temperature, also indicated by the average and standard deviations of the velocities shown in Table 5.3. As the flow rate was increased to 6 ACH (Figures 5.A11-15), reductions in velocity occur with increasing supply air temperature, in the north-eastern sector of the occupied zone in what may be described as a large triangular circulating zone, from the low end of the east-wall flowing upwards towards the high end of the west-wall and there being entrained with the supply airflow towards the east-wall. As the airflow rate was further increased to 9 ACH (Figures 5.A16-18), clear reductions in air velocity can be seen throughout the occupied zone, with increasing supply air temperature. In the outer plane, these reductions in velocity are seen to be accompanied by changes in

the flow direction, with an increasing upward-flow tendency leading to a similar circulating flow pattern as described at 6 ACH.

Reductions in air velocities in the occupied zone occur with increasing supply air temperature (at fixed airflow rates), despite greater entrainment of the room air by the supply air stream at higher supply air temperatures. Greater entrainment is indicated by the increasing velocities in the reverse airflow immediately below the supply air stream. The reduction in air velocity appears to be due to two effects:

- greater spreading across the ceiling and thereby more even distribution of the supply air stream. Evidence of greater spread of the supply air stream with increasing supply air temperature is seen by the increasing air movement towards the west-end of the outer planes.

- greater concentration/volume of the flow near the (cold) side walls due to large downward flow in this regions. This would be caused by the increasing temperature difference between the room air and the side wall surfaces.

The variation of the average velocity (over the range of supply air temperatures) with flow rate is shown in Figure 5.1. This shows a near exponential increase in average air velocity with increasing airflow rate.
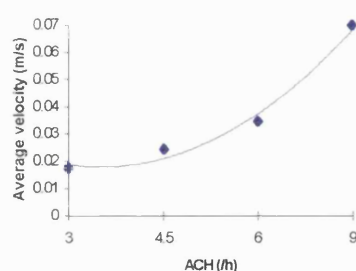
Figure 5.1 Variation of average velocity (over range of supply air temperatures) with flow rate (ACH).

Air temperature distributions in the mid-height of the room are shown in Figures 5.A19 - 5.A22 for cases 3, 4.5, 6 and 9 ACH respectively. These reveal uniformity of air temperature distribution across the occupied zone for most of the investigated range. The non-uniformity in Figure 5.A20, at the supply air temperature of 45 °C, was believed to be due to a weakness in the numerical scheme (which was commented

upon in Section 2.2.5). At 9 ACH however, at the supply air temperature of 25 °C a gradual air temperature rise occurs from a distance of approximately 1 m from the side wall until very close to the wall surface. Greater temperature uniformity is obtained with increasing supply air temperature as a result of the increase in the spread/distribution of the supply air stream across the ceiling.

The vertical air temperature distributions at the mid-point of the occupied zone are shown in Figures 5.2a-d. At low flow rates, the temperature variation with height is approximately linear over most of the occupied zone. As the flow rate increases a reduction in temperature gradient, with increasing height, is observed. As would be expected, at similar average temperatures, lower temperature gradients occur at increased flow rates (as illustrated in Figure 5.3).

(a)   (b)

(c)   (d)

Figure 5.2 a-d Vertical air temperature variation in the occupied zone of the 'standard' case at (a) 3 ACH (b) 4.5 ACH (c) 6 ACH (d) 9 ACH.

Similarities in airflow patterns are observed at similar Archimedes numbers (Table 5.3), naturally at different magnitudes of velocity. In would appear that the Archimedes

number may be used to quantify the spread of the air-stream, with the increasing Archimedes numbers resulting in greater spreading. The spread of the supply air stream was found to influence both the non-uniformities in the thermal env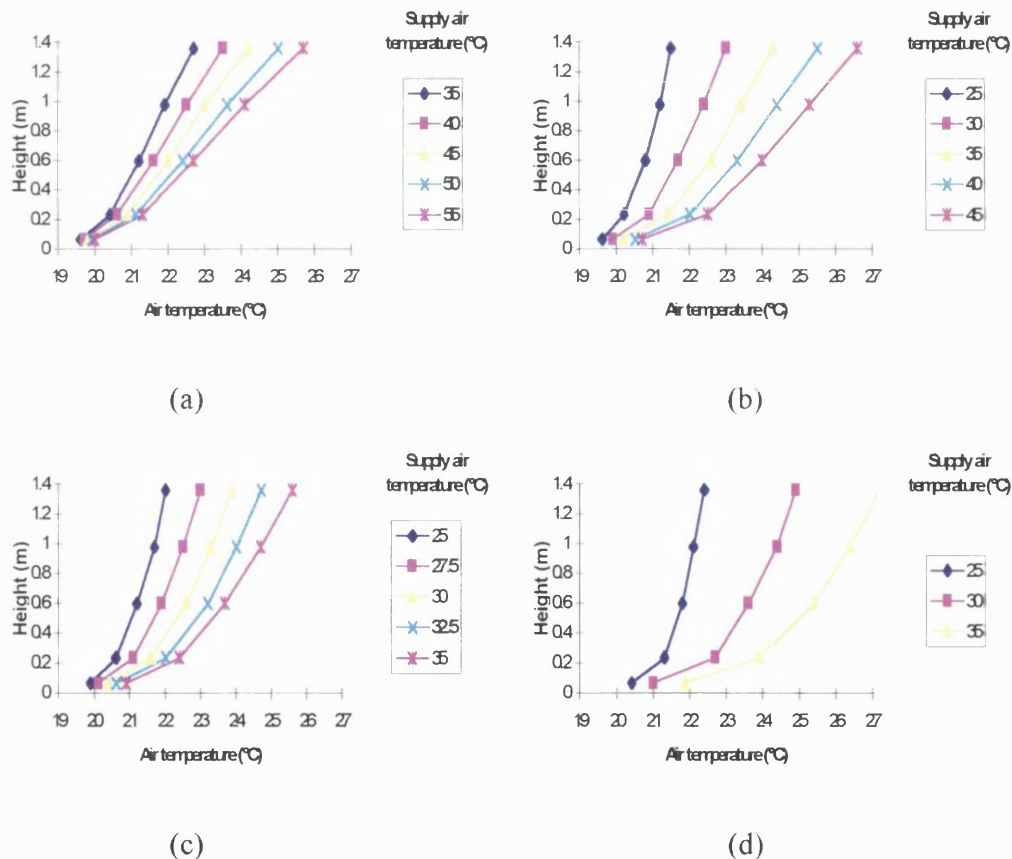ironment and the velocities in the occupied zone. At low Archimedes numbers, the high momentum carries the majority of the air-stream into the occupied zone in the eastern sector. This results in unacceptably high magnitudes of velocity as well as non-uniformities in temperature in the occupied zone. It may therefore be useful to identify a limiting Archimedes number in order to prevent such non-uniformities in temperature.
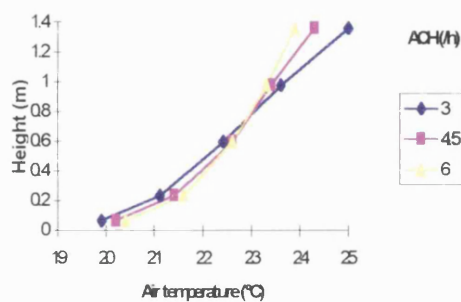
Figure 5.3 Vertical air temperature variation at similar average air temperatures (22.4 °C) at 3, 4.5 and 6 ACH.
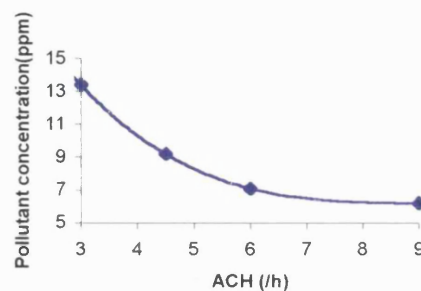
Figure 5.4 Variation of average pollutant concentration with flow rate (ACH).

At fixed flow rates, there is a reduction in the average pollutant concentration values (Table 5.3) within the occupied zone with increasing supply air temperature. As the pollutant sources are located on the wall surfaces, this reduction is no doubt due to the increasing airflow (downward) in the wall region, which is then purged by the low level extract. These variations in pollutant concentration with supply air temperature (or room temperature) are however, minimal in comparison with the changes in pollutant concentration with flow rate. The variation in average pollutant concentration (over the range of supply air temperatures) is shown in Figure 5.4. The effect of pollutants generated within the occupied zone is assessed in the transient investigation in Section 5.6.7.

Results (Table 5.3) show the possibility of unacceptably high discomfort levels due to high vertical air temperature differences at low flow rates and draught at high flow rates. These will be discussed together with observations made on the effects of the room-specific parameters.

ACH	t_{on}	t_{ave}	t_{sd}	v_{ave}	v_{sd}	v_{wwall}	PDv_{ave}	PDv_{sd}	$PD_{\delta T\,ave}$	$PD_{\delta T\,sd}$	c_{ave}	c_{sd}	Ar $\times 10^{-3}$
(/h)	(°C)	(°C)	(°C)	(m/s)	(m/s)	(m/s)	(%)	(%)	(%)	(%)	(ppm)	(ppm)	
3	35	21.2	1.1	0.018	0.021	0.128	0.5	1.7	3.5	1.9	13.4	6.8	11.6
	40	21.6	1.3	0.018	0.021	0.132	0.5	1.7	5.3	2.4	13.2	6.5	15.5
	45	22.0	1.5	0.018	0.021	0.137	0.5	1.7	7.5	2.8	13.2	6.3	19.3
	50	22.4	1.8	0.018	0.021	0.140	0.5	1.6	10.0	3.2	13.1	6.2	23.2
	55	22.8	2.0	0.018	0.021	0.142	0.5	1.6	12.8	3.7	13.1	6.0	27.1
4.5	25	20.7	0.7	0.025	0.031	0.138	1.1	3.4	1.5	1.2	9.2	5.2	1.6
	30	21.6	1.1	0.024	0.031	0.154	1.1	3.2	3.6	2.1	9.1	4.9	3.2
	35	22.4	1.4	0.024	0.031	0.160	1.0	2.9	7.2	2.9	9.0	4.6	4.8
	40	23.2	1.7	0.025	0.030	0.170	1.0	2.7	11.6	3.8	8.9	4.4	6.4
	45	23.9	2.0	0.025	0.031	0.176	0.9	2.6	17.0	4.7	8.8	4.2	8.0
6	25	21.2	0.7	0.035	0.041	0.152	1.9	4.7	1.8	1.4	7.1	4.2	0.8
	27.5	21.8	1.0	0.035	0.041	0.167	1.8	4.5	3.2	2.0	6.9	3.8	1.2
	30	22.4	1.2	0.035	0.041	0.172	1.7	4.3	5.2	2.6	6.9	3.8	1.6
	32.5	23.0	1.4	0.034	0.041	0.179	1.7	4.1	7.7	3.3	6.8	3.6	2.0
	35	23.6	1.6	0.034	0.040	0.186	1.6	3.9	10.6	4.0	6.8	3.5	2.4
9	25	21.8	0.7	0.079	0.054	0.162	6.0	7.1	2.0	1.8	6.2	6.0	0.3
	30	23.5	1.3	0.073	0.057	0.214	4.3	6.3	6.9	3.7	5.6	5.3	0.6
	35	25.2	1.8	0.067	0.058	0.241	3.1	5.4	14.7	15.9	5.1	3.8	0.9

Table 5.3 Summary of numerical evaluation results for the standard case.

5.6 Sensitivity studies

The room specific parameters are covered one-by-one and comparisons made between these and the standard case. The focus of the comparison is on the differences in flow behaviour and the consequent influence on thermal comfort. The effects on the IAQ are included in the time dependent investigations. In each of the following sections, observations are made on the effect of the room-specific parameter on the local thermal discomforts (vertical air temperature gradient and draught) and compared to those obtained for the uniform wall temperature case. The implications of these observations on the limits of operation of the H & V system to prevent local thermal discomforts are discussed (Section 5.7) after observations on each of the room specific parameters.

5.6.1 Vertical temperature gradients (vtg) in the side walls

The influence of side wall temperature gradients was investigated and comparisons made with the uniform wall temperature case. Surface temperature gradients were approximated by equal temperatures steps in three equidistant vertical sections of the side walls, as shown in Table 5.1. Three cases were considered: Case A is the uniform

wall temperature case with B and C representing increasing temperature differences between the low and high end of the wall of 1 °C and 2 °C respectively. The average surface temperature of 20 °C was the same in all the cases. Initial comparisons were made for cases A, B and C at 3 ACH at supply air temperature of 30 °C to observe the effect of an increasing temperature gradient. Further to this, comparisons were extended to include variations in flow rate and supply air temperature. These were restricted to cases A and C at 3 ACH (supply air temperatures of 40 °C and 50 °C) and 9 ACH (supply air temperatures of 25 °C and 30 °C).

Results

The airflow patterns obtained for cases A, B and C at 3 ACH and supply air temperature of 30°C are shown in Figures 5.A23, 5.A24 and 5.A25 respectively. The simulated wall temperature gradients seem to have little effect on the flow pattern and air velocity distributions within the room. This is also confirmed by the similarity in average velocity and its standard deviation in the occupied zone (Table 5.4, Run Nos. 1,4, and 5). Similar average air temperatures were obtained for all three cases. There are however, increases in the vertical air temperature gradient within the occupied zone (Figure 5.5) with increases in wall temperature gradients.

The investigation also showed a reduced influence of the wall temperature gradient on the vertical air temperature gradients (Figure 5.6) at higher supply air temperatures. Similar average temperatures of the occupied zone were maintained between the cases with and without wall temperature gradients.
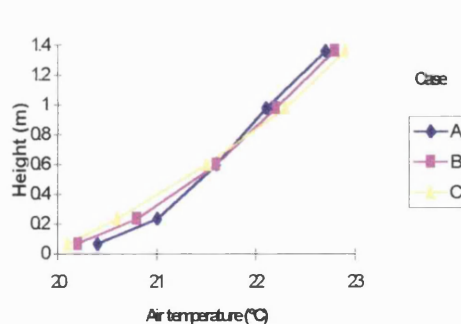

Figure 5.5 Vertical air temperatures for cases A, B and C at 3 ACH and supply air temperature of 30 °C.
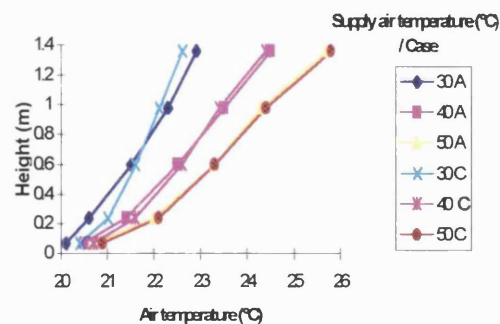
Figure 5.6 Vertical air temperature gradients for cases A and C at 3 ACH and various supply air temperatures.

At 9 ACH the airflow patterns were again similar, both without (Figure 5.A26, case *A*) and with (Figure 5.A27, case *C*) wall temperature gradients. Some differences in magnitudes of air velocity are seen in the supply air stream along the ceiling and down the east-wall, with higher velocities occurring for the case with wall temperature gradients. In the occupied zone though, despite minor variations in the flow pattern between the cases with and without wall temperature gradients, similar magnitudes of velocity were obtained. The similarity in overall magnitudes of velocity is supported by the figures in Table 5.4. (Run. Nos. 8 and 10). As with the comparisons at 3 ACH, similar average and standard deviations of air temperature occur for the cases both with and without the wall temperature gradient. The vertical air temperature gradients (Figure 5.7) of cases *A* and *C* in the occupied zone were similar, at both of the supply air temperatures.
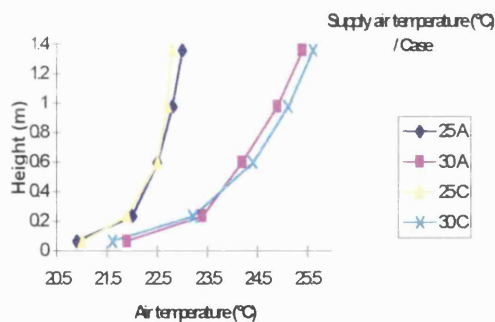

Figure 5.7 Vertical air temperatures of cases *A* and *C* at 9 ACH.

The occurrence of similar air temperatures and magnitudes of velocity in the occupied zone both with and without the side wall temperature gradients implies similar discomfort levels due to draught.

CASE	ACH	t_{on}	t_{ave}	t_{sd}	v_{ave}	v_{sd}	PDv_{ave}	PDv_{sd}	$PD_{\delta T\,ave}$	$PD_{\delta T\,sd}$	Run. No.
	(/h)	(°C)	(°C)	(°C)	(m/s)	(m/s)	(%)	(%)	(%)	(%)	
A	3	30	21.6	0.8	0.016	0.021	0.4	1.6	1.8	1.4	1
		40	22.5	1.3	0.017	0.021	0.5	1.6	4.9	2.3	2
		50	23.4	1.7	0.017	0.022	0.4	1.5	9.5	3.3	3
B	3	30	21.5	0.9	0.016	0.021	0.4	1.6	2.4	1.6	4
C	3	30	21.5	1.0	0.017	0.021	0.4	1.6	3.1	1.8	5
		40	22.5	1.4	0.017	0.022	0.5	1.6	6.1	2.5	6
		50	23.1	1.9	0.016	0.021	0.3	1.4	12.3	5.2	7
A	9	25	22.4	0.6	0.062	0.059	4.4	6.9	1.6	1.6	8
		30	24.2	1.2	0.074	0.056	4.1	6.3	5.9	3.3	9
C	9	25	22.4	0.6	0.065	0.062	5.1	7.6	1.4	1.3	10
		30	24.2	1.4	0.072	0.061	4.5	6.2	8.0	4.3	11

Table 5.4 Numerical evaluation values for walls with vertical temperature gradients.

5.6.2 Obstacles

The influence of solid objects such as people and furniture on the flow behaviour within a room was assessed. Simulations were performed at two flow rates of 3 and 9 ACH with two solid objects (dimensions 0.4 x 0.4 x 1.4 m³) located near the centre of the room. The locations can be seen in the graphical result in Figure 5.A28. The size of the obstacles was increased (0.8 x 0.8 x 1.4 m³) and the location of one of these changed as may be seen in Figure 5.A29. The effect of the variation in size and location of the objects was investigated only at the high flow rate, at which a larger influence was expected than at low flow rates. The two obstacle sizes will be referred to as the small and large obstacles.

Results

The numerical values in Table 5.5 (Run Nos. 1 and 2) suggests little influence of the small obstacles on the overall flow conditions in the occupied zone. At the high flow rate of 9 ACH, the presence of the small obstacles (Figure 5.A28) resulted in lower velocities throughout the occupied zone compared to the standard case (Figure 5.A16) also shown in Table 5.5 (Run. Nos. 3 and 5). The obstacles appear to restrict the entrainment of the air in the occupied zone, as a result of the high velocity supply air stream in the high region of the room. Evidence of this reduction in entrained airflow is also seen in the reduced velocities in the 'return airflow' in the outer plane. The increase in size of the obstacles and change in location of one of these (Figure 5.A29) had insignificant impact on the flow distributions compared to those with small

obstacles (Figure 5.A28). This is reflected by the overall flow conditions obtained in Table 5.5 (Run. Nos. 3 and 4).

Similar air temperature distributions occurred irrespective of the presence of obstacles as seen in the Figure 5.8 and the average and standard deviation of air temperatures in Table 5.5.

Similarity in the air temperatures and reductions in air velocity would lead to the expectation of reduced levels of discomfort due to draught. This would be the case, as long as the presence of obstacles does not cause increases in turbulence intensity, large enough to counter-act the effect of the reductions in velocity. To investigate the draught levels experienced, spot values at different locations in the occupied zone were examined including in the vicinity of the obstacles. The magnitudes of velocity, turbulence intensity and draught perception were determined at these spot values and compared with the standard case. Spot values were selected to show vertical variations of the variables at three locations in the room, at a distance of approximately 0.7, 3.0 and 5.5 m from the west-wall and all at 1.7 m from the south wall. These locations are labelled A, B and C respectively. Spot values of the data obtained for the cases with (small obstacles) and without obstacles at 9 ACH are shown in Figures 5.9-5.11.
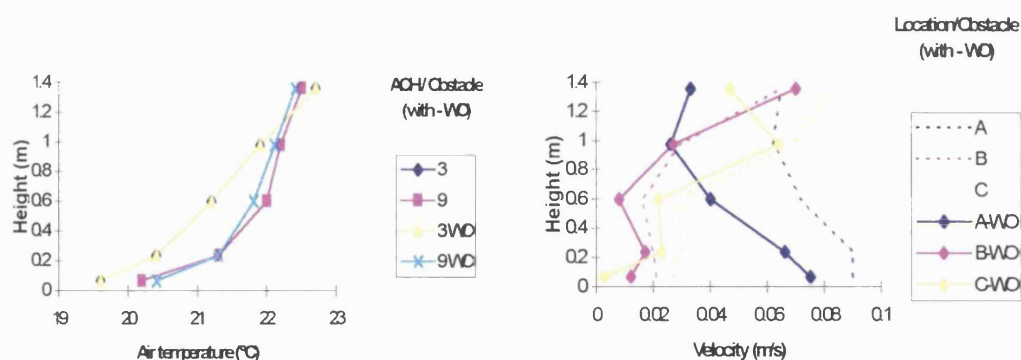

Figure 5.8 Vertical air temperatures with and without obstacles. WO - With Obstacle.

Figure 5.9 Velocities at the spot values (A, B, C) with and without obstacles.
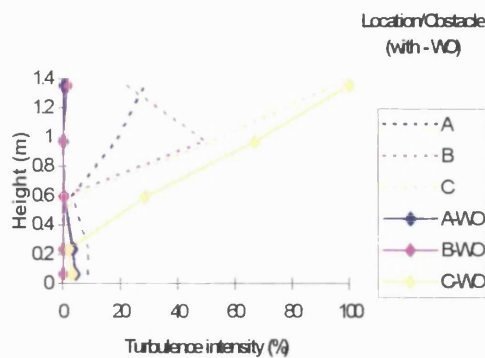
Figure 5.10 Turbulence intensities at the spot values (A, B, C), with and without obstacles.
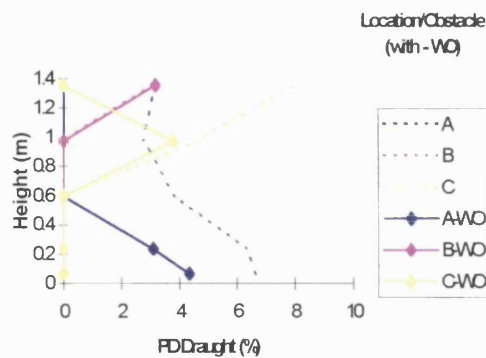
Figure 5.11 Percentage dissatisfaction due to draught at the spot values (A, B, C), with and without obstacles.

The velocity variations in Figure 5.9 confirm velocity reductions with the presence of obstacles. The presence of the obstacles caused lower turbulence intensities at locations A and B and higher turbulence intensities at location C (Figure 5.10). The flow patterns with the presence of obstacles (Figure 5.A.28) are seen to undergo large changes in the magnitudes and direction of the flow in the region of location C, which would appear to result in the increased turbulence intensity. This increase in turbulence intensity counteracts the reduction in velocity, resulting in similar draught discomfort level (Figure 5.11) in the region to the mid-height and lower levels at the high end of the occupied zone. Overall draught levels (as represented by locations A, B and C) of the cases with obstacles, do not exceed those of the standard case. These draught levels are in general similar to or lower than those obtained from the standard case.

Obstacle	ACH	t_{on}	t_{ave}	t_{sd}	v_{ave}	v_{sd}	PDv_{ave}	PDv_{sd}	$PD_{\delta T ave}$	$PD_{\delta T sd}$	Run No.
	(/h)	(°C)	(°C)	(°C)	(m/s)	(m/s)	(%)	(%)	(%)	(%)	
small	3	35	21.2	1.1	0.016	0.021	0.5	1.7	3.5	1.9	1
-	3	35	21.2	1.1	0.018	0.021	0.5	1.7	3.5	1.9	2
small	9	25	21.8	0.8	0.062	0.061	4.7	7.4	2.1	2.0	3
large	9	25	21.8	0.8	0.059	0.064	4.6	7.4	2.1	2.0	4
-	9	25	21.8	0.7	0.079	0.054	6.0	7.1	2.0	1.8	5

Table 5.5 Numerical evaluation data for an enclosure with and without internal obstacles. (Excludes data for the change in size and location of the obstacles)

5.6.3 Heat sources

The influence of heat sources on the flow behaviour was investigated for heat sources both *within* and *above* the occupied zone. Heat sources within the occupied zone were specified as emanating from the surfaces of two small objects (as defined in the previous section - dimensions 0.4 x 0.4 x 1.4 m^3). Total heat sources of magnitude 220 W and 440 W were used and represent the heat sources from two persons at two activity levels, a standing activity and high activity level respectively. These will be referred to in the dialogue as the 'unit heat sources' and 'doubled heat sources'.

The effect of the heat sources within the occupied zone (as located in Figure 5.A30) was investigated at various flow rates (3, 4.5 and 9 ACH) and supply air temperatures, as specified in Table 5.1. The supply air temperatures were selected to coincide with conditions used in the standard case at the same flow rate. The effect of the doubled heat sources was investigated at the intermediate flow rate of 4.5 ACH. The effect of a change in location (as shown in Figure 5.A39) of the unit heat sources was assessed (at an airflow rate of 4.5 ACH).

A high level heat source of 200 W located on the ceiling was also assessed, both individually and in combination with a unit heat source within the occupied zone. The 200 W heat source was to represent sensible heat gains from lighting. This was investigated at a low airflow rate of 3 ACH.

Results

Heat sources within the occupied zone

Comparison of airflow patterns obtained with the unit heat sources (Figures 5.A30 and 5.A33) at 3 , 4.5 and those of the standard cases (Figures5.A1 and 5.A7) at the same supply air temperature show the main difference in the flow distribution being the presence of higher velocities in localised regions above the heat sources. These high velocities are created by the thermal plume from the heat sources. Away from the immediate vicinity of the heat sources, the flow patterns and magnitudes of velocity are similar for the cases with and without heat sources. At 9 ACH a larger difference in airflow pattern is observed between that obtained with the unit heat sources (Figure

5.A36) and the standard case (Figure 5.A16). Lower air velocities occur in the occupied zone than for the standard case.

A change in location of the unit heat sources (Figure 5.A39) had little influence on the velocity distributions produced at the original location (Figure 5.A30). Negligible change to the overall velocity distribution is suggested by the similarity in average and standard deviation of velocities in Table 5.6 (Run. Nos.1 and 8). Doubling of the heat source (Figure 5.A40) similarly, had little additional impact on the velocity distribution obtained for the unit heat sources (Figure 5.A33).

Temperature contours in the symmetry plane and in the plane through the mid-height of the room are shown in Figures 5.A31-32, 5.A34-35 and 5.A37-38 for the unit heat sources at 3, 4.5 and 9 ACH respectively and in Figures 5.A41-42 for the doubled heat sources at 4.5 ACH. These show a uniformity of air temperature across the occupied zone with large temperature variations only in the immediate vicinity of the heat sources. The thermal plume from the heat sources causes localised zones of high temperature mainly above the occupied zone.

Vertical temperature variations at the mid-point of the room are shown in Figure 5.12 (at 3 ACH), Figure 5.13 (at 9 ACH) for the unit heat sources and in Figure 5.14 (at 4.5 ACH) for the doubled heat sources. The effect of these on the air temperature distribution appears to be fairly uniform over the occupied zone, with fairly consistent increases in air temperature throughout the occupied zone, thus maintaining similar air temperature gradients in the occupied zone as for the standard case. This similarity in vertical air temperature gradient over the occupied zone is considered to be of greater importance than the absolute temperature differential between the fixed points of 0.1 m and 1.0 m, which are used in estimating the percentage dissatisfaction. The temperature differentials would indicate considerable influence of the heat sources on the dissatisfaction level (Table 5.6). This will be discussed in Section 5.7.1.

Draught is first of all assessed in comparison to the standard case at the same supply air temperature and flow rate and is then extended to a comparison at similar average air temperatures. Spot values of velocity, turbulence intensity and draught perception are shown in Figures 5.15 - 5.17 for the case with unit heat sources and the standard

case both at 9 ACH and supply air temperature of 25 °C. In comparison to the standard case, there are minor increases in the velocities (Figure 5.15) in the immediate vicinity of the heat sources and reductions in the regions further away. The presence of the heat source led to increases in the turbulence intensity (Figure 5.16) in the central and western regions of the room and reductions in the eastern region. Increased air temperatures and reduced air velocities however compensate for these increases in turbulence intensity, resulting in generally reduced levels of discomfort due to draught (Figure 5.17).
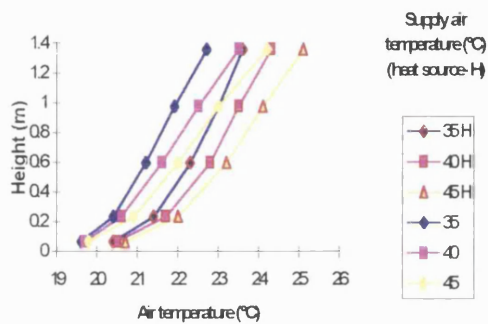

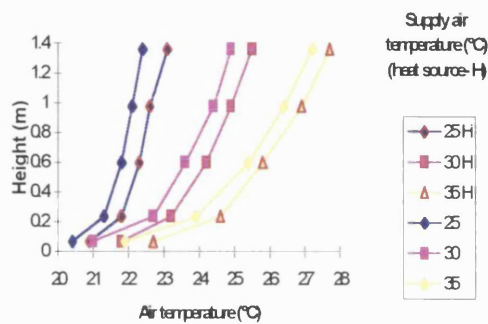**Figure 5.12** Vertical temperatures at 3 ACH with and without the unit heat sources.

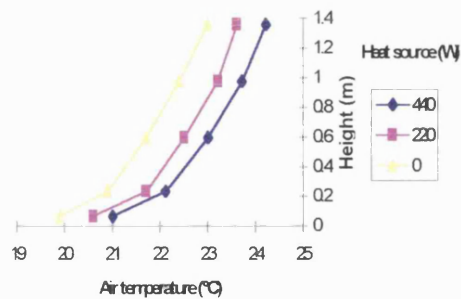**Figure 5.13** Vertical temperatures at 9 ACH with and without the unit heat sources.

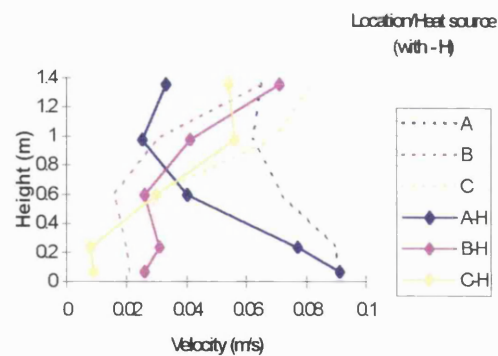**Figure 5.14** Vertical temperature variation at 4.5 ACH with various heat sources

Figure 5.15 Velocities at the spot values (A, B, C), with and without 220W heat source
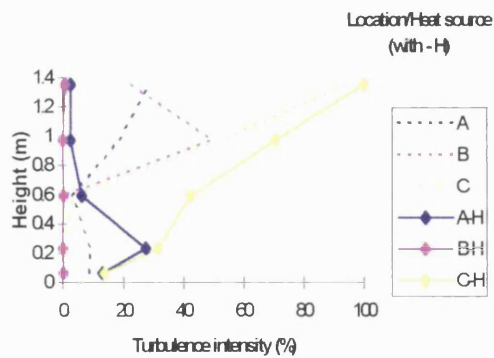
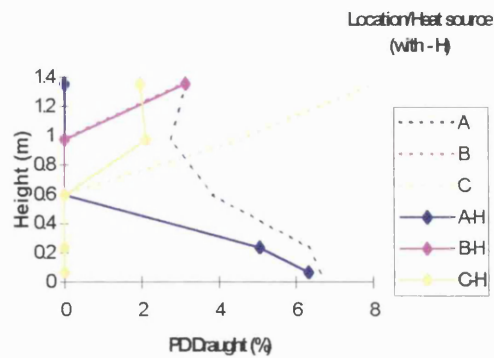**Figure 5.16** Turbulence intensities at the spot values (A, B, C), with and without 220 W heat source.

Figure 5.17 Percentage dissatisfaction due to draught at the spot values (A, B, C) with and without 220W heat source.

It is however more useful to perform a comparison of draught levels at similar average air temperatures of both cases. On the basis of the simulation results, a direct comparison at similar average temperatures was not possible. This was done by interpolation of data from the standard case (Table 5.6, Run. Nos. 16 and 17) to conditions at an average air temperature of 22.2 °C to coincide with the average air temperature of the case with the unit heat sources (Run. No. 5). At the same average air temperature, similar levels of draught (Figure 5.18) are estimated for both cases over large parts of the occupied zone.
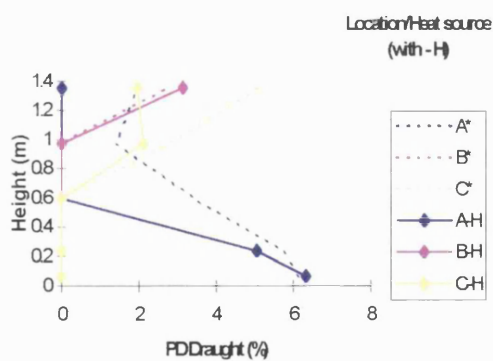

Figure 5.18 Percentage dissatisfaction due to draught at spot values A,B,C at an average air temperature of 22.2 °C (* - interpolated case)
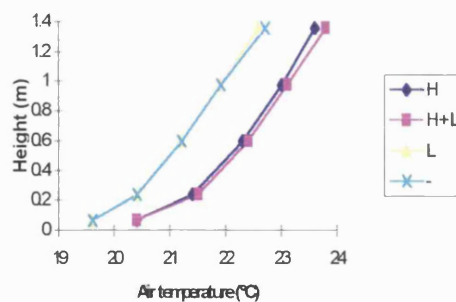
Figure 5.19 Vertical temperatures with and without high level heat sources , H - heat source in the occupied zone, L - light.

Heat sources above the occupied zone

The high level heat source appears to have negligible influence on the flow pattern in the room, neither as the sole heat source within the room (Figure 5.A43 compared to Figure 5.A1 of the standard case) nor in combination with a heat source within the occupied zone (Figure 5.A45 compared to Figure 5.A32 for the heat source within the occupied zone only). The high level heat source is not found to have an impact on the uniformity of temperature distribution across the occupied zone (Figures 5.A44 and 5.A46). The influence of the heat source is mainly in the ceiling region, with little effect on the occupied zone, as can be seen in the vertical air temperature variations in Figure 5.19.

Heat sources from lights would not be expected to exceed these levels, particularly when using low energy emitters. These should therefore have no influence on the determination of limits of operation due to vertical air temperature differences or draught.

Heat source (W)	loc-ation	ACH (/h)	t_{on} (°C)	t_{ave} (°C)	t_{sd} (°C)	v_{ave} (m/s)	v_{sd} (m/s)	PDv_{ave} (%)	PDv_{sd} (%)	$PD_{\delta T\,ave}$ (%)	$PD_{\delta T\,sd}$ (%)	Run No.
220	low	3	35	22.2	1.1	0.024	0.030	1.1	3.0	4.5	2.3	1
		3	40	22.7	1.3	0.023	0.030	1.1	2.8	6.6	2.9	2
		3	45	23.1	1.5	0.022	0.028	1.0	2.6	8.8	3.4	3
220	low	4.5	30	22.4	1.0	0.032	0.038	1.8	4.2	4.0	2.3	4
220	low	9	25	22.2	0.7	0.069	0.061	5.1	7.4	1.6	1.4	5
		9	30	24.1	1.2	0.062	0.066	3.9	6.7	5.9	3.8	6
		9	35	25.7	1.7	0.057	0.067	2.9	5.7	12.7	5.5	7
220*	low	3	35	22.2	1.1	0.024	0.031	1.2	3.1	4.5	2.3	8
440	low	4.5	30	22.9	1.1	0.038	0.040	2.0	4.4	4.6	2.6	9
200	high	3	35	21.3	1.1	0.016	0.021	0.4	1.7	3.8	2.0	11
220 + 200	low + high	3	35	22.3	1.2	0.024	0.031	1.2	3.1	4.8	2.4	10
-	-	3	35	21.2	1.1	0.018	0.021	0.5	1.7	3.5	1.9	12
-	-	3	40	21.6	1.3	0.018	0.021	0.5	1.7	5.3	2.4	13
-	-	3	45	22.0	1.5	0.018	0.021	0.5	1.7	7.5	2.8	14
-	-	4.5	30	21.6	1.1	0.023	0.031	1.1	3.2	3.6	2.1	15
-	-	9	25	21.8	0.7	0.079	0.054	6.0	7.1	2.0	1.8	16
-	-	9	30	23.5	1.3	0.073	0.057	4.3	6.3	6.9	3.7	17
-	-	9	35	25.2	1.8	0.067	0.058	3.1	5.4	14.7	15.9	18

Table 5.6 Numerical evaluation data for simulations with and without internal heat sources.(* heat source moved)

5.6.4 Unequal wall surface temperatures

The influence of differences in the wall surface temperatures within the room was investigated. Individual wall surfaces were specified to be at uniform temperatures. These investigations were conducted at low flow rates of 3 and 4.5 ACH and at a combination of the surface temperatures shown in Table 5.7. Cases 1 and 6 are effectively the standard case with wall temperature of 19 and 20 °C. The numerical evaluation results in Table 5.8 include the average surface temperature in the enclosure (t_w).

Wall Case	W-wall	E-wall	N-wall	S-wall	H-wall (ceiling)	L-wall (floor)
1						
2						20
3			20			20
4					20	20
5			18	20		20
6	20	20	20	20	20	20

Table 5.7 Surface temperatures (°C), default 19 °C.

Results

The variations in wall surface temperature are seen to have little effect on the flow patterns and velocity distributions as shown in Figures 5.A47-52 for cases 1-6 at 3 ACH. Average velocities in the occupied zone were of similar magnitudes for all the cases, with the largest variation observed for case 5 which had the lowest side wall temperature (Table 5.8).

Temperature distributions across the occupied zone are uniform, with temperature variations confined to areas in the immediate vicinity of the walls as shown in Figure 5.A53 for cases 3 and 4 at 4.5 ACH. The vertical air temperature profiles in the occupied zone are shown in Figure 5.20 at 3 ACH (cases 1-6) and Figure 5.21 at 4.5 ACH (cases 1,3,4,6). The effect of the increase in floor temperature is confined to a small region near the floor. Although this causes a significant difference in numerical values (Table 5.8) of the percentage dissatisfaction due to the vertical air temperature difference, the air temperature variation or gradient over most of the occupied zone and therefore the body, is similar for all six cases.
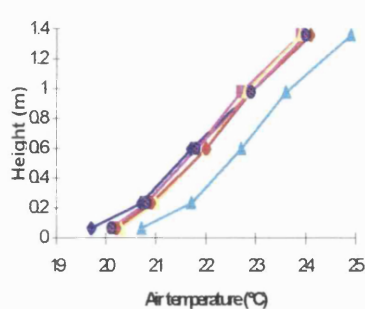
Figure 5.20 Vertical air temperatures at various wall surface temperatures (3 ACH). Cases as defined in Table 5.8.
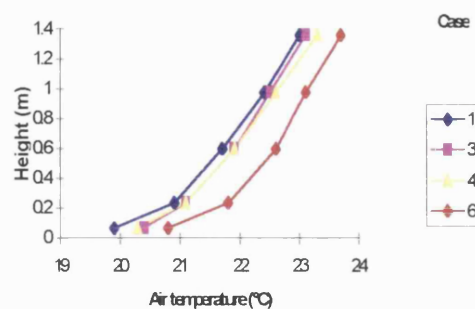
Figure 5.21 Vertical air temperatures at various wall surface temperatures (4.5 ACH)

Temperature distributions in the occupied zone are seen to be less dependent on the average enclosure surface temperature than on the average surface temperature of the *side walls*. The vertical air temperatures of cases 2-5 are closer in magnitude to case *1* than case *6*, despite average surface of approximately the average of cases 1 and 6 (Table 5.8). The average surface temperatures of the *side walls* (cases 2,4,5 = 19 °C and case 3 = 19.25 °C) however are identical or closer in magnitude to those of case *1*. This suggests that the surface temperatures of side walls have a greater impact on the temperature gradient in the occupied zone than the floor or ceiling. Furthermore, similar average temperatures of the side walls result in similar vertical temperature gradients despite differences in the individual wall temperatures, therefore indicating similar and collective influences of the side walls.

As the non-uniformity in wall temperatures had little effect on the flow pattern and velocity distribution in the occupied zone, similar draught levels were experienced as with the standard case at the same average temperatures (Table 5.8).

Case	ACH	t_{on}	t_w	t_{ave}	t_{sd}	v_{ave}	v_{sd}	PDv_{ave}	PDv_{sd}	$PD_{\delta T\,ave}$	$PD_{\delta T\,sd}$
	(/h)	(°C)	(°C)	(°C)	(°C)	(m/s)	(m/s)	(%)	(%)	(%)	(%)
1	3	42	19	21.78	1.4	0.017	0.022	0.5	1.7	6.1	2.6
2	3	42	19.27	21.88	1.3	0.017	0.021	0.5	1.7	4.5	2.1
3	3	42	19.39	22.04	1.3	0.018	0.022	0.6	1.8	4.6	2.2
4	3	42	19.55	22.00	1.4	0.017	0.021	0.5	1.6	5.0	2.3
5	3	42	19.27	21.87	1.3	0.014	0.019	0.2	1.4	4.6	2.2
6	3	42	20	22.70	1.4	0.016	0.022	0.4	1.5	5.7	2.5
1	4.5	30	19	21.6	1.1	0.023	0.031	1.1	3.2	3.6	2.1
3	4.5	30	19.39	21.84	0.9	0.025	0.032	1.2	3.3	2.7	1.7
4	4.5	30	19.55	21.88	1.0	0.023	0.031	1.1	3.1	3.3	1.9
6	4.5	30	20	22.4	1.0	0.025	0.031	1.0	3.0	3.2	1.9

Table 5.8 Numerical evaluation data for non uniform surface temperatures.

5.6.5 Cold window surface

A window was located on the east-wall with the low edge at a height of 1m and spanning the width of the room. This was assumed to be at a temperature of 16 °C, with the remaining room surfaces at 20 °C. The effect of this was investigated at a low airflow rate of 3 ACH.

Results

Similar flow patterns were obtained with the presence of the cold window surface (Figure 5.A54) as with the standard case (Figure 5.A23) at the same wall temperature and supply parameters, with mainly a greater downward airflow occurring on the east-wall due to the cold window surface. These high velocities however, do not carry through into the occupied zone and have minimal effect on the magnitude of velocities in the occupied zone as shown in Table 5.9

Air temperature distributions across the occupied zone remain fairly uniform, with larger variations only in the immediate vicinity of the window (Figure 5.A55). The influence of the cold window on the temperature distribution in the occupied zone occurs mainly in the mid-height of the occupied zone, as illustrated in Figure 5.22 which shows the vertical air temperatures with and without the presence of the window. The effect of this change in air temperature profile on the discomfort due to vertical air temperature differences/gradients is difficult to assess and will be discussed in Section 5.7.1.
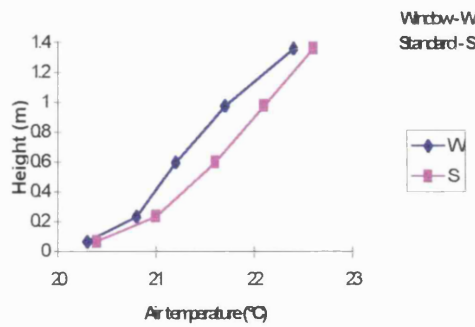
Figure 5.22 Vertical temperature variations for a room with a cold window and a standard room.

No notable difference in draught perception are expected from those obtained for the standard case at similar average air temperatures. This is because the air temperature dip caused by the cold window surface in comparison to the standard case, occurred in the mid-height of the room where air velocities are anyhow low. The regional influence of the cold window would be expected to diminish with increasing flow rates. Adverse effects due to the cold window surface on the draught discomfort level are therefore not anticipated at high flow rates.

Case	ACH	t_{on}	t_w	t_{ave}	t_{sd}	v_{ave}	v_{sd}	PDv_{ave}	PDv_{sd}	$PD_{\delta T\,ave}$	$PD_{\delta T\,sd}$
	(/h)	(°C)	(°C)	(°C)	(°C)	(m/s)	(m/s)	(%)	(%)	(%)	(%)
window	3	30	19.84	21.33	0.7	0.015	0.018	0.2	1.4	1.2	1.1
standard	3	30	20	21.6	0.8	0.016	0.021	0.4	1.6	1.8	1.4

Table 5.9 Numerical evaluation data for a room with a cold window surface

5.6.6 Room geometry

In addition to the room of dimensions 6 x 6 x 2.5 m^3 (geometry 1) used in the preceding investigations, a room of 4 x 4 x 2.5 m^3 (geometry 2) was investigated. The simulations were performed at flow rates of 3 and 6 ACH and at supply air temperatures as used in the standard case, with uniform wall surface temperatures of 19 °C. Comparison between the two geometries were based on numerical evaluation results and the use of spot values at the same normalised locations.

Results

Lower average velocities are obtained for geometry 2 as shown in Figure 5.23 (from Tables 5.3 and 5.11). Examinations of the spot values of the air velocities (again in the

same locations as defined in Section 5.6.2), shows the reduction in velocity to be throughout the occupied zone at 3 ACH (Figure 5.24). However at 6 ACH (Figure 5.25) higher velocities occurred in the lower regions of the occupied zone of geometry 2, with the reverse in the high regions.
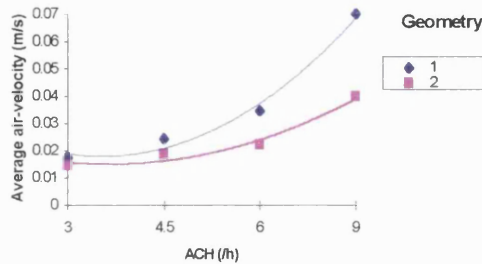

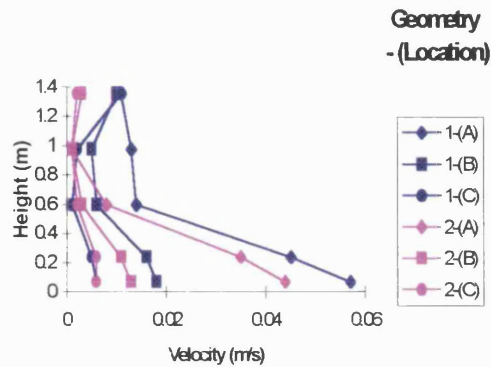**Figure 5.23** Average velocities of geometries 1 and 2.

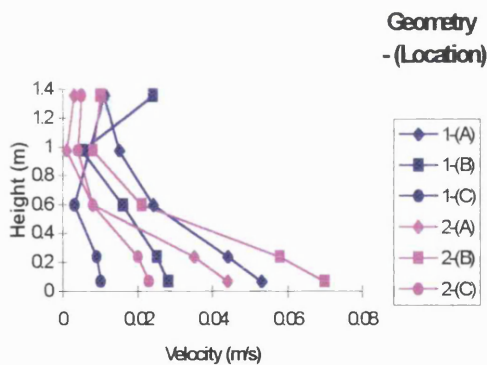**Figure 5.24** Spot values of geometries 1 and 2 at 3 ACH (locations A, B, C)

Figure 5.25 Spot values of geometries 1 and 2 at 6 ACH (locations A, B, C)

At the same ACH and supply air temperature of both geometries lower average air temperatures were obtained for geometry 2. The results obtained earlier, on the effect of unequal wall surface temperatures (Section 5.6.4) would suggest the reduction in average air temperature may be as a result of the increased heat transfer (heat loss of the room air), due to the larger percentage of *side wall* to *total wall* surface area. The reduced floor area (of geometry 2) also appears to be responsible for the reduced temperature 'step' seen in the floor region in the vertical air temperature profile (Figures 5.26 and 5.27) in comparison to geometry 1. This results in lower air temperature differences between the designated points for evaluation of discomfort due

to vertical air temperature differences. However, apart from the temperature step in the vicinity of the floor, the temperature gradients are almost identical for both geometries over the majority of the occupied zone. This, together with the previous result on the collective influence of the side walls on the temperature distribution within the room (Section 5.6.4), would suggest that similar temperature gradients would occur with other room geometries of similar height.
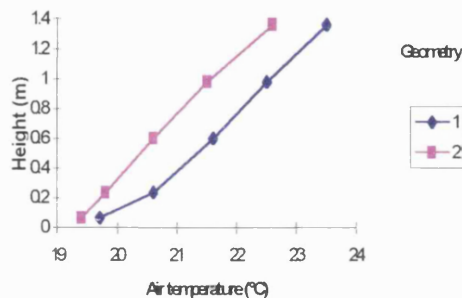

Figure 5.26 Vertical air temperatures of geometries 1 and 2 at 3 ACH.
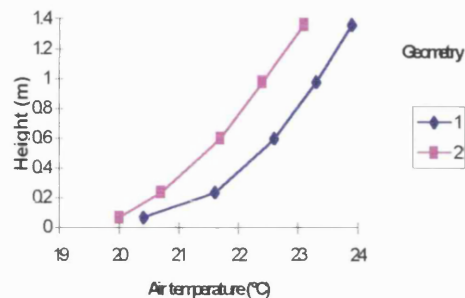
Figure 5.27 Vertical air temperatures of geometries 1 and 2 at 6 ACH.

The figures in Table 5.10 indicate lower discomforts due to draught at both ACH of the smaller room. At 6 ACH however, increased velocities were obtained in the lower regions of the room in comparison to the larger room geometry. At the high airflow rates where draught could cause problems, the overall discomfort levels would appear to be similar to those obtained at the larger geometry at similar ACH.

Geom.	ACH	t_{on}	t_{ave}	t_{sd}	v_{ave}	v_{sd}	PDv_{ave}	PDv_{sd}	$PD_{\delta T\,ave}$	$PD_{\delta T\,sd}$
	(/h)	(°C)	(°C)	(°C)	(m/s)	(m/s)	(%)	(%)	(%)	(%)
2	3	40	20.9	1.0	0.015	0.020	0.5	1.6	1.9	1.4
2	6	30	21.6	1.1	0.022	0.028	0.9	2.8	3.7	2.0
1	3	40	21.6	1.3	0.018	0.021	0.5	1.7	5.3	2.4
1	6	30	22.4	1.2	0.034	0.041	1.7	4.3	5.2	2.6

Table 5.10 Numerical evaluation data at varied geometries.

5.6.7 Time dependent variations

The investigations so far have been based on steady state conditions. The variation of flow behaviour in time is of importance, particularly due to the mode of operation of the expected H & V system involving intermittent operation over a wide range of conditions. Of particular importance is the time taken to approach the steady state

values of temperature and pollutant concentration. Also of interest is the variation in comfort conditions in this transition towards steady state conditions. Initial room temperatures were assumed to be equal to the wall surface temperature of 19 °C. Equal and uniform wall temperatures were assumed. Two scenarios were considered with regard to pollutant concentration:

a) initial concentration of pollutant in the room equal to zero, and

b) initial concentration equal to the average value of pollutant concentration obtained at a continuous base rate ventilation of 1 ACH .

The former is more realistic if the main source of pollution is from the occupants. The latter is more useful in investigating possible lead times for the ventilation system to reduce the pollution level due to internal pollutants to acceptable levels before room utilisation.

Results

Flow patterns at 3 ACH, at time intervals of 15, 30 and 45 minutes after start-up are shown in Figures 5.A56, 5.A57 and 5.A58. These show the flow pattern approaching that of the steady state condition (Figure 5.A47) at the first time interval (15 minutes). At the subsequent time intervals (30, 45 minutes), only small changes are observed in the upper-west quadrant of the outer plane. These changes however, have little influence on the occupied zone, where the bulk of distributions and magnitudes of velocity remain similar from the first time interval onwards.

It was assumed that flow patterns at higher ACH would approach steady state conditions more rapidly than at lower ACH. This assumption proved to be wrong and resulted in incomplete extraction of graphical results for the flow patterns at the higher ACH. A limited number of these were obtained and are used together with the numerical evaluation results, in the analysis of the time dependent variations at 6 and 9 ACH.

Flow patterns at 6 ACH, at a time interval of 30 minutes and 9 ACH, at a time interval of 15 minutes after start-up, are shown in Figures 5.A62 and 5.A64, with the corresponding steady state flow patterns in Figures 5.A13 and 5.A16. Observation of

these and the velocities in Table 5.11 show an increase in flow rate, resulting in longer time periods for the flow conditions to settle.

Temperature distributions at both 3 ACH (Figures 5.A59, 5.A60 and 5.A61 at 15, 30 and 45 minutes) and 6 ACH (Figure 5.A63 at 15 minutes) exhibit uniform air temperature distributions across the occupied zone throughout the transient. Comparisons of air temperature distribution in the occupied zone may thus be made in terms of the vertical temperature distributions in the occupied zone. These are shown in Figures 5.28 and 5.30 at 3 and 6 ACH, respectively, and suggest that steady values are approached within 30 minutes at 3 ACH and within 15 minutes at 6 ACH. At 9 ACH, although the steady state average air temperature is approached by the first time interval of 15 minutes (Table 5.11), this is at a higher air temperature gradient (Figure 5.32) than at the steady condition. The steady state air temperature gradients are approached at the second time interval (i.e. 30 minutes after start-up). These increased air temperature gradients, during the early stages of the transient, are however fairly modest. This would suggest the acceptability of limits of operation of the H & V equipment (to prevent discomfort due vertical air temperature differences) based on steady state conditions. During early periods of operation of the H & V equipment (i.e. the warming up period) the local thermal discomforts would be expected to be of reduced importance *until* thermal neutrality is achieved (i.e. until thermal neutrality has been achieved, local discomfort is a secondary issue).
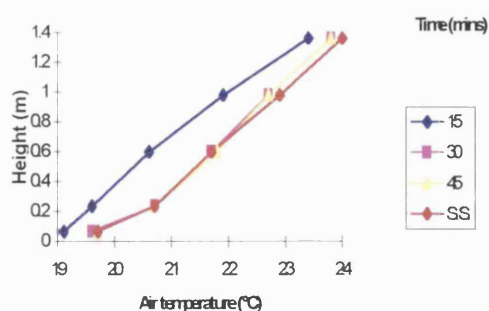
Figure 5.28 Vertical air temperatures at times of 15, 30, 45 mins. and at the steady state (S.S.) at 3 ACH.
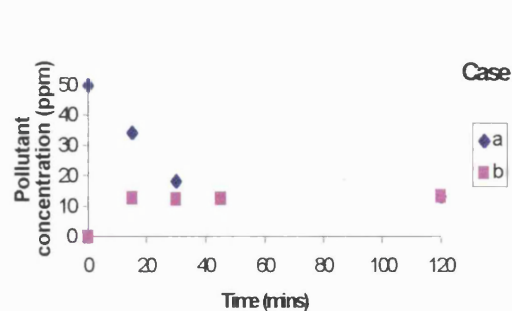
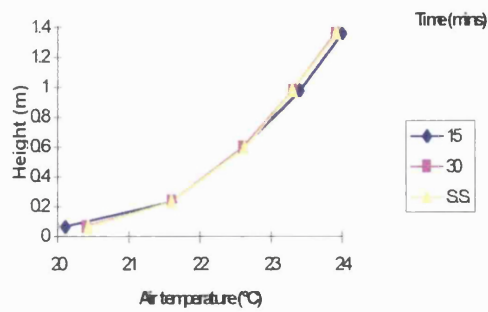**Figure 5.29** Variation of pollutant concentration with time at 3 ACH.

Figure 5.30 Vertical air temperatures at times of 15, 30 mins. and the steady state (S.S.) at 6 ACH.
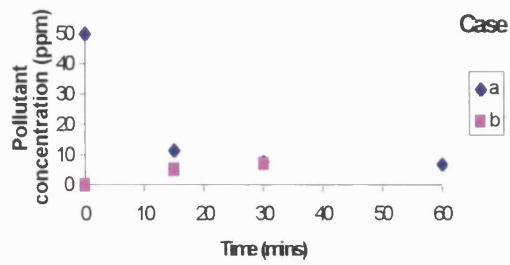

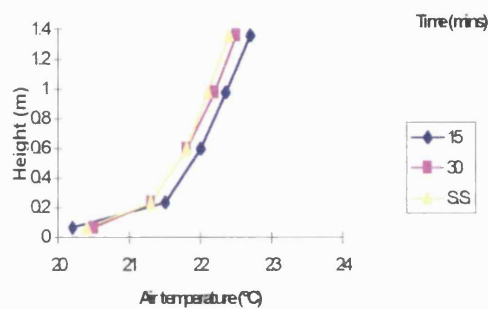**Figure 5.31** Variation of pollutant concentration with time at 6 ACH.

Figure 5.32 Vertical air temperatures at times of 15, 30 mins. and the steady state (S.S.) at 9 ACH.
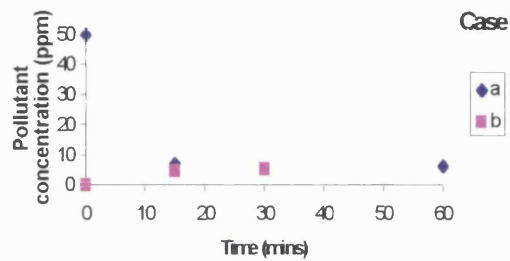

Figure 5.33 Variation of pollutant concentration with time at 9 ACH.

With average temperatures in the occupied zone approaching constant values fairly rapidly (Figure 5.34), the main difference between the time steps which may influence discomfort due to draught is the magnitude of velocity. In this case, there is an improvement in the discomfort levels in the approach to steady state values due to the lower velocities experienced en-route. The discomfort levels would appear to always fall within the limits set by steady state criteria.

The variation in average pollutant concentration with time, both for zero initial pollutant concentration in the room and for the initial pollutant concentration of 50 ppm, are shown in Figures 5.29, 5.31 and 5.33 at flow rates of 3, 6 and 9 ACH respectively. With the introduction of pollutant concentrations at start-up (i.e. initial concentrations in the room being zero) steady state conditions were approached fairly rapidly. This would suggest that thermal conditions permitting, no substantial lead times in start-up of the H & V system would be required. Comparison of the average

pollutant concentrations obtained with an initial concentration of 50 ppm in the room are shown in Figure 5.35 for all three ACH. The plot indicates a minor difference in the pollutant removal effectiveness at airflow rates of 6 and 9 ACH. Therefore, for rapid achievement of acceptable IAQ levels, it may not be necessary to exceed flow rates of approximately 6 ACH.
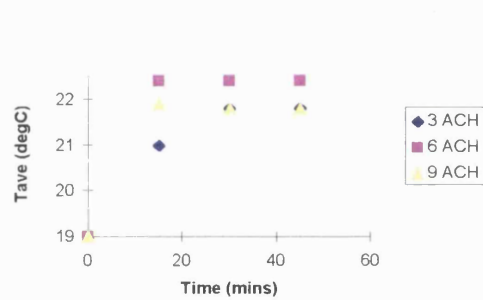

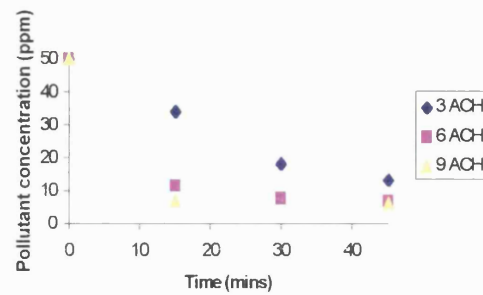**Figure 5.34** Average air temperature variation with time at 3, 6, and 9 ACH.

Figure 5.35 Average pollutant concentration with time at 3, 6 and 9 ACH. (Initial pollutant concentration of 50 ppm)

Time	ACH	t_{on}	t_{ave}	t_{sd}	v_{ave}	v_{sd}	PDv_{ave}	PDv_{sd}	$PD_{\delta Tave}$	$PD_{\delta T sd}$
	(/h)	(°C)	(°C)	(°C)	(m/s)	(m/s)	(%)	(%)	(%)	(%)
15	3	42	21.0	1.6	0.012	0.018	0.3	1.5	5.5	2.4
30	3	42	21.8	1.4	0.016	0.021	0.5	1.7	6.3	2.6
45	3	42	21.8	1.4	0.016	0.022	0.5	1.7	6.2	2.5
S.S.	3	42	21.8	1.4	0.017	0.022	0.5	1.7	6.1	2.6
15	6	30	22.4	1.4	0.030	0.040	1.6	4.2	7.5	3.1
30	6	30	22.4	1.2	0.032	0.042	1.7	4.4	5.2	2.6
S.S.	6	30	22.4	1.2	0.034	0.041	1.7	4.3	5.2	2.6
15	9	25	21.9	0.8	0.059	0.059	4.0	6.8	2.0	1.7
30	9	25	21.8	0.7	0.064	0.059	4.9	7.3	1.8	1.8
S.S.	9	25	21.8	0.7	0.079	0.054	6.0	7.1	2.0	1.8

Table 5.11 Numerical evaluation data for the time dependent cases.

5.7 Limits of operation of the H & V equipment

This section addresses the determination of limits of operation of the H & V system in order to prevent the local thermal discomforts from exceeding acceptable limits. This was done using the observations made in the parametric and sensitivity studies on the effect of various parameters (the supply and room specific parameters) on the local

thermal discomforts.. The limits of operation were evaluated independently for each of the local thermal discomforts: a) vertical temperature gradients and b) draught.

A summary of the observations made in the sensitivity studies, on the influences of the room specific parameters (RSPs) on the vertical air temperatures and draught is listed in Table 5.1λ. The comparisons are made relative to the results of the standard case.

5.7.1 Vertical air temperature gradient

The introduction of room specific effects was not found to cause appreciable changes in the vertical air temperature *gradients* over most of the occupied zone and therefore the body. Differences in temperature gradients occurred over small regions, some resulting in greater temperature differences between the head and ankle level.

Comparatively little research has been performed on the effects of vertical air temperature gradients or variations on thermal discomfort. All the existing studies, including the data by *Olesen et Al.* (1979)   which was used in this study, correlate the discomfort level to air temperature differences between two fixed heights. These investigations do not address the effects of the temperature profile between the fixed heights. This profile is mostly assumed to be linear, which may be a reasonable assumption when cooling, but is not necessarily the case for heating, as seen in the present results. The view taken in this study, is that similar levels of comfort/discomfort would be perceived where similar temperature profiles or gradients occur over most of the body.

Of the RSPs investigated, excluding the effect of the large cold window, differences in temperature gradients from those of the standard case occurred over small zones, the largest being in the floor region at reduced room geometries (geometry B) and for a difference in floor temperature. Although these localised temperature variations, or steps, caused significant reductions in the temperature differences between the prescribed points (0.07 - 1 m), the majority of the body (~80% for a seated person and 90% for a standing person) experienced similar temperature gradients.

Case	Vertical temperature distribution	Draught
Vertical wall temperature gradients	Similar gradients were observed over most of the range of the investigation.	Similar temperature and velocity distribution resulted in similar magnitudes of draught.
Obstacles	Negligible influence	Lower velocities occurred throughout the occupied zone. These were however accompanied by increased turbulence in some locations. In these locations draught levels were similar to those of the standard case.
Heat sources	At the same supply air temperature and flow rates heat sources within the occupied zone naturally resulted in higher air temperatures. These increases were fairly evenly distributed over the occupied zone, therefore maintaining similar temperature gradients (as for the standard case). Heat sources above the occupied zone, had very little impact on temperatures in the occupied zone.	At the same average air temperature of the occupied zone, similar levels of draught were obtained over large parts of the occupied zone.
Unequal wall surface temperatures .	The side wall surface temperatures were found to have the greatest influence on the vertical air temperature distribution in the occupied zone. These side walls were observed to have a collective influence on the temperature gradient (i.e. similar influences of the individual side walls, therefore average surface temperatures of side walls may be used in the characterisation process).	Over the range of wall surface temperatures investigated (and expected), no significant variation occurred. Similar levels of draught were experienced at similar average temperatures.
Window	A cold window affected mainly the region in the mid-height of the occupied zone. The lower and higher regions were at similar temperatures as those of the standard case (at the same wall surface temperatures) . A dip in the temperature occurred in the mid-region in comparison to the standard case..	The dip in temperature was coincident with the lowest velocities in the occupied zone and therefore had no effect on the overall draught level.
Geometry	Similar temperature gradients occurred over most of the occupied zone. Smaller temperature steps were experienced in the vicinity of the floor at the reduced room geometry.	Higher velocities were experienced in the floor region, but lower velocities in the higher end of the occupied zone, including the head region. Similar draught levels and limits were estimated as for the geometry in the standard case.
Time	Over most of the flow range the temperature gradients were at, or below, those experienced at steady conditions. At high ACH there was an initial increase in temperature gradient dropping to the steady values within 15-30 mins.	A gradual build up of the velocities towards the steady values was noted. Temperatures were attained more rapidly, therefore draught levels were not expected to exceed the limits established on the basis of the standard case at known average air temperatures.

Table 5.12 Summary of observations made in the sensitivity studies on the effect of the RSPs on the local thermal discomforts.

The position/view herein adopted, is not to suggest that a large air temperature reduction in a locality would not cause local thermal discomfort. However, due to the location at which the temperature reductions occurred (for the change in geometry and unequal wall surface temperatures) i.e. in the ankle region, these are not expected to have a notable impact during cold periods when the ankles are unlikely to be exposed and thus more sensitive to draught.

Assuming a greater importance of the temperature gradient over the absolute temperature differences, the results of the sensitivity studies would indicate *similar* limits of operation for all rooms of similar surface temperatures and supply parameters of the H & V system. Although the analysis indicated a greater correlation between the temperature gradients and the side wall surface temperatures as opposed to the average surface temperatures, determination of individual (and therefore average) side wall temperatures would in practice be an unlikely prospect.

For practical application of the limits of operation obtained from the standard case, a number of considerations need to be made. This is because in 'real' rooms differences in wall surface temperatures will occur. These conditions in the room need to be *linked* to an equivalent average surface temperature of the equivalent standard case. Assuming the ACH and supply air temperatures will be measured, the link remains to be made between the wall surface temperatures. Two options which may be considered to achieve this are:

a) measurement of the mean radiant temperature in the room.

b) measurement of one or more of the side wall temperatures.

In the first of these, the measurement of mean radiant temperature, which will be needed for thermal comfort purposes anyway, relies on the absence of other radiant sources and may therefore not be a reliable option. In the second option, the use of an exterior wall surface may lead to an underestimation of the average surface temperatures. An interior wall surface on the other hand could have the opposite effect. The safer option for measurement of a single surface temperature, would be the measurement of an exterior wall surface temperature.

An alternative to the options listed above would be the use of a 'design' surface temperature in determining the limiting supply air temperatures. This may be a fixed temperature based on the minimum wall surface temperatures expected, but may also incorporate the use of outside air temperature compensation, similar to boiler run-up temperature's i.e. changing 'design conditions' on the basis of the outside air temperature and knowledge of the insulation level.

The use of fixed operation limits would appear to be a reasonable option for the H & V system. At design wall surface temperatures in the region of 19 °C, the maximum wall surface temperatures during the heating season would be unlikely to exceed the design surface temperature by more than 2-3 °C. This would imply allowable increments in supply air temperature of 2-3 °C to achieve similar limits of discomfort due to vertical air temperature differences. At low airflow rates these increments in supply air temperature are unlikely to have significant economic repercussions. Higher flow rates and supply air temperatures are anyhow less likely with increasing wall surface temperatures and therefore also reductions in the space heat load. Therefore the greater the insulation value of the building, the greater the applicability of fixed limits of operation.

The estimated limits of operation to prevent discomfort due to vertical air temperature gradients will be defined in terms of: flow rates and corresponding supply air temperatures at which the prescribed limit of discomfort of 6.5% is achieved at wall surface temperatures of 19 °C. These were determined by linear interpolation of the data in Table 5.3 and are shown graphically in Figure 5.36. This includes a polynomial fit through the points to allow continuous evaluation over the range of flow rates between 3 and 9 ACH.
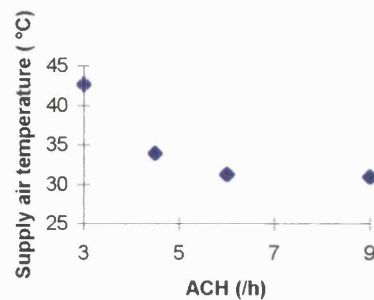
Figure 5.36 Limits of operation of supply air temperature in order not to exceed 6.5% dissatisfaction due to vertical air temperature gradients.

5.7.2   Draught

Heat sources, obstacles and a change in the room geometry had the largest impact on the velocities in the occupied zone in comparison to the standard case. The presence of the heat sources and obstacles generally resulted in reductions in the velocities within the occupied zone. These reductions in velocity were accompanied by increases in the turbulence intensity in localised regions. This resulted in similar overall draught levels as those of the standard case at similar average air temperature.

A reduction in the room geometry, at the same ACH and supply air temperature, resulted in lower velocities in the occupied zone. The reduction in the magnitudes of velocity were however not uniform over the occupied zone. Although lower velocities occurred over most of the occupied zone including in the head region, increases in velocity occurred in the floor region. Both the head and ankles are particularly sensitive to draught, with the head being the more sensitive of the two. This greater sensitivity of the head region and the fact that the ankles are likely to be clothed during the colder periods and therefore less sensitive to draught than when exposed, lends support to the reduction in draught indicated by the average velocities (Table 5.10). It would appear therefore that a reduction in draught levels is obtained in the smaller room (with the room height maintained). The draught levels obtained from the numerical evaluations were in both cases considered to be good representati ons of the occupied zone as a whole.

Over the investigated range, overall draught levels in the room did not exceed the acceptable limit of 6.5 %. If average air temperatures were to fall below those used/obtained in the investigation, then at the high flow rate (9 ACH), discomfort due to draught is likely to exceed the acceptable limits. The results obtained from the time dependent simulations however indicate little benefit for IAQ purposes, in operating at flow rates as high as 9 ACH. Similarly, the thermal environment was observed to be achieved fairly rapidly thus implying that at the high flow rates, average air temperatures below those obtained in the investigation would be unlikely to occur for substantial periods.

For the H & V system under current investigation, no restriction would therefore appear to be required with respect to discomfort due to draught. This is assuming the supply ATD has been sized to prevent draught e.g. at the total effective area of 0.25 m^2 for the room of 6 x 6 x 2.5 m^3.

5.8   Thermal comfort control

The feasibility of thermal comfort control using an index such as the *PMV* was assessed. As a result of the assessment the measurements which would be required to control thermal comfort in the room were determined. The necessary number and location of these measurements were also identified.

5.8.1   Feasibility of *PMV* control

Air movement (or velocity) influences the thermal sensation only when it results in additional cooling of the body. This occurs when the mode of heat transfer is by forced convection. As mentioned in Chapter 4 the transition from free to forced convection occurs at flow rates of between 1-2 m/s. From the velocities obtained in the occupied zone, it would therefore be expected that over the range of operation of the potential H & V systems the velocities will have little or no impact on the *PMV*. The highest velocities obtained did not to exceed 0.1 m/s as shown by the vector magnitudes in Figure 5A.16 (9 ACH, supply air temperature of 25 °C) for the standard case. Lower

velocities occurred with room specific effects such as obstacles and heat sources in the room.

To confirm negligible influence of the velocities on the *PMV*, a comparison was made of the *PMVs* with and without the inclusion of the velocity magnitude i.e. comparison of the *PMVs* obtained with the simulated velocities included in the *PMV* equation to the *PMVs* obtained with a zero velocity. The results of this comparison (9 ACH, 25 °C) are shown in Table 5.13. The *PMVs* were calculated at a combination of two activity levels 58 W and 70 W and two clothing insulation values, 0.11, 0.16 m² °C/W. The Table as expected, shows a greater influence of velocity at lower activity and lighter clothing. The impact of the velocity on the PMV even at these values is minor and can be neglected.

M	Icl=0.11		Icl=0.16		Icl=0.23	
	PMV	*PMV**	*PMV*	*PMV**	*PMV*	*PMV**
70	-0.72	-0.67	-0.15	-0.11	0.37	0.40
58	-1.41	-1.34	-0.67	-0.62	-0.01	0.04

Table 5.13 Average *PMVs* calculated with and without (*) the influence of velocity at activity rates (*M*) of 58 and 70 W/m², clothing insulation values (*I$_{cl}$*) of 0.11 and 0.16 at a partial water vapour pressure of 1400 Pa.

In the current application of the H & V system, velocity measurements are therefore not needed to determine the thermal sensation in the room as represented by the *PMV*. Thermal comfort control for this application may therefore be restricted to the measurement of air temperature, mean radiant temperature and the relative humidity. These measurements are addressed below.

5.8.2 Sensor locations and measurements

Within this section, the minimum number of sensor locations/measurements are determined with which representative conditions within the occupied zone can be established for application in the control of the thermal environment. The use of a thermal comfort sensor was not specifically investigated. This was taken into account indirectly by consideration of the four environmental parameters, the air temperature,

velocity, mean radiant temperature and the partial water vapour pressure measured by the relative humidity.

The environmental parameter singled out for investigation was the air temperature. The remaining parameters were not investigated for the following reasons:

1. The previous section established that a *velocity* measurement is not required for the evaluation of *PMV* for the application range of the H & V system.

2. In practice only minor variations in *relative humidity* occur within a room. This means that the location of the measurement point within the occupied zone is not really of consequence so far as relative humidity is concerned.

3. The *mean radiant temperature* of the room is influenced not by a persons location in the room but by the persons orientation relative to the radiant heat source which were assumed to be the wall surfaces. The mean radiant temperature is also independent of the flow variables.

Measurement of air temperature

Uniform air temperature distributions were observed across the room in the parametric studies. This was maintained with the introduction of the RSPs. The choice of location of the air temperature sensor(s) within the occupied zone, was thus confined to a selection of suitable height(s) at which these should be located. A number of locations were considered for the potential measurement points of the air temperature, as shown in Table 5.14. These consisted essentially, of two location types:

1. a conventional near wall location (representing a wall mounted thermostat), and
2. a central location within the occupied zone.

Location No.	Location	Height (m)
1	Near wall, approximately 1 cm from West wall	0.6, 1.0, 1.4
2	Central	0.6, 1.0, 1.4

Table 5.14 Locations of sensor 'measurement' points

Initial assessment of the air temperature measurements showed better agreement and consistency between the measurements obtained at a height of 0.6 m and the average air temperatures than the measurements at the other heights. The measurements

obtained at this height for both the central and wall location are shown and discussed below.

Comparison between the measurements obtained at the two locations and the average air temperature of the occupied zone are shown in Figure 5.37a-h for a low flow rate of 3 ACH and a high flow rate of 9 ACH. These are for three cases, the standard, the case with side wall temperature gradients and the case with internal heat sources. The comparisons indicate increases in the offsets between the average and measurement temperatures with both increasing supply air temperatures and flow rates. This occurs at both thermostat locations with smaller differences in the offsets at the central location. The maximum and minimum temperature offsets are shown in Table 5.15. These maximum and minimum offsets occurred at the lowest and highest supply air temperatures respectively.

From these results, a central thermostat location would appear to offer distinct advantages compared to the wall location in the determination and control of the air temperature of the occupied zone. The distinction between temperature determination and control is made because in the control of the thermal environment, the consistency of the measurement (i.e. constant offsets through different supply parameters) is of greater importance than the actual reading obtained.

The results obtained for the standard case indicate a possible benefit of air temperature setback of the control set point, with increasing flow rate. The magnitude of temperature setback required was seen to decrease with the presence of the wall temperature gradient and internal heat sources. Similar magnitudes of temperature offsets were however obtained irrespective of flow rate when internal heat sources were present. The measurements obtained from the remaining steady state cases were similar to those of the standard case and have not been listed.
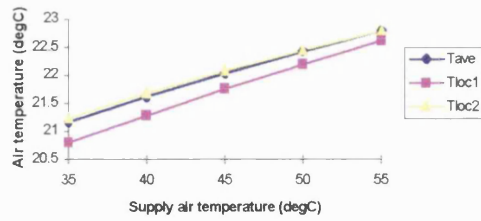
(a) standard case, 3 ACH
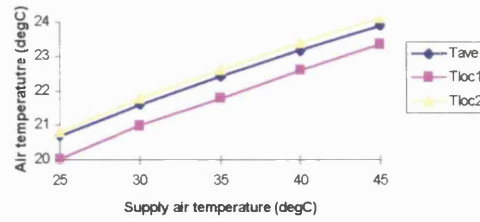
(b) standard case 4.5 ACH
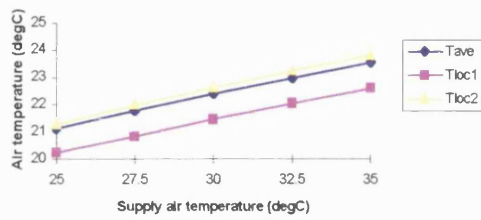
(c) standard case, 6 ACH
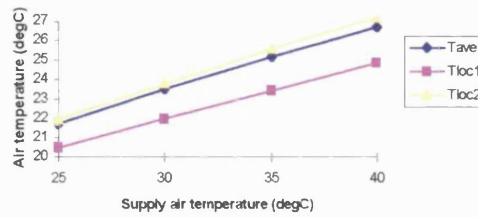
d) standard case, 9 ACH
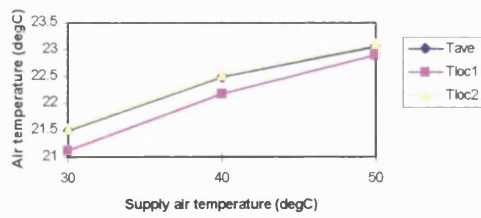
(e) with wall temperature gradient, 3 ACH
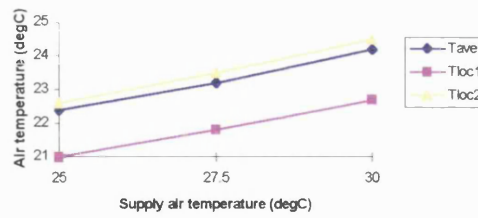
(f) with wall temperature gradient, 9 ACH
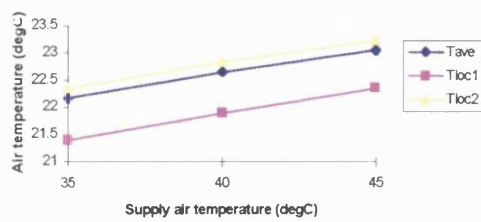
(g) with internal heat source, 3 ACH
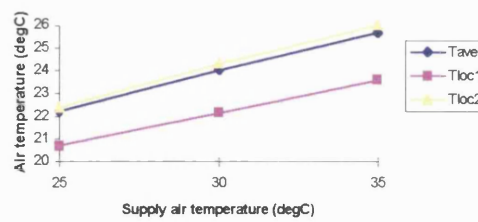
(h) with internal heat source, 9 ACH

Figure 5.37a-h Temperature 'measurements' at specified sensor locations. Tloc1 - air temperature at location 1, Tloc2 - air temperature at location 2, Tave - average air temperature in the occupied zone.

Case	Offset of measurements from average temperature (°C)	
	Central location	Wall location
Standard 3 ACH	-0.06 → 0.00	-0.37 → -0.18
Standard 4.5 ACH	0.12 → 0.22	-0.67 → -0.55
Standard 6 ACH	0.15 → 0.29	-0.91 → -0.95
Standard 9 ACH	0.23 → 0.51	-1.25 → -1.84
Wall temperature gradient 3 ACH	0.02 → 0.04	-0.38 → -0.16
Wall temperature gradient 9 ACH	0.2 → 0.3	-1.4 → -1.5
Internal heat source (unit) 3 ACH	0.2	-0.78 → -0.70
Internal heat source (unit) 9 ACH	0.16 → 0.34	-1.52 → -2.09

Table 5.15 Range of temperature offsets between measurements at a height of 0.6 m and average temperatures. The range represents the offsets with increasing supply air temperature.

The measurements obtained with internal heat sources are considered to be the most important assessment criteria. This is because internal heat sources are bound to be generated during occupancy periods. The small variations in offsets observed with internal heat sources, would therefore not appear to warrant variations in the control temperature set-points of the system.

The evaluation shows the ability to obtain good representation of the air temperature in the occupied zone of the room using a single centrally located sensor. Measurement of the mean radiant temperature and relative humidity in the room can be made were convenient. The location of these is commented on in the discussion below.

5.9 Discussion

5.9.1 Overview of the results

A detailed study has been performed to investigate the influence of a wide range of parameters on a combined heating and ventilation system using a high level supply and low level extract device. The parameters investigated included, the supply airflow rate and temperature, room surface temperatures, internal heat sources, obstacles, a cold window surface, the room geometry and transient effects. These parameters were

grouped into two categories, the parametric studies and the sensitivity studies. The parametric studies were performed on a simple flow model with the room represented as a bare enclosure with all the enclosure surfaces at the same temperature. The parametric studies investigated the effect of comprehensive range of airflow rates and supply air temperatures on the flow behaviour in the room. Sensitivity studies were then performed to observe the effects of the remaining parameters, the so-called room specific parameters, on the flow behaviour. These sensitivity studies were performed at supply parameters to coincide with some of the conditions used in the parametric studies. The idea behind this approach was to create a web of linkages using the parametric studies and a limited number of investigations for each of the sensitivity studies. This was to allow extrapolation of results to conditions not investigated.

The influence of the investigated parameters on the flow behaviour was analysed and as a consequence the effects of these on the thermal comfort and IAQ in the room assessed. The observations made have been discussed within the text. This investigation appears to be the most comprehensive study to date on the effects of a combined heating and ventilation system on the thermal comfort and IAQ in a room, with no comparable results to refer to. The discussion in this Section has a bias towards the implication of the results obtained on the control of the H & V system and the indoor environment. A brief summary of some of the salient features observed in the course of the investigation will be provided, leading on to the recommendation of a control strategy to achieve thermal comfort control while providing good IAQ in an energy efficient manner.

In the parametric studies it was observed that the airflow patterns and distributions of air velocity and temperature in the room had a dependency on both the buoyancy and the momentum of the supply air stream. The influence of the two factors may be combined by using the non-dimensional Archimedes number (Ar), which from preliminary results would appear to lend itself to characterisation of the flow distribution in the room. The use of this characterisation criteria may be used to achieve effective air distribution within the room, eliminating excessive air movement and non-uniformities in air temperature across the room. This would be considered as part of the design process as opposed to the control and is not discussed further.

In the sensitivity studies it was observed that despite differences in airflow patterns and magnitudes of air velocity and temperature , similar local thermal discomfort levels were obtained at similar average air temperatures and boundary conditions irrespective of the room specific parameters. The boundary conditions hereby referred to are the supply parameters i.e. airflow rate and supply temperature and the average room surface temperatures. This is a very useful result both for design and control purposes. In the design process it implies that calculated or pre-calculated results using a simple flow model, with the room represented by a bare enclosure, can be used in the assessment of the potential discomfort levels in rooms for most standard applications. In the control of the thermal environment, this implies that the limits of operation of the H & V system to prevent discomfort due vertical air temperature differences and draught will be valid throughout.

Draught was found not to exceed specified discomfort levels of 6.5 % over the expected range of flow rates. Restrictions in the limits of operation to prevent discomfort due to draught are thus not required. Limits of operation of the H & V systems were thus determined only for prevention of discomfort due to vertical air temperature differences. The limits of operation were defined in terms of the airflow rate, supply air temperature and average surface temperature in the room. In deducing similar limits of operation irrespective of the room specific effects, it was assumed that the profile or gradient of the air temperature variation over the occupied zone was of greater importance than the air temperature differential between fixed heights. The influence of the profile of air temperature variation does not appear to have been studied and the results highlight the need for more research into this field.

The thermal sensation of a person or persons at predefined activity and clothing insulation levels was measured using Fanger's *PMV*. Over the expected range of flow rates of the H & V system, the air velocity had negligible influence on the *PMV*. The implication of this is that a simplification of the *PMV* model can be used in the control of thermal comfort in the room. The simplified *PMV* model would take into consideration only the air temperature, mean radiant temperature and relative humidity in the room.

The need for a measurement of air velocity in the room is made redundant based on the results on the thermal comfort analysis. The air temperature in the room was found to be well represented by a single centrally located measurement device (within the occupied zone) in approximately the mid-height of the occupied zone. At this location the measurement gave good representations of the average air temperature in the occupied zone irrespective of the operating conditions. The relative humidity in the room can be measured at any convenient location, either at the same point as the air temperature or together with the mean radiant temperature. A high location measurement point for the mean radiant temperature would probably be most suitable to eliminate the effect of localised solar radiation. This would suggest the need for at least two measurement locations in the room, which does not support the use of a combined thermal comfort sensor.

5.9.2 Recommended control strategy

The control strategy outlined below uses a simplified form of the *PMV* i.e. it does not utilise all seven personal and environmental parameters, but assumes some of these to be constant with the control based on the relation between the remaining parameters. This control strategy will be referred to as Simple Comfort Control (SCC).

The aim of the control strategy is to achieve and maintain a comfortable thermal environment through a user friendly interface with minimal user interaction. The concept proposed for SCC is described in the following points:

1. Control of the thermal environment is to be based on the relationship between the air temperature, mean radiant temperature and relative humidity alone. This will use the *PMV* algorithm with a zero velocity and constant values of the personal parameters. The precise value of the personal parameters used is not relevant. These can mathematically be shown to have a linear relationship with the *PMV*. Changes in the personal parameters will therefore result in constant offsets of the *PMV*s from those obtained at the reference values. The significance of this is that SCC is not concerned with the actual *PMV* obtained. The reason for this will become apparent in the following points.

2. The users preferred comfort level in the thermal environment is not to be based on predictions of a neutral *PMV*, but on the user response to the thermal environment. Once this preferred comfort level and therefore *PMV* is obtained, SCC will maintain this *PMV* level by controlling the room air temperature and possibly relative humidity to maintain a constant *PMV*. Various preferred comfort levels may be stored by the user for specific activities e.g. a night time setting in a similar manner as used in thermostat setback.

3. At the preferred comfort level SCC will modulate the supply air conditions (flow rate, temperature and humidity) to maintain the comfort level or *PMV* whilst preventing vertical air temperature gradients from exceeding acceptable limits i.e. maintaining operation of the H & V equipment within defined operating limits. (Limits of operation for the prevention of draught are not required in the current application).

4. A user request for a warmer environment is met by preset increases in the average air temperature as opposed to fixed *PMV* increments. This avoids the necessity of the input of personal parameters. Although this approach would imply inconsistent increases in thermal sensation during different seasons, the seasonal change in clothing trends is relatively slow and the user would get used to the system response.

SCC achieves thermal comfort control, which is not possible with conventional thermostat control. The main advantages of SCC over a complete (7 variable) *PMV* comfort control system is:

- It eliminates the error aspect which is often reported in the prediction of the *PMV*. SCC does not require the *PMV* to predict the users comfort conditions. The mathematical consistency of the *PMV* in relation to the individual variables is the most important aspect of SCC.

- It avoids the complex and inaccurate task of the user specification of activity and clothing insulation level.

- Achieves comfort control in a simple manner.

A schematic representation of the control strategy is shown in Figure 5.38. With the aid of examples a basic implementation strategy of SCC is outlined below. This will demonstrate the integration of SCC with specific IAQ and energy policies or requirements. The potential contribution of other information gained in the course of this investigation is also highlighted.
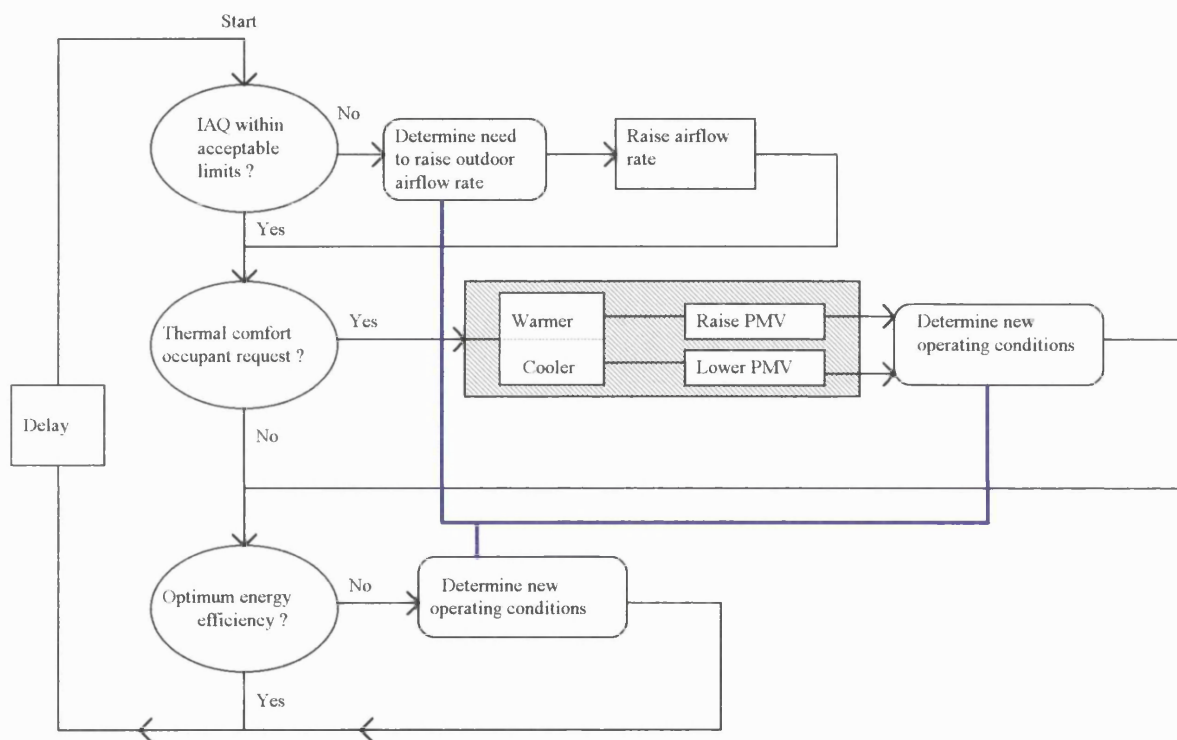
Figure 5.38 Control scheme integrating the use of SCC.

The control loop consists essentially of three distinct levels: the IAQ, the thermal comfort and the energy efficiency levels. Within each of these levels pre-stored knowledge is utilised in effecting a control decision or action. These 'knowledge centres' are shown in Figure 5.38, linked by a blue line which represent two way links of information flow. The implication of this is that any action taken in any of the three levels, is performed with consideration of the knowledge and requirements of the other levels. The user interface, marked as the shaded area in Figure 5.38 is shown in Figure 5.39.

The control action taken with the use of information from these 'knowledge centres' is described using two scenarios (A and B) showing a sequence of events. These will

serve to explain the control scheme with the aid of two specific examples to follow, on the control action during operation of the system.

A. (Outdoor air flow rate requirements).

1. Assuming measurements are made of various pollutants and outside air supply is controlled in DCV principles.

2. One or more pollutant concentrations might exceed the AIC limit (e.g. limits in Table 1.4).

3. An increased outdoor airflow rate is required to reduce the relevant pollutant concentration levels to their AIC values. This increase in outdoor airflow rate may be estimated using for example the pollutant variation with airflow rate as shown in Figure 5.4. This is however established on the basis of 100 % outside air supply and is not necessarily valid for recirculating systems.

B. (Thermal comfort and Energy requirements).

1. Assuming a fixed design wall surface temperature of 19 °C has been specified. The operation limits of supply temperature and airflow rate (in ACH) are as shown in Figure 5.36.

2. Assuming the increase in PMV is most efficiently brought about by an increase in average air temperature. This will mostly be the case.

3. An increase in average air temperature may be brought about by increasing the heat supply rate to the room either by raising the supply air temperature or the airflow rate or both.

4. While maintaining the minimum outdoor airflow rate required for IAQ purposes, the operating conditions need to be maintained within the specified operating limits and provide energy efficient operation. As a consequence of a request for a warmer environment, optional supply conditions can be determined to obtain the required increase in average air temperatures (as shown in Figure 5.39). At a fixed airflow rate the required supply air temperature can be estimated using the gradients obtained from Figures 5.37a-d. (e.g. at the airflow rates used of 3, 4.5 6 and 9 ACH the rate of increase of average air temperature vs. supply air temperature was 0.09, 0.18, 0.26 and 0.36). If the required supply air temperature exceeds the

operating limit a new and equivalent pair of supply conditions can be estimated i.e. an airflow rate and supply air temperature that obtain the same average air temperature. The pairing of supply conditions (to obtain the same average air temperature) can be made from the data in Table 5.3. e.g. the ratio of supply enthalpies to obtain similar average air temperature (22.4 °C) at 4.5 and 6 ACH is 1.07 and 1.2 respectively, relative to that at 3 ACH. This is as a result of increasing heat transfer at the wall surfaces with increasing airflow rate. The ratio can be used in establishing/estimating a new operating condition which falls within the operation limits (Figure 5.36).

5. At the optional supply conditions, the most energy efficient action may be taken. In the absence of alternative or waste heat sources (e.g. from other zones in the building) the minimum required airflow rate would be used to obtain the required increase in average air temperature.

Occupant Response	Increment average air temperature (°C)
Much warmer	+ 1.5
Warmer	+ 1.0
Slightly warmer	+ 0.5
Slightly cooler	- 0.5
Cooler	- 1.0
Much cooler	- 1.5

Figure 5.39 SCC control interface and response
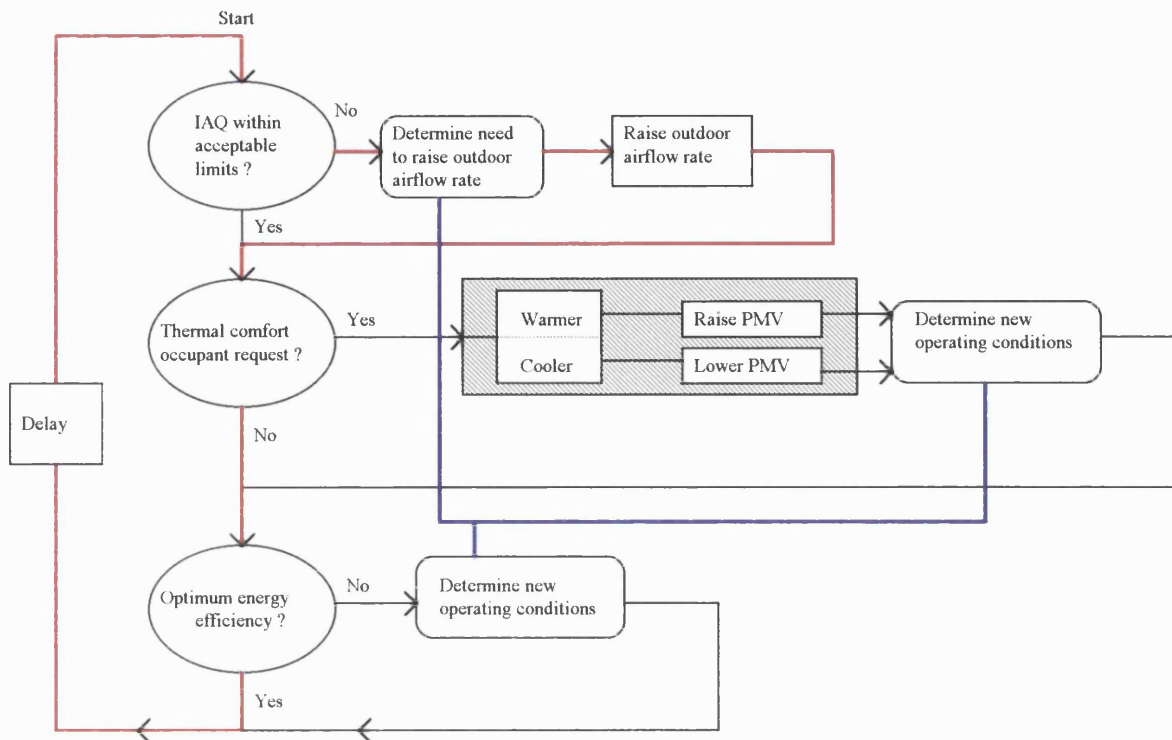
Figure 5.40 Control scheme integrating the use of SCC, Example 1.

Example 1

Status

The system is in operation at 3 ACH, supply air temperature of 35 °C. The system operates on 100 % outside air (with heat recovery). Thermal comfort is fine. The concentration level of CO_2 reaches a concentration level of 1500 ppm, as a result of a an increase in the number of persons in the room.

System response

The outdoor airflow rate is to be increased to reduce the CO_2 concentration in the room back to its AIC level of 1200 ppm. The outside airflow rate would be estimated to require an increase of 1 ACH (Figure 5.4) to reduce the concentration to its required level (based on the ratio of reduction of concentration levels). At the new airflow rate of 4 ACH a new supply air temperature is required to maintain the same average room air temperature. This can be estimated from the procedure described in Scenario B to be 27 °C (assuming an enthalpy ratio of 1.03 : 3 x 35 x 1.03 / 4).
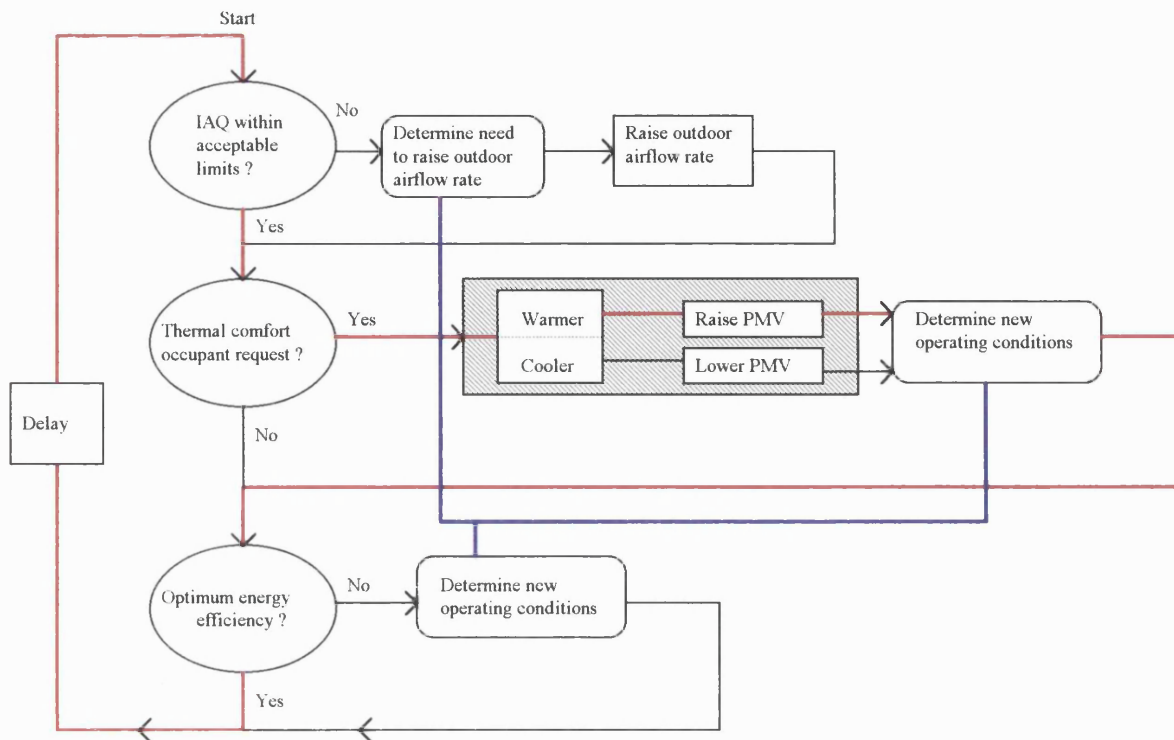
Figure 5.41 Control scheme integrating the use of SCC, Example 2.

Example 2

Status

The system is in operation at 3 ACH and supply air temperature of 40 °C. IAQ is fine. The user requests a 'warmer' environment via a user interface as shown in Figure 5.39.

System response

The outdoor airflow rate is maintained. The average air temperature in the room is to be raised by 1 °C. At 3 ACH, this would require an estimated increase in supply air temperature to 51 °C. This exceeds the operation limits as shown in Figure 5.36. New supply conditions may therefore be estimated at e.g. 4.5 ACH and a supply air temperature of 36.4 °C (3 x 51 x 1.07 / 4.5). Assuming no alternative energy implications, the system would readjust to these new operating conditions. At these conditions, after a delay, the system would fine-tune the supply air temperature to match the average air temperature required.

A rough outline has been provided of a control scheme. The IAQ and Energy policies have been vague. IAQ requirements are currently under review in many countries and the energy policy will depend on the available components and integration with the complete H & V system of the house. The essence of the outline was however to demonstrate the possibility of integration of specific IAQ and energy policies together with thermal comfort control such as SCC in the control of the indoor environment. The concept also demonstrates the potential use of data obtained from pre-calculated CFD simulations in the control of the thermal environment.

The implementation of such a control strategy would appear to be suited to expert system techniques which are increasingly being applied in Building Energy Management systems (Shaw, 1987). The integration of the control strategy in an expert system application is currently under development with plans of testing this in a demonstration building of the Daimler Benz Research Institute in Frankfurt. The demonstration project at Daimler Benz is targeted at future intelligent homes as part of the ESPRIT Home Systems project for integrated home applications.

Figure.5.A1

Velocity vectors for the standard case at 3 ACH, supply temperature 35 °C.
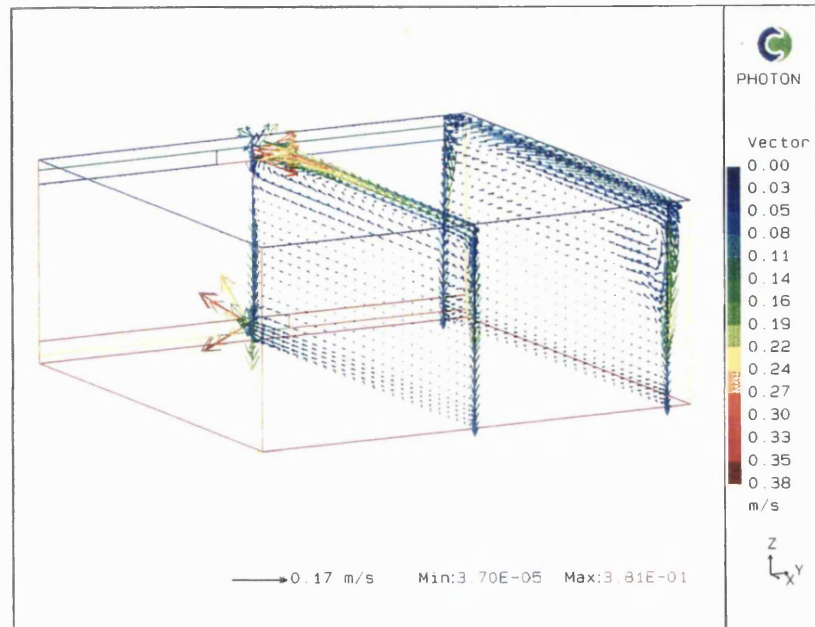
Figure.5.A2

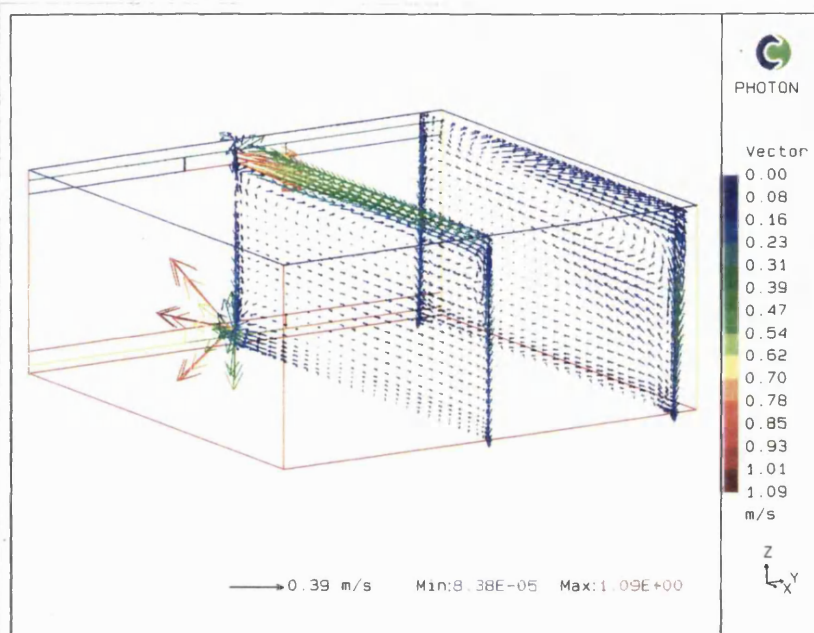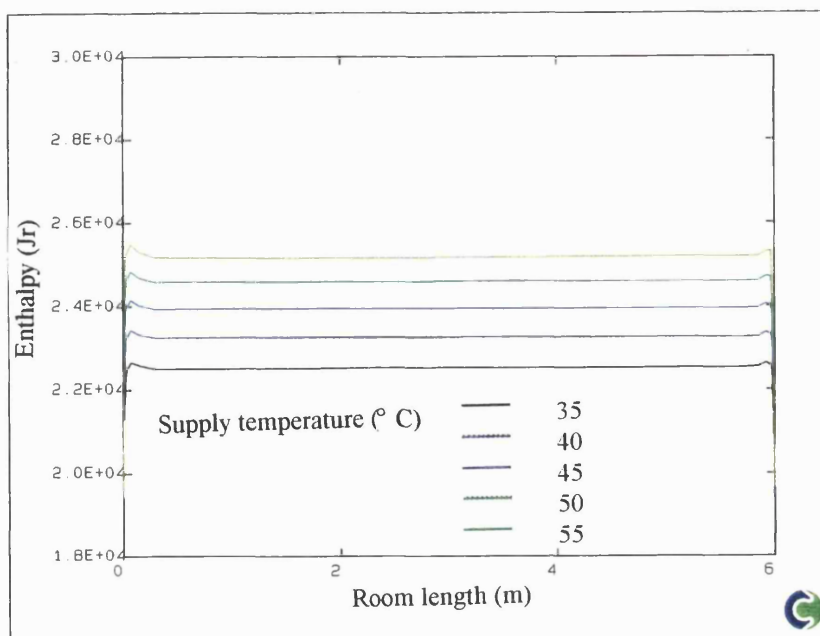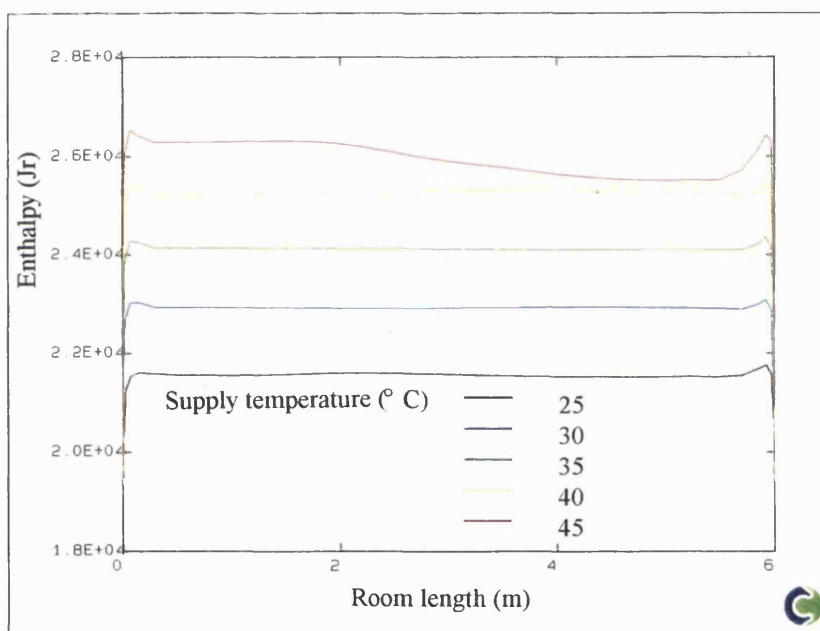Velocity vectors for the standard case at 3 ACH, supply temperature 40 °C.
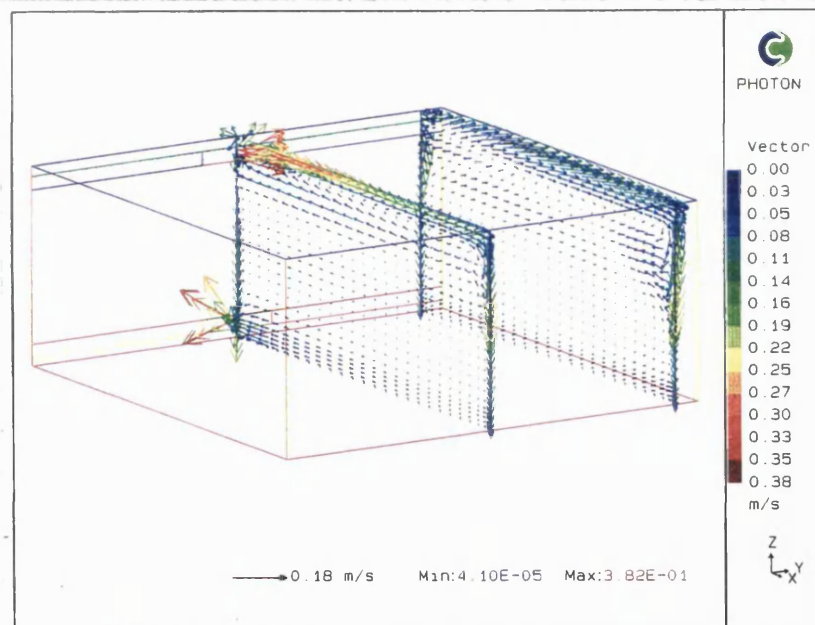
Figure.5.A3

Velocity vectors for the standard case at 3 ACH, supply temperature 45 °C.
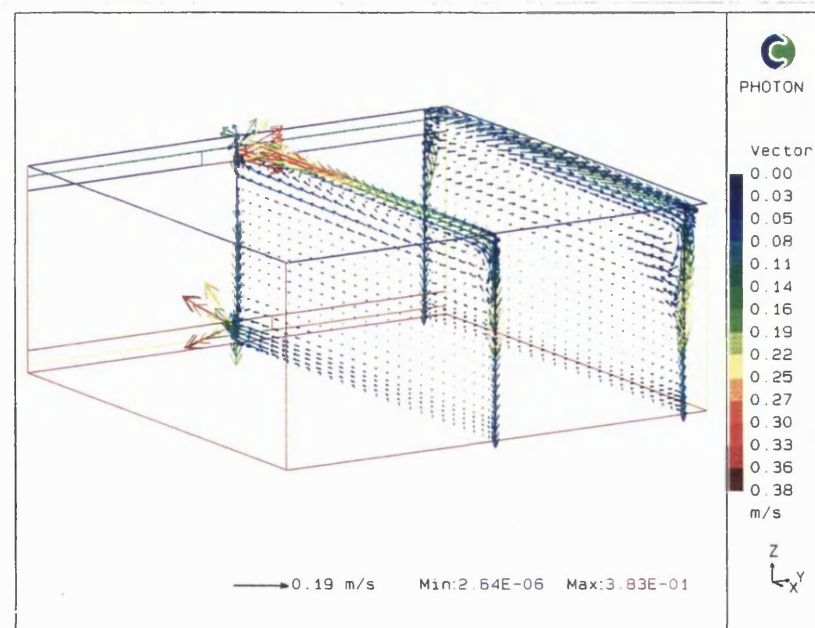
Figure.5.A4

Velocity vectors for the
standard case at 3 ACH,
supply temperature 50 °C.
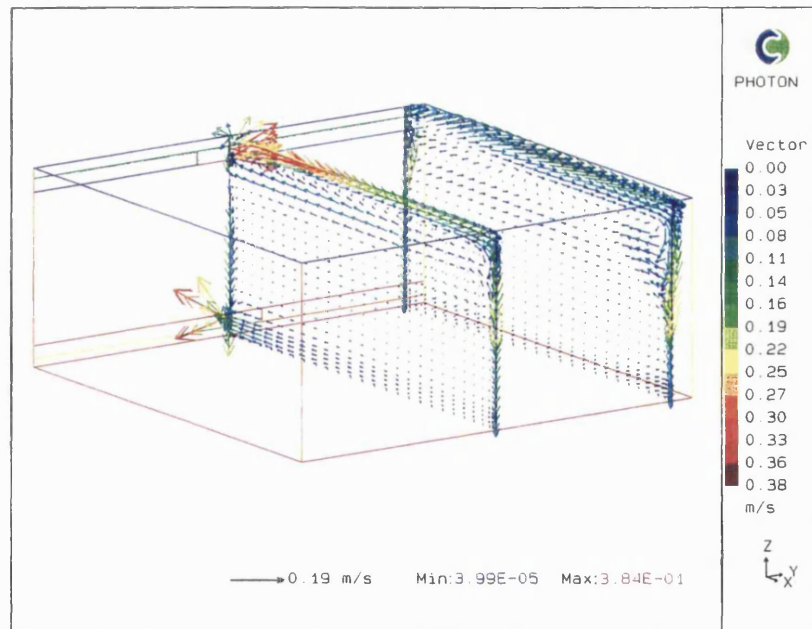
Figure.5.A5

Velocity vectors for the
standard case at 3 ACH,
supply temperature 55 °C.
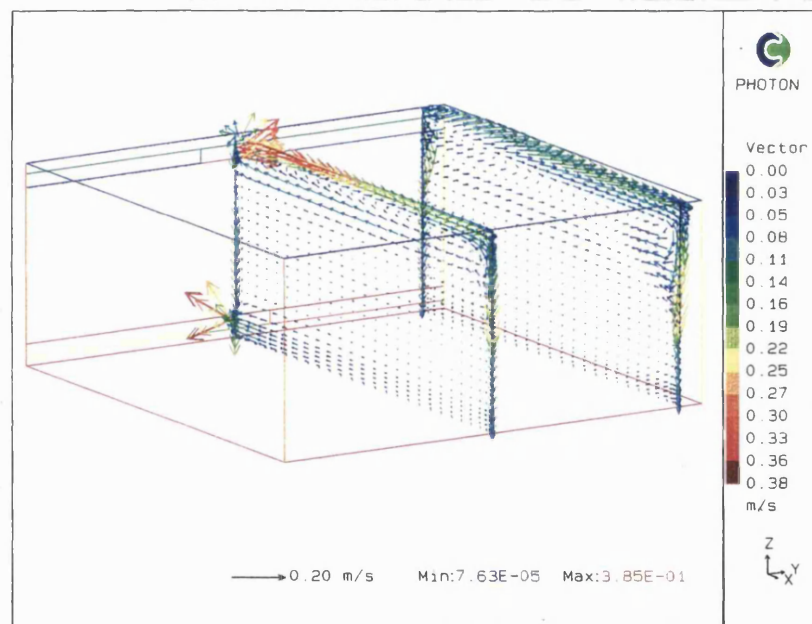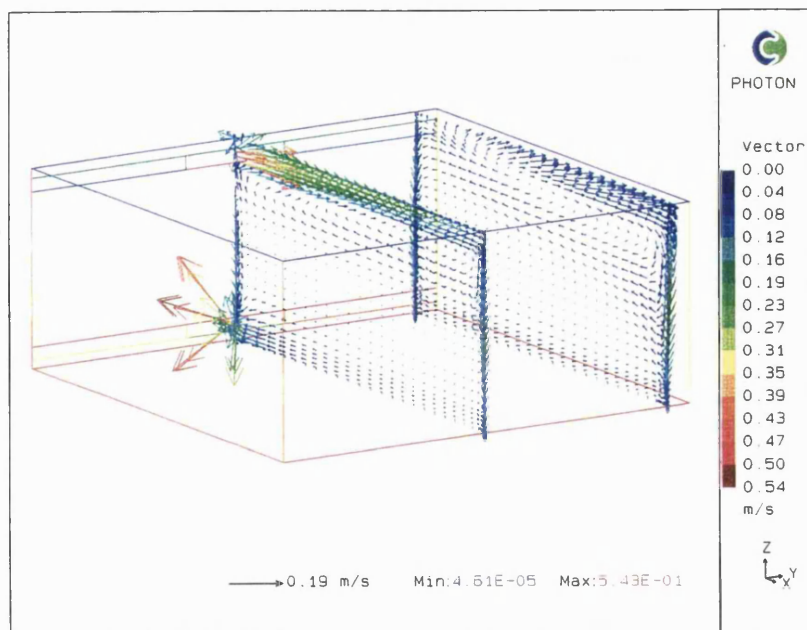
Figure.5.A6

Velocity vectors for the standard case at 4.5 ACH, supply temperature 25 °C.
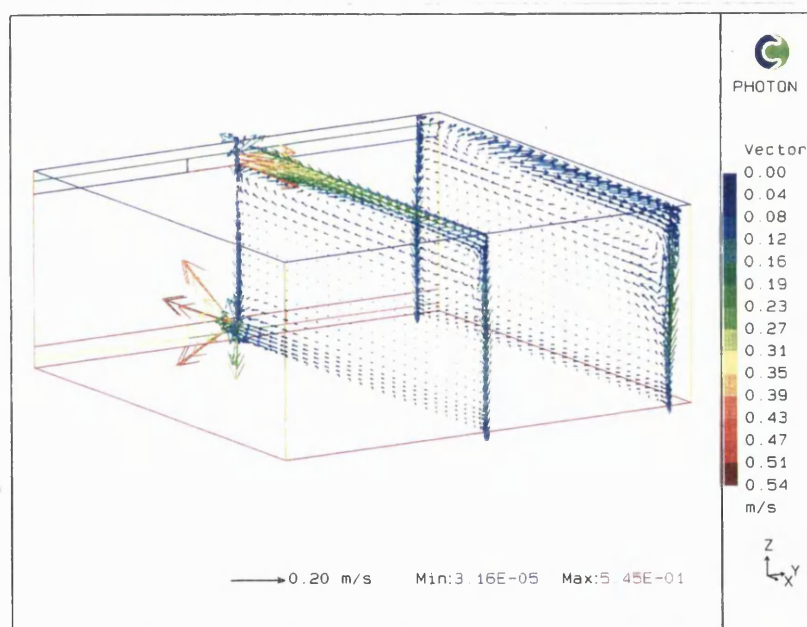
Figure.5.A7

Velocity vectors for the standard case at 4.5 ACH, supply temperature 30 °C.
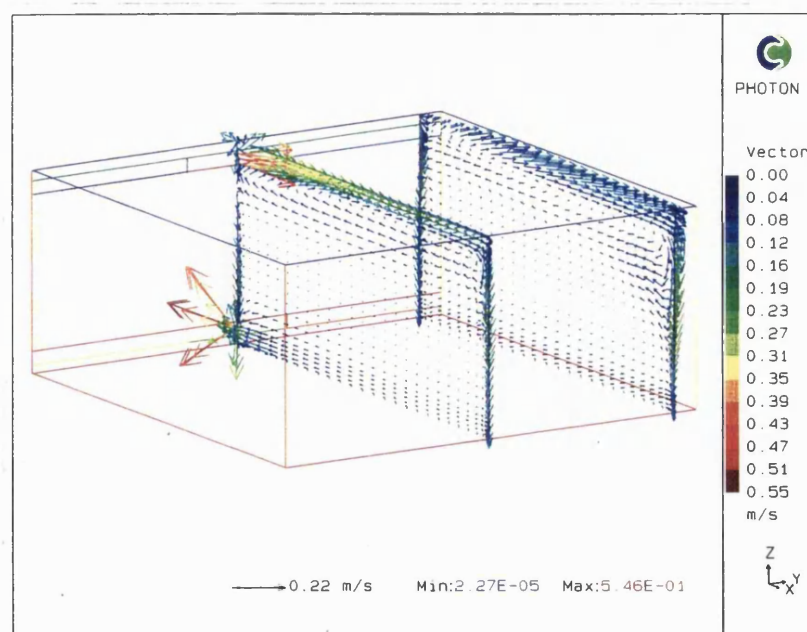
Figure.5.A8

Velocity vectors for the standard case at 4.5 ACH, supply temperature 35 °C.

Figure.5.A9

Velocity vectors for the
standard case at 4.5 ACH,
supply temperature 40 °C.
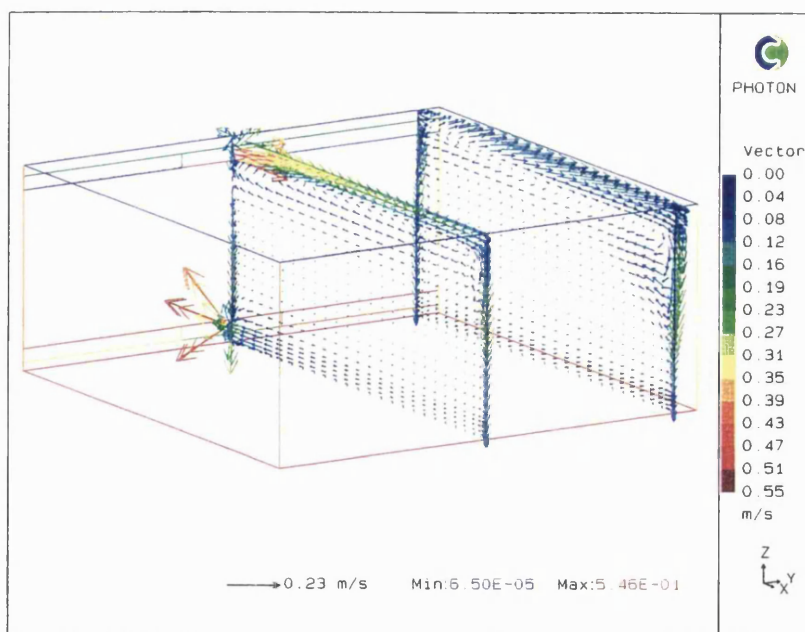
Figure.5.A10

Velocity vectors for the
standard case at 4.5 ACH,
supply temperature 45 °C.
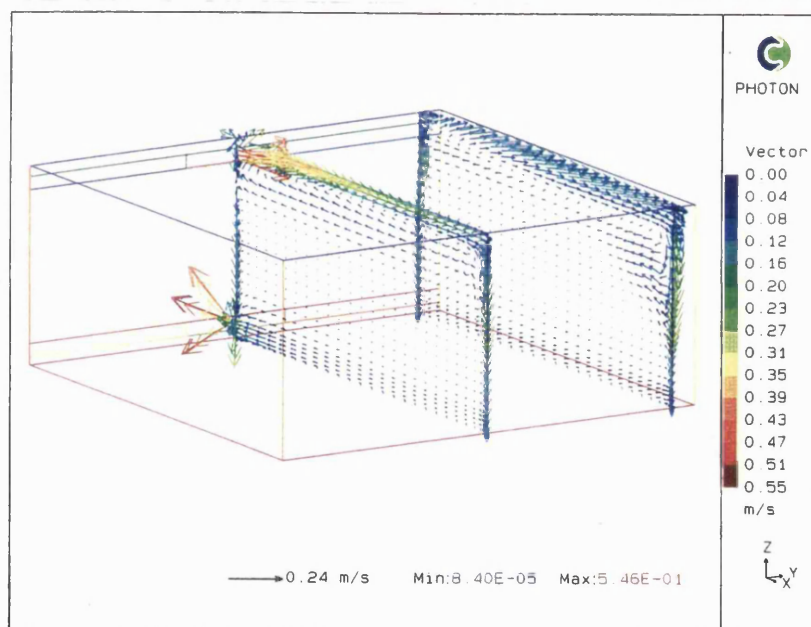
Figure.5.A11

Velocity vectors for the
standard case at 6 ACH,
supply temperature 25 °C.
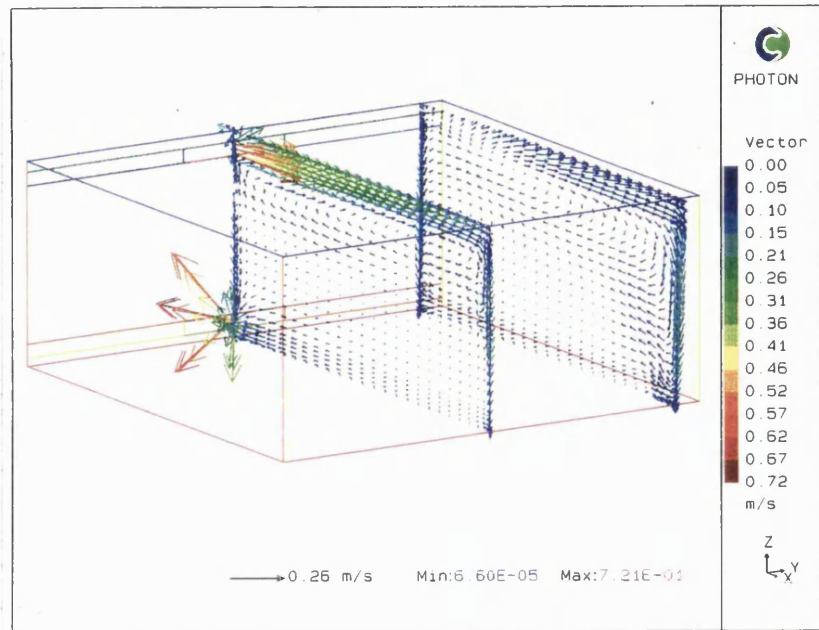
Figure.5.A12

Velocity vectors for the
standard case at 6 ACH,
supply temperature 27.5 °C.
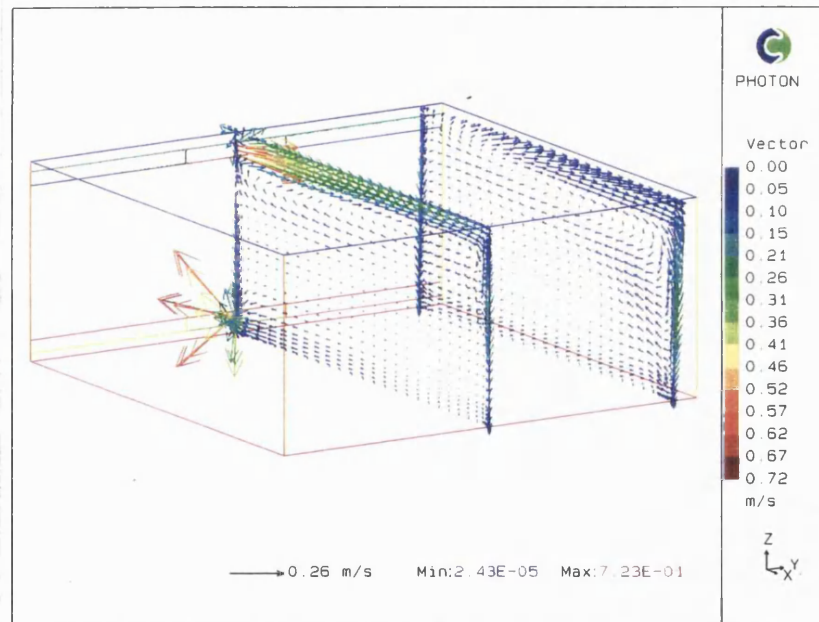
Figure.5.A13

Velocity vectors for the
standard case at 6 ACH,
supply temperature 30 °C.
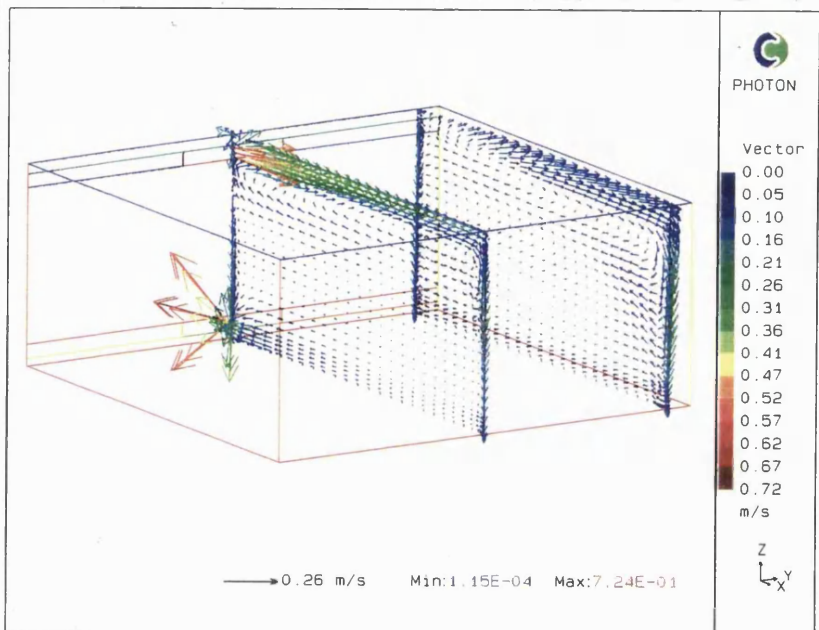
Figure.5.A14

Velocity vectors for the
standard case at 6 ACH,
supply temperature 32.5 °C.
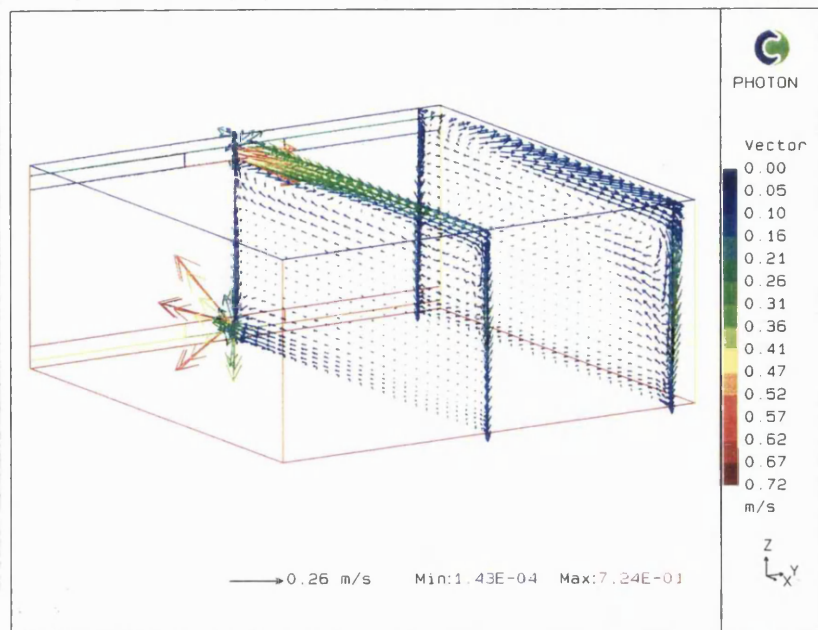
Figure.5.A15

Velocity vectors for the
standard case at 6 ACH,
supply temperature 35 °C.
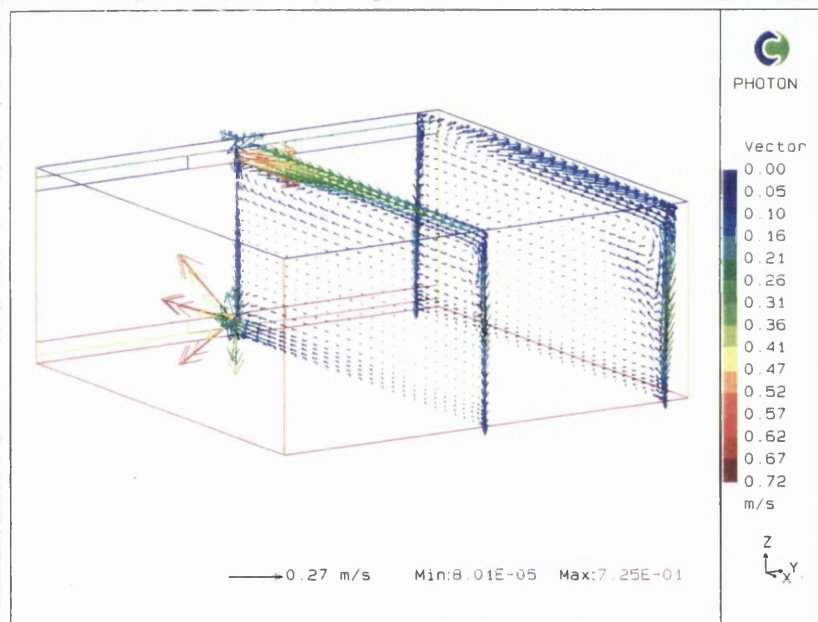
Figure.5.A16

Velocity vectors for the
standard case at 9 ACH,
supply temperature 25 °C.
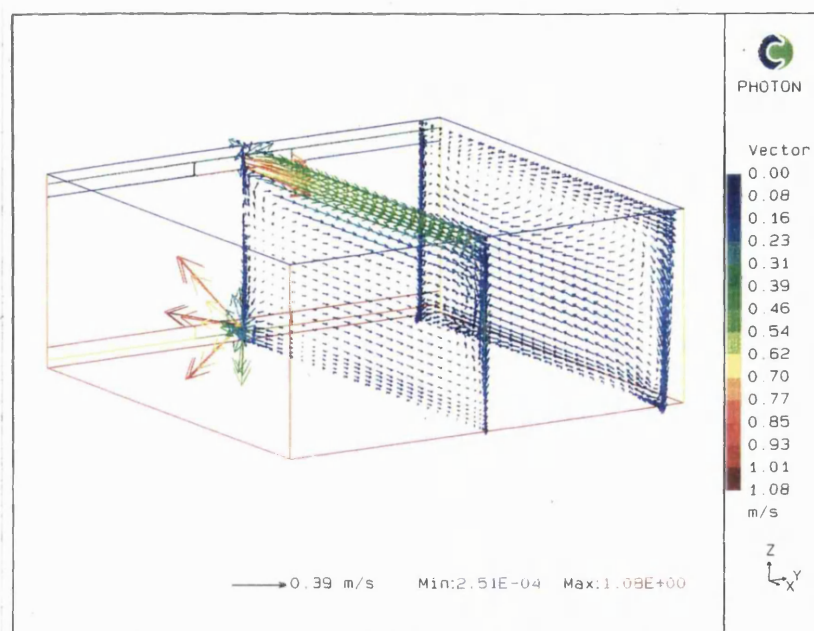
Figure.5.A17

Velocity vectors for the
standard case at 9 ACH,
supply temperature 30 °C.
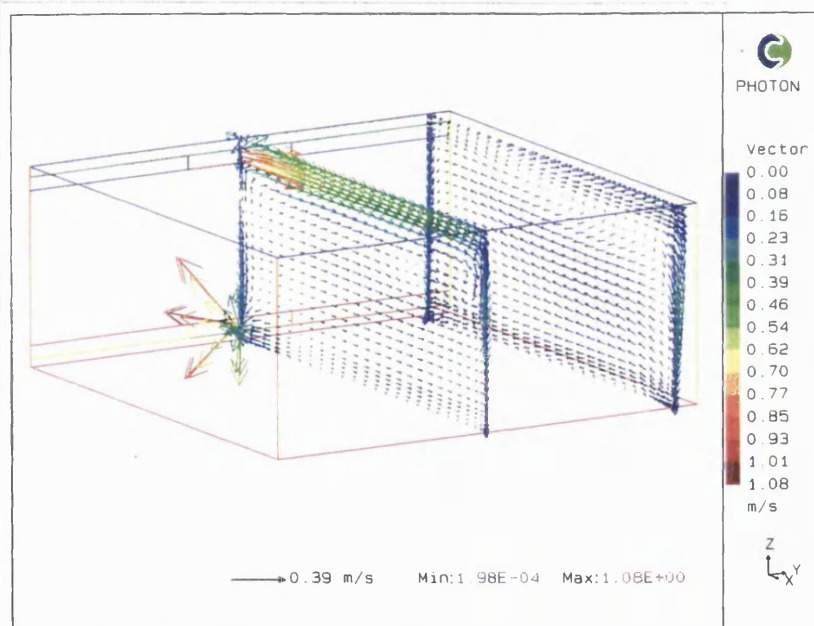
Figure.5.A18

Velocity vectors for the
standard case at 9 ACH,
supply temperature 40 °C.

Figure.5.A19

Enthalpy contours in the mid-
height of the symmetry plane for
the standard case at 3 ACH and
at supply temperatures of 35-55 °C.

Figure.5.A20

Enthalpy contours in the mid-
height of the symmetry plane for
the standard case at 4.5 ACH and
at supply temperatures of 25-45 °C.

Figure.5.A21

Enthalpy contours in the mid-
height of the symmetry plane for
the standard case at 6 ACH and
at supply temperatures of 25-35 °C.
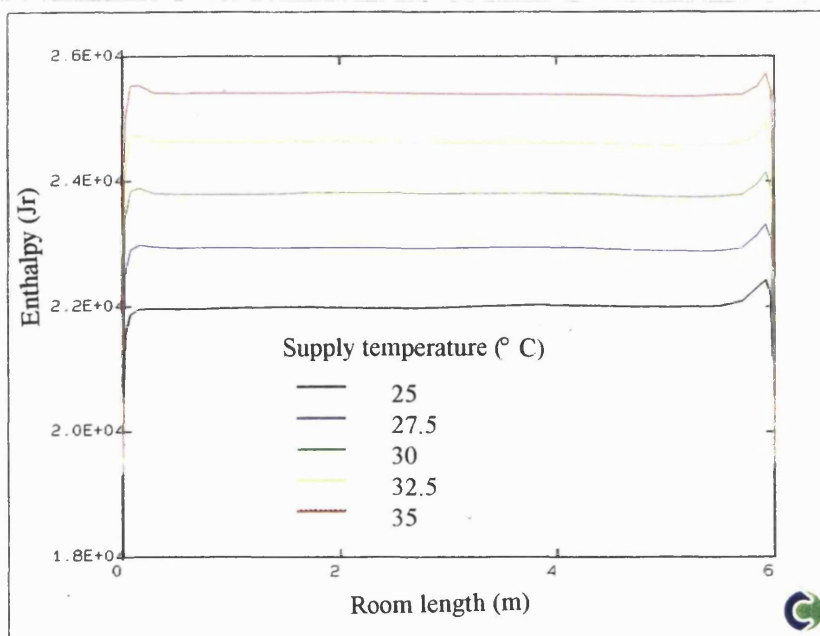
Figure.5.A22

Enthalpy contours in the mid-height of the symmetry plane for the standard case at 9 ACH and at supply temperatures of 25-35 °C.
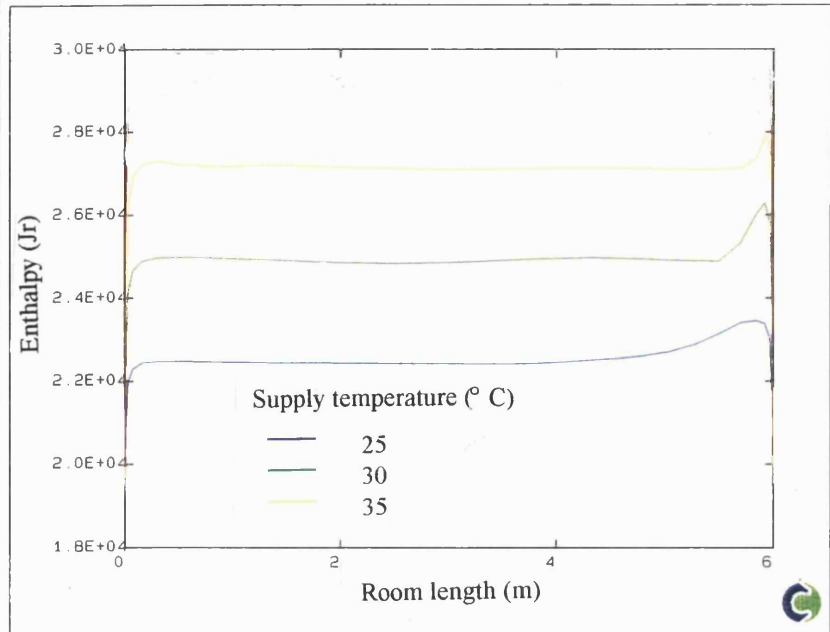
Figure.5.A23

Velocity vectors for the room without side wall temperature gradients. *Case A*, 3 ACH, supply temperature 30 °C.
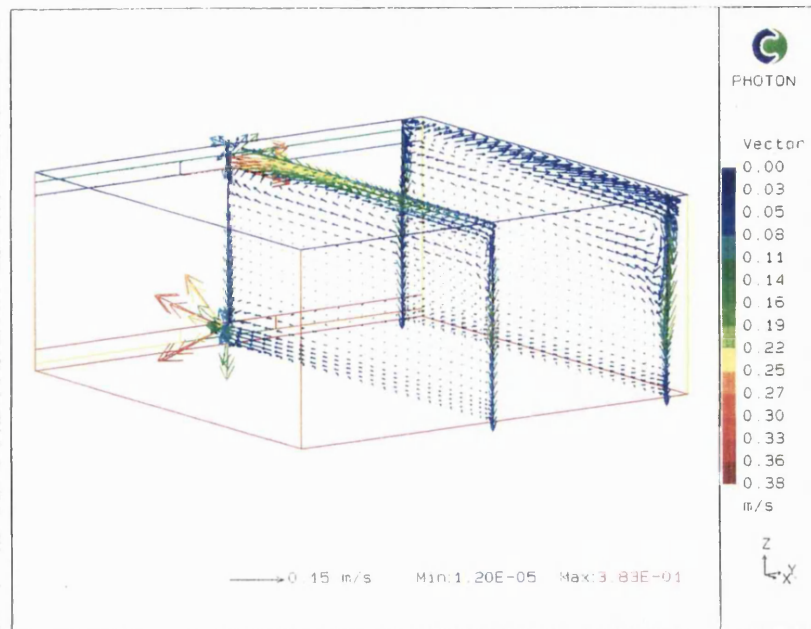
Figure.5.A24

Velocity vectors for the room with side wall temperature gradients. *Case B*, 3 ACH, supply temperature 30 °C.
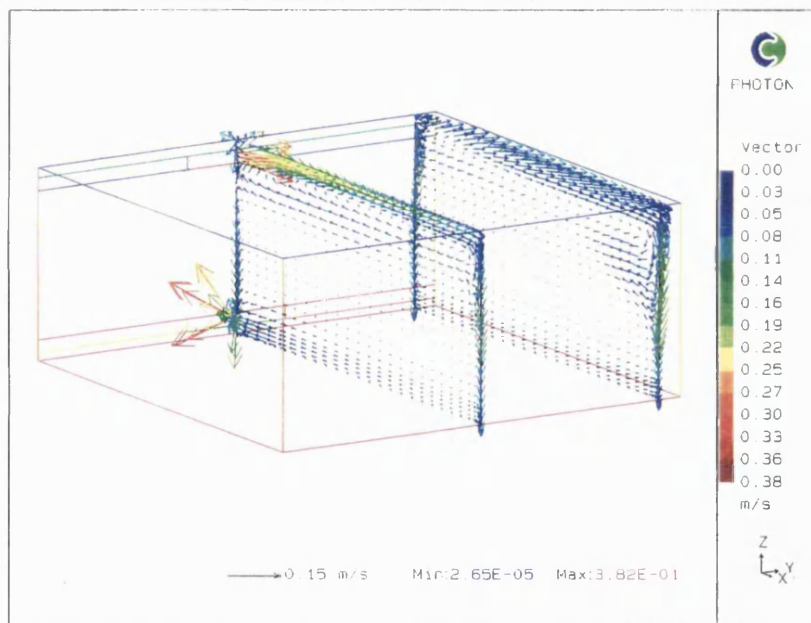
Figure.5.A25

Velocity vectors for the room with side wall temperature gradients. *Case C*, 3 ACH, supply temperature 30 °C.
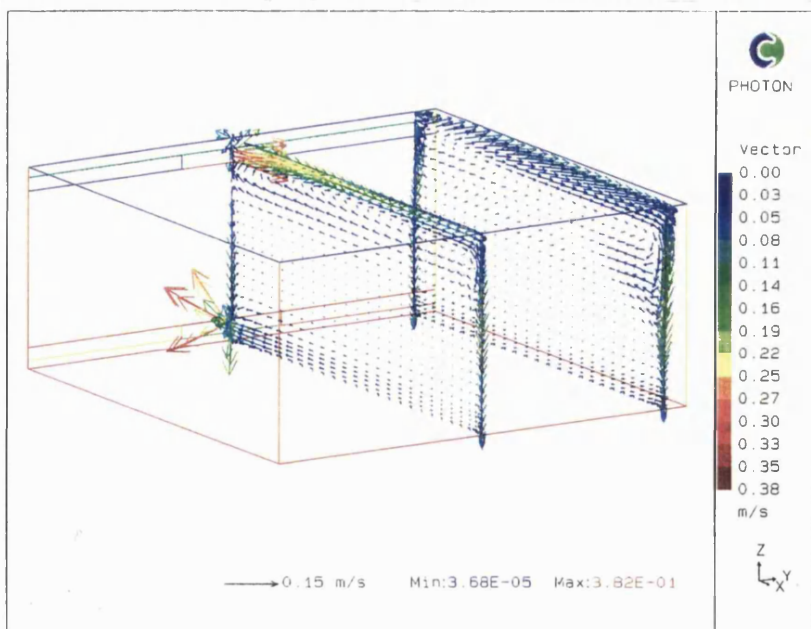
Figure.5.A26

Velocity vectors for the room without side wall temperature gradients. *Case A*, 9 ACH, supply temperature 25 °C.
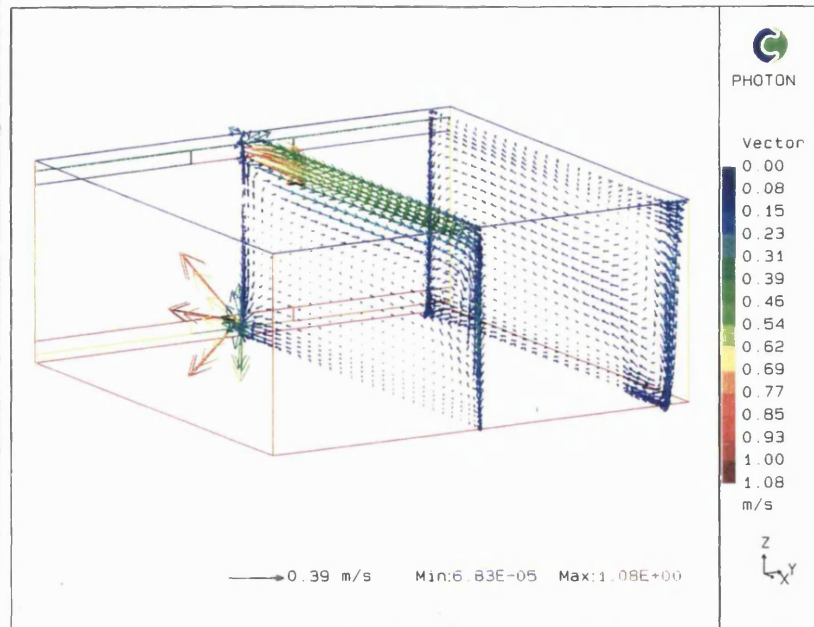
Figure.5.A27

Velocity vectors for the room with side wall temperature gradients. *Case C*, 9 ACH, supply temperature 25 °C.
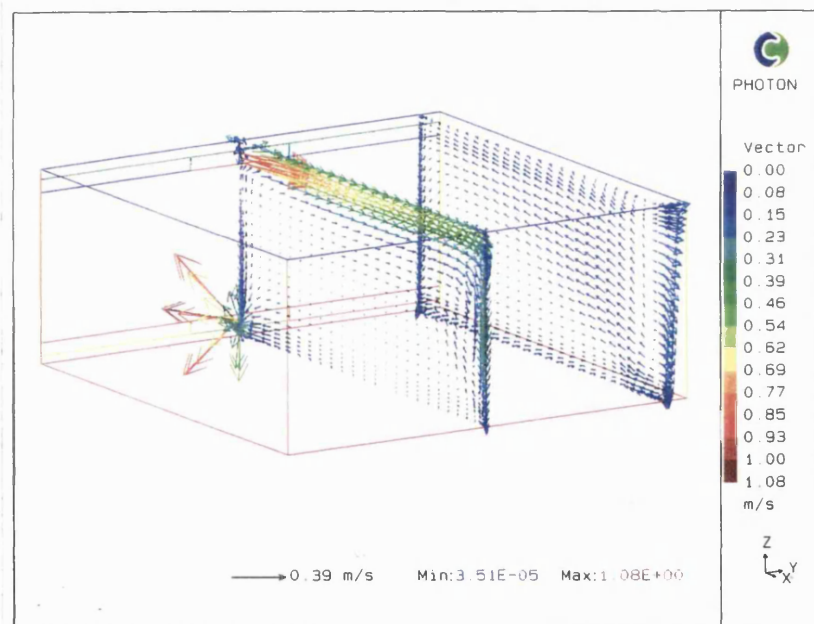
Figure.5.A28

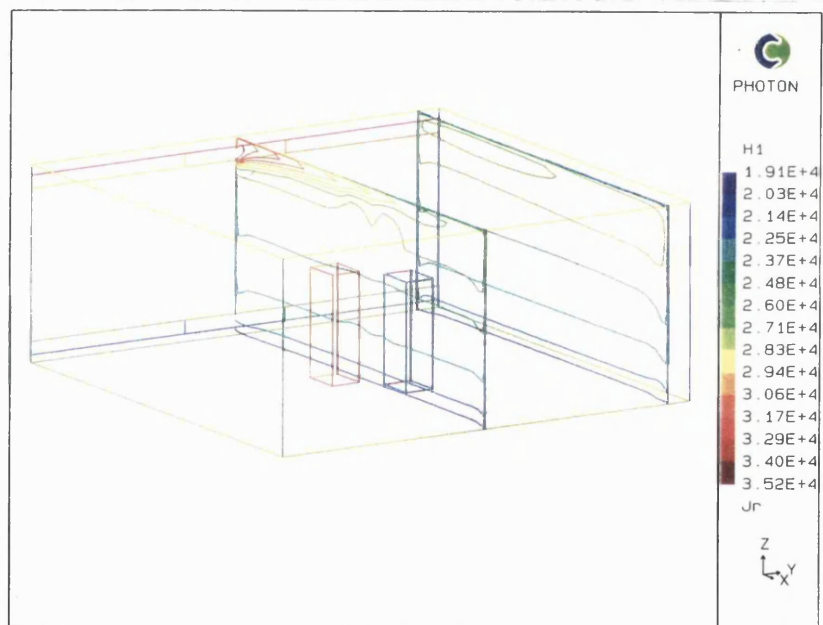Velocity vectors for the room with two obstacles of dimension 0.4 x 0.4 x 1.4 m³. 9 ACH, supply temperature 25 °C.
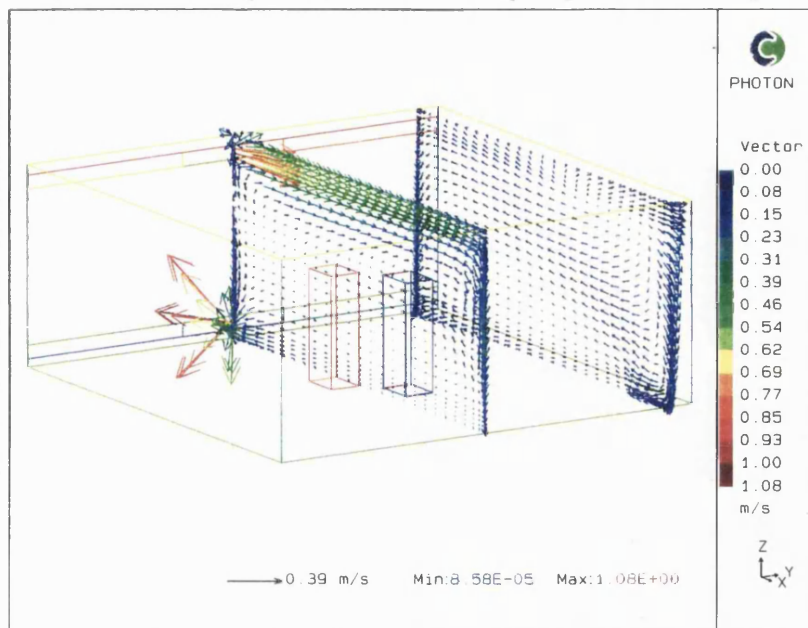
Figure.5.A29

Velocity vectors for the room with two obstacles of dimension 0.8 x 0.8 x 1.4 m³. 9 ACH, supply temperature 25 °C.
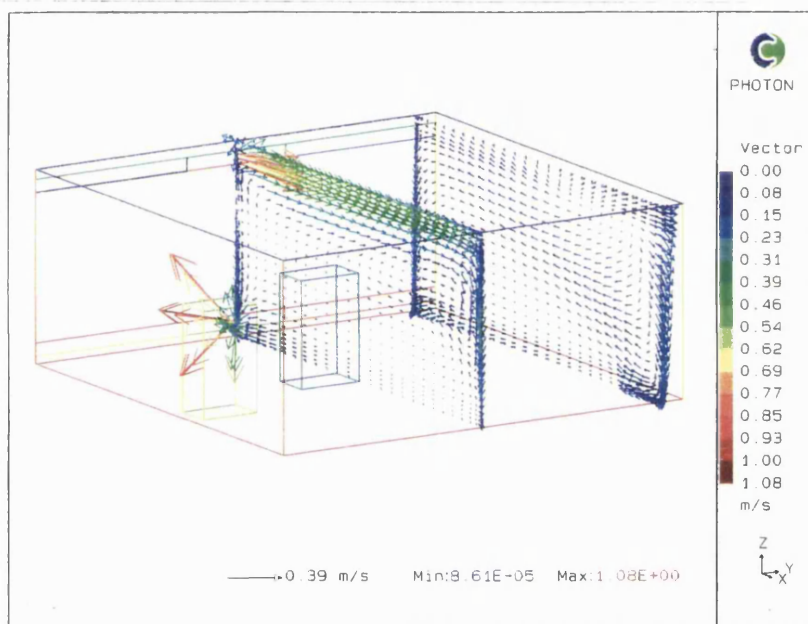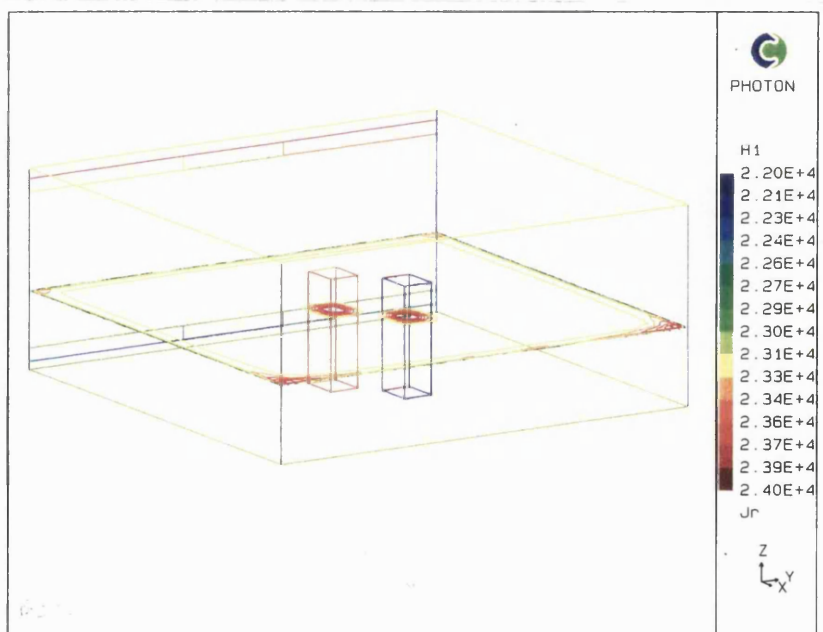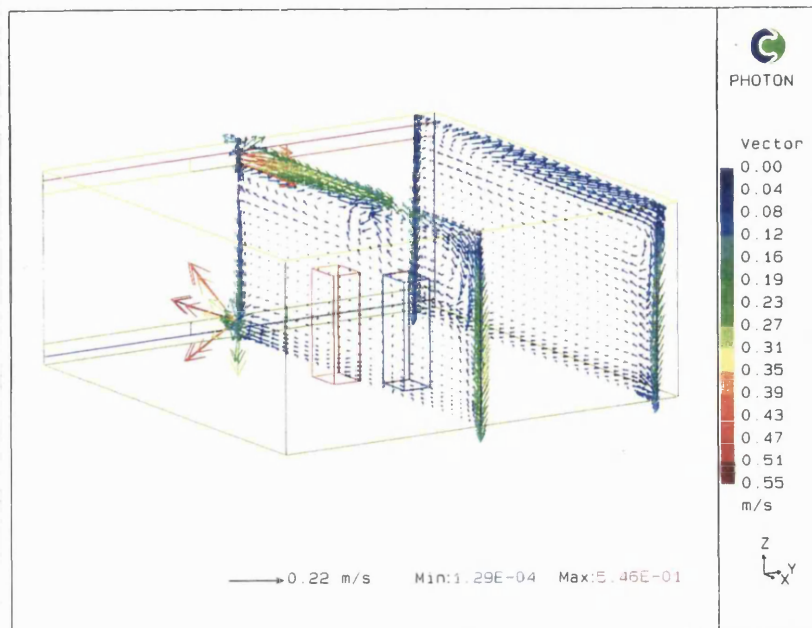
Figure.5.A30

Velocity vectors for the
room with unit heat sources
in the occupied zone, 3 ACH,
supply temperature 35 °C.
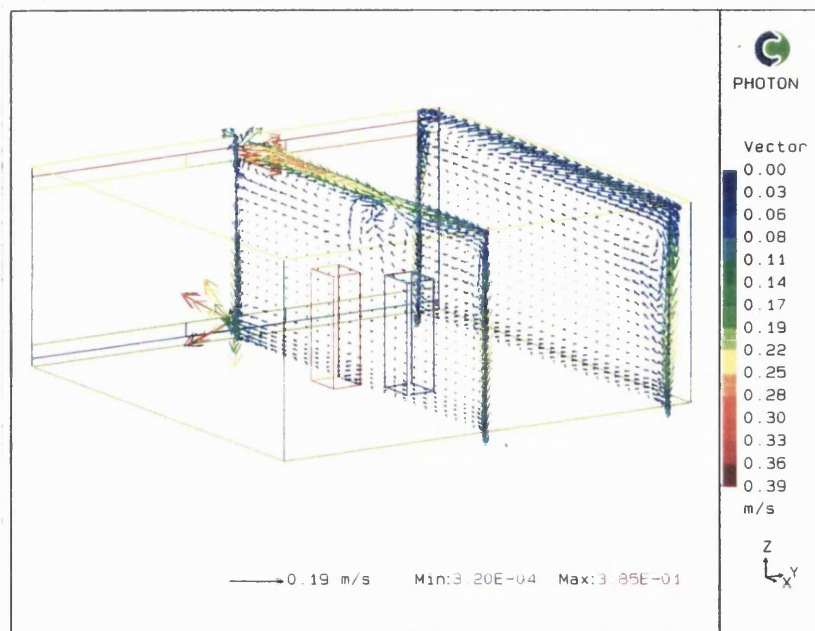
Figure.5.A31

Enthalpy contours (y plane)
for the room with unit heat
sources in the occupied zone,
3 ACH, supply temperature 35 °C.

Figure.5.A32

Enthalpy contours (z plane)
for the room with unit heat
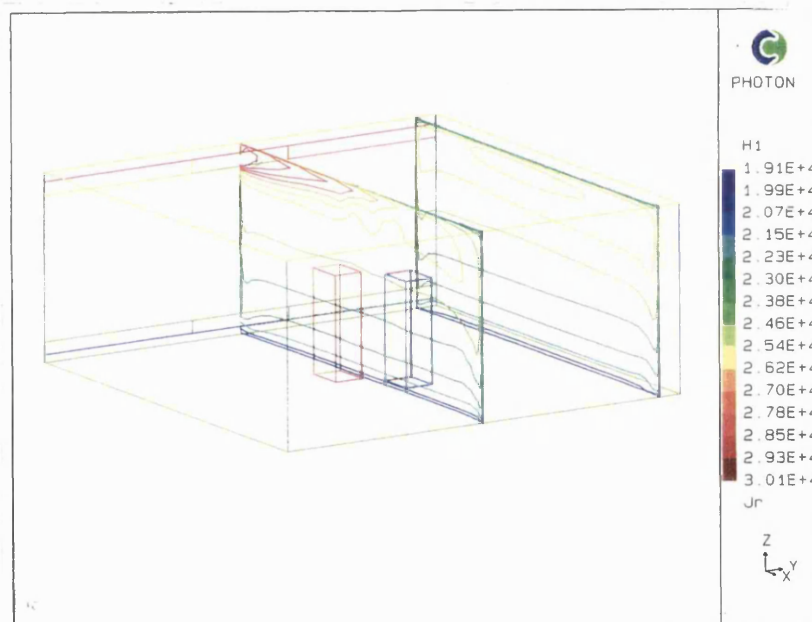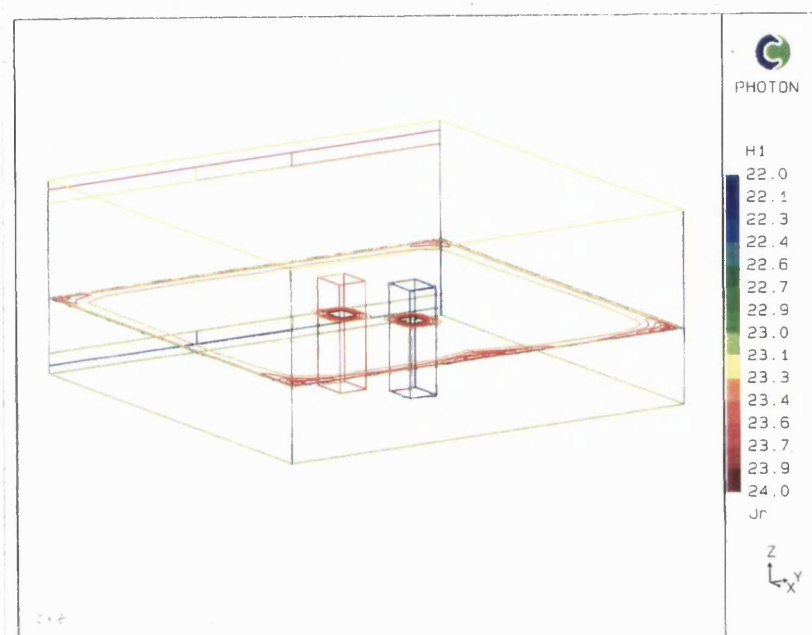source in the occupied zone,
3 ACH, supply temperature 35 °C.

Figure.5.A33

Velocity vectors for the
room with unit heat sources
in the occupied zone, 4.5 ACH,
supply temperature 30 °C.

Figure.5.A34

Enthalpy contours (y plane)
for the room with unit heat
sources in the occupied zone,
4.5 ACH, supply temperature 30 °C.

Figure.5.A35

Enthalpy contours (z plane)
for the room with unit heat
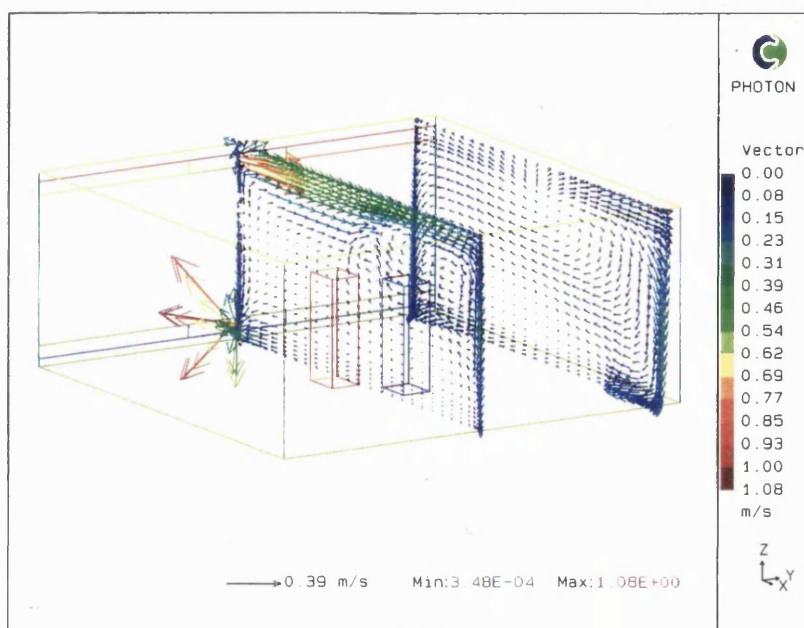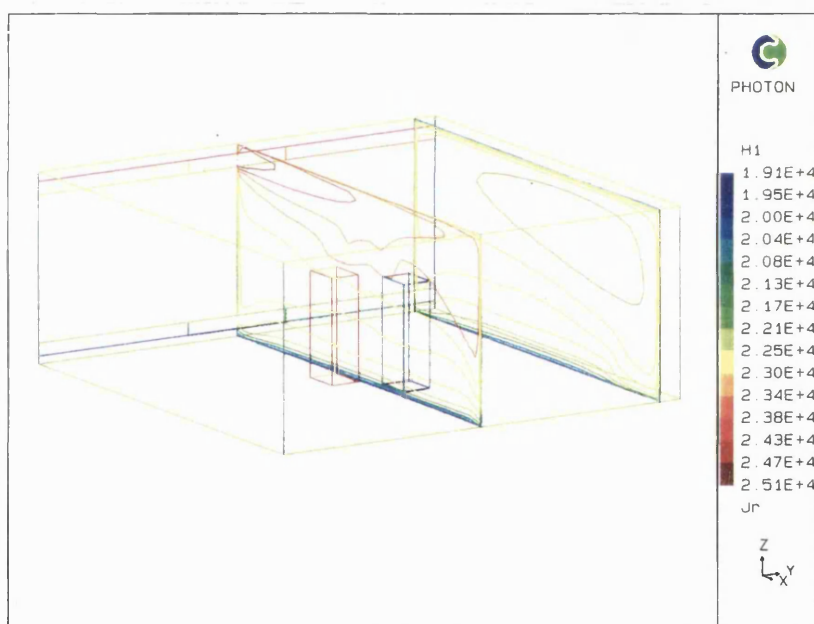source in the occupied zone,
4.5 ACH, supply temperature 30 °C.

Figure.5.A36

Velocity vectors for the
room with unit heat sources
in the occupied zone, 9 ACH,
supply temperature 25 °C.

Figure.5.A37

Enthalpy contours (y plane)
for the room with unit heat
sources in the occupied zone,
9 ACH, supply temperature 25 °C.

Figure.5.A38

Enthalpy contours (z plane)
for the room with unit heat
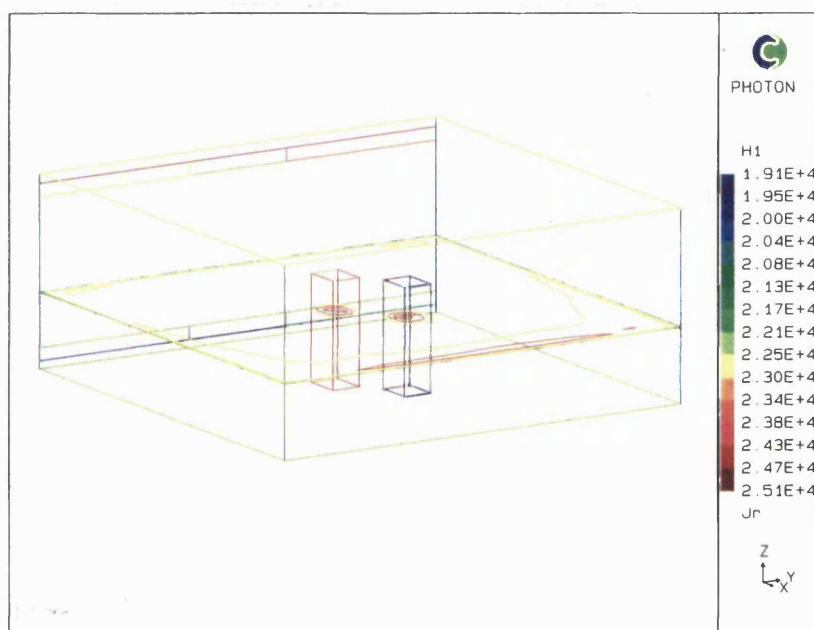source in the occupied zone,
9 ACH, supply temperature 25 °C.

Figure.5.A39

Velocity vectors for the room with unit heat sources in the occupied zone, one heat source moved, 3 ACH, supply temperature 35 °C.
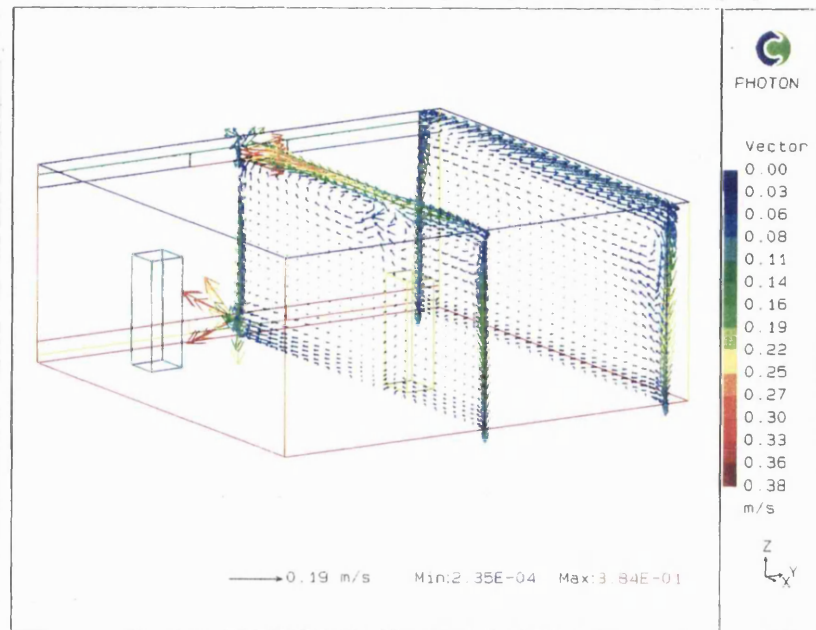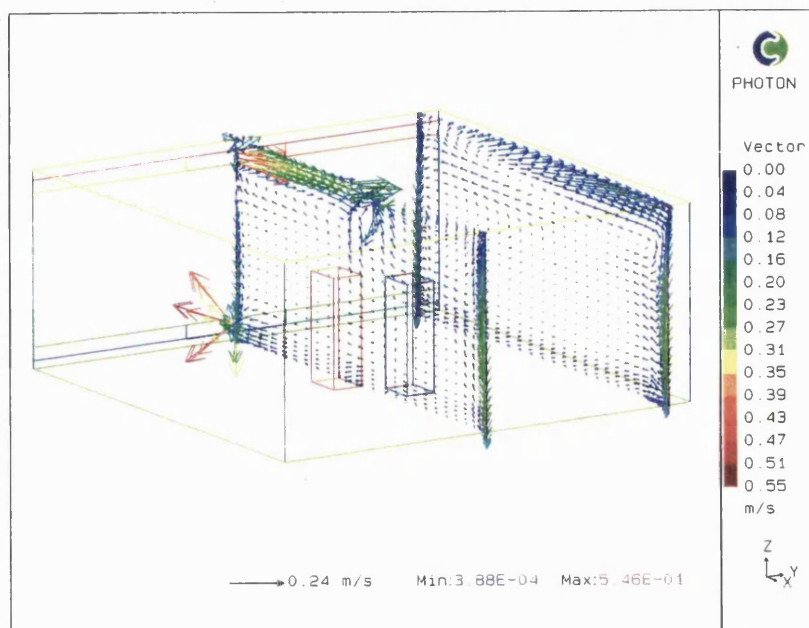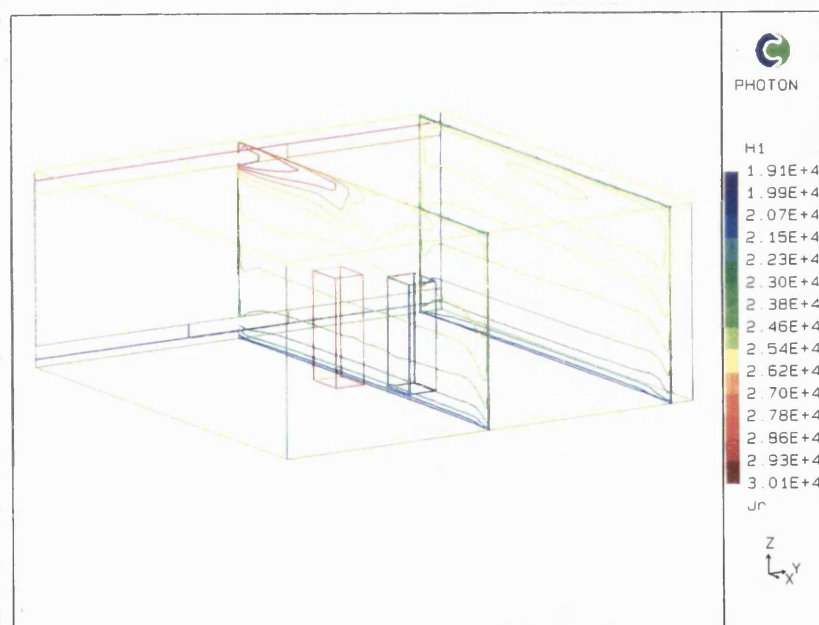
Figure.5.A40

Velocity vectors for the
room with double heat sources
in the occupied zone, 4.5 ACH,
supply temperature 30 °C.

Figure.5.A41

Enthalpy contours (y plane)
for the room with double heat
sources in the occupied zone,
4.5 ACH, supply temperature 30 °C.

Figure.5.A42

Enthalpy contours (z plane)
for the room with double heat
source in the occupied zone,
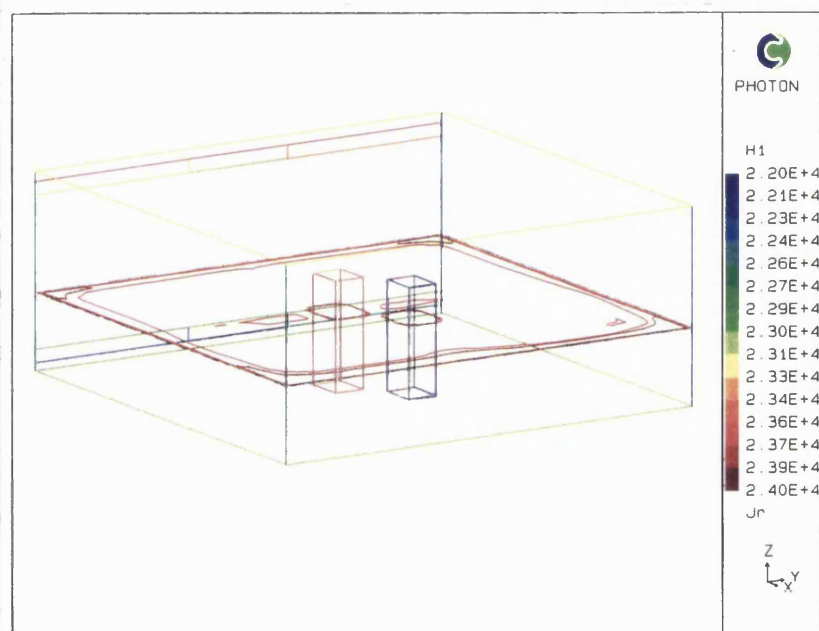4.5 ACH, supply temperature 30 °C.

Figure.5.A43

Velocity vectors for the
room with a heat source above
the occupied zone, 3 ACH,
supply temperature 35 °C.

Figure.5.A44

Enthalpy contours (y plane)
for the room with a heat source
above the occupied zone, 3 ACH,
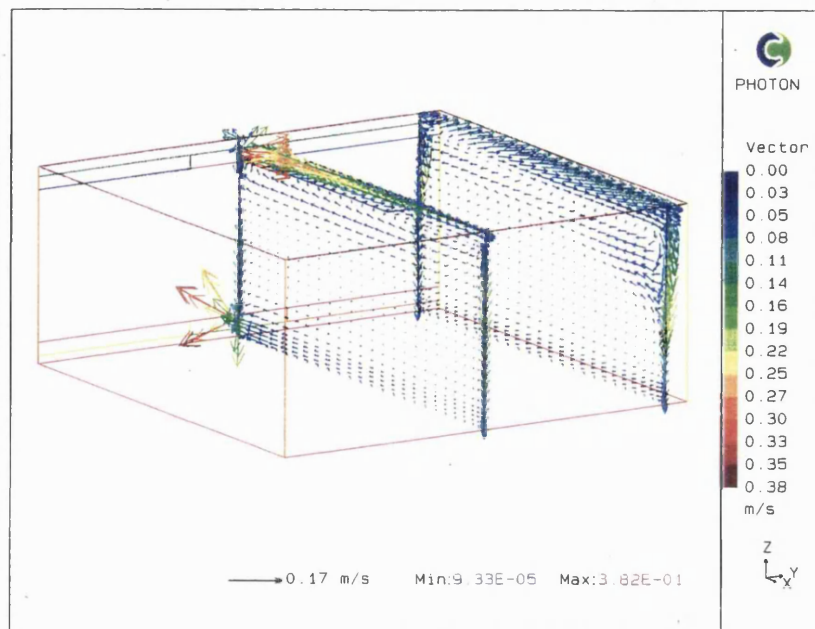supply temperature 35 °C.
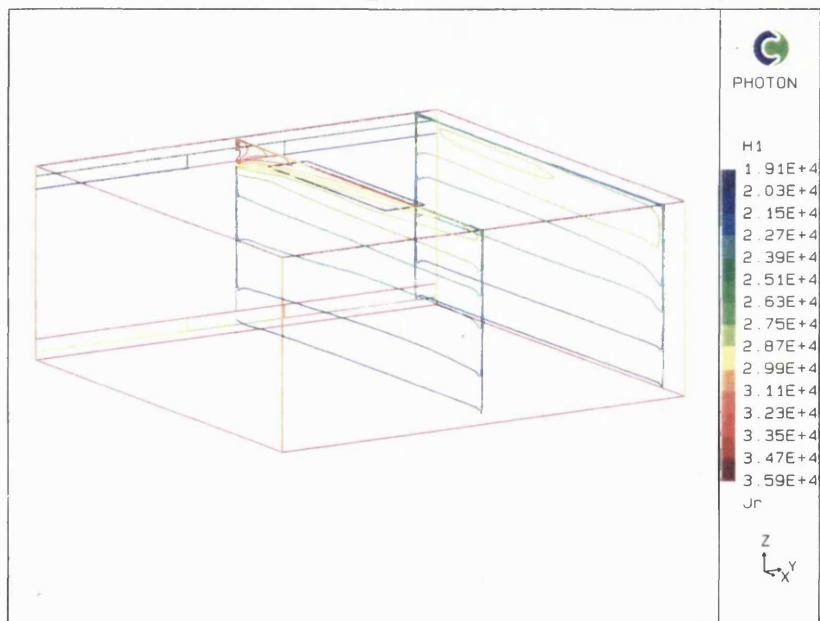
Figure.5.A45

Velocity vectors for the room with a heat source above and within the occupied zone, 3 ACH, supply temperature 35 °C.
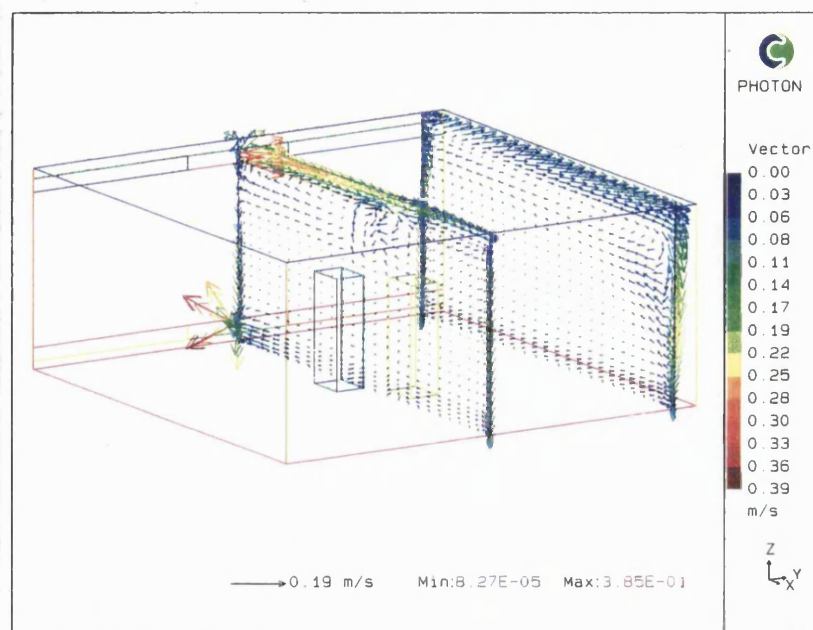
Figure.5.A46

Enthalpy contours (y plane) for the room with a heat source above and within the occupied zone, 3 ACH, supply temperature 35 °C.
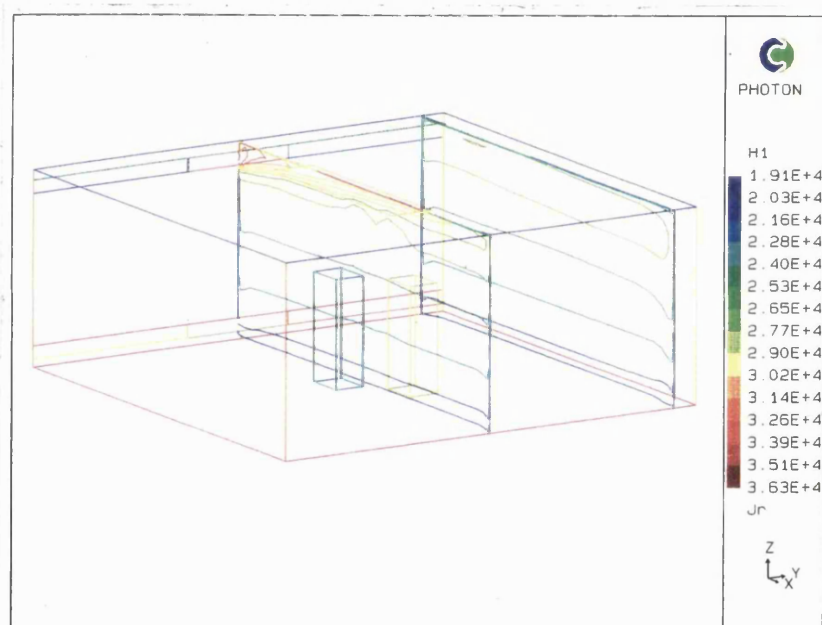
Figure.5.A47

Velocity vectors for the room with unequal wall temperatures, Case 1, 3 ACH, supply temperature 42 °C.
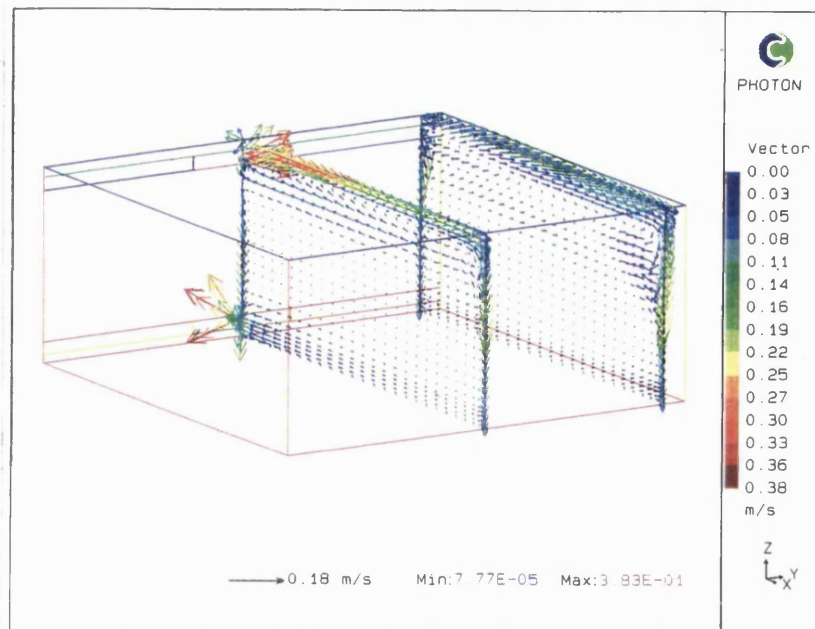
Figure.5.A48

Velocity vectors for the room with unequal wall temperatures, Case 2, 3 ACH, supply temperature 42 °C.
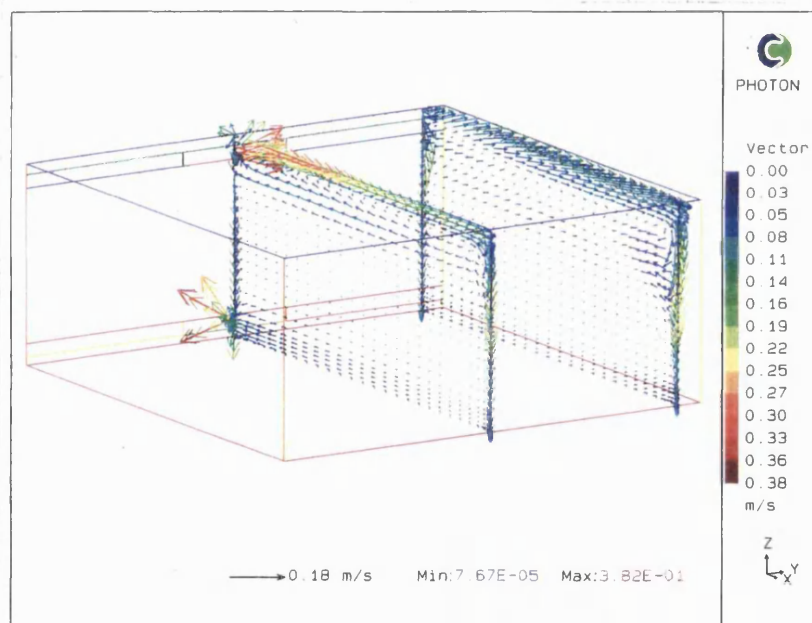
Figure.5.A49

Velocity vectors for the room with unequal wall temperatures, Case 3, 3 ACH, supply temperature 42 °C.
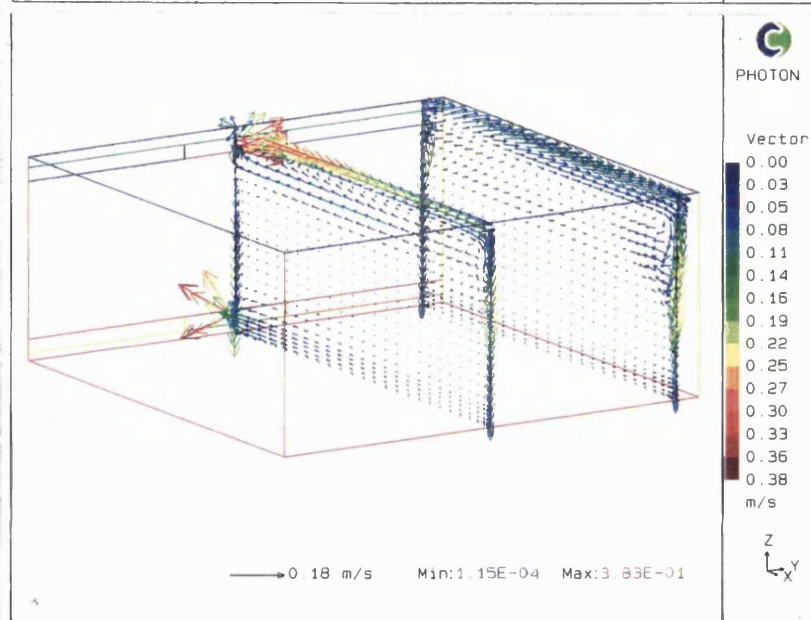
Figure.5.A50

Velocity vectors for the room with unequal wall temperatures, Case 4, 3 ACH, supply temperature 42 °C.
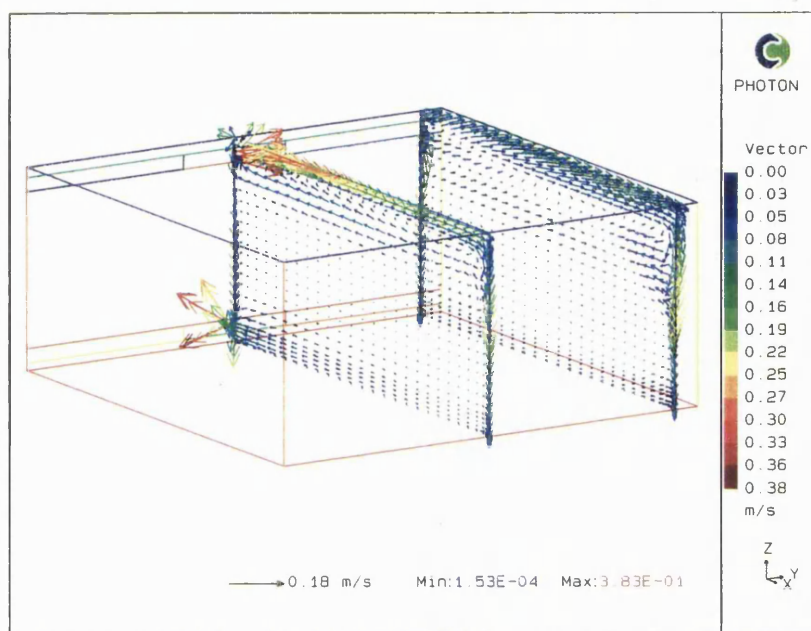
Figure.5.A51

Velocity vectors for the room with unequal wall temperatures, Case 5, 3 ACH, supply temperature 42 °C.
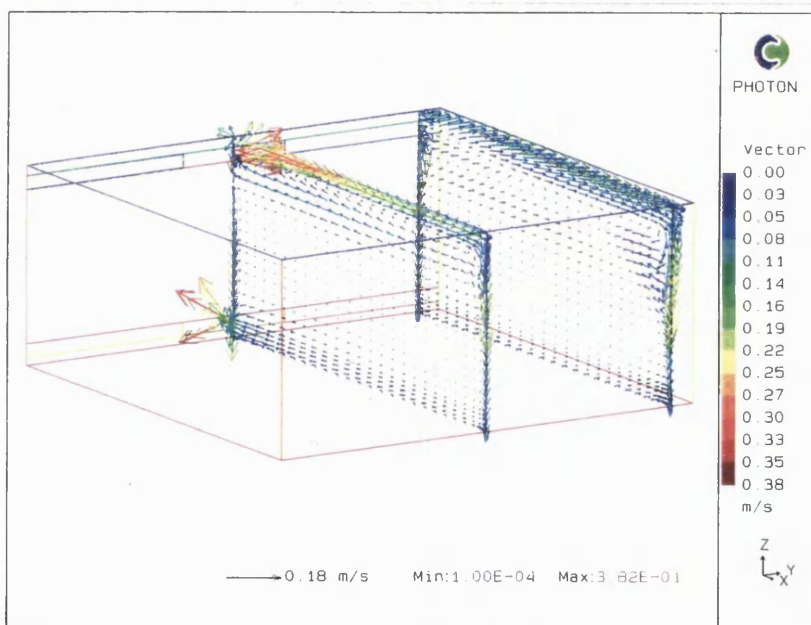
Figure.5.A52

Velocity vectors for the room with unequal wall temperatures, Case 6, 3 ACH, supply temperature 42 °C.
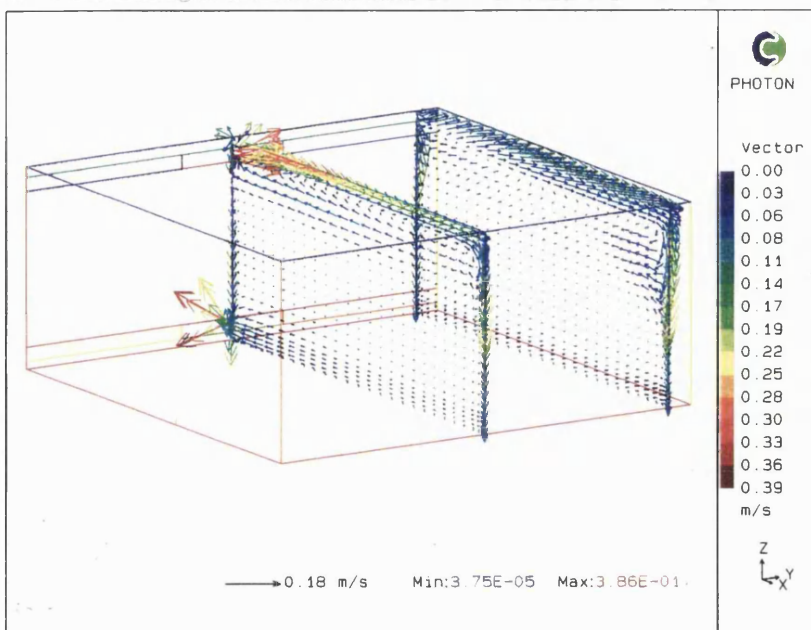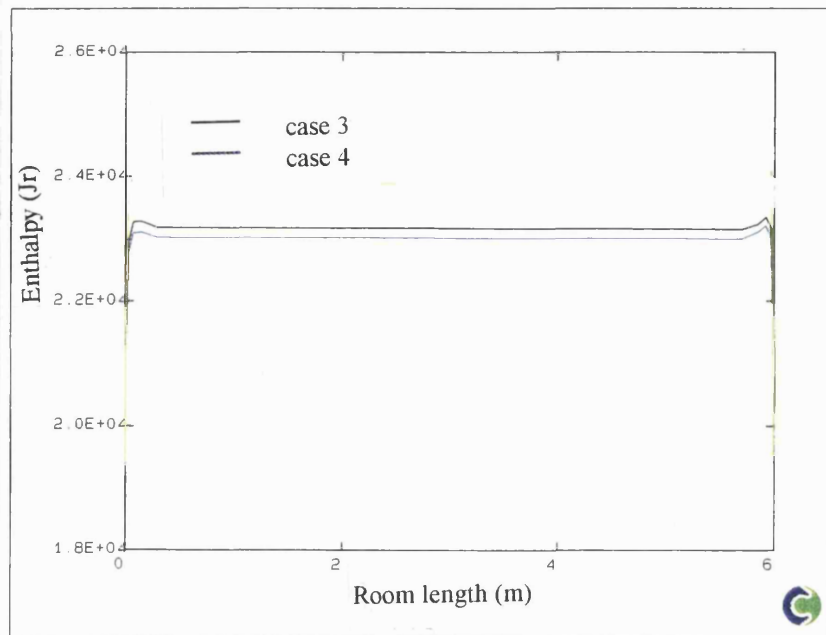
Figure.5.A53

Enthalpy contours in mid-height of the symmetry plane for the room with unequal wall temperatures, Cases 3 and 4, 4.5 ACH, supply temperature 30 °C.
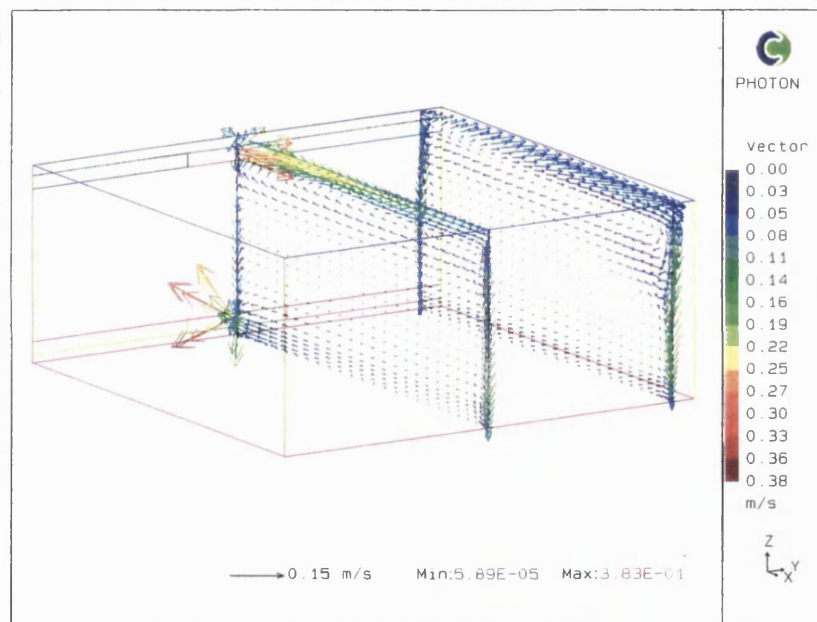
Figure.5.A54

Velocity vectors for the room with a cold window surface, 6 ACH, supply temperature 30 °C.
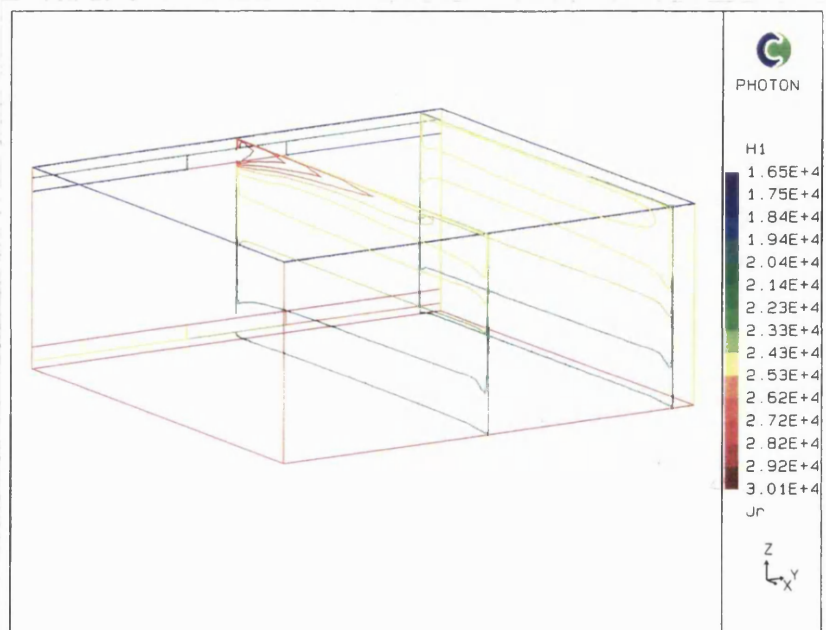
Figure.5.A55

Enthalpy contours for the room with a cold window surface, 6 ACH supply temperature 30 °C.

Figure.5.A56

Velocity vectors for the transient case at 15 mins, 3 ACH, supply temperature 42 °C.
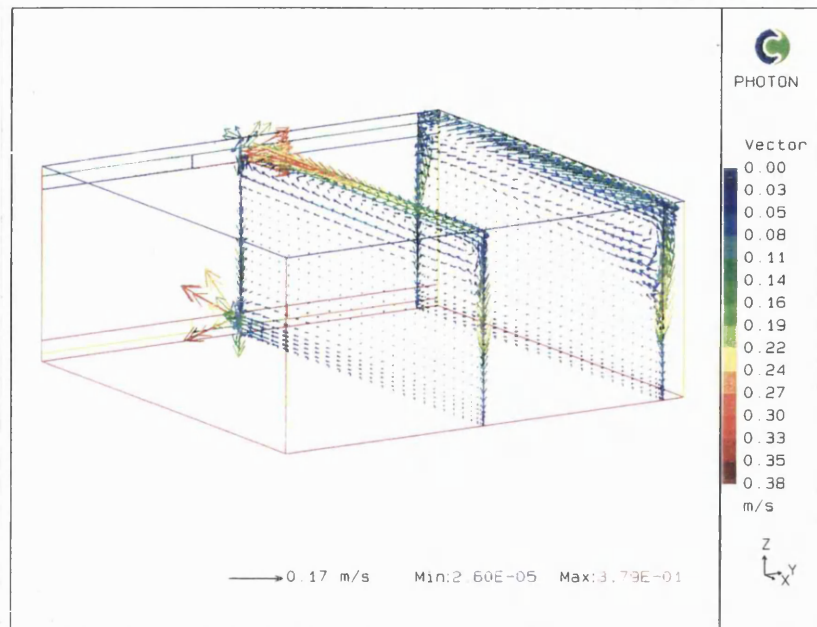
Figure.5.A57

Velocity vectors for the transient case at 30 mins, 3 ACH, supply temperature 42 °C.
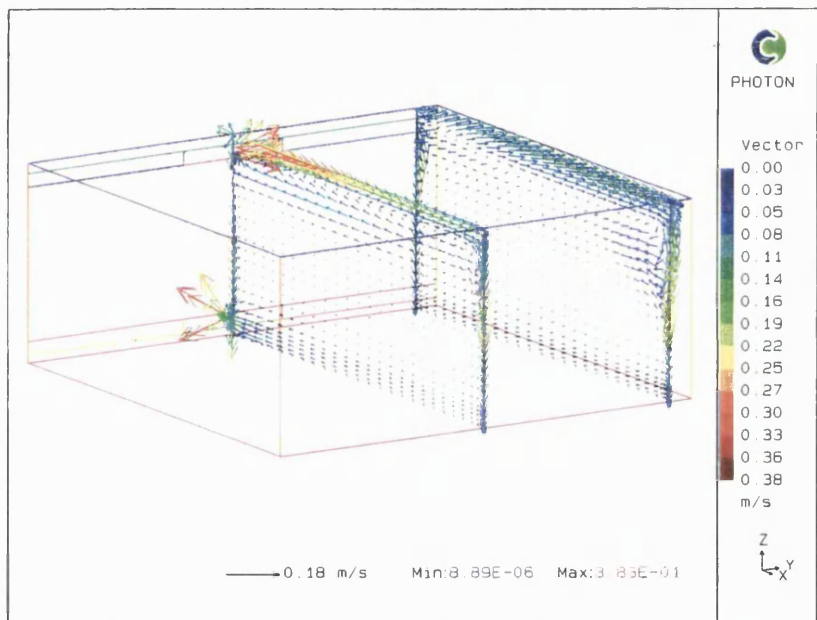
Figure.5.A58

Velocity vectors for the transient case at 45 mins, 3 ACH, supply temperature 42 °C.
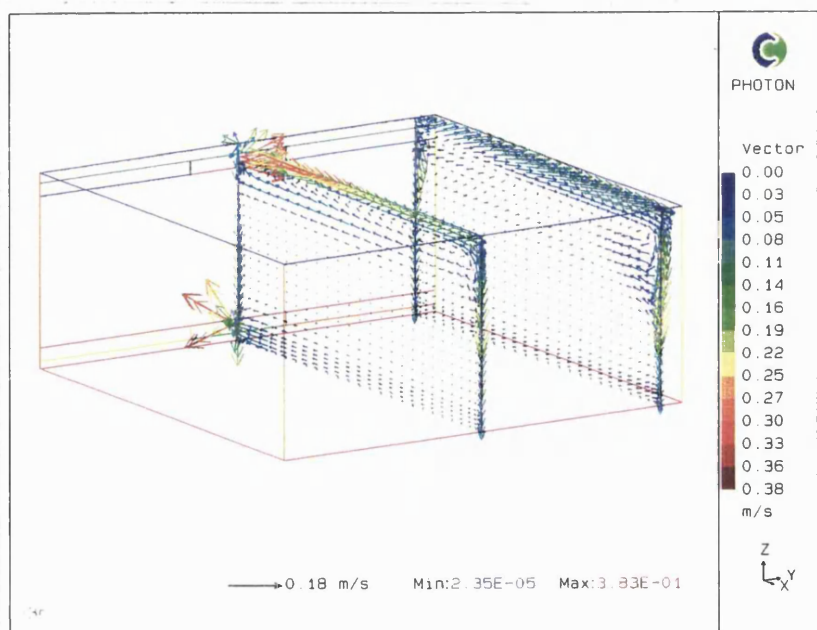
Figure.5.A59

Enthalpy contours for the
transient case at 15 mins,
3 ACH, supply temperature
42 °C.

Figure.5.A60

Enthalpy contours for the
transient case at 30 mins,
3 ACH, supply temperature
42 °C.

Figure.5.A61

Enthalpy contours for the
transient case at 45 mins,
3 ACH, supply temperature
42 °C.
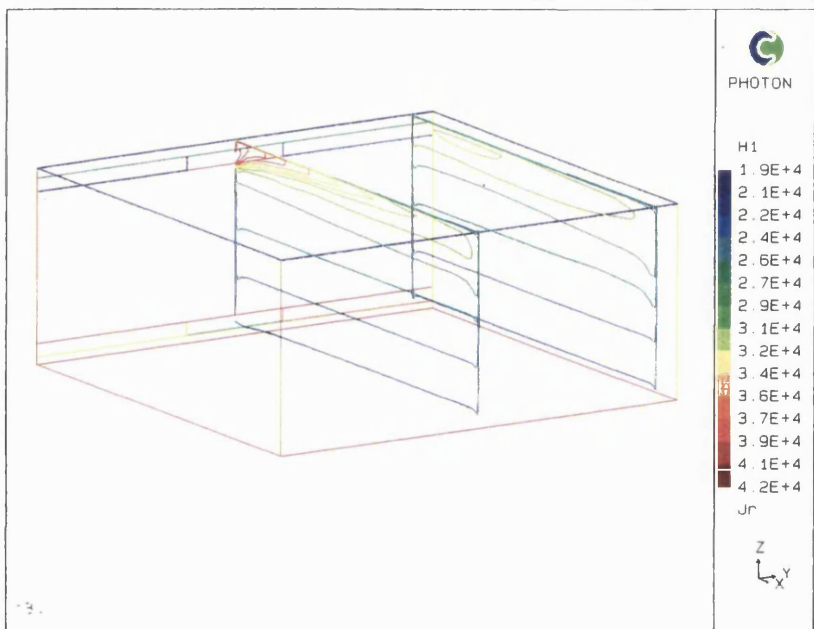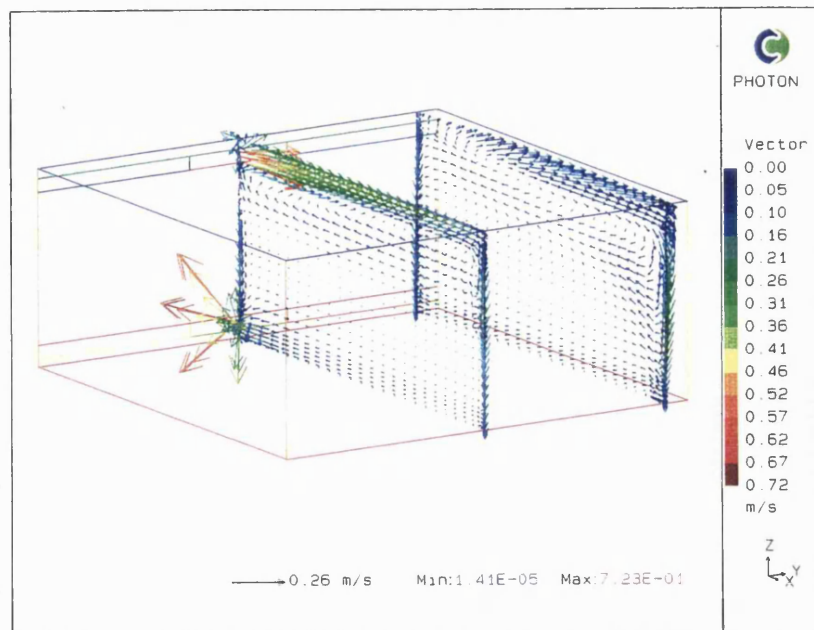
Figure.5.A62

Velocity vectors for the transient case at 30 mins, 6 ACH, supply temperature 30 °C.
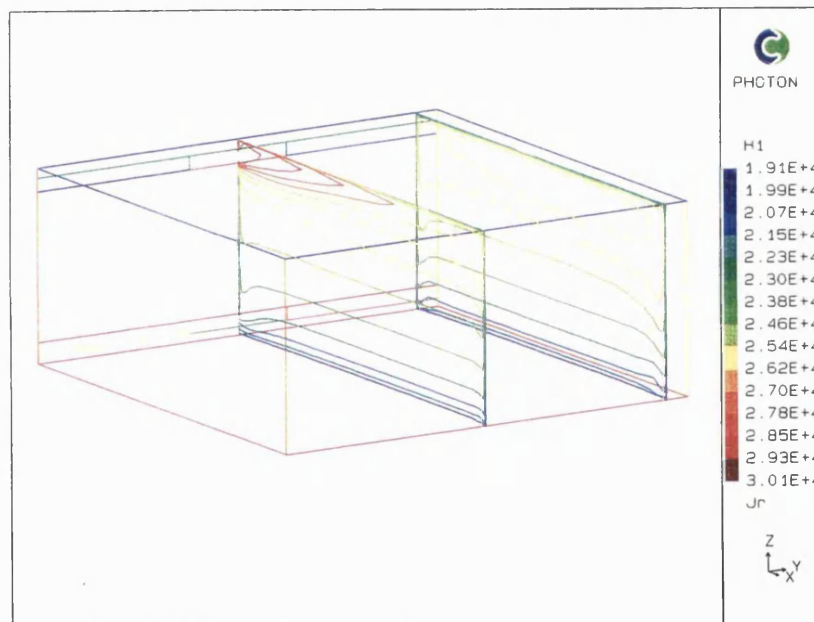
Figure.5.A63

Enthalpy contours for the transient case at 30 mins, 6 ACH, supply temperature 30 °C.
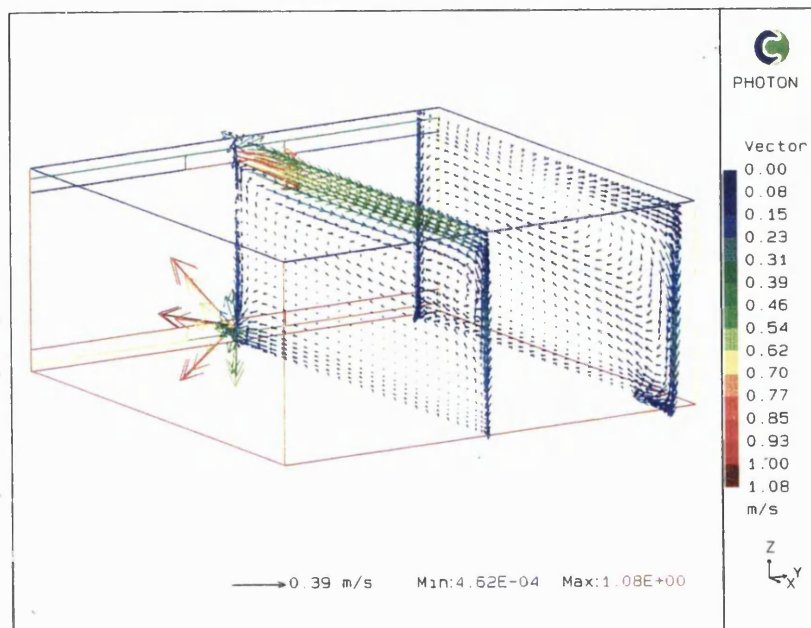
Figure.5.A64

Velocity vectors for the transient case at 15 mins, 9 ACH, supply temperature 25 °C.

6. CONCLUSIONS
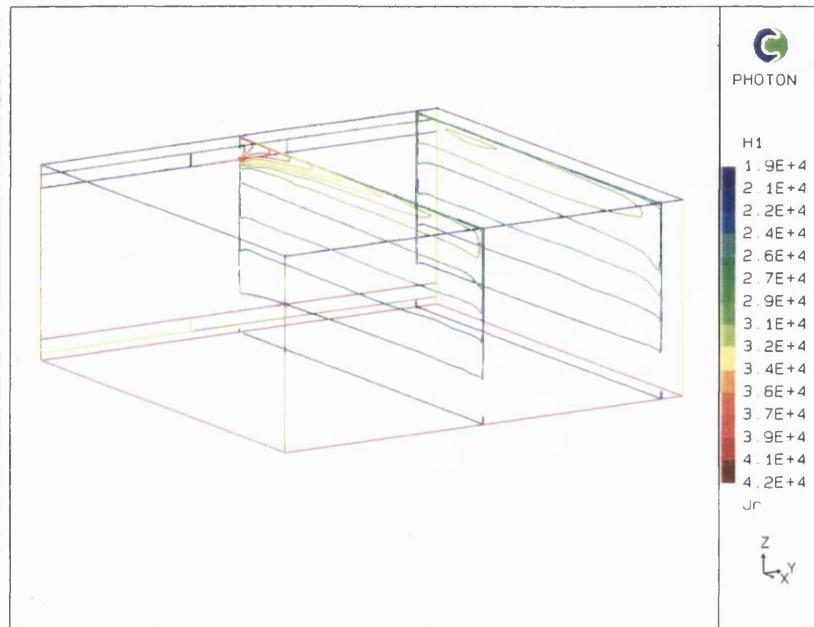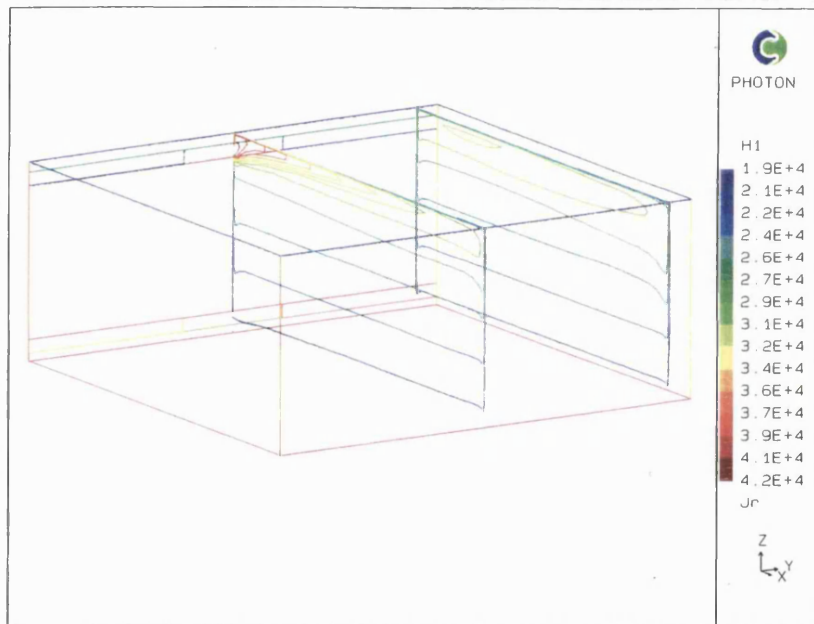
The aim of the research was to identify a suitable heating and ventilation system for the provision and control of thermal comfort in rooms of future low energy homes, whilst allowing for the provision of good indoor air quality (IAQ) and minimising the energy consumption.

Computational fluid dynamics (CFD) was used as a tool to predict indoor airflow, temperature and pollutant distributions. This involved the identification of a suitable indoor airflow model and validating this for use in the current investigation. The validation process involved the comparison of predictions of these models with existing experimental data. Two turbulence models were assessed, the Lam-Bremhorst low Reynolds number k-ε turbulence model and the two layer k-ε turbulence model. The predictions of both of these models were in good agreement with the experimental data with the two layer model making up for somewhat poorer predictive qualities by considerable computational advantages. The two layer model was chosen for application in this research. The CFD modelling of indoor air flow was a time consuming task and a considerable amount of time was dedicated to this to achieve numerically accurate solutions. The difficulties encountered and time dedicated to this confirms the view of various researchers that CFD application to indoor air flow modelling is still not a "plug and play" design tool, but requires considerable time and experience to obtain reliable predictions.

The range of investigation of the CFD modelling task was determined through analysis of the thermal and IAQ requirements in a typical room of a low energy home located in a mid-European climate. This analysis produced estimates of the airflow rates and supply air temperatures required to meet both the thermal and IAQ demands and also identified the boundary conditions i.e. wall surface temperatures which may occur in the room. The analysis estimated a required range of airflow rates of the heating and ventilation (H & V) system of up to 6 ACH in a room of volume 90 m^3.

Distributions of air velocity, temperature and pollutant concentration in a room supplied by several air distribution configurations were predicted at selected conditions

over the expected range of airflow rates. The predicted quantities were used in the assessment of the optimum configurations or locations of air terminal devices (ATDs) for the current application. The assessment criteria were the thermal comfort and IAQ provided by these configurations and the relative energy consumption in the provision of similar thermal comfort levels. Thermal comfort and IAQ were compared in terms of the uniformity and magnitude of *PMV* and pollutant concentrations in the room respectively.

On the basis of the comparisons over the range of expected airflow rates, a configuration with a single high level supply device and low level extract was chosen as most appropriate to meet the requirements of the H & V system. This performed better than other ATD configurations with respect to thermal comfort and as well as any of the other investigated configurations in terms of the IAQ. The high level supply / low level extract configuration achieved poorer energy utilisation compared to some of the other configurations at low airflow rates, however the configuration improved utilisation at high airflow rates.

In the analysis of different ATD configurations, it was found that over the range of operation low level supply devices were best combined with low level extracts . The low level supplies were found to perform well in comparison to the high level supplies at airflow rates of up to 3 ACH. At the higher end of the airflow range however, irrespective of the supply velocity, thermal discomfort due to draught in the occupied zone exceeded the specified limits of 6.5 %.

For both the low and high level supply ATD configurations, fixed geometry ATDs were found to be suitable for application in a H & V system. Negligible benefit to the thermal comfort, IAQ, energy consumption is gained from using variable geometry supply devices. The ATDs should be sized to prevent draught at the maximum airflow rate.

For the chosen configuration of the H & V system i.e. the high level supply low level extract ATD combination, investigations were performed to assess the effect of so-called room specific parameters on the thermal comfort provided by the H & V system.

The room specific parameters investigated included: differences in wall surface temperatures, the presence of internal heat sources and obstacles, a cold window surface, the room geometry and transient effects.

The room specific effects had little implication on the thermal comfort provided by the H & V system over the range of operation. Similar limits of operation of the H & V equipment (airflow rate and supply air temperature) were valid irrespective of the particular room configuration.

Discomfort due to draught was within the specified levels of 6.5 % over all of the airflow range, from 3 to 9 ACH investigated. In the current application, limits of operation of the H & V equipment for the prevention of draught therefore need not be specified.

Limits of operation of the H & V system were identified to prevent discomfort due to vertical air temperature gradients. These were determined relative to an average internal wall surface temperature and methods discussed in which this could best be applied in practice i.e. on the basis of measurements in a real room. For well insulated buildings the fixed limits of operation could be set at a design wall surface temperature determined from the insulation value of the building and the climatic data.

Over the expected range of operation, the air velocity in the occupied zone had negligible impact on the thermal sensation measured by the PMV. An air velocity measurement is thus not needed to effect thermal comfort control using a PMV based index. Simplified PMV based control could therefore be achieved with the measurement of only three of the environmental parameters: air temperature, mean radiant temperature and the relative humidity.

The air temperature in the occupied zone was best represented by a measurement point situated within the occupied zone and at the mid-height of the zone. A high level measurement location was expected of the mean radiant temperature, therefore suggesting the requirement of at least two sensor locations in the room. The use of a single thermal comfort sensor is therefore not suitable.

As a result of the observations made in the course of the study, the author recommends the use of a simple form of comfort control which is entitled Simple Comfort Control (SCC). SCC is based on the PMV algorithm without the influence of velocity and the personal parameters (activity rate, work rate and clothing insulation levels). The aim of SCC is to achieve and maintain user specified comfort levels by the use of a simple interface for user application. SCC would be expected to be integrated with specific IAQ and energy policies. The format of an integrated control scheme has been demonstrated in the thesis.

The research task has met its aims of identification of a suitable heating and ventilation system to provide and control thermal comfort in the rooms of low energy homes. In the process of attaining this goal, substantial data has been obtained which sheds new light on the thermal environment in heated and ventilated rooms. The process has also demonstrated the potential for the use of pre-calculated CFD data in application to the control of the indoor environment.

APPENDIX A1

Minimum ventilation rates for dwellings (Limb, 1994).

Country and Standard Reference	Whole Building (Dwelling) Ventilation Rates	Living Room	Bedroom	Kitchen	Bathroom + WC	WC only
Belgium (NBNB62-003)	0.7 - 1.0 ach 20 30 m^3/h per person		1.0 dm^3/s per m^2 floor area	50-75 m3/h.	14 dm^3/s	7.0 dm^3/s
Canada (CSA F3261-M1989; ASHRAE 62-1989)	>0.3 ach 5 l/s per person			Exhaust 50 l/s (inter.)30 l/s (cont.)	Exhaust 25 l/s (inter.) 15 l/s (cont.)	
Denmark (DS 418)		0.4 - 0.6 ach		0.7 ach	0.7 ach	
Finland (NBC - D2)		0.5 l/s m^2	4.0l/s.person 0.7 l/s m^2floor area	Exhaust 20 l/s	Exhaust 15 l/s	
France (Arrêté 24.03.82)				20- 135 m^3/h	15 - 30 m^3/h	15-30 m^3/h
Germany (DIN 18017; DIN1946; VDI 2088)		Min. 60-120 m^3/h Max. 60-180 m^3/h		Min. 40m^3/h Max. 60m^3/h	Min. 40m^3/h Max. 60m^3/h	Min. 20m^3/h Max 30 m^3/h
Italy (MD 05.07.75)	0.35 - 0.5 ach	15 m^3/h per person		1.0 ach	1.0 - 2.0 ach	
Netherlands (NEN 1087)		1.0 dm^3/s per m^2 floor area	1.0 dm3/s per m^2 floor area	21 dm^3/s	14 dm^3/s	7.0 dm^3/s
New Zealand (ASHRAE 62-1989)	5% of openable window floor area in each room				25 l/s per room (inter.) 10 l/s per room (const.)	
Norway (NBC ch 47 - 1987)		Supply: Openable window or inlet bigger than 100cm^2 in external wall	Supply: Openable window or inlet bigger than 100cm^2 in external wall	Extract: Mech. extract 60 m^3/h or by natural extract at least 150 cm^2 duct above roof	Extract: Mech. extract 60 m^3/h or by natural extract at least 150 cm^2 duct above roof	Extract: Mech extract 40 cm^3/h or by natural extract 100cm^2 duct above roof
Sweden (BFS 1988:18 ch 4:1)	Supply: Min 0.35 l/s m^2 floor area	Supply: 0.35 l/s m2 floor area	Supply: 4.0 l/s person	Extract: 10 l/s.room	Extract: 10 - 30 l/s	Extract: 10 l/s
Switzerland (SIA 384/2,SIA 382/1)			80 - 120 m^3/h		30 - 60 m^3/h	
United Kingdom (BS 5720-1979; BS5925-1991; Build.Regs.Pt.F, CIBSE Guides A,B)	Rec.12 - 18 l/s.person Min. 8-12 l/s.person	Vent. openings with at least 1/20th floor area and vent openings with total area not less than 4000mm^2	Vent. openings with at least 1/20th floor area and Nat. vent openings with total area not less than 4000mm^2	Mech. supply 60l/s inter or 30l/s cooker hood and Nat. vent openings with total area not less than 4000mm^2 orl ach	15l/s intermit.	1/20th floor area or 3 ach intermit. with overrun
United States of America (ASHRAE 62-1989)	0.35 ach but no less than 7.5 l/s.person			50 l/s (intermit.) or 12 l/s (cont.) or operatable windows	25 l/s per room (intermit.) orl0 l/s per room (cont.) or operatable windows	

APPENDIX A2

1. Metabolic rates of different activities (*ISO Standard 7730*, 1993).

Activity	Metabolic rate	
	(W/m²)	(met)
Reclining	46	0,8
Seated, relaxed	58	1,0
Standing, relaxed	70	1,2
Sedentary activity (office, dwelling, school, laboratory)	70	1,2
Standing activity (shopping, laboratory, light industry)	93	1,6
Standing activity (shop assistant, domestic work, machine work)	116	2,0
Medium activity (heavy machine work, garage work)	165	2,8

2. Thermal resistance of clothing ensembles (*ISO Standard 7730*, 1993).

Clothing ensemble	I_{cl}	
	(m²·°C/W)	(clo)
Nude	0	0
Shorts	0,015	0,1
Typical tropical clothing ensemble: briefs, shorts, open-neck shirt with short sleeves, light socks and sandals	0,045	0,3
Light summer clothing: briefs, long light-weight-trousers, open-neck shirt with short sleeves, light socks and shoes	0,08	0,5
Light working ensemble: light underwear, cotton work shirt with long sleeves, work trousers, woollen socks and shoes	0,11	0,7
Typical indoor winter clothing ensemble: underwear, shirt with long sleeves, trousers, jacket or sweater with long sleeves, heavy socks and shoes	0,16	1,0
Heavy traditional European business suit: cotton underwear with long legs and sleeves, shirt, suit including trousers, jacket and waistcoat, woollen socks and heavy shoes	0,23	1,5

REFERENCES

Anderson, J.D. (1995)
Computational fluid dynamics, the basics with applications. McGraw Hill.

ASHRAE (1981)
ASHRAE Standard 55-1981. *Thermal environmental conditions for human occupancy.* The American society of Heating, Refrigeration and Air-Conditioning Engineers Inc., Atlanta, GA.

ASHRAE (1989)
ASHRAE Standard 62-1989. *Ventilation for acceptable indoor air quality.* The American society of Heating, Refrigeration and Air-Conditioning Engineers Inc., Atlanta, GA.

ASHRAE (1992)
ASHRAE Standard 55-1992. *Thermal environmental conditions for human occupancy.* The American society of Heating, Refrigeration and Air-Conditioning Engineers Inc., Atlanta, GA.

ASHRAE (1993)
ASHRAE Handbook - Fundamentals. The American society of Heating, Refrigeration and Air-Conditioning Engineers Inc., Atlanta, GA.

ASHRAE (1996)
BSR/ASHRAE Standard 62-1989R, Public Review Draft. *Ventilation for acceptable indoor air quality.* (Proposed American national standard). The American society of Heating, Refrigeration and Air-Conditioning Engineers Inc., Atlanta, GA.

Awbi, H.B. (1991)
Ventilation of buildings. E & FN SPON.

BS 5925 (1980)
Code of practice for design of buildings: Ventilation principles and designing for natural ventilation. British Standards Institution.

Burberry, P. (1983)
Environment and services. Mitchell's building series

Cain, W.; See, L.; and Tosun, T. (1986)
"Irritation and odor from formaldehydes: chamber studies". Proceedings of IAQ 86 - managing indoors for health and energy conservation. The American society of Heating, Refrigeration and Air-Conditioning Engineers Inc., Atlanta, GA.

CARRIER E20-ii (1994)
Hourly analysis program & system design load program, Users manual. Carrier software systems.

Carlson, T. (1991)
"Warm air heating with a constant supply air flow rate without recirculation". Proceedings of the 12th AIVC conference, Ottawa, Volume 2, pp. 275-284.

CHAM (1993)
PHOENICS online information service: encyclopaedia. PHOENICS version 2.0. CHAM ltd.

Cheesewright, R.; King, K.J.; and Ziai, S. (1986)
"Experimental data for the validation of computer codes for the predictions of two-dimensional buoyant cavity flows". *Significant questions in buoyancy affected enclosure or cavity flows*, ed. Humphrey J.A.C et al. ASME, New York, pp. 75-81.

Chen, Q. (1988)
Indoor airflow, air quality and energy consumption of buildings. Ph.D. thesis, Delft university of technology.

Chen, Q.; Meyers, C.A.; and van der Kooi, J. (1989)
"Convective heat transfer in rooms with mixed convection". International seminar in Indoor air flow patterns, University of Liege, 14 pp.

Chen, Q.; Moser, A.; and Huber, A. (1990)
"Prediction of buoyant, turbulent flow by a low Reynolds number k - ε turbulence model". *ASHRAE Transactions*, Volume 96, Part 1, pp. 563-573.

Chen, Q. and Moser, A. (1991)
"Simulation of a multiple nozzle diffuser". Proceedings of the 12th AIVC conference, Ottawa, Volume 2, pp. 1-14.

Chen, Q. and Jiang, Z. (1992)
"Significant questions in predicting room air motion". *ASHRAE Transactions*, Volume 98, Part 1, pp. 929-939.

Chen, Q.; Moser, A.; and Suter, P. (1992)
"A database for assessing indoor airflow, air quality and draught risk". *IEA Annex 20 Air flow patterns within buildings*. International Energy Agency.

Chien, K.Y. (1982)
"Predictions of channel and boundary layer flows with a low Reynolds number turbulence model". *AIAA journal*, Volume 20, Number 1, pp. 33-38.

CIBSE (1986)
CIBSE guide Volume A, Design data. The Chartered Institute of Building Services Engineers, London.

Diamant, R.M.E. (1986)
Thermal and acoustic insulation, Butterworths.

ECA (1994)
European Collaborative Action Indoor Air Quality and Its Impact on Man: Guidelines for Ventilation Requirements in Buildings. Report Number 11, EUR 14449 EN. Luxembourg: Office for Official Publications of the European Communities.

Fanger, P.O. (1970)
Thermal comfort, McGraw Hill.

Fanger, P.O. (1988)
"Introduction of the olf and decipol units to quantify air pollution perceived by humans indoors and outdoors". *Energy and Buildings*, volume 12, pp. 1-6.

Fanger, P.O. (1996)
"Fanger gets behind ventilation pre-standard". *Heating and Air Conditioning*, September 1996.

Federspiel, C.C. and Asada, H. (1994)
"User - adaptable comfort control for HVAC systems". *Journal of dynamic systems, measurement and control. Transactions of the ASME*, Volume 116, Issue 3, pp. 474-486.

Feist, W. (1990)
Passiv Haus. Institut Wohnen und Umwelt, Darmstadt.

Foster, J.S. (1983)
Structure and Fabric part 1. Mitchell's building series

Gan, G. and Croome, D.J. (1994)
"Thermal comfort models based on field measurements". *ASHRAE Transactions*, Volume 100, Part 1, pp. 782-794.

Gan, G. (1995)
"Evaluation of room air distribution systems using computational fluid dynamics". *Energy and Buildings*, Volume 23, Number 2, pp. 83-93.

Haberda, F. and Trepte, L. (1989)
"Mindestluftwechsel und lueftungstechnische Massnahmen fuer Raumluftqualitaet und rationelle Energienutzung". *IEA Annex 9 Minimum ventilation rates and measures for controlling indoor air quality*. International Energy Agency.

Harris, S.M. and McQuiston, F.C. (1988)
"A study to categorize walls and roofs on the basis of their thermal response". *ASHRAE Transactions*, Volume 94, Part 2, pp. 688-715.

Humphreys, M.A. (1992)
"Thermal comfort requirements, climate and energy". Proceedings 2nd WREC conference, Reading, Volume 4, pp 1725-1734.

ISO (1984)
International standard ISO 7730 -1984. *Moderate thermal environments - determination of the PMV and PPD indices and specification of the conditions for thermal comfort*. International Standards Organisation.

ISO (1993)
International standard ISO 7730 -1993. *Moderate thermal environments - determination of the PMV and PPD indices and specification of the conditions for thermal comfort*. International Standards Organisation.

Jannsen, J.E. (1994)
"The V in ASHRAE: an historical perspective". *ASHRAE journal*, Volume 36, pp 126-132.

Jones, W.P. (1994)
Air conditioning engineering. Edward Arnold.

Knoll, B. (1992)
Advanced ventilation systems - state of the art and trends. Technical note AIVC 35. International Energy Agency.

Kon, A. (1994)
"Thermal comfort sensor". IEEE instrumentation and technology conference, UK, pp 454-456.

Lam, C.K.G. and Bremhorst, K. (1981)
"A modified form of the k-ε turbulence model for predicting wall turbulence". *Journal of fluids engineering*, ASME transactions, Volume 103, pp. 456-460.

Launder, B.E. and Sharma, B.I. (1974)
"Application of the energy dissipation model to the calculation of flow near a spinning disc". *Letters in heat and mass transfer*, Volume 1, pp. 131-138.

Liddament, M.W. (1986)
Air infiltration calculation techniques - an application guide, AIVC. International Energy Agency.

Liddament, M.W. (1991)
A review of building air flow simulation. Technical Note AIVC 33. International Energy Agency.

Liddament, M.W. (1994)
"Energy efficient ventilation strategies". Proceedings of innovative housing 93. Vancouver, pp. 417-426.

Limb, M.J. (1994)
Current ventilation and air conditioning systems and strategies. Technical note AIVC 42. International Energy Agency.

Limb, M.J. (1994)
Ventilation and building airtightness: an international comparison of standards, codes of practice and regulations. Technical note AIVC 43. International Energy Agency.

Ludwig, J. (1994)
Personal correspondence, CHAM Ltd., London.

MacArthur, J.W. (1986)
"Humidity and predicted mean vote based (PMV based) comfort control". *ASHRAE Transactions*, Volume 92, Part 1B, pp. 5-17.

Madhav, M. (1994)
Personal correspondence, CHAM Ltd., London.

McQuiston, F.C. and Spitler, J.D. (1992)
Cooling and heating load calculation manual. The American society of Heating, Refrigeration and Air-Conditioning Engineers Inc., Atlanta, GA.

Moser, A. (1988)
Low Reynolds number effects in single-room air flow. IEA Annex 20, Research item No. 1.1. International Energy Agency.

Nielsen, P.V. (1989)
Representation of boundary conditions at supply openings. IEA Annex 20, Research item No. 1.11. International Energy Agency.

Olesen, B.W. (1993)
"Standards for the design and evaluation of the indoor thermal environment". *ASHRAE journal*, Volume 35, pp. 20-25.

Oseland, N.A. and Humphreys, M.A. (1994)
Trends in thermal comfort research. BRE report. Building Research Establishment, UK.

Patankar, S.V. (1980)
Numerical heat transfer and fluid flow. McGraw Hill.

Patel, V.C.; Rodi, W.; and Scheuerer, G. (1984)
"Turbulence models for near wall and low Reynolds number flows: A review". *AIAA Journal*, Volume 23, No. 9, pp. 1308-1319.

Raatschen, W. (1989)
Bedarfsgeregelte Lueftungsanlagen. IEA Annex 18 Demand controlled ventilation systems - state of the art review. International Energy Agency.

Shaw, M.R. (1987)

Applying expert systems to environmental management and control. BRE report. Building research establishment, UK.

Scheatzle, D.G. (1991)

"The development of PMV-based control for a residence in a hot arid climate". *ASHRAE transactions,* Volume 97, Part 2, pp. 1002-1019.

Seyer, R. and Trepte, L. (1990)

"Intelligent buildings - innovative techniques for the environment". Proceedings of the 11th AIVC conference, Italy.

Stephenson, J. (1995)

Building regulations explained. E & FN SPON.

Veersteeg, H.K. and Malalasekera, W. (1995)

An introduction to computational fluid dynamics: the finite volume method. McGraw Hill.

Werner, G. (1990)

"Ventilation system as an air heating system measuring results in residential buildings". Proceedings of the 11th AIVC conference, Italy.

Whittle, G.E. (1986)

"Computation of air movement and convective heat transfer within buildings". *International journal of ambient energy,* Volume 3, pp. 151-164.

Zhang, J.S.; Chriastenson, L.L.; and Riskowski, G.L. (1989)

"Regional airflow characteristics in a mechanically ventilated room under non-isothermal conditions". *ASHRAE Transactions,* Volume 95, Part 2.